Microarray analysis of oxidative phosphorylation disorders

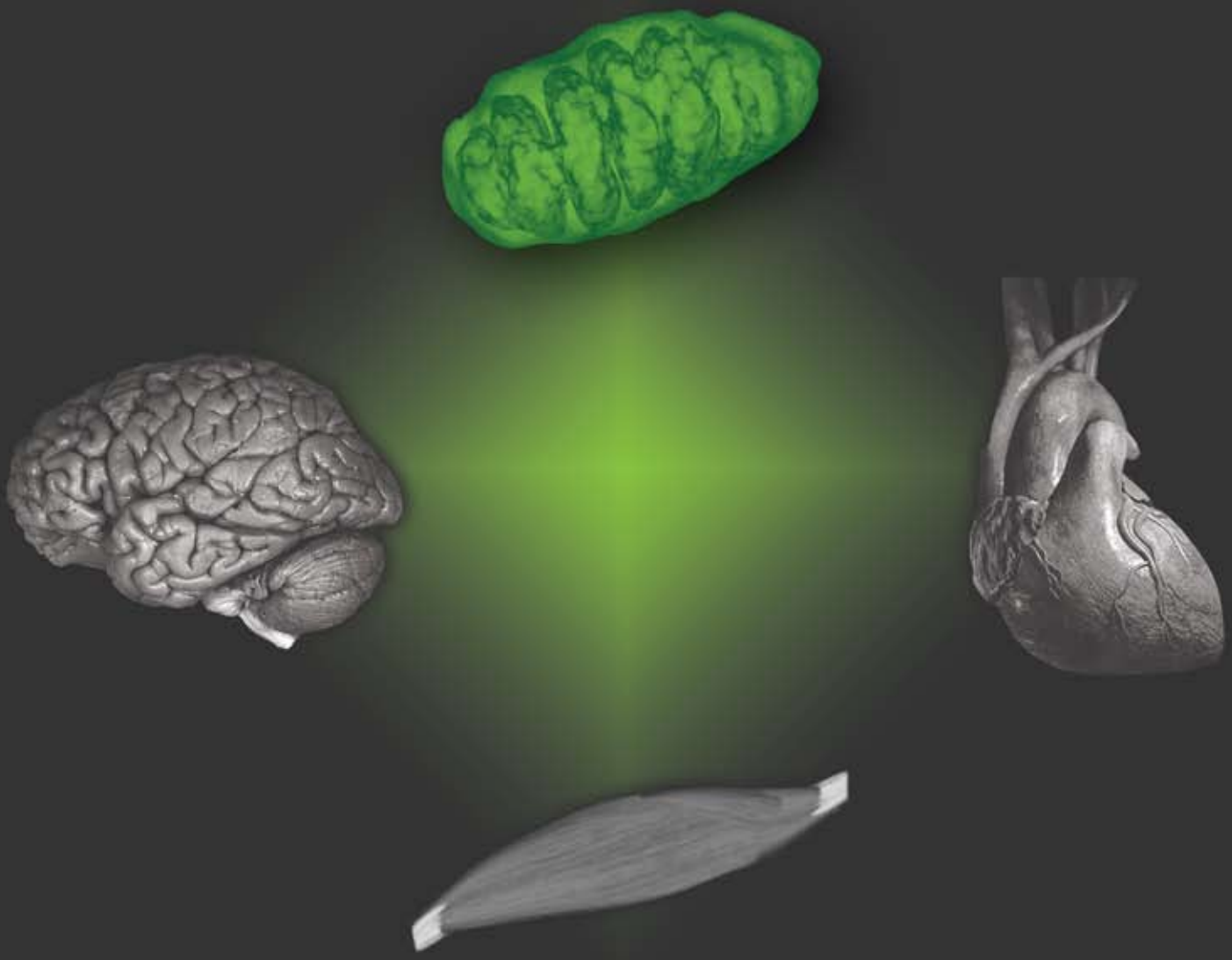

Rudy G.E. van Eijsden

Microarray analysis of oxidative phosphorylation disorders

ISBN 978-90-8891-0449

Cover design
Rudy van Eijsden

Figure 1 of chapter 1
Lars Eijssen

Printed by
Proefschriftmaken.nl

Microarray analysis of oxidative phosphorylation disorders

Proefschrift

ter verkrijging van de graad van doctor
aan de Universiteit Maastricht,
op gezag van de Rector Magnificus,
Pof. mr. G.P.M.F. Mols,
Volgens het besluit van het College van Decanen,
In het openbaar te verdedigen
op donderdag 22 mei 2008 om 12.00 uur

door

Rudy Gerardus Elisabeth van Eijsden

Geboren te Maastricht op 3 augustus 1977

Promotor
Prof. dr. J.P.M. Geraedts

Copromotor
Dr. H.J.M. Smeets

Beoordelingscommissie
Prof. dr. B. G. Wouters (voorzitter)
Prof. dr. P. Van Hummelen (VIB, K.U. Leuven)
Prof. dr. A.K. Raap (LUMC, Leiden)
Dr. M. E. Rubio-Gozalbo (AzM, Maastricht)
Prof. dr. G. J. van der Vusse

The studies described in this thesis were supported by a grant of the Princess Beatrix Foundation (MAR99-0111) and performed at the Department of Genetics and Cell Biology, Research Institute Growth and Development (GROW), Maastricht University, The Netherlands.

The beginning of knowledge is the discovery of something we do not understand

- Frank Herbert -

TABLE OF CONTENTS

CHAPTER 1

General Introduction

Mitochondrial genetics of oxidative phosphorylation disorders

Mitochondria are cellular organelles which are present in almost all eukaryotic cells. One of the most important functions of mitochondria is the production of energy in the form of ATP through the process of oxidative phosphorylation (OXPHOS). OXPHOS starts with a series of oxidation-reduction reactions carried out by a group of enzymes embedded in the mitochondrial inner membrane referred to as the respiratory chain (figure 1). The respiratory chain consists of four enzyme complexes, OXPHOS complexes I to IV. During this process a reduction of O_2 (respiration) and oxidation of NADH (and FADH2) takes place and an electrochemical gradient is created by the pumping of protons from the mitochondrial matrix to the mitochondrial inter-membrane space. The electrochemical proton gradient is the driving-force for the generation of ATP when protons flow back across the membrane. ATP is generated by the ATP synthase or ATPase complex (complex V), which is the final OXPHOS complex. During this process of aerobic energy metabolism, reactive oxygen species (ROS) are formed as a by-product, making mitochondria the main intracellular source of ROS production but also an immediate target of ROS-induced damage.

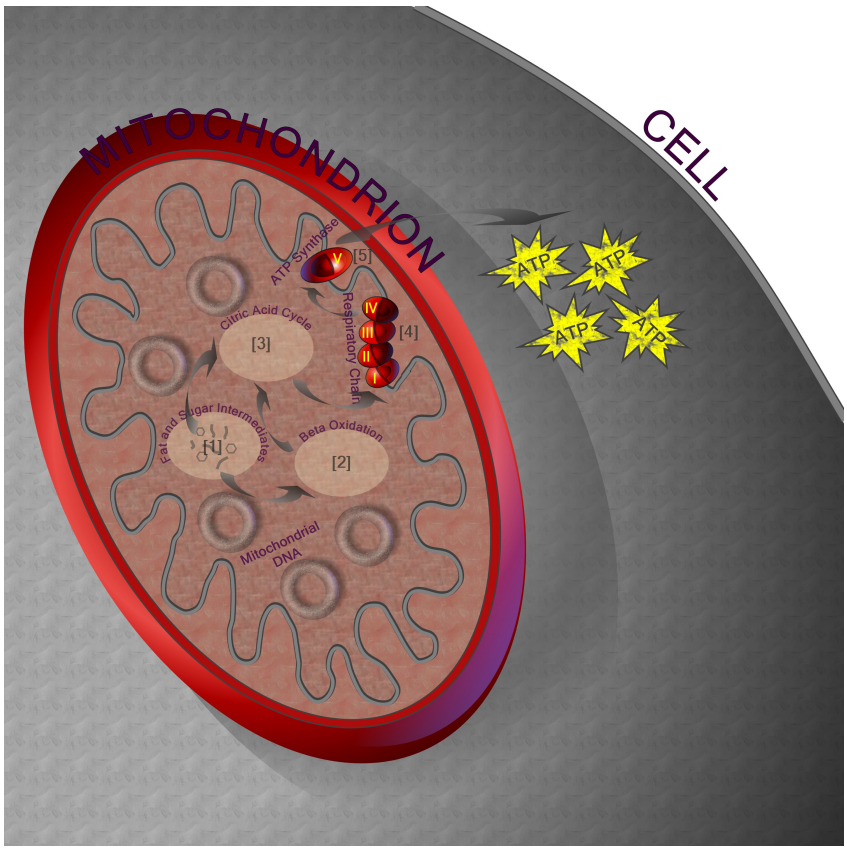

Figure 1: Mitochondria and the respiratory chain inside a cell
Fat and sugar metabolism (1) and beta oxidation (2) form intermediates for the citric acid cycle (3). Oxidation products NADH and $FADH_2$ produced by the citric acid cycle enter into the respiratory chain (4) where an electrochemical proton gradient is created which drives the ATP synthase complex (5) to produce energy in the form of ATP. The numbers I to V represent the five OXPHOS complexes.

Mitochondria are one of the few cell organelles which carry their own functional genome. The human mitochondrial DNA (mtDNA) molecule contains 16,569 bp and comprises 13 protein-encoding genes, 22 tRNA genes and 2 rRNA genes (figure 2) [1], and is inherited maternally. A cell is polyploid for the mtDNA, because each cell can contain hundreds to thousands of mitochondria and each mitochondrion contains 5 to 10 copies of the mtDNA. The proteins encoded by the mtDNA are all subunits of the different OXPHOS complexes. The mtDNA encodes seven subunits of complex I (NADH dehydrogenase), one subunit of complex III (*b-c1* complex), three subunits of complex IV (cytochrome *c* oxidase), and two subunits of complex V (ATPase). The other subunits of these complexes and the entire complex II are coded for by the nuclear DNA (nDNA). The mitochondrial tRNA and rRNA molecules are necessary for the translation and protein synthesis from these mitochondrial transcripts, because the mtDNA code differs from the nDNA code, e.g. UGA codes for tryptophan rather than being a stop codon as in the genetic code of the nDNA [2]. Pathogenic point mutations in one of the mtDNA protein encoding, tRNA or rRNA genes can lead to malfunctioning of OXPHOS and clinical symptoms. Additionally, mtDNA rearrangements (deletions/duplications) or depletions can have a similar effect. Copies of the mtDNA with pathogenic mutations usually coexist with wild-type mtDNA in the same cell or tissue, a situation referred to as heteroplasmy. Disease manifestations only occur when the level of mutated mtDNA molecules exceeds a cell or tissue specific threshold. Disorders in which OXPHOS deficiency is a central characteristic are referred to as oxidative phosphorylation disorders, or in short, OXPHOS disorders. MtDNA mutations can arise *de novo*, they can be acquired somatically, mainly due to ROS damage, or they can be maternally inherited and segregate in families. An inefficient OXPHOS function will often result in increased ROS production, thereby increasing the somatic mutation rate and causing protein and DNA damage. Besides mutations in these mtDNA genes, mutations in nuclear genes with a direct or indirect relation to OXPHOS may also result in OXPHOS deficiency. These genes may encode structural OXPHOS subunits, but it may also be genes involved in mtDNA replication and mitochondrial biogenesis, regulatory genes in the OXPHOS complex formation.

A hallmark of OXPHOS disorders is genetic and clinical heterogeneity. Genetic heterogeneity means that different mutations, i.e. mutations in different genes (mtDNA or nDNA) or at different sites in the same gene, can lead to the same clinical symptoms. Clinical heterogeneity refers to situations where the same mutation results in different clinical symptoms or syndromes. At least for mtDNA mutations, part of this can be explained by heteroplasmy and different mutation levels. Syndromic OXPHOS disorders which are caused by heteroplasmic mtDNA mutations and which have been studied for this thesis are Leigh syndrome (OMIM #256000), Neuropathy, Ataxia, and Retinitis Pigmentosa (NARP, OMIM #551500), and mitochondrial Myopathy, Encephalopathy, Lactic Acidosis, and Stroke-like episodes (OMIM #540000). Leigh syndrome is genetically heterogeneous and can be caused by a variety of mutations in mtDNA encoded as well as in nDNA encoded genes. Leigh syndrome can for example be caused by the m.9176T>C mutation in the mtDNA encoded *ATP6* gene [3-5], but also by mutations in the nuclear *SURF1* gene

which encodes a complex IV assembly factor [6-8]. A more common cause of Leigh syndrome and the milder NARP syndrome is a point mutation at position 8993 in the *ATP6* gene, where a thymidine is mutated to a cytosine or a guanine (m.8993T>C/G). For this mutation, heteroplasmy is an important factor for clinical expression as the NARP symptoms usually manifest at mutation loads above 60%, and severe Leigh syndrome above 90% [9-11]. The clinical heterogeneity for this mutation can largely be explained by the heteroplasmy level, but this is not always the case. The m.3243A>G mutation is an example of a mutation that leads to extreme clinical heterogeneity, which can not be explained by heteroplasmy differences only. This mutation may result in MELAS, cardiomyopathy, diabetes mellitus, deafness, renal failure, or a combination of these symptoms [12-21].

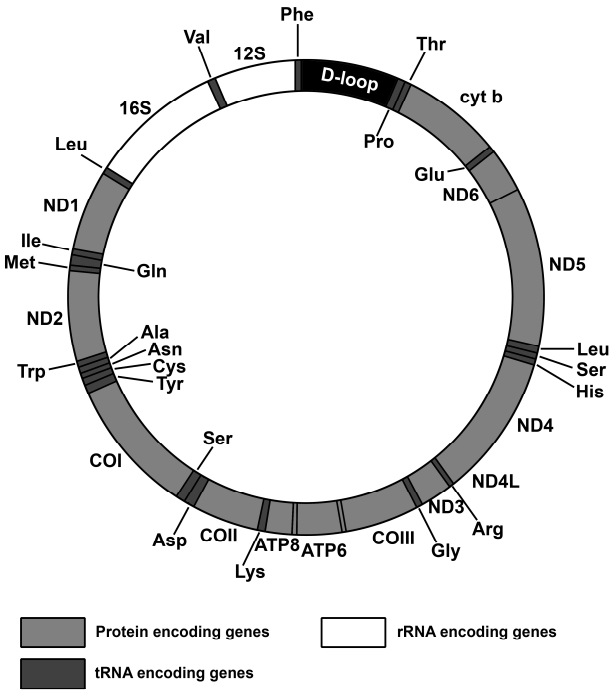

Figure 2: Schematic representation of the human mtDNA molecule
The image was downloaded and adapted from the MitoMap website: www.mitomap.org [22].

Diagnosis of OXPHOS disorders

A genetic diagnosis of OXHOS disorders can be difficult to achieve due to the genetic and clinical heterogeneity. Diagnosis of OXPHOS disease is mostly symptom based, supported by measurements of blood lactate and pyruvate levels, the activity of the separate OXPHOS complexes in muscle or cultured fibroblasts, and/or microscopy. A genetic diagnosis is required to confirm the clinical diagnosis, characterise the cause of the disease and predict the segregation pattern, and to provide more accurate information on prognosis and possible treatments. In a number of OXPHOS disorders, where symptoms are directly related to a particular mutation, a rapid genetic diagnosis is possible. However, often this can not be achieved due to the genetic

and clinical heterogeneity of OXPHOS disorders, and the genetic defect may reside in the mtDNA or in one of the many candidate genes in the nDNA, providing a major challenge for genetic testing.

As the number of patients with the same mutation or a mutation in the same gene is fairly small, diagnostic centres have access to only relatively small numbers of patients in each disease category, making it difficult for each centre to develop consensus guidelines for the investigation of OXPHOS disorders. There are only limited clinical or laboratory guidelines for the investigation of suspected mitochondrial disease. The current workflow for a genetic diagnosis usually starts with screening for several mtDNA mutations which are most common in OXPHOS disorders and screening for deletions and depletions of the mtDNA. If symptoms are likely to be linked to a specific gene or specific genes, a candidate gene approach can be chosen where genes which previously have been related to the clinical symptoms are screened for mutations. When a diagnosis OXPHOS disease is likely, it makes sense to screen the entire mtDNA for mutations. In paediatric cases of OXPHOS disease, about 25% is caused by an mtDNA defect [23]. When mtDNA screening still does not lead to a genetic diagnosis and the suspicion of an OXPHOS disorder still holds, a more detailed investigation will be necessary, which will be more time consuming, costly, and with an uncertain success rate. Of course this has to be evaluated case by case, and depends on the guidance towards candidate genes based on symptoms, laboratory investigations and family data. When the size of the family and the number of patients is sufficient, linkage analysis can be carried out in order to identify a chromosomal region and characterise the genetic defect in candidate genes. Genetic linkage analysis in a consanguineous family with an isolated cytochrome *c* oxidase (COX) deficiency indentified a locus containing the two candidate genes *SCO1* and *COX10*, which are both involved in COX assembly, and *COX10* appeared to contain a pathogenic mutation [24]. An alternative approach is a complementation study, where whole chromosomes or parts of chromosomes are transferred to cultured patient cells in order to try and compensate the OXPHOS defect. A prerequisite is that the OXPHOS defect can be measured in cell lines, which is not always the case. This approach will narrow down or will result in a list of candidate genes which subsequently can be screened for mutations. This strategy was used for the identification of chromosome 9 being the chromosome containing the genetic defect in Leigh syndrome with cytochrome *c* oxidase (COX) deficiency. Subsequently, linkage analysis was carried out to narrow down the region on chromosome 9 to a 7-cM interval on chromosome 9q34, significantly decreasing the number of candidate genes for mutation screening. Finally, the *SURF1* gene contained pathogenic mutations in these families with Leigh syndrome with COX deficiency [7].

The improvement and development of new and existing mutation detection technologies and their rapidly increasing capacity will provide an alternative for those cases in which clinical symptoms can not be directly linked to a specific gene, candidate gene list, or mtDNA mutation or when linkage analysis or complementation assays are not possible. As this is the majority of cases

and mutation screening technology is evolving extremely rapidly, this might be the better alternative. High throughput gene expression analysis would also be one of the additional methods which could be used to classify patients into groups, which could ease the identification of the underlying gene defect, or which could support positional cloning by narrowing down the list of candidate genes. The application of microarray based mutation detection and gene expression analysis for OXPHOS disorders will be the basis of this thesis.

Microarrays

Especially since the completion of the working draft of the human genome DNA sequence [25, 26], the use of microarray technology has been emerging fast as an extremely useful tool for gene expression studies, genotyping, and resequencing at "a whole genome" level and in a high throughput manner. For gene expression studies, the microarray technology makes use of complementary DNA (cDNA) or oligonucleotide probes which hybridise to the gene transcript, the messenger RNA (mRNA) (figure 3). Probes are printed or synthesised on a solid support, i.e. a microarray slide or gene chip, forming probe spots of which each represents a transcript of a gene. After extraction of RNA from two sample groups, the target (RNA) of each group is converted to cDNA and for a 2-colour microarray, labelled with different fluorescent dyes, Cy3 (green) for one group and Cy5 (red) for the other group. The labelled targets are then combined in equal amounts and hybridised to the microarray where each labelled target will bind to its complementary probe. After hybridisation, the microarray is stringently washed to remove a-specific bound targets and scanned in a microarray scanner. The scanner excites the fluochromes with a laser resulting in emission of light from the dyes with different wave lengths which can be detected and measured. For example, if a gene is over-expressed in the Cy3 labelled sample compared to the Cy5 labelled sample, more molecules of that sample will bind to the complementary probe compared to the other sample, resulting in a spot which will light up green; in case of under expression of the gene, it will light up red. When the expression for the gene is equal in both samples, the spot will light up yellow.

By measuring the intensities of the red and green signal for each probe spot, ratios in gene expression can be calculated between the two sample groups for each gene represented on the microarray. Besides the two-colour system described above, other microarray platforms use only one colour, and only one sample is hybridised to each microarray (figure 3). After a normalisation step between the different microarrays from one experiment, the absolute probe spot intensities and gene expression ratios can be calculated. Because tens to hundreds of thousands of probes can be spotted or synthesised on one microarray slide or chip, it is possible to create microarrays containing the whole human transcriptome, enabling the measurement of the expression level of all human genes in one experiment simultaneously. This allows for characterisation of gene expression signatures that can classify specific disease conditions or for identification and understanding of molecular biological pathways or single genes involved in disease or pathology.

One of the earlier reports on cancer classifications used DNA microarrays to distinguish between acute myeloid leukaemia and acute lymphoblastic leukaemia by a gene expression class predictor [27]. In an other study, a 'poor prognosis' gene expression signature was identified to predict the risk of breast cancer metastasis [28]. Mootha *et al.* used the microarray gene expression technology in combination with a specific analysis technique focussing on groups of functionally related genes and identified a number of genes involved in oxidative phosphorylation which were under-expressed in human diabetic muscle [29]. This latter study illustrated the additive value of focussing on gene groups or pathways besides focussing on significant differentially expressed genes only.

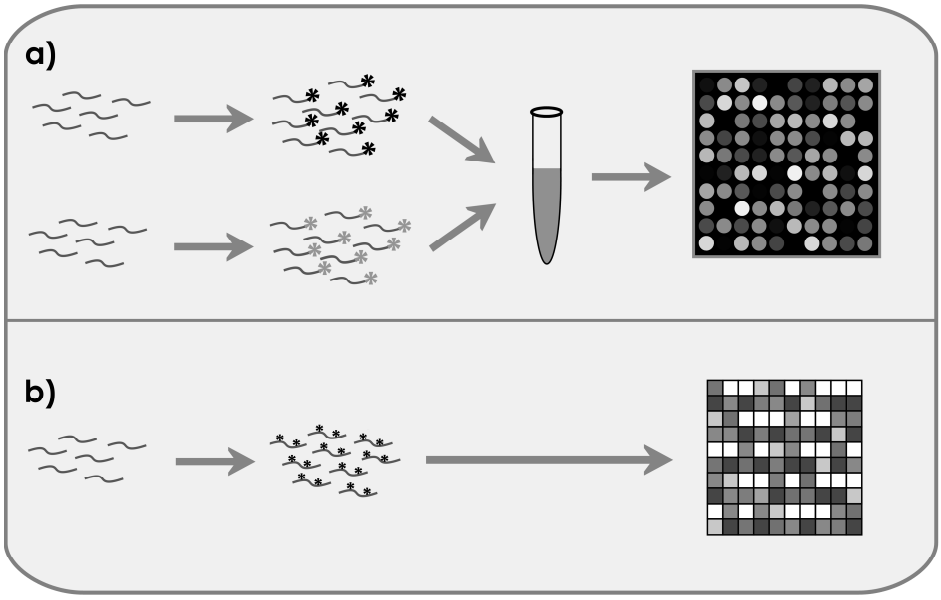

Figure 3: Microarray gene expression technique
(a) 2 colour microarray experiment: RNA from two samples is converted to cDNA and labelled with different fluorescent dyes (Cy3/green or Cy5/red). Labelled targets are subsequently co-hybridised to the microarray slide. Absolute and relative intensities are retrieved for each colour by scanning the slide in a microarray scanner. When a red spot indicates up-regulation, green will indicate down-regulation and yellow indicates no change; (b) Single colour microarray experiment: only one RNA sample is amplified, labelled and hybridised to the microarray slide. Absolute intensities are retrieved by scanning the slide in a microarray scanner. Relative intensities have to be computed by comparing intensities with other slides.
The image was taken from Eijssen [30].

As illustrated by the examples above, microarrays have already proven their value in understanding pathological processes in complex diseases like cancer and diabetes. Therefore, we explored the potential of this technology for the study of OXPHOS disorders. As a class prediction tool it could help in facilitating diagnosis by classifying patients, reducing the number of candidate genes, and specifying the candidate genes for mutation screening. One of the possibilities would be to identify a gene expression classification signature which could distinguish between OXPHOS disorders due to mtDNA or nDNA mutations. Additionally, more specific classification categories could be set, e.g. to identify whether mutations reside in genes

coding for structural components of the OXPHOS system, or in genes which are involved in mitochondrial biogenesis. Ideally, a gene expression classification would have to be identified which would be able to identify the type of OXPHOS disorder in combination with a specific genetic defect, e.g. MELAS with the m.3243A>G or Leigh syndrome with a *SURF1* mutation. The key aspect in the identification of gene expression classification signatures resides in the use of a "training" gene expression dataset coming from a first patient group to carry out supervised classification. A "test" gene expression dataset coming from a second patient group has to be generated, which is to be used to validate the established classifier. This is extremely difficult to achieve for OXPHOS disorders because of the enormous clinical and genetic heterogeneity of the patient groups. It is only possible for few conditions or genes to find homogeneous patient groups big enough to build a training and a test dataset consisting of enough samples for classification purposes. Microarray gene expression analysis is however very useful to identify molecular biological processes or gene groups involved in the onset and progression of OXPHOS disorders. As there are no established therapies for OXPHOS disorders at the moment, this will provide valuable information for understanding OXPHOS pathology and subsequently for the development of possible treatments.

Aims and contents of this thesis

OXPHOS is under dual genetic control of the nDNA and the mtDNA. OXPHOS disorders are clinically and genetically heterogeneous, which makes it difficult to determine the genetic defect and explain the pathology, and symptom-based protocols which link clinical symptoms directly to a specific gene or mtDNA mutation are often falling short. Therefore, we addressed the use of microarray gene expression profiling as a tool for classifying patients or genetic defects. As it turned out that classification was difficult, due to the genetic heterogeneity of the diseases involved, we added a chip-based approach for high-throughput screening of the mtDNA. Gene expression profiling was additionally performed to get further insight in the pathogenic molecular mechanisms involved in patients.

The aims of this thesis are:

- To develop new approaches which facilitate genetic diagnosis of OXPHOS disorders.
- To understand primary and secondary pathological molecular processes that are involved in OXPHOS disorders.
- To characterise novel therapeutic entries for the treatment of OXPHOS disorders.

Chapter two describes the use of a microarray based method to resequence the entire mtDNA in order to improve and speed up genetic diagnosis of OXPHOS disorders. A quarter of the mainly paediatric OXPHOS patients could be genetically diagnosed using this technique. The usefulness of this technique as a diagnostic tool will be discussed and a comparison will be made with other new rapidly developing mutation detection techniques. Chapters three, four and five present

microarray gene expression studies in skeletal muscle and cultured primary skin fibroblasts from OXPHOS patients in an effort to elucidate primary and secondary molecular biological pathways involved in the onset and persistence of these disorders. These pathways were evaluated to provide possible new therapeutic entries for OXPHOS disorders. A number of novel, but also known molecular processes involved in OXPHOS disorders were identified. The experimental models, the processes identified and their contribution to the identification of new therapeutic entries for the treatment of OXPHOS disorders are discussed in chapter six.

CHAPTER 2

Chip-based mtDNA mutation screening enables fast and reliable genetic diagnosis of OXPHOS patients

R.G.E. van Eijsden [1,2,^], M. Gerards [2,3,^], L.M.T. Eijssen [3,4], A.T.M. Hendrickx [1], R.J.E. Jongbloed [1,2,4], J.H.J. Wokke [5], R.Q. Hintzen [6], M.E. Rubio-Gozalbo [7], I.F.M. de Coo [6], E. Briem [8], V. Tiranti [8], H.J.M. Smeets [1,2,3]

[1]Department of Clinical Genetics, Maastricht University, The Netherlands.
[2]Research Institute Growth and Development (GROW), Maastricht University, The Netherlands.
[3]Department of Population Genetics, Genomics and Bioinformatics, Maastricht University, The Netherlands.
[4]Cardiovascular Research Institute Maastricht (CARIM), Maastricht University, The Netherlands.
[5]Department of Neurology, Rudolf Magnus Institute of Neuroscience, University Medical Centre Utrecht, Utrecht, The Netherlands.
[6]Department of Neurology, Erasmus MC, Rotterdam, The Netherlands.
[7]Department of Paediatrics and Laboratory Genetic Metabolic Diseases, Maastricht University Hospital, Maastricht, The Netherlands.
[8]Pierfranco and Luisa Mariani Centre for the Study of Children's Mitochondrial Disorders – National Neurological Institute "C. Besta," Unit of Molecular Neurogenetics, Milan, Italy.

[^]These authors contributed equally to this work.

Genetics In Medicine 2006; 8 (10): 620-627

Abstract

Purpose: Oxidative phosphorylation (OXPHOS) is under dual genetic control of the nuclear and the mitochondrial DNA (mtDNA). OXPHOS disorders are clinically and genetically heterogeneous, which makes it difficult to determine the genetic defect, and symptom-based protocols which link clinical symptoms directly to a specific gene or mtDNA mutation are falling short. Moreover, approximately 25% of the paediatric patients with oxidative phosphorylation disorders is estimated to have mutations in the mtDNA and a standard screening approach for common mutations and deletions will only explain part of these cases. Therefore, we tested a new chip-based screening method for the mtDNA. **Methods:** MitoChip (Affymetrix) resequencing was performed on three test samples and on 28 patient samples. **Results:** Call rates were 94% on average and heteroplasmy detection levels varied from 5 to 50%. A genetic diagnosis can be made in almost a quarter of the patients at a potential throughput of 8 complete mtDNA sequences per 4 days. Moreover, a number of potentially pathogenic unclassified variants (UVs) were detected. **Conclusions:** The availability of long-range PCR protocols and the predominance of single nucleotide substitutions in the mtDNA make the resequencing chip a very fast and reliable method to screen the complete mtDNA for mutations.

Introduction

Oxidative phosphorylation (OXPHOS) disorders affect at least 1 in 8000 of the general population and belong to the group of most common inherited metabolic diseases [31]. Disease manifestations due to OXPHOS defects can be highly variable, but usually involve tissues with a high energy demand like heart, muscle, renal and the endocrine systems [32]. Several well-described syndromes are known, like Kearns-Sayre syndrome (KSS) and Pearson syndrome, Neuropathy Ataxia Retinitis Pigmentosa (NARP), Mitochondrial Encephalomyopathy, Lactic Acidosis and Stroke-like episodes (MELAS) and Myoclonus Epilepsy and Ragged Red Fibres (MERRF). However, OXPHOS defects can also manifest with more common and less specific symptoms, like type 2 diabetes, deafness, encephalopathy, myopathy, and cardiomyopathy. OXPHOS disorders therefore cause significant morbidity and mortality and have a broad impact on public health.

Approximately 25% of the paediatric patients with OXPHOS disorders have mutations in the mtDNA, but these are difficult to find due to the genetic and clinical heterogeneity [23]. As the number of mtDNA mutations has increased to over 250 and the clinical specificity lags behind, symptom-based protocols fall short and screening of the entire mtDNA is preferable [22]. The recently introduced MitoChip (Affymetrix) is a new method for mtDNA resequencing [33, 34]. In this paper we describe our experience of the complete mtDNA screening of 28 patients with OXPHOS disease by MitoChip resequencing.

Materials & methods

Patient and test samples

Genomic DNA was isolated from muscle according to the protocol of Mullenbach *et al.* [35]. DNA from 3 conventionally sequenced patients, a patient with a heteroplasmic 5 bp deletion [36] and 28 patients with a clinical and/or biochemical phenotype of OXPHOS disease were analysed on the MitoChip. These patients were all negative for the MELAS m.3243A>G, MERRF m.8344A>G, and NARP m.8993T>C/G mutations, and for large deletions of the mtDNA.

MitoChip and experimental procedure

The MitoChip contains both sense and anti-sense probes specific for the forward and reverse sequence of two fragments of the mtDNA. One fragment interrogates 15,446 bases of the mtDNA minus the D-loop sequence. The other fragment is a duplicate of the first fragment, comprising 12,938 bases of the mtDNA coding sequence minus the sequence of the 12S and 16S mitochondrial ribosomal RNA genes. The two fragments are separated on the chip by a control fragment (Affymetrix). Oligonucleotide probes are synthesised *in situ* on the chip by Affymetrix by standard photolithography and solid-phase DNA synthesis [37, 38]. For each position of the mtDNA fragments, four 25-mer probes are represented on the chip, each with a different nucleotide in the middle (A, G, C, or T) allowing for the detection of all possible nucleotide substitutions. The probe with the correct corresponding nucleotide in the middle for each mtDNA position will give the highest signal intensity after hybridisation and scanning. The entire mtDNA was amplified using the Expand Long Template system (Roche) in 2 fragments (A and B) of 8466 bp and 7866 bp in length, with an overlap of 235 bp. The primers for fragment A were forward primer [5'-ccgcttctggccacagcacttaaacacatc-3'] and reverse primer [5'-aggaggttagttgtggcaat-3'], and for fragment B forward primer [5'-gcttcattcattgcccccac-3'] and reverse primer [5'-ggaggatggtggtcaagggacccctatctg-3']. The 7.5kb control sequence was amplified using the primers and template from the Customseq™ control kit (Affymetrix). PCR products were purified using the QIAQuick PCR cleanup kit (QIAGEN). Equimolar amounts of the amplified fragments A and B were pooled and fragmented together with the amplified 7.5kb control sequence, labelled and hybridised on a pre-hybridised MitoChip as described in the Affymetrix CustomSeq Resequencing protocol. Chips were washed and stained on the GeneChip fluidics station 400 (Affymetrix) using the pre-programmed CustumSeq Resequencing wash and stain protocol (DNA ARRAY-WS2). The MitoChips were scanned using the Affymetrix GeneChip scanner 3000 creating .CEL files for subsequent analysis.

Data analysis

Affymetrix GeneChip DNA Analysis Software (GDAS) version 3.0.1.3 beta was used to analyse the .CEL files, using the default program settings. A report file was created by GDAS listing the nucleotide variations for both chip fragments compared to the Revised Cambridge Reference

Sequence (RCRS) [22, 39]. Discrepancies between nucleotide calls for both chip fragments were evaluated manually. The final base changes were written to a text file ('affy output file'). A second analysis was performed using R, a free software environment for statistical computing and graphics [40]. In the R analysis, each chip (.CEL file) was analysed separately. For each position the nucleotide with the highest signal intensity was determined, not taking into account the background signal. Nucleotide changes were printed to a text file ('R output file'). Finally the 'affy output file' and the 'R output file' were compared and combined, resulting in a list of variations for each sample. Discrepancies between the GDAS and R output were evaluated manually by directly looking at the chip image or by conventional sequencing. Unless otherwise mentioned, throughout this paper the phrase 'MitoChip analysis' refers to the combined GDAS and R analysis.

Validation of variations and heteroplasmy levels

Both strands of a fragment carrying a variant were cycle sequenced using the BigDye Terminator v3.1 Cycle sequencing kit, an ABI- PRISM 3100 genetic analyser and the Sequence Analysis 3.7 software package. The level of heteroplasmy was determined by mutation specific restriction digestion. In case a restriction site was gained or lost, fragments were amplified using primers surrounding the underlying variation, otherwise a specific mismatch primer was designed in order to create a restriction site. On PCR amplification, a labelled primer was added to the reaction in the last PCR cycle to label the PCR products. Labelled PCR products were digested and the fragments were analysed on an ABI-PRISM 3100 genetic analyser using the GeneScan Analysis 3.7 software package (Applied Biosystems). The level of heteroplasmy was determined by calculating the ratio of the mutant or wild type peak area (depending on the gain or loss of a restriction site by the nucleotide variation) and the sum of the mutant and wild type peak areas. Primer sequences and reaction conditions are available on request.

Results

MitoChip performance and validation

Based on a total of 32 DNA samples, the average GDAS call rate was 94.0%, ranging from 88.9% to 96.8%. Of the GDAS 'no call' signals, 0.72% (212/29366) of the chip positions gave a 'no call' for each of the 32 chips analysed, corresponding to 134 mtDNA nucleotide positions. A GDAS call was always given for each of the 32 chips for 12200 mtDNA nucleotide position (20486 out of 29366 (70%) chip positions). For 7 chips GDAS and R analysis were compared for the entire sequence and R analysis accounted for an average of 24.2% (ranging from 13% to 37%) of the total amount of base changes in the output files. Five unclassified variants (UVs) were identified by the R analysis, which were not detected by the standard GDAS analysis. For the three test samples, which were also sequenced conventionally, 34 out of 35 (97%) variations were called correctly on the MitoChip. In two test samples, one and six variations were additionally detected by the MitoChip. By reinterpretation of the conventional sequencing results, one of the variations which were detected additionally by the MitoChip proved to be a low percentage heteroplasmic substitution

(false negative), and the other additional variants appeared to be falsely detected as a nucleotide variant by the MitoChip (false positives). A known 5 bp deletion was also tested, but not detected. Two DNA samples differing at 16 positions in their mtDNA sequence were mixed at ratios of 1:1, 1:9 and 1:19. In the mix sample analyses (only GDAS), the Total Quality Threshold Score setting was set at 30 and 75. Fifteen of sixteen positions were called correctly at a heteroplasmy level of 50% for both TQT settings. Only one position was called correctly as heteroplasmic in all three mix samples at both TQT settings. At a TQT value of 30, 'no call' signals were 3 times more often observed at the 16 investigated heteroplasmy positions than at a TQT value of 75.

mtDNA variations in 28 patients

A total of 520 variations were detected in 28 patients, comprising 197 unique nucleotide substitutions. Fifteen heteroplasmic variations were detected in a total of 11 patients. Four of these variations were confirmed by sequencing and mutation specific restriction digestion (m.15939C>T at 7%, m.13513G>A at 14%, m.3243A>T at 34%, and m.13042G>A at 84%); two proved to be homoplasmic single base pair insertions (m.3229_3230insA and m.3158_3159insT); two appeared to be false positive; one was shown to be a homoplasmic polymorphism (m.15452C>A); the remaining six were not tested because they were considered not to be pathogenic. Of all detected variations, three were known pathogenic mutations (table 1), 114 have been reported before as polymorphisms (supplementary table S1), 41 did not result in an amino acid change and were most likely polymorphisms (supplementary table S1), and 39 were unclassified variants (UVs), some of which were likely pathogenic (table 2). Eight variants were located in tRNA molecules (figure 1). In three patients known pathogenic mutations were detected and in 23 patients UVs were detected. In five patients only polymorphisms were detected.

UVs were evaluated for evolutionary conservation, for functional significance by determining the effect on the tRNA or on the protein, and - when available - for segregation in the family. Seven UVs were located in six tRNA genes (figure 1), 11 UVs in the 12S and 16S rRNA genes, one UV in the mtDNA transcription terminator site, and 20 UVs in the protein encoding genes. Of the eight tRNA variations (figure 1), the m.15939C>T variation in the tRNA-Thr gene was heteroplasmic with a mutation load of 7%. The other tRNA variations were all homoplasmic or close to homoplasmy (>98% mutation load). Two of the variations in the protein encoding genes were heteroplasmic 84% and 70%, respectively, for the m.13042G>A in the ND5 gene and m.14258G>A in the ND6 gene.

Single nucleotide insertions were detected as well. A heteroplasmic m.3158A>T transition on the chip proved to be a single nucleotide insertion (m.3158_3159insT) by standard sequencing. Additionally, the homoplasmic m.3229_3230insA insertion was initially detected by the MitoChip analysis as a heteroplasmic m.3229T>A transition.

Table 1: Evident pathogenic mutations

Position	nt change	aa change	Mutation load *	Locus	Disease **	No. of samples	aa / n Conservation ***	No. patients previously described	Reference(s)
3243	A>T	-	34%	tRNA-Leu1	MM	1	30/31 species	1	Shaag et al. (1997) [41]
3697	G>A	G-S	>97%	ND1	MELAS	1	Hs/Pt/Cf/Mm/Rn/ Gg/Dm/Ag/Ce/At/Os	1	Kirby et al. (2004) [42]
13513	G>A	D-N	13 - 15%	ND5	MELAS / Leigh Disease	1	Hs/Pt/Cf/Mm/Rn/ Gg/Dm/Ag/Ce/At/Os	1	Santorelli et al. (1997) [43]
								4	Pulkes et al. (1999) [44]
								1	Penisson-Besnier et al. (2000) [45]
								3	Chol et al. (2003) [46]
								3	Kirby et al. (2003) [47]
								6	Sudo et al. (2004) [48]

* Mutation loads are determined by mutation specific restriction digestion analysis followed by GeneScan analysis.

** MM: Mitochondrial Myopathy; MELAS = Mitochondrial Encephalomyopathy, Lactic Acidosis, and Stroke-like episodes.

*** For the tRNA variations, the nucleotide conservation is shown. For the variations in protein encoding genes, the amino acid conservation is displayed. Hs: Homo sapiens, Pt: Pan troglodytes, Cf: Canis familiaris, Mm: Mus musculus, Rn: Rattus norvegicus, Gg: Gallus gallus, Dm: Drosophila melanogaster, Ag: Anopheles gambiae, Ce: Caenorhabditis elegans, At: Arabidopsis thaliana, Os: Oryza sativa.

tRNA conservations were taken from the website dealing with the compilation of mammalian tRNA genes (http://mamit-trna.u-strasbg.fr/index.html) [49].

Discussion

MitoChip performance and validation

MitoChip resequencing is a very rapid method to screen the mtDNA for mutations. Eight samples can be analysed by one technician over a period of 4 days. The average call rate of 94.0% is within the range described by Affymetrix and others [33]. The additional R analysis led to an increase in total base calls and to the identification of 5 UVs (in 4 out of 7 samples), which would have been missed by GDAS analysis only. Of the 212 chip positions (0.72%) (134 mtDNA nucleotide positions) which consistently gave a 'no call', 197 (124 mtDNA nucleotide positions) were cytosine nucleotides. Previously, it was reported that 1.7% of the bases always gave a 'no call' in a dataset of 26 chips [33]. About 51% of these were from regions containing two or more successive C bases. R-analysis showed that in these regions especially the forward strand differed from the reference sequence, whereas the reverse sequence gave a call equal to the reference sequence. The reason for this is yet unknown. The mtDNA nucleotide positions of twelve common mtDNA mutations (m.1555A>G, m.3243A>G, m.3460G>A, m.8344A>G, m.8993T>G/C. m.9176T>C, m.10159T>C, m.11778G>A, m.13513G>A, m.14459G>A, m.14484T>C, and m.14487T>C), were not among the

nucleotide positions always giving a 'no-call'. Within-chip and between-chip reproducibility have already been determined showing a within-chip error rate of 0.0025% and a between-chip error rate of 0.0027%, illustrating that the base calls were reproducible for >99.99% [33]. In our experiments 97% of the variations was called correctly in three previously sequenced samples, which is comparable with the 95% reported before in 18 samples [33]. In the three test samples, only six variations appeared be false positive after follow-up investigation. It is unlikely that PCR errors are causative for false positive MitoChip calls since there is a large number of templates for the PCR, and the heteroplasmy levels due to sporadic PCR errors will be below the detection limit. As GeneChip Resequencing Arrays only support detection of homozygous and heterozygous single nucleotide substitutions, small deletions (5 bp) could not be detected, although 2 single nucleotide insertions were detected as heteroplasmic "substitutions". One might expect that the heteroplasmic 5 bp deletion would be detected by the MitoChip as a loss of signal, but available software is insufficient for these quantitative analyses, especially if over 50% of the wild type mtDNA is still present [36].

Although the GDAS software was designed to detect homozygous (homoplasmic) and heterozygous (50% heteroplasmy) single base pair substitutions only, it was previously shown that heteroplasmic variations at levels as low as 2% were detectable [33]. However, in our dilution experiments only one out of 16 positions could be identified correctly as a heteroplasmic variation in the 5%, 10%, and 50% mix samples. Notably, the number of 'no calls' at these 16 heteroplasmic positions was three times higher at the TQT setting of 30 compared to the GDAS default TQT setting of 75, illustrating a difficulty for the algorithm to assign a call for the particular position, probably because of the signal of the heteroplasmic variant. This suggests that further development of the data analysis algorithm and tuning of the data analysis settings can improve the detection level of heteroplasmic mutations. An option would be to customise our R-analysis to make it sensitive for heteroplasmic variations. Nevertheless, we were able to detect a heteroplasmic variation in the tRNA-Thr gene (m.15939C>T) in a patient with a mutation load as low as 7%. Additionally, a pathogenic mutation in the *ND5* gene (m.13513G>A) was identified and validated at a heteroplasmic level of 13%–15%. Apparently, the sensitivity for heteroplasmy detection is different per position and probably depends on the sequence surrounding the variation.

Table 2: Unclassified Variants

non-protein-coding region, unclassified variants

Position	nt change	aa change	Mutation load *	Locus	No. of samples	nt Conservation **
892	A>T	-	h	12S rRNA	3	-
1860	A>G	-	100% $	16S rRNA	1	-
2098	G>A	-	100% $	16S rRNA	1	-
2259	C>T	-	100% $	16S rRNA	1	-
2361	G>A	-	100% $	16S rRNA	1	-
2581	A>G	-	100% $	16S rRNA	1	-
2757	A>G	-	100% $	16S rRNA	1	-
2768	A>G	-	100% $	16S rRNA	2	-
2825	G>C	-	h	16S rRNA	4	-
3105	A>G	-	100% $	16S rRNA	1	-
3159	insT	-	100% $	16S rRNA	1	-
3229	insA	-	h	Transcription terminator	1	-
4336	T>C	-	>98%	tRNA-Gln	2	13/31 species
5558	A>G	-	100%	tRNA-Trp	1	31/31 species
5592	A>G	-	100%	tRNA-Ala	1	28/31 species
5850	T>C	-	>98%	tRNA-Tyr	1	30/31 species
12308	A>G	-	100% $	tRNA-Leu2	5	31/31 species
15890	C>T	-	100%	tRNA-Thr	1	31/31 species
15939	C>T	-	7%	tRNA-Thr	1	13/31 species

protein coding region, unclassified variants

Position	nt change	aa change	Mutation load *	Locus	No. of samples	aa Conservation **	Pathogenicity score ^
3308	T>C	M>T	100% $	ND1	2	Hs/Cf/Mm/Rn/Ag	0 (28)
4501	C>T	S>F	100% $	ND2	1	Hs/Cf	0 (20)
4561	T>C	V>A	100% $	ND2	1	Hs/Pt/Mm/Rn/At/Os	0 (20)
5319	A>G	T>A	100% $	ND2	1	Hs	0 (20)
6408	A>G	I>V	100% $	CO1	1	Hs/Pt/Cf/Mm/Rn/Gg/Dm/Ag/Sp	6 (20)
7146	A>G	T>A	100% $	CO1	2	Hs/Cf	0 (28)
7389	T>C	Y>H	100% $	CO1	2	Hs/Pt	0 (28)
8516	T>C	W>R	100% $	ATP8	1	Hs/Pt/Mm/Rn	7 (23)
8975	T>C	L>P	100% $	ATP6	1	Hs/Pt/Gg	4 (20)
10680	G>A	A>T	100% $	ND4L	1	Hs/Pt/Cf/Mm/Rn	15 (28)
11447	G>A	V>M	100% $	ND4	1	Hs/Pt/Cf	2 (20)
13042	G>A	A>T	84%	ND5	1	Hs/Pt/Cf/Mm/Rn/Gg/Dm/Ag/Ce/At/Os	18 (31)
13630	A>G	T>A	100% $	ND5	1	Hs/Pt/Gg/Dm/Ag	8 (28)
13880	C>A	S>Y	100% $	ND5	2	Hs/Pt/At	0 (28)

14207	G>A	T>I	100% $	ND6	1	Hs/Pt/Cf	8 (28)
14258	G>A	P>L	70% $$	ND6	1	Hs/Pt	5 (20)
14766	C>T	T>I	100% $	CYB	13	Hs/Pt	8 (28)
15311	A>G	I>V	100% $	CYB	1	Hs/Pt/Cf/Mm/Rn/Gg/Ag/Ce/Sp/Sc/Kl/Eg	1 (23)
15725	C>T	L>F	100% $	CYB	1	Hs/Pt/Cf/Gg/Kl/Eg/At	2 (20)
15824	A>G	T>A	100% $	CYB	1	Hs/Pt/Cf/Gg	0 (20)

***** Mutation loads are determined by mutation specific restriction digestion analysis followed by GeneScan analysis.

$ Mutations load estimated by MitoChip and/or sequencing results only.

$$ Also confirmed with denaturing high-performance liquid chromatography (dHPLC) analysis.

****** Ag: Anopheles gambiae, At: Arabidopsis thaliana, Ce: Caenorhabditis elegans, Cf: Canis familiaris, Dm: Drosophila melanogaster, Eg: Eremothecium gossypii, Gg: Gallus gallus, Hs: Homo sapiens, Kl: Kluyveromyces lactis, Mm: Mus musculus, Os: Oryza sativa, Pt: Pan troglodytes, Rn: Rattus norvegicus, Sc: Saccharomyces cerevisiae, Sp: Schizosaccharomyces pombe.

^ The pathogenicity score is calculated according to the criteria set by Mitchell et al. [50]. Since information was not available on all criteria, the maximal score using only the available information is indicated between brackets.

h Detected as heteroplasmic by MitoChip analysis.

tRNA conservations were taken from the website dealing with the compilation of mammalian tRNA genes (http://mamit-trna.u-strasbg.fr/index.html) [49].

MitoChip compared to other methods

Resequencing chips are powerful if long-range PCR protocols are available and substitutions are the predominant pathogenic mutations, which is the case for the mtDNA. Other methods for mtDNA mutation analysis are conventional sequence analysis, single strand conformation polymorphism (SSCP) analysis, denaturing gradient gel electrophoresis (DGGE), temperature gradient gel electrophoresis (TGGE), denaturant capillary electrophoresis (DCE) and denaturing high-performance liquid chromatography (dHPLC) [51-55]. These techniques all have their advantages and disadvantages with respect to costs, time consumption, high throughput possibilities, heteroplasmic detection limit, and type of mutations that can be detected (table 3). At this moment, heteroduplex based methods (dHPLC, DGGE, TGGE, and DCE) appear to be more sensitive than the MitoChip for heteroplasmy detection, with detection sensitivities as low as 0.5% [52-54, 56]. SSCP and conventional sequence analysis are not able to detect low percentages of heteroplasmy. MitoChip resequencing is able to detect heteroplasmic variants at low levels, although the data analysis needs to be optimised to reach similar detection levels. Although the costs per nucleotide are cheaper for conventional sequencing [33], considering the overall costs per sample, MitoChip resequencing is preferable over conventional sequencing, mostly due to a tremendous gain in labour costs (8 samples can be analysed by one technician over a period of 4 days) and automated analysis at comparable bench costs.

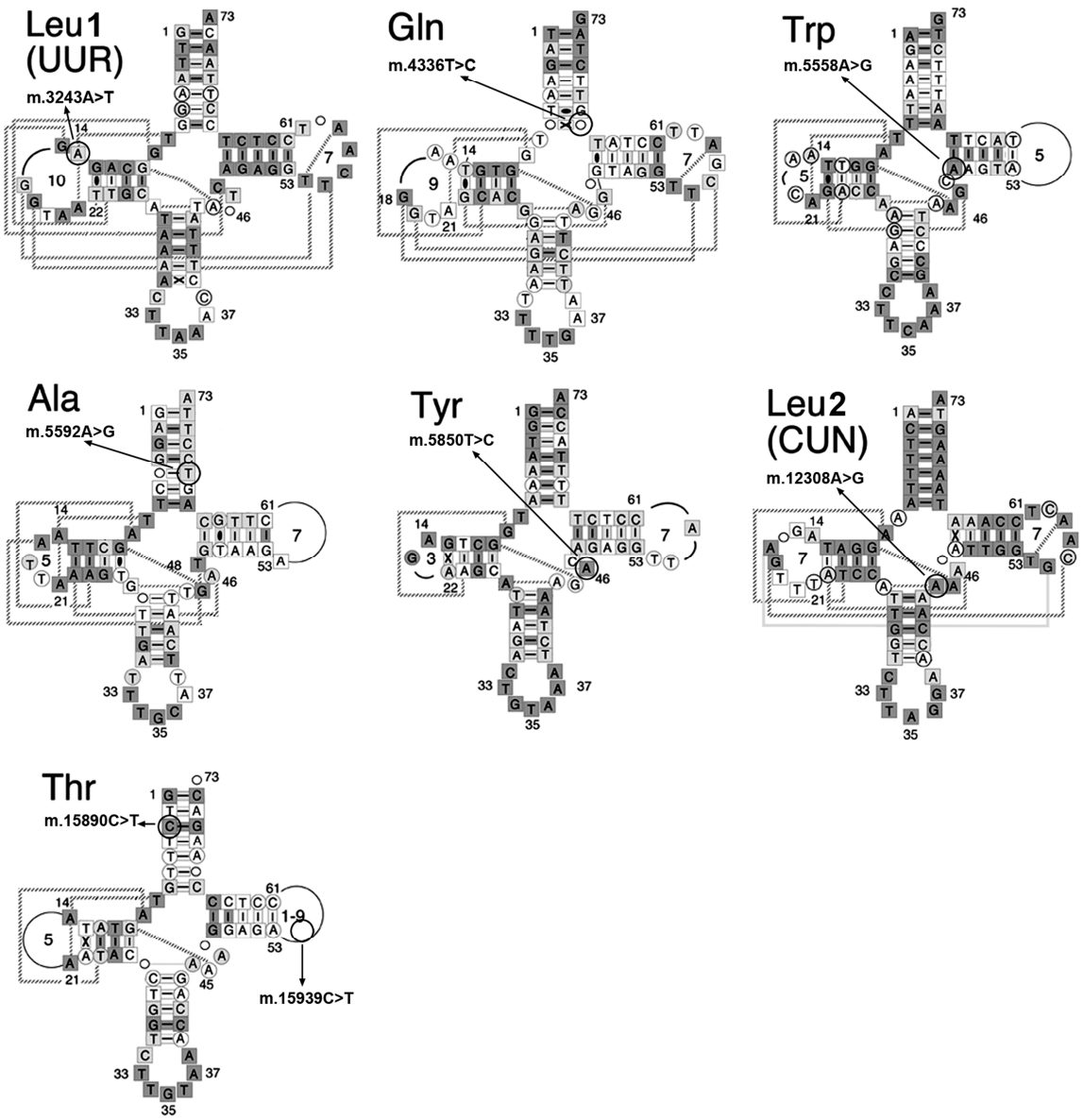

Figure 1: Eight tRNA variations (unclassified variants and mutations) detected in 28 patients with OXPHOS disease

Detected were an m.3243A>T variation in the tRNA-Leu1, an m.4336T>C variation in the tRNA-Gln gene, an m.5558A>G variation in the tRNA-Trp gene, an m.5592A>G variation in tRNA-Ala gene, an m.5850T>C variation in the tRNA-Tyr gene, an m.12308A>G variation in the tRNA-Leu2 gene, and an m.15890C>T variation and m.15939C>T variation in the tRNA-Thr gene.

The images are adapted from the website dealing with the compilation of mammalian tRNA genes (http://mamit-trna.u-strasbg.fr/index.html) [49].

Table 3: Comparison of mtDNA mutation screening methods

	SSCP	DGGE	TGGE	DCE	dHPLC	Sequencing	MitoChip
Equipment costs	low	low	low	high	high	high	high
Labour intensive	yes	yes	yes	no	no	yes	no
High throughput	-	-	-	+	+	+	++
Heteroplasmy detection	-	++	++	++	++	+	+(+)
Homoplasmy detection	+	-	-	-	-	+	+

SSCP: single strand conformation polymorphism, DGGE: denaturing gradient gel electrophoresis, TGGE: temperature gradient gel electrophoresis, DCE: denaturant capillary electrophoresis, dHPLC: denaturing high-performance liquid chromatography.

MtDNA variations in 28 clinical samples

The pathogenic m.3243A>T mutation was found in a patient with proximal myopathy, ptosis and ophthalmoplegia at a mutation level of 34%. Magnetic resonance imaging (MRI) of the brain showed white matter abnormalities and muscle creatine phosphokinase levels were elevated. Muscle biopsy histomorphology revealed ragged red fibres (RRF) and cytochrome c oxidase (COX) negative fibres. This mutation has been previously described in muscle (81.4%), skin (69.3%) and blood (13.8%) of a 9-year old girl with muscle weakness, encephalopathy and a reduction of the activity of OXPHOS complexes I, III and IV [41]. The mutation is located at the same position as the classical MELAS m.A3243A>G mutation at the first position of the D-loop in the tRNA tRNA-Leu1 molecule (figure 1), leading to a dramatic loss of aminocylation efficiency. Moreover, residue A14 of this tRNA is strongly conserved within all classical tRNA molecules and it is involved in establishing tertiary interactions with other residues of the tRNA [57]. The pathogenic m.3697G>A mutation in the ND1 gene was detected at a mutation load higher than 97% in a patient with spastic dystonia, elevated levels of lactate and pyruvate in blood serum and cerebrospinal fluid. The affected amino acid is evolutionary highly conserved (table 1) and the mutation has been described before in a MELAS patient with 80% of the m.3697G>A mutation in muscle and 79% in skin fibroblasts [42]. Pathogenicity of the mutation was confirmed by fusion experiments with ρ^0 cell lines (no restoration of complex I activity) combined with blue native polyacrylamide gel electrophoresis (BN-PAGE) (low levels of fully assembled complex I) [42]. The m.3697G>A mutations was also evaluated according to the scoring system to assess pathogenicity of complex I mutations [50]. This score can range from 0 (not pathogenic) to 40 (pathogenic) and is based on several criteria: biochemical defect, functional studies, reports by two or more independent laboratories, heteroplasmy, segregation in the family, and evolutionary conservation. The m.3697G>A mutation reached a score of 32. Our report of this mutation as a second independent laboratory will increase the score to 37 points, which is above the "pathogenic" cut-off of 30. The m.13513A>G mutation was detected in a patient with encephalopathy, strokes, dystonia, signs of Parkinsonism, mental retardation and signs of early fatigue. Biochemical analysis indicated a deficiency of the pyruvate dehydrogenase complex (PDHC) in muscle. The m.13513A>G transition in the ND5 gene changes an amino acid strongly conserved over 11 species (table 1) and has been related to MELAS and Leigh syndrome in several reports [43-48]. The pathogenicity score for this mutation is 39 [50]. The functional importance of this amino acid is further supported by the

finding of a pathogenic mutation m.13514A>G, affecting the same codon, that results in a different amino acid replacement (D393G versus D393N) in two MELAS patients [58].

UVs were evaluated with respect to heteroplasmy, evolutionary conservation, functional influence of the effect on tRNA or protein, and segregation in the family [50, 59, 60]. Several UVs were likely to be pathogenic, but the effect of others is still unclear. The m.5850T>C variation had a mutation load of >98% in muscle and 13% in urine, but it could not be detected in blood or hair of the patient. It was not present in blood, hair, or urine from the patient's clinically unaffected mother, brother, and sister. The position of this variation in the tRNA-Tyr gene is evolutionary highly conserved. These data strongly suggest a pathogenic role. A second variation with a high probability of pathogenicity was the homoplasmic m.3229-3230insA. This variation is located in the transcription terminator site and may disturb the function of this site. Moreover, the location of this variation being exactly between the 16S rRNA gene and the tRNA-Leu1 gene might result in a faulty cleavage of the RNA after transcription. A faulty cleavage could have consequences for the function of the tRNA-Leu1 and 16S rRNA genes. The m.13042G>A variation in the ND5 gene was heteroplasmic (84%) and the involved amino acid was also strongly conserved (table 2), which favours a pathogenic role. The m.14258G>A variation in the ND6 gene was also a heteroplasmic (70%) variation in a protein coding gene. Although this variation is heteroplasmic, the affected amino acid is not well conserved. The m.15939C>T variation in the tRNA-Thr gene was also heteroplasmic (7%) in the patient's muscle. The variation is located in the T-loop of the tRNA molecule and not involved in establishing tertiary interactions in the tRNA molecule, making a pathogenic role less likely. The other homoplasmic variations (table 2) have to be further evaluated, as it is difficult to determine pathogenicity solely based on criteria like heteroplasmy and conservation alone. Functional and family studies will be performed to provide the definite evidence.

Resequencing does not only detect known pathogenic mutations or polymorphisms, but also UVs and risk factors for unrelated pathology, like cancer, Alzheimer's disease or Parkinson's disease. As the significance of this latter group of variations for individual cases and their families is yet unclear and the risk factors can not explain the primary pathology, it is evident that these data have to be carefully dealt with by the clinicians. Patients should be counselled about the uncertainties of some of the observations and the difficulties to interpret part of the results. However, this is inevitable and does not counterweight the genetic diagnoses made. It will also be a temporary problem, as due to the joint sequencing efforts more and more information will become available about neutral polymorphisms, genuine risk factors of disease, and actual pathogenic mutations.

Conclusion

MitoChip resequencing is a fast, cost-effective and reliable method with high throughput capabilities for complete mtDNA screening. A quarter of the patients with OXPHOS disease can be genetically diagnosed by this technique, based on the detection of three pathogenic and three or four likely pathogenic mutations in 28 patients, which confirms the percentage previously described [23]. Because of the growing number of mtDNA mutations combined with the increasing clinical heterogeneity, MitoChip resequencing is the preferred method to screen the mtDNA for mutations, especially when symptom specific screening and screening of only the most common mtDNA mutations fall short.

Supplementary Table S1: mtDNA polymorphisms detected in 28 patients with OXPHOS disease

polymorphisms - previously reported

Position	nt-change Chip	nt-change custom sequencing	Heteroplasmic on chip	In No. of samples heteroplasmic on chip	aa-change	Locus	No. of samples	% of samples	Population frequency *
709	g>a	np	No	-	-	MT-RNR1 / 12S ribosomal RNA	3	10.7%	17.2%
710	t>c	np	No	-	-	MT-RNR1 / 12S ribosomal RNA	2	7.1%	1.0%
750	a>g	np	No	-	-	MT-RNR1 / 12S ribosomal RNA	27	96.4%	99.1%
769	g>a	np	No	-	-	MT-RNR1 / 12S ribosomal RNA	2	7.1%	6.0%
825	t>a	np	No	-	-	MT-RNR1 / 12S ribosomal RNA	2	7.1%	3.5%
930	g>a	np	No	-	-	MT-RNR1 / 12S ribosomal RNA	1	3.6%	2.1%
1018	g>a	np	No	-	-	MT-RNR1 / 12S ribosomal RNA	2	7.1%	6.1%
1189	t>c	np	No	-	-	MT-RNR1 / 12S ribosomal RNA	3	10.7%	3.2%
1438	a>g	np	No	-	-	MT-RNR1 / 12S ribosomal RNA	25	89.3%	96.5%
1721	c>t	np	No	-	-	MT-RNR2 / 16S ribosomal RNA	2	7.1%	0.5%
1738	t>c	np	No	-	-	MT-RNR2 / 16S ribosomal RNA	2	7.1%	0.9%
1811	a>g	np	No	-	-	MT-RNR2 / 16S ribosomal RNA	1	3.6%	7.0%
1888	g>a	np	No	-	-	MT-RNR2 / 16S ribosomal RNA	3	10.7%	5.6%
2352	t>c	np	No	-	-	MT-RNR2 / 16S ribosomal RNA	2	7.1%	2.1%
2706	a>g	np	No	-	-	MT-RNR2 / 16S ribosomal RNA	15	53.6%	80.7%
2758	g>a	np	No	-	-	MT-RNR2 / 16S ribosomal RNA	2	7.1%	3.4%
2885	t>c	np	No	-	-	MT-RNR2 / 16S ribosomal RNA	2	7.1%	3.4%
3010	g>a	np	No	-	-	MT-RNR2 / 16S ribosomal RNA	5	17.9%	21.7%
3106	c>g	np	No	-	-	MT-RNR2 / 16S ribosomal RNA	1	3.6%	-
3197	t>c	np	No	-	-	MT-RNR2 / 16S ribosomal RNA	2	7.1%	3.3%
3212	c>t	np	No	-	-	MT-RNR2 / 16S ribosomal RNA	1	3.6%	0.2%
3394	t>c	np	No	-	Y>H	MT-ND1	2	7.1%	1.6%
3450	c>t	np	No	-	Syn	MT-ND1	1	3.6%	0.7%
3480	a>g	np	No	-	Syn	MT-ND1	3	10.7%	4.1%
3594	c>t	np	No	-	Syn	MT-ND1	2	7.1%	6.0%
4104	a>g	np	No	-	Syn	MT-ND1	2	7.1%	6.0%
4216	t>c	t>c	No	-	Y>H	MT-ND1	6	21.4%	9.5%

4580	g>a	np	No	-	Syn	MT-ND2	1	3.6%	2.9%
4732	a>g	np	No	-	N>S	MT-ND2	1	3.6%	1.2%
4769	a>g	np	No	-	Syn	MT-ND2	27	96.4%	98.9%
4917	a>g	a>g	No	-	N>D	MT-ND2	3	10.7%	4.9%
5046	g>a	g>a	No	-	V>I	MT-ND2	2	7.1%	3.2%
5108	t>c	np	No	-	Syn	MT-ND2	1	3.6%	3.1%
5147	g>a	np	No	-	Syn	MT-ND2	1	3.6%	5.3%
5471	g>a	np	No	-	Syn	MT-ND2	1	3.6%	0.7%
5655	t>c	t>c	No	-	-	MT-TA	2	7.1%	0.9%
5773	g>a	g>a	No	-	-	MT-TC	1	3.6%	2.2%
5913	g>a	np	No	-	D>N	MT-CO1	1	3.6%	0.4%
6018	g>a	np	No	-	A>T	MT-CO1	1	3.6%	0.1%
6221	t>c	np	No	-	Syn	MT-CO1	1	3.6%	2.3%
6261	g>a	g>a	No	-	A>T	MT-CO1	1	3.6%	0.4%
6776	t>c	np	No	-	Syn	MT-CO1	2	7.1%	2.1%
6962	g>a	np	No	-	Syn	MT-CO1	1	3.6%	1.9%
7028	c>t	np	No	-	Syn	MT-CO1	15	53.6%	81.5%
7055	a>g	np	No	-	Syn	MT-CO1	2	7.1%	2.1%
7256	c>t	np	No	-	Syn	MT-CO1	2	7.1%	6.0%
7337	g>a	np	No	-	Syn	MT-CO1	1	3.6%	0.6%
7521	g>a	np	No	-	-	MT-TD	2	7.1%	6.1%
7768	a>g	np	No	-	Syn	MT-CO2	2	7.1%	1.9%
7867	c>t	np	No	-	Syn	MT-CO2	2	7.1%	1.9%
8468	c>t	np	No	-	Syn	MT-ATP8	2	7.1%	3.5%
8697	g>a	np	No	-	Syn	MT-ATP6	2	7.1%	4.9%
8701	a>g	np	No	-	T>A	MT-ATP6	3	10.7%	35.1%
8736	t>c	np	No	-	Syn	MT-ATP6	1	3.6%	-
8854	g>a	np	Yes	1	A>T	MT-ATP6	1	3.6%	0.1%
8860	a>g	np	No	-	T>A	MT-ATP6	27	96.4%	99.8%
8901	a>g	np	No	-	Syn	MT-ATP6	1	3.6%	0.1%
9055	g>a	np	No	-	A>T	MT- ATP6	3	10.7%	4.2%
9449	c>t	np	No	-	Syn	MT-CO3	1	3.6%	1.1%

9477	g>a	np	No	-	V>I	MT-CO3	2	7.1%	3.4%
9670	a>g	np	No	-	N>S	MT-CO3	1	3.6%	0.2%
9698	t>c	np	No	-	Syn	MT-CO3	3	10.7%	4.4%
9899	t>c	np	No	-	Syn	MT-CO3	2	7.1%	1.1%
10086	a>g	np	No	-	N>D	MT-ND3	1	3.6%	1.1%
10172	g>a	np	No	-	Syn	MT-ND3	1	3.6%	0.4%
10325	g>a	np	No	-	Syn	MT-ND3	1	3.6%	0.5%
10373	g>a	np	No	-	Syn	MT-ND3	1	3.6%	1.1%
10398	a>g	np	No	-	T>A	MT-ND3	8	28.6%	46.2%
10463	t>c	np	No	-	-	MT-TR	3	10.7%	4.9%
10550	a>g	np	No	-	Syn	MT-ND4L	3	10.7%	3.6%
10750	a>g	np	No	-	N>S	MT-ND4L	1	3.6%	0.2%
10873	t>c	np	No	-	Syn	MT-ND4	3	10.7%	35.5%
11002	a>g	np	No	-	Syn	MT-ND4	1	3.6%	0.6%
11251	a>g	np	No	-	Syn	MT-ND4	5	17.9%	9.1%
11299	t>c	np	No	-	Syn	MT-ND4	4	14.3%	4.3%
11467	a>g	np	No	-	Syn	MT-ND4	5	17.9%	11.0%
11653	a>g	np	No	-	Syn	MT-ND4	1	3.6%	0.2%
11719	g>a	np	No	-	Syn	MT-ND4	13	46.4%	77.8%
11812	a>g	np	No	-	Syn	MT-ND4	1	3.6%	3.3%
12338	t>c	np	No	-	M>T	MT-ND5	1	3.6%	0.2%
12372	g>a	np	No	-	Syn	MT-ND5	5	17.9%	12.8%
12612	a>g	np	No	-	Syn	MT-ND5	2	7.1%	4.4%
12634	a>g	np	No	-	I>V	MT-ND5	1	3.6%	0.1%
12705	c>t	np	No	-	Syn	MT-ND5	3	10.7%	46.6%
12717	c>t	np	No	-	Syn	MT-ND5	1	3.6%	-
12738	t>g	np	No	-	Syn	MT-ND5	1	3.6%	0.2%
13105	a>g	np	No	-	I>V	MT-ND5	4	14.3%	6.2%
13326	t>c	np	No	-	Syn	MT-ND5	1	3.6%	0.3%
13327	a>g	np	No	-	T>A	MT-ND5	1	3.6%	-
13368	g>a	np	No	-	Syn	MT-ND5	3	10.7%	5.1%
13617	t>c	np	No	-	Syn	MT-ND5	2	7.1%	3.3%

13637	a>g	np	No	-	Q>R	MT-ND5	2	7.1%	0.5%
13650	c>t	np	No	-	Syn	MT-ND5	2	7.1%	6.0%
13680	c>t	np	No	-	Syn	MT-ND5	1	3.6%	0.6%
13708	g>a	np	No	-	A>T	MT-ND5	2	7.1%	6.8%
13789	t>c	np	No	-	Y>H	MT-ND5	2	7.1%	0.1%
14178	t>c	np	No	-	I>V	MT-ND6	2	7.1%	2.2%
14182	t>c	np	No	-	Syn	MT-ND6	2	7.1%	2.3%
14233	a>g	np	No	-	Syn	MT-ND6	1	3.6%	3.4%
14470	t>a	np	No	-	Syn	MT-ND6	1	3.6%	0.3%
14560	g>a	np	No	-	Syn	MT-ND6	2	7.1%	2.3%
14769	a>g	a>g	No	-	N>S	MT-CYB	2	7.1%	1.0%
14798	t>c	np	No	-	F>L	MT-CYB	5	17.9%	7.5%
14872	c>t	np	No	-	Syn	MT-CYB	1	3.6%	0.4%
14905	g>a	np	No	-	Syn	MT-CYB	3	10.7%	5.3%
15115	t>c	np	No	-	Syn	MT-CYB	2	7.1%	1.2%
15217	g>a	np	No	-	Syn	MT-CYB	1	3.6%	1.2%
15301	g>a	np	Yes	1	Syn	MT-CYB	2	7.1%	32.4%
15326	a>g	np	No	-	T>A	MT-CYB	27	96.4%	99.3%
15452	c>a	c>a	Yes	1	L>I	MT-CYB	5	17.9%	9.1%
15607	a>g	np	No	-	Syn	MT-CYB	3	10.7%	5.7%
15833	c>t	np	No	-	Syn	MT-CYB	1	3.6%	0.9%
15904	c>t	np	No	-	-	MT-TT	1	3.6%	2.8%
15928	g>a	np	No	-	-	MT-TT	3	10.7%	5.0%

polymorphisms - synchronous variations

Position	nt-change Chip	nt-change custom sequencing	Heteroplasmic on chip	In No. of samples heteroplasmic on chip	aa-change	Locus	No. of samples	% of samples	Population frequency *
3579	a>g	np	No	-	Syn	MT-ND1	1	3.6%	-
3666	g>a	np	No	-	Syn	MT-ND1	2	7.1%	2.2%
3693	g>a	np	No	-	Syn	MT-ND1	2	7.1%	1.1%
4562	a>g	np	No	-	Syn	MT-ND2	1	3.6%	0.4%

4733	t>c	np	No	-	Syn	MT-ND2	1	3.6%	0.2%
4745	a>g	np	No	-	Syn	MT-ND2	1	3.6%	0.4%
4856	t>c	np	No	-	Syn	MT-ND2	1	3.6%	0.0%
5036	a>g	np	No	-	Syn	MT-ND2	2	7.1%	0.9%
5196	t>c	np	No	-	Syn	MT-ND2	1	3.6%	0.1%
5237	g>a	np	No	-	Syn	MT-ND2	1	3.6%	0.9%
5393	t>c	np	No	-	Syn	MT-ND2	2	7.1%	0.8%
5414	a>g	np	No	-	Syn	MT-ND2	1	3.6%	0.1%
6548	c>t	np	No	-	Syn	MT-CO1	2	7.1%	0.8%
6827	t>c	np	No	-	Syn	MT-CO1	2	7.1%	1.1%
6845	c>t	np	No	-	Syn	MT-CO1	1	3.6%	0.1%
6989	a>g	np	No	-	Syn	MT-CO1	2	7.1%	0.8%
7184	a>g	np	No	-	Syn	MT-CO1	1	3.6%	0.2%
8248	a>g	np	No	-	Syn	MT-CO2	2	7.1%	0.9%
8655	c>t	np	No	-	Syn	MT-ATP6	2	7.1%	3.5%
9033	a>g	np	No	-	Syn	MT-ATP6	1	3.6%	0.1%
9233	t>c	np	No	-	Syn	MT-CO3	1	3.6%	0.1%
10094	c>t	np	No	-	Syn	MT-ND3	1	3.6%	-
10154	a>g	np	No	-	Syn	MT-ND3	1	3.6%	0.1%
10169	c>t	np	No	-	Syn	MT-ND3	1	3.6%	0.0%
10688	g>a	np	No	-	Syn	MT-ND4L	2	7.1%	3.6%
10810	t>c	np	No	-	Syn	MT-ND4	2	7.1%	3.8%
12519	t>c	np	No	-	Syn	MT-ND5	2	7.1%	1.0%
12633	c>a	np	No	-	Syn	MT-ND5	2	7.1%	1.5%
12798	c>t	np	No	-	Syn	MT-ND5	1	3.6%	0.0%
12816	c>a	np	Yes	1	Syn	MT-ND5	1	3.6%	-
13260	t>c	np	No	-	Syn	MT-ND5	1	3.6%	0.1%
13359	g>a	np	No	-	Syn	MT-ND5	1	3.6%	0.3%
13506	c>t	np	No	-	Syn	MT-ND5	2	7.1%	3.5%
13914	c>a	np	No	-	Syn	MT-ND5	1	3.6%	0.7%
13953	t>c	np	No	-	Syn	MT-ND5	1	3.6%	-
14167	c>t	np	No	-	Syn	MT-ND6	3	10.7%	4.2%

14203	a>g	np	No	-	Syn	MT-ND6	2	7.1%	0.9%
14773	c>t	np	No	-	Syn	MT-CYB	1	3.6%	-
14956	t>c	np	No	-	Syn	MT-CYB	1	3.6%	0.0%
15340	a>g	np	Yes	1	Syn	MT-CYB	1	3.6%	0.1%
15808	a>g	np	No	-	Syn	MT-CYB	1	3.6%	0.1%

***** Frequencies in the general population were retrieved from the Human Mitochondrial Genome Database were sequence information is available from 2469 mtDNA sequences (June 28, 2006) [61].

np: Not performed.

Syn: synchronous variation (no change in amino acid)

CHAPTER 3

Gene expression profiling reveals complement mediated regeneration in skeletal muscle from Leigh syndrome patients with a SURF1 mutation

R.G.E. van Eijsden [1,2,$], R. Mineri [3,$], P.J. Lindsey [1,2], L.M.T. Eijssen [1], C.M.M. van den Burg [1,2], L.E.A. de Wit [4], T.A. Ayoubi [1], C. Di Blasi [5], J. Zeman [6], M. Zeviani [3], I.F.M. de Coo [7], W. Sluiter [4], H.J.M. Smeets [1,2,£], V. Tiranti [3,£]

[1]Department of Genetics and Cell Biology, Maastricht University, Maastricht – The Netherlands.
[2]Research Institute Growth & Development, Maastricht University, Maastricht – The Netherlands.
[3]Pierfranco and Luisa Mariani Centre for the Study of Children's Mitochondrial Disorders, IRCCS Foundation Neurological Institute "C. Besta", Unit of Molecular Neurogenetics, Milan – Italy.
[4]Department of Biochemistry, Mitochondrial Research Unit, Erasmus MC, Rotterdam – The Netherlands.
[5]Unit of Neuromuscular diseases and Neuroimmunology, IRCCS Foundation Neurological Institute "C. Besta",
[6]Department of Paediatrics, First Faculty of Medicine, Charles University, Prague, Czech Republic
[7]Department of Neurology, Erasmus MC, Rotterdam – The Netherlands.

[$]Joint first authors.
[£]Both senior authors contributed equally to this work.

Submitted

Abstract

Leigh syndrome is an early-onset and often fatal neurodegenerative disorder, characterised by necrotic lesions in the brain basal ganglia. Leigh syndrome with a decreased cytochrome c oxidase (COX) activity is frequently caused by SURF1 gene mutations. To characterise molecular pathophysiological processes, gene expression profiling was performed in skeletal muscle biopsies from SURF1 Leigh syndrome patients and controls. No significant alterations were observed for the oxidative phosphorylation (OXPHOS) genes. Altered were protein synthesis, DNA metabolism, cell cycle, skeletal muscle development, and intriguingly the complement system. Genes of the classical complement pathway (*C1R*, *C1S*, and *C3*), involved in both immune response and tissue regeneration, were significantly up-regulated. This regenerative response is also observed by other processes. Most likely, *SURF1* mutations lead to increased production of reactive oxygen species (ROS), causing protein damage and increased turnover. This could trigger complement mediated muscle regeneration as a rescue process.

Introduction

Leigh syndrome (MIM 256000) is a progressive neurodegenerative disorder of infancy and childhood. The onset of the disease is at birth or within the first months of life. It has a characteristic neuropathology of focal, bilateral symmetrical necrotic lesions in brainstem, basal ganglia, thalamus and spinal cord. Disease progression is in general very fast, resulting in death within about two years from the age of onset. A frequent cause of Leigh syndrome is a defective oxidative phosphorylation (OXPHOS) system [62]. Mutations have been identified mainly in genes coding for enzymes involved in aerobic energy metabolism, including the X-linked E1α subunit of pyruvate dehydrogenase, the subunits of the OXPHOS system, and genes involved in the assembly of these complexes. Some of these genes are encoded by the nuclear DNA, others by the mitochondrial DNA (mtDNA). Mutations in the *SURF1* gene, which is encoded by the nuclear DNA, are the main cause of Leigh syndrome with cytochrome c oxidase (COX) deficiency. Tiranti *et al.* reported 75% (18 out of 24) of the Leigh patients with COX deficiency to have a mutation in the *SURF1* gene [63], although another study reported a lower frequency of 26% (6 out of 23) [64]. The absence of the SURF1 protein causes accumulation of early assembly intermediates (S1 and S2) of the cytochrome c oxidase complex, as is illustrated by blue native two-dimensional gel electrophoresis, indicating that the SURF1 protein plays a role in the assembly of intermediate component S3 [65]. Leigh syndrome caused by mutations in the *SURF1* gene has a homogeneous clinical manifestation. Patients present with progressive encephalopathy, generalised hypotonia with sharp tendon reflexes, trunk ataxia, oculomotor abnormalities, central respiratory problems, and rapidly progressive psychomotor regression [7]. Although we know that Surf1 is an important factor for the assembly of the COX complex, the exact pathophysiological mechanism in the

development and progression of the disease is still unknown and it is also unclear whether the SURF1 protein has additional roles in other biological processes [32].

Mitochondrial diseases mainly affect tissues with a high energy demand like heart, skeletal muscle, and the renal and neuro-endocrine systems [7]. In Leigh syndrome these are the central nervous system and skeletal muscle [7]. To identify pathogenic molecular processes due to mutations in the SURF1 gene, and to gain more insight into the pathophysiology of the disease, differences in skeletal muscle gene expression levels between SURF1 patients and controls were characterised by microarray technology and validated by functional assays.

Materials & methods

Patients and controls

Needle biopsies were taken from the quadriceps muscle from six Leigh syndrome patients with a mutation in the *SURF1* gene (P60, P62, P63, P64, P65, P66) and from six controls (C3-8, table 1). For ethical reasons it was not possible to systematically get age-matched controls, which would involve healthy children of 2-4 years of age, and only one biopsy was available from a 10-year old girl with no mitochondrial disease, which was used for immunohistochemistry (see below). Three of the Leigh syndrome patients have been previously described by Tiranti *et al.* (patient 6 in table 1, patient P64 in table 1 of this study), Bruno *et al.* (patient P63 in table 1 of this study), and Zhu *et al.* (patient P60 in table 1 of this study) [8, 63, 66]. After biopsy, the muscle samples were immediately frozen in liquid nitrogen.

Microarray procedure

Total RNA was isolated using the TRIzol reagent (Invitrogen, Breda, The Netherlands) and purified with the RNeasy clean-up kit (Qiagen, Venlo, The Netherlands). RNA quantity and purity were determined spectrophotometrically using the Nanodrop ND-1000 (Nanodrop Technologies, Wilmington, DE, USA) and RNA integrity was assessed by determining the RNA 28S/18S ratio using a Bioanalyser 2100 (Agilent, Santa Clara , CA, USA). Muscle RNA spiked with four bacterial RNA transcripts was reverse transcribed into cDNA and amplified in a two-round amplification reaction according to the manufacturer's protocol (Affymetrix, Santa Clara, CA, USA). A mixture of cDNA and added hybridisation controls was hybridised on Affymetrix HG-U95Av2 chips, followed by staining and washing steps in the GeneChip fluidics station according to the manufacturer's procedures. To assess the raw probe signal intensities, chips were scanned using the GeneChip scanner 3000 (Affymetrix, Santa Clara, CA, USA).

Table 1: Patients and controls

Subject-Code	SURF1 Mutations	Sex	Age at muscle biopsy	COX activity	Blood lactate level
P60	[312_321del 311_312insAT] + [312_321del 311_312insAT]	M	3	4%	increased
P62	[19_35dup (now 37_38ins)] + [19_35dup (now 37_38ins)]	M	4	21%	mildly increased
P63	[240+1G>T] + [531_534del]	M	2	reported reduced	increased
P64	[19_35dup (now 37_38ins)] + [19_35dup (now 37_38ins)]	F	2	13%	increased
P65	[722_723insC] + [722_723insC]	M	3	NA	NA
P66	[240+1G>T] + [T844C]	M	2	39%	increased
P1	[552delG] +[790-791delAG]	F	10	15%	increased
P2	[312_321del 311_312insAT] + [821del18]	F	2	5%	Increased
C3	-	F	34	NA	NA
C4	-	F	64	NA	NA
C5	-	F	17	NA	NA
C6	-	F	22	NA	NA
C7	-	M	53	NA	NA
C8	-	M	25	NA	NA

Overview of patients and controls used for the microarray study and follow-up investigations.
COX activity and blood lactate levels for the controls were not determined but were assumed to be normal.
P = patient, C = control, M = Male F = Female, NA = Not available, COX=cytochrome c oxidase.
The nomenclature of the SURF1 mutations is as suggested by Péquignot et al. [6] according to the guidelines by Dunnen and Antonarakis [67].

Microarray data analysis

R, a free software environment for statistical computing and graphics, was used with the *gnlm* and the *affy* libraries to perform the data preparation and analysis [40, 68-70]. Version 8 of the Unigene-based probe set definition files (CDF files) as described by Dai *et al.* was used to combine the individual probes into probe sets [71]. These CDF files are based on Unigene build #192. The *expresso* method of the *affy* library, without background correction, with constant normalisation, use of perfect match signal intensities only, and the "mas" summarisation method was used to calculate the probe set intensities from the individual probe signals. Normal linear regression models, implemented by the *gnlr* function within the *gnlm* library, were used to asses significantly differentially expressed genes between patients and controls. Differences due to experimental variation were corrected for by including the data from the RNA spikes and hybridisation controls as covariates in the models. Because not all microarray experiments were carried out on the same day, the hybridisation days were also included in the modelling procedure. The Akaike information criterion (AIC), representing the likeliness of each model penalised for its complexity, was used to identify genes with a significant change in expression between the two groups [72]. The AIC was adjusted to be comparable to a two-sided chi-squared test with a significance level of 99.9%, making the analysis more stringent [73]. To test for age differences we used 2 additional data sets from the Public Expression Profiling Resource (pepr.cnmcresearch.org). The first consisted of 10 controls (age 10 –20 years) and the other of 2 controls *in duplo* (mixed samples with age between 4 and 13 and 5 and 12 years). Because these muscle RNA samples were run on different version of

Affymetrix CHIPs, respectively, the 133A and the U95, we could only use the genes with overlapping probes or probe sets.

Data mining

To identify biological processes in which the significantly differentially expressed genes were involved, the Gene Map Annotator and Pathway Profiler (GenMAPP, version 2.1, build 20060809) and MAPPFinder (version 2.0, build 20041218) programs were used [74, 75]. The gene database version "Hs-Std_20060526.gdb" and the Mapps version "Hs_Contributed_20060605" were used for both programs. Additionally the web-based Database for Annotation, Visualisation and Integrated Discovery (DAVID) was used to assess enriched gene ontology terms within the significantly differentially expressed gene list [76].

Quantitative Real-time PCR

Primers were designed using Primer Express® software version 3.0 (Applied Biosystems, Foster City, CA, USA). cDNA was prepared from 2 µg of total RNA in a standard reverse transcriptase reaction. PCR was performed in a 7700 Realtime PCR System (Applied Biosystems, Foster City, CA, USA) and a MyiQ Single-Colour Real-Time PCR Detection System (Biorad, Hercules, CA, USA) using Eurogentec qPCR™ Mastermix Plus for SYBR Green® I (Eurogentec, Seraing, Belgium). The cycling conditions were: an initial step of 2 minutes at 50°C, activation of the Hot Goldstar enzyme at 95°C for 10 minutes, and 40 cycles of 15 seconds at 95°C followed by 1 minute at 60°C (denaturation, annealing, and elongation). The ADP-ribosylation factor 1 (*ARF1*) gene was used as an internal reference because of its constant expression level in muscle [77]. The other 8 genes for which quantitative real-time PCR (QRT-PCR) was performed were complement component 1, r subcomponent (*C1R*), complement component, s subcomponent (*C1S*), complement component 3 (*C3*), clusterin (*CLU*), pyruvate kinase, muscle (*PKM2*), peripheral myelin protein 22 (*PMP22*), ryanodine receptor 3 (*RYR3*), and solute carrier family 16, member 3 (*SLC16A3*). Primers used for amplification are listed in supplementary table S1. QRT-PCR was carried out once on the same RNA samples as used for the microarray experiments. Data was analyzed in R using the *elliptic* function of the *growth* library to implement normal linear regression models [69, 70]. The AIC was adjusted to be comparable to a two-sided chi-squared test with a significance level of 99.0%, making the analysis more stringent [73].

Immunohistochemistry

For immunohistochemistry needle biopsies, taken from the quadriceps muscle patient P1 (table 1) and the age-matched control biopsy were frozen in isopentane, cooled in liquid nitrogen, and stored in liquid nitrogen until use. Immunohistochemical staining was performed on acetone-fixed 6 µm-thick cryosections using anti-C3 and anti-C5b-9 monoclonal antibodies (Dako, Copenhagen, Denmark) diluted 1:10 and 1: 25, respectively. Sections were incubated in primary antibody, then in biotinylated goat anti-mouse IgG (Jackson ImmunoResearch Labs. Inc, West

Grove, PA, USA), and finally treated with rhodamine-avidin D (Vector Labs, Burlingame, CA, USA). As a positive control for the anti-C3 staining, a cryosection of a quadriceps muscle needle biopsy from a Duchene muscular dystrophy (DMD) patient was included. For double immunolabelling, a C3c polyclonal antibody (Dako, Copenhagen, Denmark) was used in combination with an anti-collagen fraction VI (membrane of muscle fibres; Chemicon, Temecula, Canada), anti-laminin α5 (subendothelial extracellular matrix; Chemicon, Temecula, Canada), and an anti-foetal or anti-neonatal myosin (muscle development; Novocastra, Newcastle Upon Tyne, United Kingdom) monoclonal antibody. The antibodies were diluted 1:1000, 1:250, 1:50, 1:20, and 1:20 respectively. In all cases the primary antibodies were used in the first incubation step, followed by biotinylated goat anti-rabbit IgG, by rhodamine avidin D and by Cy2-labelled goat anti-mouse IgG (Jackson, West Grove, PA, USA). As a control, sections were either incubated with isotype-specific IgG or the primary antibody was omitted.

Oxidative protein damage

Oxidative damage to proteins in the muscle biopsies was determined by quantifying the amount of carbonyl groups per mg protein using an ELISA assay optimised for small amounts of proteins (Oxprot assay). For this assay, a small part of about 10 mg wet weight (ww) of the skeletal muscle biopsies from four controls and from the same six patients used for the microarray experiments (P60, P62, P63, P64, P65, P66, table 1) was used. The snap-frozen biopsies were pulverised in the presence of 19 mL/g ww of RIPA buffer (50 mM Tris-HCl, 150 mM NaCl, 1 mM EDTA, pH 7.4, containing 0.25% sodium deoxycholate, 1% NP40 and supplemented with a protease inhibitor mixture (PIM) of one Complete tablet per 50 mL (Roche Diagnostics, Almere, The Netherlands), 1 mM 4-(2-aminoethyl)-benzenesulfonyl-fluoride hydrochloride (Pefabloc SC, Roche Diagnostics, Almere, The Netherlands) and 2 mM diisopropyl fluorophosphate (DFP) (Fluka Chemica, Steinheim, Switzerland)) in a small Bessman tissue pulveriser (Fisher Scientific, Pittsburg, PA, USA) precooled with liquid nitrogen. For carbonyl determination the tissue homogenate was first incubated on ice for 30 min, and then centrifuged at 16,000 g for 20 min at 4°C, and the supernatant was diluted in PBS to 0.5 µg/mL protein. Next 200 µl was transferred into triplicate wells of a Nunc Maxisorp microplate. The amount of carbonylgroups resulting from protein oxidation were determined as described by Alamdari *et al.* [78]. A technical replicate was performed for four out of eight patient samples and for four out of seven control samples. A one-sided t-test on the averages of the replicate measurements was used to assess statistical differences between the patient and the control groups.

Detection of superoxide-producing enzymes in muscle

The expression of superoxide radical-producing enzymes in muscle was quantified by enzyme histochemistry of skeletal muscle cryosections from two *SURF1* patients P1 and P2 and the 6 controls, using dihydroethidium (DHE) to trap superoxide as the enzyme product. Ten-µm thick cryosections were stored at -80°C and after thawing the sections were stained by 5 µM

dihydroethidium and 0.5 µg/mL Hoechst 33258 in phosphate-buffered saline (PBS) for 30 min at 37°C in a humidified atmosphere [42]. The orange fluorescence of the superoxide-specific product of DHE oxidation [79] was measured using a fluorescence inverted microscope (Olympus IX50) equipped with a 460-490 nm band pass excitation filter and 515-nm emission IF-barrier filter, digitised with a F-view camera (Soft Imaging System, Münster, Germany), and analyzed offline (AnalySIS 3.1; Soft Imaging System, Münster, Germany). The signal was expressed in arbitrary units reflecting the total fluorescence intensity of all events divided by the number of blue fluorescent nuclei. At least 300 nuclei per section were counted in two to three consecutive sections.

Results

Gene expression profiling of muscle from SURF1 patients

Probe signal intensities specific for 7084 transcripts were obtained for each of the six *SURF1* and six control samples (table 1). Normal linear regression modelling indicated 369 transcripts to be significantly differentially expressed between the *SURF1* patients and the control group (supplementary table S2), 313 of which were up-regulated and 56 were down-regulated. The majority of the changes was rather small, with only 14.1% (44) of the up-regulated genes and 8.9% (5) of the down-regulated genes having fold changes of more than 2. Expression of the *SURF1* transcript was significantly down-regulated with a fold change of 2.5. Other genes which were significantly more than 2.5-fold down-regulated were *PKM2* (Pyruvate kinase - muscle), *RYR3* (Ryanodine receptor 3), and *SLC16A3* (Solute carrier family 16 - member 3). Other up-regulated genes with a fold change of more than 2 were *CLU* (Clusterin), *C1R* (Complement component 1-r subcomponent), *C1S* (Complement component 1-s subcomponent), and *PMP22* (Peripheral myelin protein 22), with fold changes of 3.7, 3.1, 2.3, and 4.9, respectively. As 4 out of 6 controls were females and 5 out of the 6 analysed patients were males we tested whether the expression differences could be explained by sex differences between patients and controls. Reanalysis of the 369 significant genes with sex added to the model has yielded a difference for 8 genes, 2 of which only had a sex difference and 6 of which both had a difference between patients and controls and a sex difference, so we concluded that sex did not explain our results. The age difference between patients and controls could also play a role in the gene expression changes. To test this, we used 2 control data sets of the Public Expression Profiling Resource (pepr.cnmcresearch.org). The first consisted of 10 controls (age 10 –20 years) and the other of 2 controls *in duplo* (mixed samples with age between 4 and 13 and 5 and 12 years). Because these muscle RNA samples were run on different version of Affymetrix CHIPs, respectively, the 133A and the U95, we could only use the genes with overlapping probes or probe sets. In the first data set our results were confirmed by 75% of the genes and in the second by 43%. For the other genes in the second data set it was not possible to show a difference between patients and controls, probably because of the small sample size (only 2 control mixtures) and the lab variability.

However, the initial results of the complement system were confirmed in both additional analyses.

To identify altered processes in our own patient control dataset, an additional pathway analysis was performed. MAPPFinder analysis showed that the three most significantly changed ($p<0.05$) local pathways or gene groups were Complement Activation (classical pathway), Ribosomal Proteins, and Regulation of Actin Cytoskeleton (table 2). Because there were two maps including the complement activation pathway, this pathway is listed twice. The most significantly changed gene ontology pathways or gene groups in the biological process category can be linked to protein synthesis, DNA metabolism, cell cycle, skeletal muscle development, and the immune system with the majority of these gene expression changes pointing towards a stimulation of these processes (table 3), which are the same process terms ($p<0.05$) as determined by DAVID (supplementary table S3).

Table 2: MAPPFinder results for local pathways or gene groups

MAPP Name	# Changed	# Measured	# On MAPP	% Present	P-value
Hs_Complement_and_Coagulation_Cascades_KEGG	7	39	63	61.9	0.013
Hs_Ribosomal_Proteins	6	31	88	35.2	0.016
Hs_Regulation_of_Actin_Cytoskeleton_KEGG	10	74	146	50.7	0.023
Hs_Complement_Activation_Classical	3	9	17	52.9	0.024

MAPPFinder results listing the significantly changed ($p<0.05$) local pathways or gene groups between Leigh syndrome patients with a SURF1 mutation and control subjects.

Table 3: MAPPFinder results for gene ontology pathways or gene groups

GO ID	GO Name	# Changed	# Measured	# in GO	% Present	P-value
7046	ribosome biogenesis	3	10	61	16.4	0.009
42254	ribosome biogenesis and assembly	3	10	72	13.9	0.009
1558	regulation of cell growth	6	41	108	38.0	0.013
40008	regulation of growth	6	43	120	35.8	0.016
45445	myoblast differentiation	2	5	10	50.0	0.017
6974	response to DNA damage stimulus	7	57	224	25.4	0.017
6289	nucleotide-excision repair	2	5	19	26.3	0.018
9719	response to endogenous stimulus	7	58	238	24.4	0.018
1649	osteoblast differentiation	2	4	18	22.2	0.019
45165	cell fate commitment	2	4	18	22.2	0.019
6956	complement activation	3	13	33	39.4	0.021
7028	cytoplasm organization and biogenesis	3	14	84	16.7	0.023
7049	cell cycle	18	211	653	32.3	0.023
48747	muscle fiber development	2	6	17	35.3	0.024
48741	skeletal muscle fiber development	2	6	17	35.3	0.024
48637	skeletal muscle development	2	6	17	35.3	0.024
16049	cell growth	6	48	141	34.0	0.026
8361	regulation of cell size	6	48	141	34.0	0.026
6259	DNA metabolism	14	156	645	24.2	0.026
1666	response to hypoxia	2	5	8	62.5	0.028
43087	regulation of GTPase activity	2	5	39	12.8	0.029
51336	regulation of hydrolase activity	3	13	66	19.7	0.029

50793	regulation of development	4	24	63	38.1	0.03
6281	DNA repair	6	51	202	25.2	0.032
40007	growth	7	59	177	33.3	0.032
48625	myoblast cell fate commitment	1	1	2	50.0	0.036
7518	myoblast cell fate determination	1	1	2	50.0	0.036
16570	histone modification	2	6	23	26.1	0.037
16569	covalent chromatin modification	2	6	23	26.1	0.037
48175	hepatocyte growth factor biosynthesis	1	1	1	100.0	0.042
48176	regulation of hepatocyte growth factor biosynthesis	1	1	1	100.0	0.042
48178	negative regulation of hepatocyte growth factor biosynthesis	1	1	1	100.0	0.042
45663	positive regulation of myoblast differentiation	1	1	2	50.0	0.042
45661	regulation of myoblast differentiation	1	1	2	50.0	0.042
46881	positive regulation of follicle-stimulating hormone secretion	1	1	3	33.3	0.042
46887	positive regulation of hormone secretion	1	1	3	33.3	0.042
46882	negative regulation of follicle-stimulating hormone secretion	1	1	4	25.0	0.042
46884	follicle-stimulating hormone secretion	1	1	4	25.0	0.042
46880	regulation of follicle-stimulating hormone secretion	1	1	4	25.0	0.042
46888	negative regulation of hormone secretion	1	1	5	20.0	0.042
51048	negative regulation of secretion	1	1	7	14.3	0.042
51128	regulation of cell organization and biogenesis	3	16	45	35.6	0.042
51014	actin filament severing	1	1	2	50.0	0.043
7346	regulation of progression through mitotic cell cycle	2	6	13	46.2	0.043
46902	regulation of mitochondrial membrane permeability	1	1	1	100.0	0.044
51095	regulation of helicase activity	1	1	1	100.0	0.044
51097	negative regulation of helicase activity	1	1	1	100.0	0.044
7569	cell aging	1	1	4	25.0	0.044
8635	caspase activation via cytochrome c	1	1	6	16.7	0.044
7568	aging	1	1	8	12.5	0.044
9440	cyanate catabolism	1	1	2	50.0	0.045
9439	cyanate metabolism	1	1	2	50.0	0.045
19754	one-carbon compound catabolism	1	1	2	50.0	0.045
7022	chaperonin-mediated tubulin folding	1	1	2	50.0	0.045
42692	muscle cell differentiation	2	7	12	58.3	0.045
15918	sterol transport	1	1	3	33.3	0.047
30301	cholesterol transport	1	1	3	33.3	0.047
42546	cell wall biosynthesis	1	1	1	100.0	0.048
45229	external encapsulating structure organization and biogenesis	1	1	1	100.0	0.048
9273	cell wall biosynthesis (sensu Bacteria)	1	1	1	100.0	0.048
9252	peptidoglycan biosynthesis	1	1	1	100.0	0.048
7047	cell wall organization and biogenesis	1	1	1	100.0	0.048
31504	cell wall organization and biogenesis (sensu Bacteria)	1	1	1	100.0	0.048
9214	cyclic nucleotide catabolism	1	1	1	100.0	0.048
30202	heparin metabolism	1	1	2	50.0	0.048
30210	heparin biosynthesis	1	1	2	50.0	0.048
48247	lymphocyte chemotaxis	1	1	4	25.0	0.048
15012	heparan sulfate proteoglycan biosynthesis	1	1	6	16.7	0.048

MAPPFinder results listing the significantly changed ($p<0.05$) gene ontology pathways or gene groups between Leigh syndrome patients with a SURF1 mutation and control subjects.

Microarray results were validated by QRT-PCR for a number of transcripts which showed a significant 2 fold or more increase or decrease according to the microarray data analysis (*C1R*, *C1S*, *CLU*, *PKM2*, *PMP22*, *RYR3*, *SLC16A3* – supplementary table S2). To confirm the role of the complement system, we determined differences in gene transcript levels for complement component 3 (*C3*) as well. Transcript levels for these complement proteins were highly up-regulated in the *SURF1* patient samples (table 4). The expression of the transcripts coding for the pyruvate kinase muscle (PKM2), peripheral myelin protein 22 (PMP22), ryanodine receptor 3 (RYR3), and solute carrier family 16 member 3 (SLC16A3) were also significantly differentially expressed in the patient samples (table 4). QRT-PCR confirmed the results of the microarray experiment, although the fold changes were consistently larger.

Table 4: QRT-PCR validation

			Array		QRT-PCR	
Symbol	**Name**	**Process**	**Significant**	**FC**	**Significant**	**FC**
C1R	Complement component 1, r subcomponent	classical pathway	Yes	3.1 ↑	Yes	9.2 ↑
C1S	Complement component 1, s subcomponent	classical pathway	Yes	2.3 ↑	Yes	10.5 ↑
C3	Complement component 3	classical/alternative pathway	-	-	Yes	9.7 ↑
CLU	Clusterin	Complement	Yes	3.7 ↑	Yes	9.1 ↑
PKM2	Pyruvate kinase, muscle	Energy metabolism	Yes	2.5 ↓	Yes	5.0 ↓
PMP22	Peripheral myelin protein 22	Myelinisation	Yes	4.9 ↑	Yes	10.0 ↑
RYR3	Ryanodine receptor 3	Calcium metabolism	Yes	2.5 ↓	Yes	3.3 ↓
SLC16A3	Solute carrier family 16 (monocarboxylic acid transporters), member 3	Lactate transport	Yes	2.5 ↓	Yes	5.0 ↓

Gene transcript fold changes for SURF1 Leigh patients compared to controls determined by microarray analysis (Array) and quantitative realtime pcr (QRT-PCR) with addition of complement component C3 (not on the array). FC: fold change, ↑: up-regulation, ↓: down-regulation.

Immunohistochemistry of the complement system in muscle of a SURF1 patient

Immunohistochemical staining of complement component C3 was much stronger in muscle of an *SURF1* patient P1 (table 1) compared to an age-matched control, in which practically no staining was observed (figure 1). Staining of C3 in muscle of a Duchene muscular dystrophy patient showed a more diffuse pattern than the *SURF1* patient (figure 1, panel A). The C3 positive staining in the *SURF1* patient was localised at the muscle fibre membranes, as illustrated by the co-localisation of complement component C3c and collagen fraction VI (figure 1, panel B). No co-localisation in the double staining of C3c and laminin α5 could be identified, indicating that the complement C3c presence was confined to the muscle fibre membranes (figure 1, panel C). The double staining of C3c and anti-foetal or anti-neonatal myosin showed a few myosin positive muscle fibres in the patient samples only (figure 1, panels D and E). Immunohistochemical staining of C5b-9 complement components to identify the membrane attack complex (MAC) indicated no difference between the patient and the control (figure 1, panel F).

Oxidative protein damage and expression of enzymes producing superoxide radicals in muscle of SURF1 patients

Oxidative damage to muscle proteins determined by the amount of carbonyl groups in the *SURF1* patients was not different (p=0.07 in a one-sided t-test) from that in the controls, respectively amounting to 1.98 (SD: 0.97) and 1.29 (SD: 0.74) nmol per mg protein based on 4 patients and four controls. The expression of superoxide producing enzymes was significantly increased in *SURF1* muscle. As shown in figure 2, the staining intensity for these enzymes in *SURF1* muscle cryosections was 2.5 fold higher than in the control samples with a p-value of < 0.005 in a one-sided t-test.

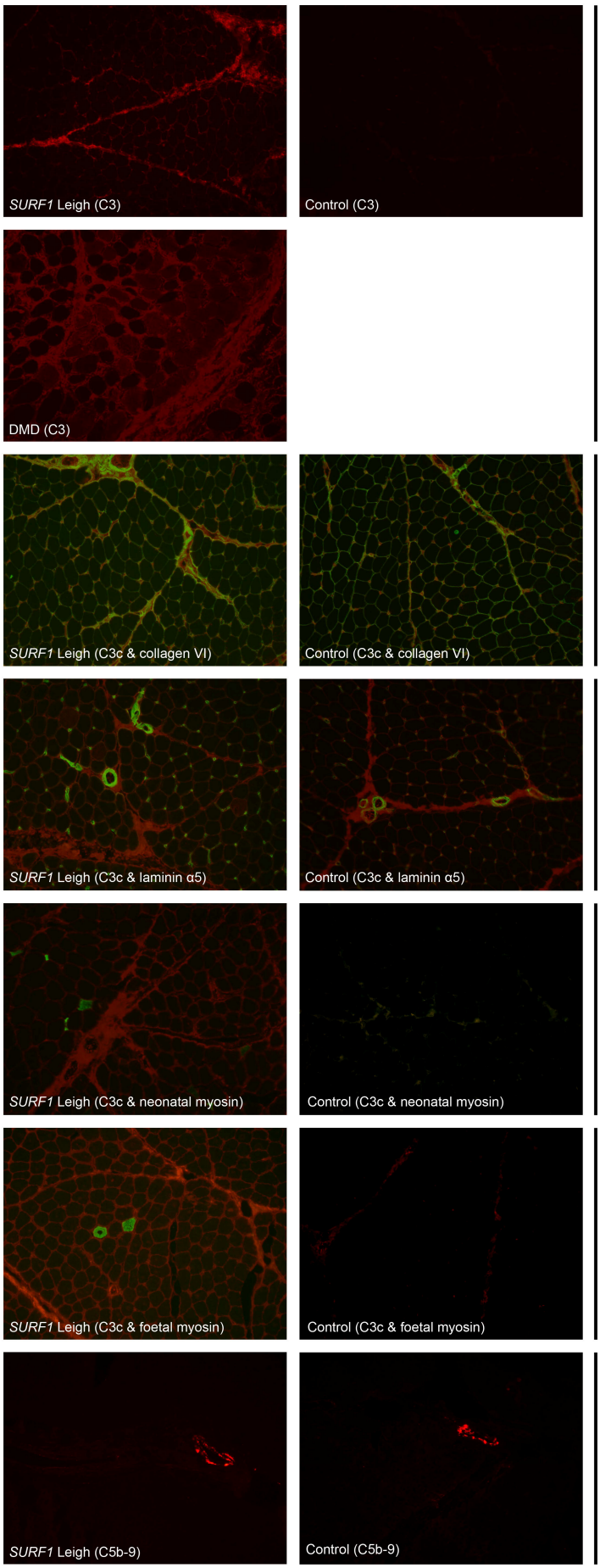

Figure 1: Immunohistochemical staining of complement factors C3 and C5b-9 in muscle of SURF1 patients

Immunohistochemical staining was performed on skeletal muscle cryosections from a control and SURF1 patient P1 for complement factor C3 alone (panel A), complement factor C3c in combination with anti-collagen fraction VI (panel B), anti-laminin α5 (panel C), an -neonatal (panel D) or anti-foetal (panel E) myosin monoclonal antibody and for complement component C5b-9 (panel F). Immunohistochemical staining for C3 was also performed on a skeletal muscle cryosection from a Duchene muscular dystrophy (DMD) patient (panel A). Staining for complement component C3 was positive for muscle of the SURF1 patient and negative for control muscle. Staining of C3 showed a diffuse pattern for muscle of the DMD patient. C3c staining (green) of muscle of the SURF1 patient co-localised with collagen fraction VI (red) but not with laminin α5 (red). A number of muscle fibres of the SURF1 patient stained positively for both C3c (green) and anti foetal or anti neonatal myosin (red). Control muscle staining was negative for double staining against C3c and anti foetal or anti neonatal myosin. Staining for C5b-9 was negative for patient P1 (panel F, left) and the control (panel F, right).

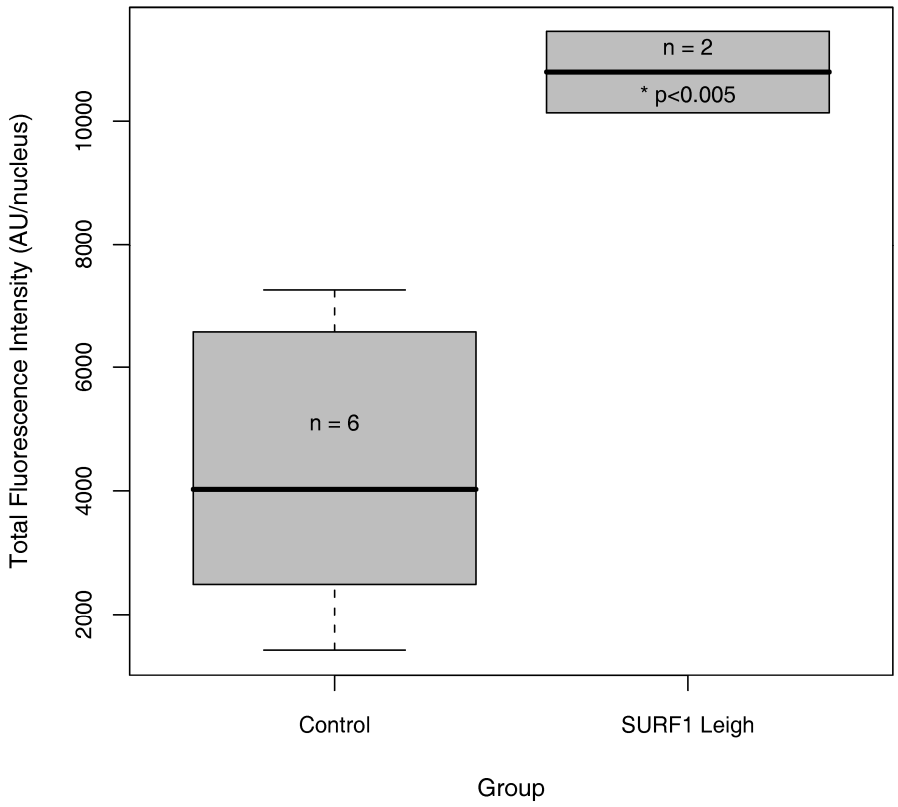

Figure 2: DHE staining

Cryosections of skeletal muscle samples of controls (n=6) and *SURF1* patients P1 and P2 (n=2) were stained with dihydroethidium (DHE) to assess the amounts of superoxide radicals present. A one-sided t-test showed that muscle of *SURF1* patients contained a 2.5 fold significantly higher amount of superoxide radicals ($p<0.005$). The whiskers in the box plot indicate the extreme values. The boxes indicate the median (thick line) and the interquartile ranges (grey area).

Discussion

Gene expression profiling of skeletal muscle of Leigh syndrome patients with a *SURF1* mutation compared to controls revealed 369 transcripts to be significantly differentially expressed (supplementary table S2). The majority (313) of the significantly differentially expressed transcripts were up-regulated, with only 14.1% of these genes having a fold change higher than 2.0. Of the 56 significantly differentially expressed transcripts which were down-regulated, 8.9% had a fold change of more than 2.0, a number of which were involved in the complement system (*CLU*, *C1R*, and *C1S*). The expression of 7 transcripts was confirmed by QRT-PCR (table 4). MAPPFinder and DAVID pathway and gene ontology based analyses revealed that protein synthesis, DNA metabolism, cell cycle, skeletal muscle development, and the immune system were the most significantly altered processes (tables 2, 3, and supplementary table S3). Some of

the altered processes may not solely relate to the difference in patients and controls due to the Surf1 defect, but also to a difference in sex or age. A sex effect was excluded as an explanation for the significantly different expression of the 369 genes. An age-effect was unlikely for the majority of changes observed, although the possibility to test this properly was limited due to the data sets and the number of controls and type of CHIPs available. In addition, any control set from a different lab introduces a lab difference between patients and controls. An age-effect was unlikely to explain the differences in the complement system. It was for ethical reasons not possible to obtain systematically muscle biopsies from age-matched normal controls. The significance of the altered processes was independently validated by immunohistochemistry of a patient and the only age-matched control available and by measurement of the amount of oxidatively damaged proteins and expression of superoxide producing enzymes.

Alterations in OXHPOS gene expression and energy metabolism

The down-regulation of the *SURF1* transcript (2.5 fold) was the only significant change in transcripts directly related to the OXPHOS system. This indicates that compensation for the defect in complex IV assembly does not occur by either up-regulating complex IV or other OXPHOS related genes, or genes involved in mitochondrial biogenesis in general. The significant down-regulation of PKM2 and SLC16A3 could be related to the high levels of lactate in blood and urine which are often found in Leigh syndrome patients [7]. Pyruvate kinase is responsible for the conversion of phosphoenolpyruvate to pyruvate at the end of the glycolysis reaction. If the OXPHOS system does not function properly, pyruvate will be converted to lactate resulting in higher blood and urine lactate levels. Down-regulation of the PKM2 gene coding for the pyruvate kinase enzyme might help in preventing lactic acidosis from occurring. *SLC16A3*, also known as monocarboxylate transporter 4 (*MCT4*) is mainly expressed in glycolytic skeletal muscle fibres and mediates the efflux of lactate from those fibres [80]. As the regulation of the monocarboxylate transporters is pH dependent, down-regulation of the *MCT4* gene could be an additional factor in trying to repress the high blood lactate levels. This, is in contrast with previous findings where the MCT4 protein was 40% more abundant in a patient with mitochondrial myopathy [81], but the disease manifestation of this patient appears to be much milder and lactic acidosis may be less of a problem. Additionally, it has been reported that exercise training can increase the expression of *MCT4* [82]. Because of the strong muscle weakness in Leigh syndrome patients resulting in the inability of a normal active life and especially in the inability of physical exercise, this could also contribute to the down-regulation of the *MCT4* gene.

Alterations in protein turnover due to oxidative damage

Protein turnover appears to be altered in muscle of *SURF1* patients. The increase in protein synthesis is mainly based on the significant up-regulation of members of the 40S (*RPS11* and *FAU*) and 60S (*RPL3*, *RPL11*, and *RPL28*) subunits of the cytoplasmic ribosomal proteins. In addition 14 transcripts coding for other subunits of the cytoplasmic ribosomal proteins tended to be more

than 1.2 fold up-regulated and only one component of the 60S subunit was down-regulated, suggesting that the process as a whole appears to be up-regulated. The small sample size and the relatively small changes in gene expression could explain why the results for the majority of these genes were not significantly differentially expressed. On the other hand, there are also indications towards an increase in protein degradation by the proteasome, in particular the 20S proteasome. One transcript, encoding subunit PSMB9, was significantly up-regulated having a fold-change of 1.3, and six transcripts coding for other subunits of the 20S proteasome were up-regulated (> 1.2-fold), although not significantly. Moreover, one of the activators of the 20S complex (*PSME1*) was significantly up-regulated with a fold-change of 2.0. The 20S complex of the proteasome is mainly associated with the breakdown of proteins with oxidative damage [83].

The increased production of reactive oxygen species (ROS) in the muscle of *SURF1* patients is not uncommon for OXPHOS disease since impairment of the OXPHOS system can result in increased ROS production [32, 84]. Increased ROS production in the muscle of *SURF1* patients is supported by a significant 1.8 fold up-regulation of glutathione peroxidase 3 (*GPX3*) and a significant 2.0 fold up-regulation of thioredoxin reductase 1 (*TXNRD1*), both having a protective effect as oxidoreductases. Although the apparent increase in oxidative protein damage observed in muscle of *SURF1* patients was not statistically significant, *SURF1* muscle cryosections contained significantly more enzymes able to produce superoxide radicals than the control samples, consistent with increased ROS production in muscle of *SURF1* patients. We hypothesise that the increase in protein turnover due to the increased ROS production, results in efficient removal of the ROS damaged proteins.

Increased expression of complement component genes

A striking observation is the involvement of the immune system in *SURF1* patients as illustrated by the up-regulation of a number of transcripts coding for complement components (table 4). Because of the physiological abundance of complement proteins, mainly produced by the liver and released in the serum, it was unexpected that the muscle itself showed an increased expression of complement components. The up-regulation of transcription of the C1QB, C1R and C1S genes in *SURF1* patients points towards the activation of complement via classical pathway [85, 86]. The end-route of the complement cascade is usually the formation of the membrane attack complex (MAC) which leads to membrane leakage resulting in cell lyses. However, no difference in the amount of MAC for a *SURF1* patient compared to an age-matched control could be identified by immunohistochemical staining against the complement C5b-9 complex. Additionally, necrosis has not been described in muscle fibres of *SURF1* patients [3]. This indicates that the activation of complement in muscle of *SURF1* patients must have a different purpose than cell lyses. This was corroborated by the fact that no signs of inflammation were observed by haematoxylin and eosin staining (data not shown) and no gene expression changes were detected for macrophage or B-lymphocyte specific genes. Further support for an alternative

explanation was based on comparing data from Duchene muscular dystrophy (DMD) models with our data, as up-regulation of complement components of the classical pathway has also been identified in mouse models for DMD [87, 88]. Like *SURF1* patients, DMD patients and mouse models showed a reduction of the activities of the OXPHOS complexes, secondary to the primary cytoskeleton defect. These activities were decreased to 50% of the normal activity in skeletal muscle (*m.quadriceps*) of dystrophin-deficient mdx mice [16]. No signs of inflammation were observed in *SURF1* patients, whereas infiltration of inflammatory cells has been identified in these mouse models [87]. Moreover, complement activation in DMD most likely results in necrosis of the muscle fibres [89, 90], which is not the case in muscle fibres of *SURF1* patients. This is also illustrated by the difference in the immunohistochemical staining pattern for complement component C3c for a *SURF1* patient, where C3c is mostly confined to muscle fibre membranes, and that of a muscle cryosection of a Duchene muscular dystrophy patient, which shows a more diffuse staining pattern (figure 1).

It has been reported that human skeletal myoblasts are able to express transcripts coding for complement components of the classical complement pathway themselves [91, 92]. The role of complement is broader than the immune system function alone and is also involved in bone and cartilage development, mammalian reproduction, and tissue and organ regeneration [93]. More specifically, complement component C3 can have a specific tissue regenerative effect in the urodeles limb after amputation. Blastema cells (embryonic-like cells as precursors for regeneration) derived from muscle, which have the ability to differentiate into myotubes, express C3 in regenerating limbs of urodeles [94]. C3 has also been directly related to regeneration of the liver. After partial hepatectomy and after toxic injury [95, 96], $C3^{-/-}$ mice showed a significant decrease in ability for liver regeneration, leading to an increased mortality. Rescuing of $C3^{-/-}$ mice by using human or murine C3 or C3a respectively, restored the regeneration process as illustrated by decreased parenchymal damage and increased hepatocyte proliferation. Similar observations were made in $C3^{-/-}$ mice treated with CCl_4 resulting in toxic injury of the liver [95].

The possibility of a regeneration process in muscle of *SURF1* patients was further supported by the microarray data. Two genes, interferon-related developmental regulator 1 (*IFRD1*) and insulin-like growth factor binding protein 3 (*IGFBP3*), which are involved in skeletal muscle development were both significantly up-regulated (1.7 and 4.5 fold respectively) in muscle of *SURF1* patients. IFRD1 is classified in the gene-ontology biological process myoblast cell fate determination and it has been described that deprivation of the protein results in an inhibition of differentiation in myoblasts [24]. IGFBP3 is annotated as a positive regulator of myoblast differentiation and it has been reported that IGFBP3 has a role in the differentiation of primary human adult skeletal myoblasts [25]. Evidence for the occurrence of muscle development in our *SURF1* patients is provided by the immunohistochemical data (figure 1), showing a positive staining of a number of muscle fibres for neonatal and foetal myosin. Finally, the *PMP22* gene, which encodes an integral membrane protein being a major component of myelin in the peripheral nervous system, was

significantly up-regulated. Various mutations in this gene are causative for Charcot-Marie-Tooth disease (MIM #118220), which is a demyelinating neuropathy. The role of PMP22 in other tissues appears to be more complex and PMP22 has been shown to regulate cell growth [97]. Taking all data together, the complement activation in muscle of *SURF1* patients most likely reflects a regeneration process rather than an immunological response, that might be triggered by the increased superoxide production of the impaired mitochondria and the resulting protein damage [98].

Conclusion

Mutations in the *SURF1* gene lead to a defect in complex IV assembly and to a deficient OXPHOS system. Although this does not lead to major alterations in transcription of OXPHOS genes, it leads to significantly increased levels of ROS due to an increased expression of ROS producing enzymes, resulting in extensive protein damage. This may trigger the activation of on the one hand the 20S complex of the proteasome to increase the capacity to breakdown damaged proteins and on the other hand of the complement system in turn inducing the process of muscle regeneration. A causative relation between these processes has to be established, but our data provide a new explanation on the pathological and rescue processes occurring in muscle of *SURF1* patients, which can assist in finding therapeutic approaches. Whether the processes observed are common to other OXPHOS disorders or OXHPOS disorders in general remains to be determined.

Supplementary table S1: QRT-PCR primers

Gene symbol	Forward primer (5'-3')	Reverse primer (5'-3')
ARF1	AATCAGCTCCGGAACCAGAA	GCAGAGGGCAAGAGGAGTGA
C1R	TCTGTGCTGGACACCCATCTC	GCAAAAACGCCCCCACTAT
C1S	TGGATAATGAAGACTATGCAGGAAAA	GGAGAGGCTGGTGGGATGTA
C3	TGGCCATTGAGCAGACCAT	CGTGCGCTGCTGTCCA
CLU	GCTGCAGGAATACCGCAAA	CCGTAGGTGCAAAAGCAACA
PKM2	TCATTGCTGTGACCCGGA	ACAGGGAAGATGCCACGGTA
PMP22	GGGACCGTGAGTTCCTAGAGC	CATTGCCAGACAGTCCTTGGA
RYR3	AGGAGAGCACCGGGTATATGG	GACTAGAGAGATGATGGTATGGATGATG
SLC16A3	GGGTGGGAACCGTGTCATT	GATGCCTTGTAACCTTGCGG

QRT-PCR primer sequences for ADP-ribosylation factor 1 (ARF1), complement component 1, r subcomponent (C1R), complement component, s subcomponent (C1S), complement component 3 (C3), clusterin (CLU), pyruvate kinase, muscle (PKM2), peripheral myelin protein 22 (PMP22), ryanodine receptor 3 (RYR3), and solute carrier family 16, member 3 (SLC16A3).

Supplementary Table S2: Differentially expressed genes

Unigene ID	FC	Symbol	Name	GO Biological Process	GO Level
Hs.436657	3.7	CLU	Clusterin	complement activation; innate immune response	5
Hs.155597	3.5	CFD	Complement factor D (adipsin)	complement activation; innate immune response	5
Hs.384598	2.7	SERPING1	Serpin peptidase inhibitor, clade G (C1 inhibitor), member 1, (angioedema, hereditary)	complement activation; innate immune response	5
Hs.363396	2.6	CFH	Complement factor H	complement activation; innate immune response	5
Hs.458355	2.3	C1S	Complement component 1, s subcomponent	complement activation; innate immune response	5
Hs.8986	1.4	C1QB	Complement component 1, q subcomponent, B chain	complement activation; innate immune response	5
Hs.502705	1.4	PRPF19	PRP19/PSO4 pre-mRNA processing factor 19 homolog (S. cerevisiae)	DNA metabolism	5
Hs.258429	1.4	ERCC5	Excision repair cross-complementing rodent repair deficiency, complementation group 5 (xeroderma pigmentosum, complementation group G (Cockayne syndrome))	DNA metabolism	5
Hs.519474	1.4		Transcribed locus, strongly similar to NP_001261.1 chromodomain helicase DNA binding protein 1 [Homo sapiens]	DNA metabolism	5
Hs.445078	1.3	TLK2	Tousled-like kinase 2	DNA metabolism	5
Hs.444118	1.3	MCM6	MCM6 minichromosome maintenance deficient 6 (MIS5 homolog, S. pombe) (S. cerevisiae)	DNA metabolism	5
Hs.475538	1.3	XPC	Xeroderma pigmentosum, complementation group C	DNA metabolism	5
Hs.53454	1.2	TOPBP1	Topoisomerase (DNA) II binding protein 1	DNA metabolism	5
Hs.88556	1.2	HDAC1	Histone deacetylase 1	DNA metabolism	5
Hs.501522	1.2	MGMT	O-6-methylguanine-DNA methyltransferase	DNA metabolism	5
Hs.269092	1.2	CDYL	Chromodomain protein, Y-like	DNA metabolism	5
Hs.555936	1.2	APEX2	APEX nuclease (apurinic/apyrimidinic endonuclease) 2	DNA metabolism	5
Hs.534331	1.2	NUDT1	Nudix (nucleoside diphosphate linked moiety X)-type motif 1	DNA metabolism	5
Hs.202672	1.1	DNMT1	DNA (cytosine-5-)-methyltransferase 1	DNA metabolism	5
Hs.1770	1.1	LIG1	Ligase I, DNA, ATP-dependent	DNA metabolism	5
Hs.75307	1.3	H1FX	H1 histone family, member X	DNA metabolism; protein complex assembly	5
Hs.76090	1.2	TNFAIP1	Tumor necrosis factor, alpha-induced protein 1 (endothelial)	DNA metabolism; protein complex assembly	5
Hs.406300	2.0	RPL23	Ribosomal protein L23	nuclear transport	5
Hs.247077	1.7	RHOA	Ras homolog gene family, member A	nuclear transport	5
Hs.12457	1.5	NUP133	Nucleoporin 133kDa	nuclear transport	5
Hs.523739	1.3	STX5	Syntaxin 5	nuclear transport	5
Hs.501023	1.3	MXI1	MAX interactor 1	nuclear transport	5
Hs.430589	1.2	CBLB	Cas-Br-M (murine) ecotropic retroviral transforming sequence b	nuclear transport	5
Hs.534373	1.4	VAMP8	Vesicle-associated membrane protein 8 (endobrevin)	protein complex assembly	5
Hs.31334	1.4	PRPF6	PRP6 pre-mRNA processing factor 6 homolog (S. cerevisiae)	protein complex assembly	5
Hs.459759	1.3	CREBBP	CREB binding protein (Rubinstein-Taybi syndrome)	protein complex assembly	5

Hs.502872	1.2	MAP3K11	Mitogen-activated protein kinase kinase kinase 11	protein complex assembly	5
Hs.87726	1.1	GGA3	Golgi associated, gamma adaptin ear containing, ARF binding protein 3	protein complex assembly	5
Hs.512464	0.4	SURF1	Surfeit 1	protein complex assembly	5
Hs.450230	4.5	IGFBP3	Insulin-like growth factor binding protein 3	regulation of cell size; cell growth	5
Hs.4055	2.2	KLF6	Kruppel-like factor 6	regulation of cell size; cell growth	5
Hs.274313	1.6	IGFBP6	Insulin-like growth factor binding protein 6	regulation of cell size; cell growth	5
Hs.67896	1.5	OGFR	Opioid growth factor receptor	regulation of cell size; cell growth	5
Hs.235935	1.3	NOV	Nephroblastoma overexpressed gene	regulation of cell size; cell growth	5
Hs.435326	1.5	ACTL6A	Actin-like 6A	regulation of cell size; cell growth; DNA metabolism	5
Hs.528299	1.1	HTATIP	HIV-1 Tat interacting protein, 60kDa	regulation of cell size; cell growth; DNA metabolism	5
Hs.23361	0.6	ABTB2	Ankyrin repeat and BTB (POZ) domain containing 2	regulation of cell size; cell growth; DNA metabolism; protein complex assembly	5
Hs.65029	2.3	GAS1	Growth arrest-specific 1	regulation of progression through cell cycle	5
Hs.282113	2.0	SNF1LK	SNF1-like kinase	regulation of progression through cell cycle	5
Hs.153752	1.6	CDC25B	Cell division cycle 25B	regulation of progression through cell cycle	5
Hs.371249	1.6	PTN	Pleiotrophin (heparin binding growth factor 8, neurite growth-promoting factor 1)	regulation of progression through cell cycle	5
Hs.504609	1.6	ID1	Inhibitor of DNA binding 1, dominant negative helix-loop-helix protein	regulation of progression through cell cycle	5
Hs.434286	1.5	CHES1	Checkpoint suppressor 1	regulation of progression through cell cycle	5
Hs.106070	1.5	CDKN1C	Cyclin-dependent kinase inhibitor 1C (p57, Kip2)	regulation of progression through cell cycle	5
Hs.82045	1.4	MDK	Midkine (neurite growth-promoting factor 2)	regulation of progression through cell cycle	5
Hs.336994	1.4	MTSS1	Metastasis suppressor 1	regulation of progression through cell cycle	5
Hs.483635	1.3	FGF1	Fibroblast growth factor 1 (acidic)	regulation of progression through cell cycle	5
Hs.152944	1.3	LOH11CR2A	Loss of heterozygosity, 11, chromosomal region 2, gene A	regulation of progression through cell cycle	5
Hs.505033	1.2	KRAS	V-Ki-ras2 Kirsten rat sarcoma viral oncogene homolog	regulation of progression through cell cycle	5
Hs.189772	1.2	CCT2	Chaperonin containing TCP1, subunit 2 (beta)	regulation of progression through cell cycle	5
Hs.202453	1.2	MYC	V-myc myelocytomatosis viral oncogene homolog (avian)	regulation of progression through cell cycle	5
Hs.239818	0.8	PIK3CB	Phosphoinositide-3-kinase, catalytic, beta polypeptide	regulation of progression through cell cycle	5
Hs.438720	1.3	MCM7	MCM7 minichromosome maintenance deficient 7 (S. cerevisiae)	regulation of progression through cell cycle; DNA metabolism	5
Hs.156519	1.3	MSH2	MutS homolog 2, colon cancer, nonpolyposis type 1 (E. coli)	regulation of progression through cell cycle; DNA metabolism	5
Hs.240457	1.2	RAD9A	RAD9 homolog A (S. pombe)	regulation of progression through cell cycle; DNA metabolism	5
Hs.446376	1.1	APC2	Adenomatosis polyposis coli 2	regulation of progression through cell cycle; protein complex assembly	5
Hs.50130	2.5	NDN	Necdin homolog (mouse)	regulation of progression through cell cycle; regulation of cell size; cell growth	5
Hs.408312	1.1	TP53	Tumor protein p53 (Li-Fraumeni syndrome)	regulation of progression through cell cycle; regulation of cell size; cell growth; DNA metabolism; protein complex assembly	5

Hs.512963	1.5	ALG11	Asparagine-linked glycosylation 11 homolog (S. cerevisiae, alpha-1,2-mannosyltransferase)	ribosome biogenesis and assembly	5
Hs.389649	1.4	DDX48	DEAD (Asp-Glu-Ala-Asp) box polypeptide 48	ribosome biogenesis and assembly	5
Hs.75528	1.3	GNL2	Guanine nucleotide binding protein-like 2 (nucleolar)	ribosome biogenesis and assembly	5
Hs.10848	1.3	BMS1L	BMS1-like, ribosome assembly protein (yeast)	ribosome biogenesis and assembly	5
Hs.499620	1.2	GEMIN4	Gem (nuclear organelle) associated protein 4	ribosome biogenesis and assembly	5
Hs.558447	1.2	EMG1	EMG1 nucleolar protein homolog (S. cerevisiae)	ribosome biogenesis and assembly	5
Hs.425777	1.8	UBE2L6	Ubiquitin-conjugating enzyme E2L 6	biopolymer metabolism	4
Hs.121575	1.6	CTSD	Cathepsin D (lysosomal aspartyl peptidase)	biopolymer metabolism	4
Hs.398157	1.6	PLK2	Polo-like kinase 2 (Drosophila)	biopolymer metabolism	4
Hs.480415	1.6	MANBA	Mannosidase, beta A, lysosomal	biopolymer metabolism	4
Hs.513617	1.5	MMP2	Matrix metallopeptidase 2 (gelatinase A, 72kDa gelatinase, 72kDa type IV collagenase)	biopolymer metabolism	4
Hs.12813	1.5	TIPARP	TCDD-inducible poly(ADP-ribose) polymerase	biopolymer metabolism	4
Hs.65436	1.4	LOXL1	Lysyl oxidase-like 1	biopolymer metabolism	4
Hs.184523	1.4	STK38L	Serine/threonine kinase 38 like	biopolymer metabolism	4
Hs.532357	1.4	TRIM21	Tripartite motif-containing 21	biopolymer metabolism	4
Hs.387208	1.4	FAU	Finkel-Biskis-Reilly murine sarcoma virus (FBR-MuSV) ubiquitously expressed (fox derived); ribosomal protein S30	biopolymer metabolism	4
Hs.154163	1.3	PRMT2	Protein arginine methyltransferase 2	biopolymer metabolism	4
Hs.524692	1.3	NUAK1	NUAK family, SNF1-like kinase, 1	biopolymer metabolism	4
Hs.529420	1.3	UBE2G2	Ubiquitin-conjugating enzyme E2G 2 (UBC7 homolog, yeast)	biopolymer metabolism	4
Hs.433728	1.2	MAPK4	Mitogen-activated protein kinase 4	biopolymer metabolism	4
Hs.234282	1.2	VPS11	Vacuolar protein sorting 11 (yeast)	biopolymer metabolism	4
Hs.171596	1.2	EPHA2	EPH receptor A2	biopolymer metabolism	4
Hs.422662	1.1	VRK1	Vaccinia related kinase 1	biopolymer metabolism	4
Hs.59138	1.1	GYPC	Glycophorin C (Gerbich blood group)	biopolymer metabolism	4
Hs.513926	1.1	SENP3	SUMO1/sentrin/SMT3 specific peptidase 3	biopolymer metabolism	4
Hs.95424	0.9	MAP4K1	Mitogen-activated protein kinase kinase kinase kinase 1	biopolymer metabolism	4
Hs.469809	0.8	PTPN4	Protein tyrosine phosphatase, non-receptor type 4 (megakaryocyte)	biopolymer metabolism	4
Hs.51133	0.8	PTK6	PTK6 protein tyrosine kinase 6	biopolymer metabolism	4
Hs.132760	0.7	SLC37A4	Solute carrier family 37 (glycerol-6-phosphate transporter), member 4	biopolymer metabolism	4
Hs.227777	0.4	PTP4A1	Protein tyrosine phosphatase type IVA, member 1	biopolymer metabolism	4
Hs.467097	2.1	SNRP70	Small nuclear ribonucleoprotein 70kDa polypeptide (RNP antigen)	biopolymer metabolism; nucleobase, nucleoside, nucleotide and nucleic acid metabolism	4
Hs.474018	1.7	ADARB1	Adenosine deaminase, RNA-specific, B1 (RED1 homolog rat)	biopolymer metabolism; nucleobase, nucleoside, nucleotide and nucleic acid metabolism	4

Hs.493202	1.5	CPSF1	Cleavage and polyadenylation specific factor 1, 160kDa	biopolymer metabolism; nucleobase, nucleoside, nucleotide and nucleic acid metabolism	4
Hs.83753	1.5	SNRPB	Small nuclear ribonucleoprotein polypeptides B and B1	biopolymer metabolism; nucleobase, nucleoside, nucleotide and nucleic acid metabolism	4
Hs.525006	1.4	NUFIP1	Nuclear fragile X mental retardation protein interacting protein 1	biopolymer metabolism; nucleobase, nucleoside, nucleotide and nucleic acid metabolism	4
Hs.512610	1.3	LSM7	LSM7 homolog, U6 small nuclear RNA associated (S. cerevisiae)	biopolymer metabolism; nucleobase, nucleoside, nucleotide and nucleic acid metabolism	4
Hs.188879	1.2	RBM6	RNA binding motif protein 6	biopolymer metabolism; nucleobase, nucleoside, nucleotide and nucleic acid metabolism	4
Hs.380277	1.3	DAPK1	Death-associated protein kinase 1	biopolymer metabolism; positive regulation of cellular physiological process	4
Hs.510528	1.1	TRAF3	TNF receptor-associated factor 3	biopolymer metabolism; positive regulation of cellular physiological process	4
Hs.183006	1.3	GLCE	UDP-glucuronic acid epimerase	cellular morphogenesis	4
Hs.522632	1.8	TIMP1	TIMP metallopeptidase inhibitor 1	cellular morphogenesis; regulation of cell proliferation; negative regulation of cellular physiological process; positive regulation of cellular physiological process	4
Hs.1735	3.1	INHBB	Inhibin, beta B (activin AB beta polypeptide)	negative regulation of cellular physiological process	4
Hs.370666	2.0	FOXO1A	Forkhead box O1A (rhabdomyosarcoma)	negative regulation of cellular physiological process; nucleobase, nucleoside, nucleotide and nucleic acid metabolism	4
Hs.373550	1.4	TGIF	TGFB-induced factor (TALE family homeobox)	negative regulation of cellular physiological process; nucleobase, nucleoside, nucleotide and nucleic acid metabolism	4
Hs.377090	1.3	ZHX2	Zinc fingers and homeoboxes 2	negative regulation of cellular physiological process; nucleobase, nucleoside, nucleotide and nucleic acid metabolism	4
Hs.522373	3.0	GSN	Gelsolin (amyloidosis, Finnish type)	negative regulation of cellular physiological process; organelle organization and biogenesis	4
Hs.440829	4.6	CEBPD	CCAAT/enhancer binding protein (C/EBP), delta	nucleobase, nucleoside, nucleotide and nucleic acid metabolism	4
Hs.513305	1.8	TFAP4	Transcription factor AP-4 (activating enhancer binding protein 4)	nucleobase, nucleoside, nucleotide and nucleic acid metabolism	4
Hs.462693	1.7	ZNF22	Zinc finger protein 22 (KOX 15)	nucleobase, nucleoside, nucleotide and nucleic acid metabolism	4
Hs.288856	1.6	PFDN5	Prefoldin subunit 5	nucleobase, nucleoside, nucleotide and nucleic acid metabolism	4
Hs.14839	1.6	POLR2G	Polymerase (RNA) II (DNA directed) polypeptide G	nucleobase, nucleoside, nucleotide and nucleic acid metabolism	4
Hs.76884	1.6	ID3	Inhibitor of DNA binding 3, dominant negative helix-loop-helix protein	nucleobase, nucleoside, nucleotide and nucleic acid metabolism	4
Hs.82071	1.6	CITED2	Cbp/p300-interacting transactivator, with Glu/Asp-rich carboxy-terminal domain, 2	nucleobase, nucleoside, nucleotide and nucleic acid metabolism	4
Hs.522074	1.6	TSC22D3	TSC22 domain family, member 3	nucleobase, nucleoside, nucleotide and nucleic acid metabolism	4
Hs.77890	1.5	GUCY1B3	Guanylate cyclase 1, soluble, beta 3	nucleobase, nucleoside, nucleotide and nucleic acid metabolism	4
Hs.194669	1.4	EZH1	Enhancer of zeste homolog 1 (Drosophila)	nucleobase, nucleoside, nucleotide and nucleic acid metabolism	4

Hs.43697	1.3	ETV5	Ets variant gene 5 (ets-related molecule)	nucleobase, nucleoside, nucleotide and nucleic acid metabolism	4
Hs.327527	1.3	SMARCA4	SWI/SNF related, matrix associated, actin dependent regulator of chromatin, subfamily a, member 4	nucleobase, nucleoside, nucleotide and nucleic acid metabolism	4
Hs.532277	1.3	ZNF250	Zinc finger protein 250	nucleobase, nucleoside, nucleotide and nucleic acid metabolism	4
Hs.200250	1.3	CREM	CAMP responsive element modulator	nucleobase, nucleoside, nucleotide and nucleic acid metabolism	4
Hs.388236	1.2	CIC	Capicua homolog (Drosophila)	nucleobase, nucleoside, nucleotide and nucleic acid metabolism	4
Hs.273621	1.2	CNP	2',3'-cyclic nucleotide 3' phosphodiesterase	nucleobase, nucleoside, nucleotide and nucleic acid metabolism	4
Hs.505004	1.2	TCEA2	Transcription elongation factor A (SII), 2	nucleobase, nucleoside, nucleotide and nucleic acid metabolism	4
Hs.584839	1.2	POLR1C	Polymerase (RNA) I polypeptide C, 30kDa	nucleobase, nucleoside, nucleotide and nucleic acid metabolism	4
Hs.371987	1.2	NFAT5	Nuclear factor of activated T-cells 5, tonicity-responsive	nucleobase, nucleoside, nucleotide and nucleic acid metabolism	4
Hs.89781	1.2	UBTF	Upstream binding transcription factor, RNA polymerase I	nucleobase, nucleoside, nucleotide and nucleic acid metabolism	4
Hs.440219	1.1	UBN1	Ubinuclein 1	nucleobase, nucleoside, nucleotide and nucleic acid metabolism	4
Hs.158174	1.1	ZNF184	Zinc finger protein 184 (Kruppel-like)	nucleobase, nucleoside, nucleotide and nucleic acid metabolism	4
Hs.432574	1.1	POLR2H	Polymerase (RNA) II (DNA directed) polypeptide H	nucleobase, nucleoside, nucleotide and nucleic acid metabolism	4
Hs.124553	1.1	ZNF263	Zinc finger protein 263	nucleobase, nucleoside, nucleotide and nucleic acid metabolism	4
Hs.409876	1.1	ZBTB24	Zinc finger and BTB domain containing 24	nucleobase, nucleoside, nucleotide and nucleic acid metabolism	4
Hs.21771	1.1	WHSC2	Wolf-Hirschhorn syndrome candidate 2	nucleobase, nucleoside, nucleotide and nucleic acid metabolism	4
Hs.178728	0.8	MBD3	Methyl-CpG binding domain protein 3	nucleobase, nucleoside, nucleotide and nucleic acid metabolism	4
Hs.515053	0.8	AES	Amino-terminal enhancer of split	nucleobase, nucleoside, nucleotide and nucleic acid metabolism	4
Hs.332173	0.7	TLE2	Transducin-like enhancer of split 2 (E(sp1) homolog, Drosophila)	nucleobase, nucleoside, nucleotide and nucleic acid metabolism	4
Hs.518249	0.6	CNBP	Zinc finger protein 9	nucleobase, nucleoside, nucleotide and nucleic acid metabolism	4
Hs.300701	1.9	TUBB2B	Tubulin, beta 2B	organelle organization and biogenesis	4
Hs.444767	1.5	KIF13B	Kinesin family member 13B	organelle organization and biogenesis	4
Hs.325528	1.2		Transcribed locus, strongly similar to NP_004937.1 dedicator of cytokinesis 2; dedicator of cyto-kinesis 2 [Homo sapiens]	organelle organization and biogenesis	4
Hs.138378	1.8	CASP4	Caspase 4, apoptosis-related cysteine peptidase	positive regulation of cellular physiological process	4
Hs.432330	0.8	RRAGA	Ras-related GTP binding A	positive regulation of cellular physiological process	4
Hs.367725	1.4	GATA2	GATA binding protein 2	positive regulation of cellular physiological process; nucleobase, nucleoside, nucleotide and nucleic acid metabolism	4
Hs.459070	0.5	ARNT2	Aryl-hydrocarbon receptor nuclear translocator 2	positive regulation of cellular physiological process; nucleobase, nucleoside, nucleotide and nucleic acid metabolism	4
Hs.1565	0.6	NEDD4	Neural precursor cell expressed, developmentally down-regulated 4	regulation of cell cycle; DNA repair; negative regulation of cellular physiological process; biopolymer metabolism; biopolymer metabolism; nucleobase, nucleoside, nucleotide and nucleic acid metabolism	4
Hs.372031	4.9	PMP22	Peripheral myelin protein 22	regulation of cell proliferation; negative regulation of cellular physiological process	4

Hs.17466	1.9	RARRES3	Retinoic acid receptor responder (tazarotene induced) 3	regulation of cell proliferation; negative regulation of cellular physiological process	4
Hs.512680	1.4	CLEC11A	C-type lectin domain family 11, member A	regulation of cell proliferation; positive regulation of cellular physiological process	4
Hs.514581	2.2	ACTG1	Actin, gamma 1	cell cycle	3
Hs.469615	1.7	sep-10	Septin 10	cell cycle	3
Hs.244580	1.2	TPX2	TPX2, microtubule-associated, homolog (Xenopus laevis)	cell cycle; cell proliferation	3
Hs.522114	1.6	CLTA	Clathrin, light polypeptide (Lca)	cell organization and biogenesis	3
Hs.441498	1.3	STAM	Signal transducing adaptor molecule (SH3 domain and ITAM motif) 1	cell organization and biogenesis	3
Hs.464779	1.3	NPC1	Niemann-Pick disease, type C1	cell organization and biogenesis	3
Hs.531752	1.1	RANBP3	RAN binding protein 3	cell organization and biogenesis	3
Hs.531561	1.8	EMP2	Epithelial membrane protein 2	cell proliferation	3
Hs.315177	0.8	IFRD2	Interferon-related developmental regulator 2	cell proliferation	3
Hs.567497	3.1	C1R	Complement component 1, r subcomponent	macromolecule metabolism; primary metabolism	3
Hs.356794	1.8	RPS24	Ribosomal protein S24	macromolecule metabolism; primary metabolism	3
Hs.496593	1.7	CAPN6	Calpain 6	macromolecule metabolism; primary metabolism	3
Hs.433529	1.6	RPS11	Ribosomal protein S11	macromolecule metabolism; primary metabolism	3
Hs.516493	1.6	FAP	Fibroblast activation protein, alpha	macromolecule metabolism; primary metabolism	3
Hs.408073	1.6	RPS6	Ribosomal protein S6	macromolecule metabolism; primary metabolism	3
Hs.429180	1.5	EIF2S2	Eukaryotic translation initiation factor 2, subunit 2 beta, 38kDa	macromolecule metabolism; primary metabolism	3
Hs.477891	1.4	CPB1	Carboxypeptidase B1 (tissue)	macromolecule metabolism; primary metabolism	3
Hs.438429	1.4	RPS19	Ribosomal protein S19	macromolecule metabolism; primary metabolism	3
Hs.419240	1.3	SLC2A14	Solute carrier family 2 (facilitated glucose transporter), member 14	macromolecule metabolism; primary metabolism	3
Hs.436405	1.2	IDH3B	Isocitrate dehydrogenase 3 (NAD+) beta	macromolecule metabolism; primary metabolism	3
Hs.75859	1.2	MRPL49	Mitochondrial ribosomal protein L49	macromolecule metabolism; primary metabolism	3
Hs.412433	1.2	AIP	Aryl hydrocarbon receptor interacting protein	macromolecule metabolism; primary metabolism	3
Hs.91161	1.2	PFDN4	Prefoldin subunit 4	macromolecule metabolism; primary metabolism	3
Hs.500156	1.1	DNAJC7	DnaJ (Hsp40) homolog, subfamily C, member 7	macromolecule metabolism; primary metabolism	3
Hs.54470	0.9	ABCC8	ATP-binding cassette, sub-family C (CFTR/MRP), member 8	macromolecule metabolism; primary metabolism	3
Hs.298469	0.9	ACE	Angiotensin I converting enzyme (peptidyl-dipeptidase A) 1	macromolecule metabolism; primary metabolism	3
Hs.179704	0.7	MEP1A	Meprin A, alpha (PABA peptide hydrolase)	macromolecule metabolism; primary metabolism	3
Hs.466471	0.7	GPI	Glucose phosphate isomerase	macromolecule metabolism; primary metabolism	3
Hs.501200	1.6	RGS10	Regulator of G-protein signalling 10	negative regulation of cellular process	3
Hs.9914	1.8	FST	Follistatin	negative regulation of cellular process; negative regulation of physiological process	3

Hs.443625	3.7	COL3A1	Collagen, type III, alpha 1 (Ehlers-Danlos syndrome type IV, autosomal dominant)	organ morphogenesis	3
Hs.409034	2.2	COL15A1	Collagen, type XV, alpha 1	organ morphogenesis	3
Hs.82116	1.8	MYD88	Myeloid differentiation primary response gene (88)	positive regulation of cellular process	3
Hs.1116	1.2	LTBR	Lymphotoxin beta receptor (TNFR superfamily, member 3)	positive regulation of cellular process	3
Hs.405156	2.0	PPAP2B	Phosphatidic acid phosphatase type 2B	primary metabolism	3
Hs.200136	1.8	ACAA2	Acetyl-Coenzyme A acyltransferase 2 (mitochondrial 3-oxoacyl-Coenzyme A thiolase)	primary metabolism	3
Hs.533514	1.7	ASMTL	Acetylserotonin O-methyltransferase-like	primary metabolism	3
Hs.195040	1.5	HSD11B1	Hydroxysteroid (11-beta) dehydrogenase 1	primary metabolism	3
Hs.512670	1.3	BCAT2	Branched chain aminotransferase 2, mitochondrial	primary metabolism	3
Hs.467554	1.1	TPO	Thyroid peroxidase	primary metabolism	3
Hs.319438	1.1	PLA2G5	Phospholipase A2, group V	primary metabolism	3
Hs.75069	1.1	SHMT2	Serine hydroxymethyltransferase 2 (mitochondrial)	primary metabolism	3
Hs.481551	0.8	MTRR	5-methyltetrahydrofolate-homocysteine methyltransferase reductase	primary metabolism	3
Hs.76244	0.7	SRM	Spermidine synthase	primary metabolism	3
Hs.200841	1.6	LAMA2	Laminin, alpha 2 (merosin, congenital muscular dystrophy)	regulation of cellular physiological process	3
Hs.192233	2.7	PPL	Periplakin	cell differentiation	2
Hs.516505	1.6	S100A13	S100 calcium binding protein A13	cell differentiation	2
Hs.495710	1.5	GPM6B	Glycoprotein M6B	cell differentiation	2
Hs.7879	1.7	IFRD1	Interferon-related developmental regulator 1	cell differentiation; organ development	2
Hs.533317	3.7	VIM	Vimentin	cellular physiological process	2
Hs.508716	3.1	COL4A2	Collagen, type IV, alpha 2	cellular physiological process	2
Hs.514412	2.2	PECAM1	Platelet/endothelial cell adhesion molecule (CD31 antigen)	cellular physiological process	2
Hs.519909	2.0	MARCKS	Myristoylated alanine-rich protein kinase C substrate	cellular physiological process	2
Hs.529571	2.0	RBP1	Retinol binding protein 1, cellular	cellular physiological process	2
Hs.58351	2.0	ABCA8	ATP-binding cassette, sub-family A (ABC1), member 8	cellular physiological process	2
Hs.567352	1.9	TXNRD1	Thioredoxin reductase 1	cellular physiological process	2
Hs.513058	1.6	TMED3	Transmembrane emp24 protein transport domain containing 3	cellular physiological process	2
Hs.77422	1.5	PLP2	Proteolipid protein 2 (colonic epithelium-enriched)	cellular physiological process	2
Hs.47629	1.5	COL21A1	Collagen, type XXI, alpha 1	cellular physiological process	2
Hs.474783	1.4	TST	Thiosulfate sulfurtransferase (rhodanese)	cellular physiological process	2
Hs.501868	1.4	TMEM41B	Transmembrane protein 41B	cellular physiological process	2
Hs.32309	1.3	INPP1	Inositol polyphosphate-1-phosphatase	cellular physiological process	2
Hs.472270	1.3	RIN2	Ras and Rab interactor 2	cellular physiological process	2
Hs.253420	0.8	NOS1	Nitric oxide synthase 1 (neuronal)	cellular physiological process	2
Hs.323878	0.7	SLC1A4	Solute carrier family 1 (glutamate/neutral amino acid transporter), member 4	cellular physiological process	2

Hs.587054	0.7	G3BP	Ras-GTPase-activating protein SH3-domain-binding protein	cellular physiological process	2
Hs.369250	0.4	RYR3	Ryanodine receptor 3	cellular physiological process	2
Hs.500761	0.4	SLC16A3	Solute carrier family 16 (monocarboxylic acid transporters), member 3	cellular physiological process	2
Hs.200629	0.7	KCNJ12	Potassium inwardly-rectifying channel, subfamily J, member 12	cellular physiological process; regulation of physiological process	2
Hs.476092	3.3	CLEC3B	C-type lectin domain family 3, member B	organ development	2
Hs.515369	1.9	TYROBP	TYRO protein tyrosine kinase binding protein	response to stress	2
Hs.325978	1.3	NUMA1	Nuclear mitotic apparatus protein 1	response to stress	2
Hs.1570	1.3	HRH1	Histamine receptor H1	response to stress	2
Hs.275775	2.5	SEPP1	Selenoprotein P, plasma, 1	response to stress; cellular physiological process	2
Hs.386793	1.8	GPX3	Glutathione peroxidase 3 (plasma)	response to stress; cellular physiological process	2
Hs.2030	1.5	THBD	Thrombomodulin	response to stress; cellular physiological process	2
Hs.153381	2.5	DARC	Duffy blood group, chemokine receptor	cellular process	1
Hs.505337	2.3	CLDN5	Claudin 5 (transmembrane protein deleted in velocardiofacial syndrome)	cellular process	1
Hs.356624	2.0	NID1	Nidogen 1	cellular process	1
Hs.471751	1.8	CMKOR1	Chemokine orphan receptor 1	cellular process	1
Hs.2465	1.6	P2RY14	Purinergic receptor P2Y, G-protein coupled, 14	cellular process	1
Hs.421986	1.5	CXCR4	Chemokine (C-X-C motif) receptor 4	cellular process	1
Hs.514242	1.4	PLEKHM1	Pleckstrin homology domain containing, family M (with RUN domain) member 1	cellular process	1
Hs.109225	1.4	VCAM1	Vascular cell adhesion molecule 1	cellular process	1
Hs.444362	1.3	LPP	LIM domain containing preferred translocation partner in lipoma	cellular process	1
Hs.56045	1.2	STAC	SH3 and cysteine rich domain	cellular process	1
Hs.433300	1.2	FCER1G	Fc fragment of IgE, high affinity I, receptor for; gamma polypeptide	cellular process	1
Hs.500771	1.2	DNMBP	Dynamin binding protein	cellular process	1
Hs.529846	1.2	CAMLG	Calcium modulating ligand	cellular process	1
Hs.449076	1.2	PWP2H	PWP2 periodic tryptophan protein homolog (yeast)	cellular process	1
Hs.67846	1.1	LILRB1	Leukocyte immunoglobulin-like receptor, subfamily B (with TM and ITIM domains), member 1	cellular process	1
Hs.529449	0.9	APBB3	Amyloid beta (A4) precursor protein-binding, family B, member 3	cellular process	1
Hs.523360	0.9	INPP5A	Inositol polyphosphate-5-phosphatase, 40kDa	cellular process	1
Hs.519873	1.5	DSP	Desmoplakin	development	1
Hs.97616	1.3	SH3GL1	SH3-domain GRB2-like 1	development; cellular process	1
Hs.434971	1.2	TRO	Trophinin	development; cellular process	1
Hs.524116	1.2	NRGN	Neurogranin (protein kinase C substrate, RC3)	development; cellular process	1
Hs.440168	0.6	DSCR1L1	Down syndrome critical region gene 1-like 1	development; cellular process	1
Hs.436204	1.4	ZNF289	Zinc finger protein 289, ID1 regulated	regulation of biological process	1
Hs.485717	0.9	SMAP1	Stromal membrane-associated protein 1	regulation of biological process	1

Hs.503165	1.3	CENTD2	Centaurin, delta 2	regulation of biological process; cellular process	1
Hs.503911	7.1	NNMT	Nicotinamide N-methyltransferase	NA	0
Hs.593775	4.7		Data not found	NA	0
Hs.604114	3.6		Transcribed locus	NA	0
Hs.597039	2.8		Transcribed locus	NA	0
Hs.593731	2.6		Transcribed locus	NA	0
Hs.523012	2.6	DDIT4	DNA-damage-inducible transcript 4	NA	0
Hs.503709	2.6	TMEM123	Transmembrane protein 123	NA	0
Hs.630569	2.5		Transcribed locus	NA	0
Hs.85155	2.4	ZFP36L1	Zinc finger protein 36, C3H type-like 1	NA	0
Hs.458573	2.4	PDGFRL	Platelet-derived growth factor receptor-like	NA	0
Hs.6434	2.4	C14orf132	Chromosome 14 open reading frame 132	NA	0
Hs.533977	2.1	TXNIP	Thioredoxin interacting protein	NA	0
Hs.633687	2.1		Transcribed locus	NA	0
Hs.630420	2.0		Transcribed locus	NA	0
Hs.75348	2.0	PSME1	Proteasome (prosome, macropain) activator subunit 1 (PA28 alpha)	NA	0
Hs.465761	1.9	ARHGEF18	Rho/rac guanine nucleotide exchange factor (GEF) 18	NA	0
Hs.523414	1.9	IGF2	Insulin-like growth factor 2 (somatomedin A)	NA	0
Hs.522665	1.8	MAGED2	Melanoma antigen family D, 2	NA	0
Hs.376046	1.7	BTN3A2	Butyrophilin, subfamily 3, member A2	NA	0
Hs.594675	1.7		Transcribed locus	NA	0
Hs.150718	1.7	JAM3	Junctional adhesion molecule 3	NA	0
Hs.642681	1.7		Data not found	NA	0
Hs.633245	1.6		Data not found	NA	0
Hs.631504	1.5	RASSF2	Ras association (RalGDS/AF-6) domain family 2	NA	0
Hs.525462	1.5	C1orf41	Chromosome 1 open reading frame 41	NA	0
Hs.591258	1.5	CD74	CD74 molecule, major histocompatibility complex, class II invariant chain	NA	0
Hs.632486	1.5	MCL1	Myeloid cell leukemia sequence 1 (BCL2-related)	NA	0
Hs.412117	1.5	ANXA6	Annexin A6	NA	0
Hs.602328	1.5		Transcribed locus	NA	0
Hs.144492	1.5	PLCE1	Phospholipase C, epsilon 1	NA	0
Hs.434219	1.5	ANKHD1	Ankyrin repeat and KH domain containing 1	NA	0
Hs.592158	1.5		Data not found	NA	0
Hs.603387	1.5		Transcribed locus	NA	0
Hs.562227	1.5	HSPG2	Heparan sulfate proteoglycan 2 (perlecan)	NA	0

Hs.592182	1.5	AMPH	Amphiphysin (Stiff-Man syndrome with breast cancer 128kDa autoantigen)	NA	0
Hs.520102	1.4	KIAA0082	KIAA0082	NA	0
Hs.632776	1.4	C22orf28	Hypothetical protein HSPC117	NA	0
Hs.429434	1.4	GAB2	GRB2-associated binding protein 2	NA	0
Hs.194816	1.4	STOML1	Stomatin (EPB72)-like 1	NA	0
Hs.304682	1.4	CST3	Cystatin C (amyloid angiopathy and cerebral hemorrhage)	NA	0
Hs.195740	1.4	AATF	Apoptosis antagonizing transcription factor	NA	0
Hs.508010	1.4	FNDC3A	Fibronectin type III domain containing 3A	NA	0
Hs.279902	1.4	CRSP9	Cofactor required for Sp1 transcriptional activation, subunit 9, 33kDa	NA	0
Hs.617685	1.4		Transcribed locus	NA	0
Hs.592088	1.4	ZNF205	Zinc finger protein 205	NA	0
Hs.593551	1.4		Transcribed locus	NA	0
Hs.447458	1.4	C10orf6	Chromosome 10 open reading frame 6	NA	0
Hs.20013	1.4	SYF2	SYF2 homolog, RNA splicing factor (S. cerevisiae)	NA	0
Hs.637254	1.4		Transcribed locus	NA	0
Hs.556496	1.4	TANK	TRAF family member-associated NFKB activator	NA	0
Hs.592324	1.4	PSEN1	Presenilin 1 (Alzheimer disease 3)	NA	0
Hs.592044	1.4	RSL1D1	Ribosomal L1 domain containing 1	NA	0
Hs.198853	1.3	C12orf32	Chromosome 12 open reading frame 32	NA	0
Hs.47338	1.3	IFIT3	Interferon-induced protein with tetratricopeptide repeats 3	NA	0
Hs.103834	1.3	TMEM106C	Transmembrane protein 106C	NA	0
Hs.643014	1.3		Transcribed locus	NA	0
Hs.98041	1.3	ZFYVE26	Zinc finger, FYVE domain containing 26	NA	0
Hs.632264	1.3	TGIF2	TGFB-induced factor 2 (TALE family homeobox)	NA	0
Hs.631844	1.3	DAPK3	Death-associated protein kinase 3	NA	0
Hs.484242	1.3	UBXD8	UBX domain containing 8	NA	0
Hs.597347	1.3		Transcribed locus	NA	0
Hs.595312	1.3		Transcribed locus	NA	0
Hs.99093	1.3	ZNF428	Chromosome 19 open reading frame 37	NA	0
Hs.458644	1.3	R3HCC1	R3H domain and coiled-coil containing 1	NA	0
Hs.591457	1.3	POLR3C	Polymerase (RNA) III (DNA directed) polypeptide C (62kD)	NA	0
Hs.631919	1.3	USP4	Ubiquitin specific peptidase 4 (proto-oncogene)	NA	0
Hs.622982	1.3		Transcribed locus	NA	0
Hs.37616	1.3	STRA13	Stimulated by retinoic acid 13 homolog (mouse)	NA	0
Hs.594086	1.2		Transcribed locus	NA	0

Hs.104661	1.2	C19orf7	Chromosome 19 open reading frame 7	NA	0
Hs.99821	1.2	C10orf22	Chromosome 10 open reading frame 22	NA	0
Hs.461860	1.2	NUP214	Nucleoporin 214kDa	NA	0
Hs.466714	1.2	PAF1	Paf1, RNA polymerase II associated factor, homolog (S. cerevisiae)	NA	0
Hs.65234	1.2	DDX27	DEAD (Asp-Glu-Ala-Asp) box polypeptide 27	NA	0
Hs.591449	1.2	MTF2	Metal response element binding transcription factor 2	NA	0
Hs.493309	1.2	KIAA0020	KIAA0020	NA	0
Hs.89497	1.2	LMNB1	Lamin B1	NA	0
Hs.522662	1.2	TSR2	Hypothetical protein DT1P1A10	NA	0
Hs.613614	1.2		Transcribed locus	NA	0
Hs.634602	1.2		Transcribed locus	NA	0
Hs.433269	1.2	C14orf11	Chromosome 14 open reading frame 11	NA	0
Hs.191046	1.2	PDE1A	Phosphodiesterase 1A, calmodulin-dependent	NA	0
Hs.606668	1.2		Transcribed locus	NA	0
Hs.591036	1.2	MDM1	Mdm4, transformed 3T3 cell double minute 1, p53 binding protein (mouse)	NA	0
Hs.592298	1.2	PPM1A	Protein phosphatase 1A (formerly 2C), magnesium-dependent, alpha isoform	NA	0
Hs.352614	1.2	AGPAT7	1-acylglycerol-3-phosphate O-acyltransferase 7 (lysophosphatidic acid acyltransferase, eta)	NA	0
Hs.557646	1.2	CDK9	Cyclin-dependent kinase 9 (CDC2-related kinase)	NA	0
Hs.567236	1.2	SHROOM2	Apical protein-like (Xenopus laevis)	NA	0
Hs.458360	1.2	UCK2	Uridine-cytidine kinase 2	NA	0
Hs.642711	1.2		Data not found	NA	0
Hs.512627	1.2	INTS10	Integrator complex subunit 10	NA	0
Hs.21811	1.1	CCDC94	Coiled-coil domain containing 94	NA	0
Hs.9043	1.1	C14orf120	Chromosome 14 open reading frame 120	NA	0
Hs.618686	1.1		Transcribed locus	NA	0
Hs.596659	0.9		Data not found	NA	0
Hs.517331	0.9	C21orf2	Chromosome 21 open reading frame 2	NA	0
Hs.519702	0.9	CYFIP2	Cytoplasmic FMR1 interacting protein 2	NA	0
Hs.213666	0.9	KIAA0460	KIAA0460	NA	0
Hs.603821	0.9		Transcribed locus	NA	0
Hs.460499	0.9	ATXN2L	Ataxin 2-like	NA	0
Hs.440364	0.8	DYNC1I1	Dynein, cytoplasmic 1, intermediate chain 1	NA	0
Hs.491354	0.8	EXTL3	Exostoses (multiple)-like 3	NA	0
Hs.444212	0.8	VSNL1	Visinin-like 1	NA	0
Hs.371222	0.8	TMEM110	Transmembrane protein 110	NA	0

Hs.568509	0.8	ARHGEF2	Rho/rac guanine nucleotide exchange factor (GEF) 2	NA	0
Hs.475125	0.8	ATXN10	Ataxin 10	NA	0
Hs.145269	0.8	TNFRSF10C	Tumor necrosis factor receptor superfamily, member 10c, decoy without an intracellular domain	NA	0
Hs.637251	0.8		Transcribed locus	NA	0
Hs.632200	0.8	THAP11	THAP domain containing 11	NA	0
Hs.598124	0.7		Transcribed locus	NA	0
Hs.370187	0.7	STAU1	Staufen, RNA binding protein, homolog 1 (Drosophila)	NA	0
Hs.632480	0.7	DENND4B	DENN/MADD domain containing 4B	NA	0
Hs.468140	0.7	FAM98A	Family with sequence similarity 98, member A	NA	0
Hs.635459	0.7		Transcribed locus	NA	0
Hs.116244	0.6	WDR62	WD repeat domain 62	NA	0
Hs.591761	0.6	HOMER1	Homer homolog 1 (Drosophila)	NA	0
Hs.600886	0.5		Transcribed locus	NA	0
Hs.534770	0.4	PKM2	Pyruvate kinase, muscle	NA	0

Differentially expressed genes between Leigh patients with a SURF1 mutation and controls. Gene Ontology annotations are listed as specific as possible (highest level). FC: fold change, NA: not annotated.

Supplementary table S3: Significantly enriched gene ontology biological process terms

GO Level	GO Term	Count	%	p-value
5	regulation of progression through cell cycle	21	6.8%	0.0003
5	complement activation	6	1.9%	0.0005
5	regulation of cell size	10	3.2%	0.0020
5	cell growth	10	3.2%	0.0020
5	DNA metabolism	23	7.4%	0.0044
5	innate immune response	6	1.9%	0.0074
5	ribosome biogenesis and assembly	6	1.94%	0.0116
5	protein complex assembly	11	3.6%	0.0313
5	nuclear transport	6	1.9%	0.0452
4	regulation of cell cycle	21	6.8%	0.0002
4	DNA repair	13	4.2%	0.0009
4	regulation of cell growth	9	2.9%	0.0013
4	regulation of cell size	10	3.2%	0.0018
4	cellular morphogenesis	13	4.2%	0.0036
4	innate immune response	6	1.9%	0.0070
4	regulation of cell proliferation	12	3.9%	0.0175
4	negative regulation of cellular physiological process	20	6.5%	0.0192
4	biopolymer metabolism	65	21.0%	0.0240
4	cytoplasm organization and biogenesis	6	1.9%	0.0253
4	positive regulation of cellular physiological process	15	4.8%	0.0302
4	nucleobase, nucleoside, nucleotide and nucleic acid metabolism	77	24.9%	0.0340
4	organelle organization and biogenesis	23	7.4%	0.0432
3	cell cycle	31	10.0%	0.0000
3	response to DNA damage stimulus	15	4.8%	0.0002
3	regulation of cell growth	9	2.9%	0.0014
3	cell growth	10	3.2%	0.0019
3	regulation of cellular physiological process	80	25.9%	0.0033
3	cellular morphogenesis	13	4.2%	0.0039
3	cell organization and biogenesis	42	13.6%	0.0047
3	positive regulation of cellular process	19	6.1%	0.0079
3	cell proliferation	19	6.1%	0.0080
3	negative regulation of cellular process	23	7.4%	0.0084
3	organ morphogenesis	10	3.2%	0.0157
3	negative regulation of physiological process	21	6.8%	0.0160
3	positive regulation of physiological process	16	5.2%	0.0223
3	macromolecule metabolism	100	32.4%	0.0289
3	primary metabolism	151	48.9%	0.0478
2	Morphogenesis	25	8.1%	0.0002
2	response to endogenous stimulus	15	4.8%	0.0004
2	response to stress	36	11.6%	0.0005
2	regulation of cellular process	86	27.8%	0.0007
2	cell differentiation	20	6.5%	0.0016
2	cell growth	10	3.2%	0.0018
2	cellular physiological process	213	68.9%	0.0019
2	regulation of growth	9	2.9%	0.0022
2	regulation of physiological process	82	26.5%	0.0025
2	organ development	20	6.5%	0.0029
2	positive regulation of biological process	22	7.1%	0.0039
2	negative regulation of biological process	23	7.4%	0.0167
1	Development	58	18.8%	0.0000
1	regulation of biological process	91	29.4%	0.0006
1	Growth	11	3.6%	0.0023
1	cellular process	244	79.0%	0.0054

Significantly enriched gene ontology biological process terms ($p<0.05$) in the list of differentially expressed genes, as determined by DAVID.

CHAPTER 4

Termination of damaged protein repair defines the occurrence of symptoms in carriers of the m.3243A>G tRNA^{Leu} mutation

R.G.E. van Eijsden [1, 2, 3$], L.M.T. Eijssen [4, 5$], P.J. Lindsey [4], C.M.M. van den Burg [4], L.E. A. de Wit [6], M.E. Rubio-Gozalbo [7], C.E.M. de Die [8], T. Ayoubi [4, 9], W. Sluiter [6], I.F.M. de Coo [10], H.J.M. Smeets [1, 2, 4]

[1]Department of Genetics and Cell Biology - Clinical Genetics, Maastricht University, Maastricht – The Netherlands.
[2]Research Institute Growth & Development, Maastricht University, Maastricht – The Netherlands.
[3]MicroArray Facility, VIB, Leuven – Belgium.
[4]Department of Population Genetics, Genomics & Bioinformatics, Maastricht University, Maastricht – The Netherlands.
[5]BiGCaT Bioinformatics, Maastricht University, Maastricht – The Netherlands.
[6]Department of Biochemistry, Mitochondrial Research Unit, Erasmus MC, Rotterdam – The Netherlands.
[7]Department of Paediatrics and Laboratory Genetic Metabolic Diseases, Maastricht University Hospital, Maastricht – The Netherlands.
[8]Department of Clinical Genetics, Maastricht University Hospital, Maastricht – The Netherlands.
[9]Cardiovascular Research Institute Maastricht (CARIM), Maastricht University – Maastricht – The Netherlands.
[10]Department of Neurology, Erasmus MC, Rotterdam – The Netherlands.

[$]Current affiliation.

Journal of Medical Genetics, *in press*

Abstract

The m.3243A>G mutation in the mitochondrial $tRNA^{Leu(UUR)}$ gene is an example of a mutation causing a very heterogeneous phenotype. It is the most frequent cause (80%) of the MELAS syndrome (Mitochondrial Myopathy, Encephalopathy, Lactic Acidosis and Stroke-like episodes), but it can also lead in addition or separately to type 2 diabetes, deafness, renal tubulopathy and/or cardiomyopathy. To identify pathogenic processes induced by this mutation, we compared global gene expression levels of muscle biopsies from affected and unaffected mutation carriers with controls. Gene expression changes were relatively subtle. In the a-symptomatic group 200 transcripts were up- and 12 were down-regulated, whereas in the symptomatic group this was 15 and 52 respectively. In the a-symptomatic group, oxidative phosphorylation (OXPHOS) complex I and IV genes were induced. Protein turnover and apoptosis were elevated, most likely due to the formation of dysfunctional and reactive oxygen species (ROS) damaged proteins. These processes returned to normal in symptomatic patients. Components of the complement system were up-regulated in both groups, but the strongest in the symptomatic group, which might indicate muscle regeneration. Most likely, protein damage and OXPHOS dysfunction stimulate repair (protein regeneration) and metabolic adaptation (OXPHOS). In a-symptomatic individuals these processes suffice to prevent the occurrence of symptoms. However, in affected individuals the repair process terminates, presumably because of excessive damage, and switches to muscle regeneration, as indicated by a stronger complement activation. This switch leaves increasingly damaged tissue in place and muscle pathology becomes manifest. Therefore, the expression of complement components might be a marker for the severity and progression of MELAS clinical course.

Introduction

Mitochondrial encephalomyopathies due to defects in oxidative phosphorylation (OXPHOS) are genetically and clinically heterogeneous disorders. Different mutations in different genes can lead to the same disease manifestation, whereas one single mutation can result into a variety of clinical symptoms. Approximately 25% of the paediatric cases of OXPHOS disease is caused by a mutation in the mtDNA [23]. An example of a clinically heterogeneous mutation is the m.3243A>G point mutation in the mitochondrial $tRNA^{Leu(UUR)}$ gene. This is the most frequent (80%) cause of MELAS syndrome (Mitochondrial Myopathy, Encephalopathy, Lactic Acidosis and Stroke-like episodes, OMIM # 540000), but can also lead in addition or separately to type 2 diabetes, deafness, renal tubulopathy and/or cardiomyopathy. Differences in mutation load can only partly explain the differences in disease severity and symptoms, but effects are not consistent and it is not the only factor involved [99]. A variety of studies have been performed to investigate possible correlations between mtDNA haplo groups or polymorphisms and clinical phenotypes, or to study clinical and pathophysiological features among individuals carrying the m.3243A>G

mutation [100-105]. However, an explanation for the differences in threshold for clinical expression and for the clinical heterogeneity has not yet been found.

Therefore, we applied gene expression profiling as an unbiased approach to identify the molecular processes which are induced by the m.3243A>G mutation in different individuals and lead to the development and progression of clinical symptoms. Microarray gene expression experiments were carried out on skeletal muscle from subjects carrying the m.3243A>G mutation and controls. Gene expression differences were compared between mutation carriers with and without symptoms to characterise the pathogenic processes involved.

Materials & Methods

Patients and controls

For gene expression profiling, needle biopsies from the quadriceps muscle were obtained from seven subjects carrying the MELAS m.3243A>G mutation (two men and five women, age at diagnosis 32 to 70 years, table 1) and six controls (two men and four women, age at muscle biopsy between 17 and 64 years). After biopsy, the muscle samples were immediately frozen in liquid nitrogen. The mutation carriers (Mut3243 group) were subdivided into two groups: one group (n=4, three women and one man) having the classical clinical MELAS symptoms which is the symptomatic group (S3243 group) and a second group (n=3, two women and one man) without clinical symptoms, the a-symptomatic group (AS3243 group). For enzyme histochemistry to detect the expression of superoxide-producing enzymes (see below), muscle cryosections were used from seven MELAS m.3243A>G mutation carriers (three symptomatic and four a-symptomatic, table 1) of which two were also used for the gene expression experiment, and nine additional controls (age at muscle biopsy between 2 and 55 years). For the oxprot assay (see below), muscle biopsies were used from 11 MELAS m.3243A>G mutation carriers (eight symptomatic and three a-symptomatic, table 1), of which five were also used for the microarray experiment, and nine controls of which three were also used in the microarray experiment (age at muscle biopsy between 2 and 53 years).

Table 1: Mutation carriers

Subject ID	m.3243A>G skeletal muscle heteroplasmy level	(A-)Symptomatic	Sex	Age at diagnosis	Microarray experiment	Oxprot assay	DHE staining
5	50%	S	F	52	+	+	-
12	53%	S	F	36	+	+	-
13	16%	AS	F	70	+	-	-
17	32%	S	M	44	+	-	-
24	73%	S	F	33	+	+	+
25	60%	AS	M	32	+	+	+
26	15%	AS	F	49	-	+	+
27	28%	AS	F	15	-	-	+
28	28%	AS	F	23	-	-	+
29	63%*	S	M	25	-	-	+
30	65%	AS	F	69	+	+	-
37	56%	S	M	46	-	+	-
38	92%	S	M	6	-	+	-
41	82%	S	M	28	-	+	-
45	64%	S	M	49	-	+	-
46	75%	S	F	37	-	+	+

Overview of m.3243A>G mutation carriers used for the microarray gene expression experiment, oxprot assay, and DHE staining.

***** Mutation percentage in fibroblast cells.

F: Female, M: Male, S: with clinical symptoms (symptomatic), AS: without clinical symptoms (a-symptomatic).

m.3243A>G mutation detection

Forward 5'-CAACTTAGTATTATACCCACAC-3' and reverse primers 5'-GATTACGAATGGCTTGCTTT-3' were used to amplify the fragment carrying the m.3243A>G mutation by polymerase chain reaction (PCR) using a FAM-labelled primer in the last PCR cycle. Heteroplasmy levels were determined by mutation specific restriction digestion with the *Haw*aii enzyme resulting in a wild-type fragment of 128 bases and a mutant fragment of 56 bases long. Digested products were analyzed on an ABI-PRISM 3100 genetic analyzer using the GeneScan Analysis 3.7 software package (Applied Biosystems, Foster City, CA, USA). The ratio of the area under the mutant peak and the sum of the areas under the mutant and wild-type peaks were calculated to determine the heteroplasmy levels of the m.3243A>G mutation.

Microarray procedure

Total RNA was isolated using the TRIzol reagent (Invitrogen, Carlsbad, CA, USA) and purified with the RNeasy clean-up kit (Qiagen, Hilden, Germany). RNA quantity and purity were determined spectrophotometrically using the Nanodrop ND-1000 (Nanodrop Technologies, Wilmington, DE, USA) and RNA integrity was assessed by determining the RNA 28S/18S ratio using the Bioanalyser 2100 (Agilent Technologies, Santa Clara, CA, USA). Muscle RNA spiked with four bacterial RNA transcripts was reverse transcribed into cDNA and amplified in a two-round amplification reaction according to the manufacturer's protocol (Affymetrix, Santa Clara, CA, USA). A mixture of cDNA and added hybridisation controls was hybridised on Affymetrix HG-U95Av2 chips, followed by staining and washing steps in the GeneChip fluidics station 400 (Affymetrix, Santa Clara, CA, USA)

according to the manufacturer's procedures. To assess the raw probe signal intensities, chips were scanned using the GeneChip scanner 3000 (Affymetrix, Santa Clara, CA, USA).

Microarray data analysis and data mining

R, a free software environment for statistical computing and graphics, was used in combination with the *gnlm* and the *affy* libraries to perform the data preparation and analysis [40, 68-70]. Version 8 of the Unigene-based probe set definition files (CDF files) as described by Dai *et al.* was used to combine the individual probes into probe sets [71]. These CDF files are based on Unigene build #192. The *expresso* method of the *affy* library, without background correction, with constant normalisation, use of perfect match signal intensities only, and the "mas" summarisation method were used to calculate the probeset intensities from the individual probe signals.

Normal linear regression models, implemented by the *gnlr* function within the *gnlm* library, were used to asses differentially expressed genes between m.3243A>G subjects and controls. For the patient versus control comparisons, two models were fitted. In one model all mutation carriers (Mut3243 group) were compared to the controls, to select the genes which have an effect due the presence of the mutation, irrespective of the presence of clinical symptoms or not. A second model was fitted to select the genes with a significant different expression for the S3243 or the AS3243 group compared to the controls, but also with a significant difference in expression between the S3243 and the AS3243 group. Differences due to experimental variation were corrected for by including the data from the RNA spikes and hybridisation controls as covariates in the models. Because hybridisations were carried out on two days, the hybridisation days were also taken into account in the modelling procedure. The Akaike information criterion (AIC), representing the likeliness of each model penalised for the complexity of the model, was used to identify the best fitting models and genes with a significant change in expression between two groups [72]. The AIC was adjusted to be comparable to a two-sided chi-squared test with a significance level of 99.9% (p-value<0.001), making the analysis more stringent [73]. The web-based Database for Annotation, Visualisation and Integrated Discovery (DAVID) was used to assess enriched gene ontology terms within the gene lists produced by the microarray data analysis [76].

Quantitative Real-time PCR

Primers were designed using Primer Express® software version 3.0 (Applied Biosystems, Foster City, CA, USA). cDNA was prepared from 2 µg of total RNA in a standard reverse transcriptase reaction. PCR was performed in a 7700 Realtime PCR System (Applied Biosystems, Foster City, CA, USA) and a BioRad MyiQ Single-Colour Real-Time PCR Detection System (Bio-Rad, Hercules, CA, USA) using Eurogentec qPCR™ Mastermix Plus for SYBR Green® I. Cycling conditions were: an initial step of 2 minutes at 50°C, activation of the Hot Goldstar enzyme at 95°C for 10 minutes, and 40 cycles of 15 seconds at 95°C followed by 1 minute at 60°C (denaturation, annealing, and

elongation). The ADP-ribosylation factor 1 (*ARF1*) gene was used as an internal reference because of its constant expression level in muscle [77]. Genes for which QRT-PCR was performed were complement component 1, r subcomponent (*C1R*), complement component, s subcomponent (*C1S*), complement component 3 (*C3*), and clusterin (*CLU*). Primers used for amplification are listed in table 2. Data was analyzed in R using the *elliptic* function of the *growth* library to implement normal linear regression models [69, 70]. The AIC was adjusted to be comparable to a two-sided chi-squared test with a significance level of 95%, making the analysis more stringent [73].

Table 2: QRT-PCR primers

Gene symbol	Description	Forward primer (5'-3')	Reverse primer (5'-3')
ARF1	ADP-ribosylation factor 1	AATCAGCTCCGGAACCAGAA	GCAGAGGGCAAGAGGAGTGA
C1R	Complement component 1, r subcomponent	TCTGTGCTGGACACCCATCTC	GCAAAAACGCCCCCACTAT
C1S	Complement component 1, s subcomponent	TGGATAATGAAGACTATGCAGGAAAA	GGAGAGGCTGGTGGGATGTA
C3	Complement component 3	TGGCCATTGAGCAGACCAT	CGTGCGCTGCTGTCCA
CLU	Clusterin	GCTGCAGGAATACCGCAAA	CCGTAGGTGCAAAAGCAACA

Primer sequences of the primers used for quantitative real-time PCR validation of microarray gene expression data.

Detection of superoxide-generating enzymes in muscle

The expression of superoxide radical-producing enzymes in muscle was quantified by enzyme histochemistry of skeletal muscle cryosections from seven MELAS m.3243A>G mutation carriers (three symptomatic and four a-symptomatic, table 1) of which two were also used for the gene expression experiment and nine additional controls (age at muscle biopsy between 2 and 55 years) using dihydroethidium (DHE) as a probe for superoxide. Ten-µm thick cryosections were stored at -80°C. After thawing the sections, they were stained by 5 µM dihydroethidium and 0.5 µg/mL Hoechst 33258 in phosphate-buffered saline (PBS) for 30 min at 37°C in a humidified atmosphere as described previously [106]. The orange fluorescence of the superoxide-specific reaction product of DHE oxidation [79] was measured using a fluorescence inverted microscope (Olympus IX50) equipped with a 460-490 nm band pass excitation filter and 515-nm emission IF-barrier filter, digitised with a F-view camera (Soft Imaging System), and analyzed offline (AnalySIS 3.1; Soft Imaging System, Münster, Germany). The signal was expressed in arbitrary units reflecting the total fluorescence intensity of all events divided by the number of blue fluorescent nuclei. At least 300 nuclei per section were counted in two to three consecutive sections. One-sided and two-sided t-tests on the averages of the replicate measurements were used to assess statistical differences between the m.3243A>G mutation carriers in general and the control groups, and between the AS3243 and S3243 group respectively.

Oxidative protein damage

Oxidative damage to proteins in the muscle biopsies was determined by quantifying the amount of carbonyl groups per mg protein using an ELISA assay optimised for small amounts of proteins (Oxprot assay). For this assay, 10 mg wet weight (ww) of the skeletal muscle biopsies was used

from nine controls (age at muscle biopsy between 2 and 53 years), of which three were also used in the microarray experiment. Additionally, skeletal muscle biopsies were used from 11 MELAS m.3243A>G mutation carriers (eight symptomatic and three a-symptomatic, table 1), of which five were also used for the microarray experiment. The snap-frozen biopsies were pulverised in the presence of 19 mL/g ww of RIPA buffer (50 mM Tris-HCl, 150 mM NaCl, 1 mM EDTA, pH 7.4, containing 0.25% sodium deoxycholate, 1% NP40 and supplemented with a protease inhibitor mixture (PIM) of one Complete tablet per 50 mL (Roche Diagnostics, Almere, The Netherlands), 1 mM 4-(2-aminoethyl)-benzenesulfonyl-fluoride hydrochloride (Pefabloc SC, Roche) and 2 mM diisopropyl fluorophosphate (DFP) (Fluka Chemica, Steinheim, Switzerland) in a small Bessman tissue pulveriser (Fisher Scientific) precooled with liquid nitrogen. For carbonyl determination the tissue homogenate was first incubated on ice for 30 min, and then centrifuged at 16,000 g for 20 min at 4°C, and the supernatant was diluted in PBS to 0.5 µg/mL protein. Next 200 µl was transferred into triplicate wells of a Nunc Maxisorp microplate. The amount of carbonyl groups resulting from protein oxidation were determined as described by Alamdari *et al* .[78]. A technical replicate was performed for seven out of nine patient samples and for three out of seven control samples. A one-sided t-test on the averages of the replicate measurements was used to assess statistical differences between the patient and the control groups.

Results

Gene expression profiling of symptomatic and a-symptomatic m.3243A>G mutation carriers

Gene expression levels were measured for 7084 transcripts in each sample. The expression of 407 transcripts was significantly different between one of the patient groups and the control group (supplementary table 1 and table 3). For 128 transcripts, the expression level differed significantly between all mutation carriers (Mut3243), irrespective of the presence of clinical symptoms, and controls. The majority (112 out of 128 or 87.5%) of these transcripts was up-regulated and 16 (12.5%) transcripts were down-regulated. The expression level of 212 transcripts differed between the a-symptomatic group (AS3243) and the controls. The vast majority (94.3% or 200 transcripts) was up-regulated and only 5.7% (12 transcripts) was down-regulated. A total of 67 (15 up- and 52 down-regulated) transcripts was significantly different between the symptomatic group (S3243) and the controls. Gene expression differences were in general small. For the Mut3243 versus controls comparison there were 18 up-regulated genes and no down-regulated genes with a fold-change larger than 1.5. In the AS3243 versus controls comparison, none of the down-regulated genes and seven of the up-regulated genes had a fold change larger than 1.5. In the S3243 versus controls comparison, only one of the down-regulated genes and four of the up-regulated genes had a fold-change larger than 1.5.

Because of the subtle gene expression differences, a process based analysis was carried out. DAVID functional annotation clustering was performed on the differentially expressed genes at

the GO biological process level 5. For the Mut3243 versus controls comparison, processes related to protein transport, programmed cell death, and the immune system, more specifically the complement system, were identified as functional gene clusters (table 4). In addition to the complement related genes identified on the microarray, a number of other complement components were shown to be differentially expressed by QRT-PCR (see below). The gene expression changes pointed to stimulation of the complement system, stimulation of protein transport, and both stimulation and inhibition of programmed cell death. Upon further analysis, the stimulation of the protein transport process in fact more closely resembled a stimulation of protein synthesis. Three out of the eight genes are related to the ribosome or the endoplasmatic reticulum (ER). The ribosomal protein L23 (*RPL23*), which is 1.5-fold up-regulated in the Mut3243 group compared to the controls, is a component of the 60S ribosomal subunit and is involved in protein synthesis. The gene coding for the translocation associated membrane protein 2 (*TRAM2*) was 1.4-fold up-regulated in Mut3243 group compared to controls. The TRAM2 protein is involved in the posttranslational processing of secretory and membrane proteins at the ER membrane [107]. The ribosome binding protein 1 homolog (*RRBP1*) gene is 1.2-fold up-regulated in the Mut3243 group compared to the controls. It mediates the interaction between the ribosome and the ER and has an mRNA stabilizing function in yeast [108]. Programmed cell death appeared to be both stimulated and inhibited in the Mut3243 group compared to controls. Pro-apoptotic processes are the 1.2 fold up-regulation of the death-associated protein (*DAP*), a stimulator of a variety of cell death systems [109, 110], the 1.2 fold up-regulation of p8 protein, also known as COM1, which is a cell cycle regulator [111] and the 0.7 fold down-regulation of the testis enhanced gene transcript (*TEGT*), which is also known as the inhibitor of the pro-apoptotic BAX protein (BI-1). Apoptosis inhibiting effects are the 1.7 fold up-regulation of annexin A1 (*ANXA1*), also known as a p35 gene, which inhibits caspase [112, 113] and the 1.1 fold up-regulation of histone deacetylase 1 (*HDAC1*). HDAC1 inhibitors have been used in cancer treatment due to their pro-apoptotic effect [114]. Finally, the 2.1 fold up-regulation of clusterin (*CLU*) is more ambiguous as CLU has been related to both stimulation and inhibition of programmed cell death [115]. For the AS3243 versus controls comparison, four functional gene clusters were identified. The gene clusters were involved in oxidative energy metabolism, programmed cell death, protein synthesis, and intracellular protein trafficking (table 5). According to the direction of the gene expression level changes, each of these processes was up-regulated. Changes in oxidative energy metabolism included the up-regulation of the genes coding for three subunits of the NADH dedydrogenase complex (complex I of the OXPHOS system): *NDUFB8* (1.4-fold), *NDUFC1* (1.2-fold), and *NDUFS3* (1.3-fold). Moreover, one subunit of the cytochrome-c-oxidase (COX) complex (complex IV of the OXPHOS system), *COX4I1*, was 1.2-fold up-regulated. Induction of protein synthesis is illustrated by the up-regulation of a number translation initiation factors, *EIF2AK1* (1.2-fold), *EIF2B4* (1.3-fold), and *EIF2S1* (1.4-fold). Furthermore, a subunit of the ribosomal 40S complex (*RPS21*) and the mitochondrial ribosomal protein L23 (*MRPL23*) were 1.5-fold and 1.3-fold up-regulated respectively. The 1.1 fold up-regulation of the p53 gene, the 1.2 fold up-regulation of homeodomain interacting protein kinase 2 (*HIPK2*), which phosphorylates the p53 genes and thereby induces apoptosis

[116], and the 1.1 fold up-regulation of serine/threonine kinase 17a (*STK17A* or *DRAK1*), which has a catalytic domain related to that of death-associated protein kinase and can induce the morphological changes of apoptosis in NIH 3T3 cells [117], point to a stimulation of apoptosis in a-symptomatic m.3243A>G mutation carriers compared to controls. No functional gene clusters were identified for the S3243 versus controls comparison.

Based on previous microarray results and observations in Leigh syndrome patients with a mutation in the *SURF1* gene (unpublished results) we investigated the gene expression changes of a number of genes of the complement system by QRT-PCR (table 6). Although the microarray analysis indicated that the complement component *C1R* was differentially expressed in mutation carriers in general compared to controls, QRT-PCR analysis showed a significantly stronger up-regulation of *C1R* in the S3243 group (6.8-fold) compared to the AS3243 group (2.7-fold) when compared to controls. Although the data for complement component *C1S* was not significant by microarray analysis, QRT-PCR analysis indicated that this transcript was significantly up-regulated in the Mut3243 group compared to the control group. QRT-PCR analysis of complement component *C3*, which was not present in the microarray dataset, indicated a significant 4.1-fold up-regulation in the Mut3243 group compared to controls. The up-regulation of clusterin was also confirmed by QRT-PCR, indicating a 4.3-fold up-regulation in the Mut3243 group compared to controls. There was a good correspondence between the microarray and QRT-PCR results, which is in general the experience with Affymetrix microarray results.

Table 3: Overview of the gene expression changes comparing mutation carriers with or without clinical symptoms to the control group

Comparison	UP		DOWN		TOTAL
S3243 versus controls	15	56.7%	52	43.3%	67
FC > 1.5	4	3.3%	1	0.8%	
Max. FC	2.2		1.7		
AS3243 versus controls	200	94.3%	12	5.7%	212
FC > 1.5	7	3.3%	0	0.0%	
Max. FC	4.9		1.4		
Mut3243 versus controls	112	87.5%	16	12.5%	128
FC > 1.5	18	14.1%	0	0.0%	
Max. FC	2.7		1.5		

For the symptomatic group 15 (56.7%) transcripts were up-regulated and 52 (43.3%) were down-regulated. In the a-symptomatic group 200 (94.3%) transcripts were up-regulated and 12 (5.7%) were down-regulated. For the mutation carriers in general, 112 (87.5%) transcripts were up-regulated and 16 (12.5%) were down-regulated.
S3243: m.3243A>G mutation carriers with clinical symptoms. AS3243: m.3243A>G mutation carriers without clinical symptoms. Mut3243: m.3243A>G mutation carriers in general, irrespective of the presence of clinical symptoms. FC: fold change. Max. FC: Maximum fold change.

Oxidative protein damage and superoxide radicals in muscle of m.3243A>G mutation carriers

Oxidative damage to muscle proteins determined by the amount of carbonyl groups was significantly increased in nine subjects carrying the m.3243A>G mutation at levels between 50-92% ($p=0.03$ in a one-sided t-test) compared to controls. The amount of carbonyl groups was 2.06 (SD: 0.86) and 1.34 (SD: 0.65) nmol per mg protein for the mutation carriers and controls respectively, illustrating a significant 1.5-fold increase. Although there was no significant difference in the amount of carbonyl groups between the S3243 and the AS3243 group, the detected amount of carbonyl groups per mg protein for one of the a-symptomatic mutation carriers was much less than the amount in the other two a-symptomatic mutation carriers (0.27 compared to 2.04 and 3.29 ng carbonyl/mg protein respectively). The expression of superoxide-production enzymes was significantly increased in muscle of m.3243A>G mutation carriers. As shown in figure 1, the staining intensity for these enzymes in muscle cryosections of five muscle biopsies from m.3243A>G mutation carriers (mutation loads between 15-73%) was significantly ($p=0.001$ in a one-sided t-test) 3.8-fold higher compared to control samples. There were no significant differences in the expression of superoxide-producing enzymes between symptomatic and a-symptomatic mutation carriers compared to controls according to a two-sided t-test.

Table 4: David functional annotation clustering results at the level of GO biological process level 5 for the Mut3243 versus control comparison

Functional Group 1: Immune response				
GO terms	**UG ID**	**Symbol**	**FC**	**Genes**
complement activation	Hs.169998	BST1	1.2	bone marrow stromal cell antigen 1
innate immune response	Hs.436657	CLU	2.1	clusterin
humoral immune response	Hs.155597	CFD	1.7	complement factor d (adipsin)
	Hs.384598	SERPING1	1.9	serpin peptidase inhibitor, clade g (c1 inhibitor), member 1, (angioedema, hereditary)
Functional Group 2: Protein transport				
GO terms	**UG ID**	**Symbol**	**FC**	**Genes**
intracellular protein transport	Hs.507755	DCAMKL1	1.4	doublecortin and cam kinase-like 1
protein transport	Hs.527919	KPNA3	0.7	karyopherin alpha 3 (importin alpha 4)
intracellular transport	Hs.444767	KIF13B	1.3	kinesin family member 13b
establishment of cellular localization	Hs.29282	MAP3K3	0.9	mitogen-activated protein kinase kinase kinase 3
	Hs.529044	RAB22A	1.2	rab22a, member ras oncogene family
	Hs.516790	ARHGEF2	1.2	rho/rac guanine nucleotide exchange factor (gef) 2
	Hs.406300	RPL23	1.5	ribosomal protein l23
	Hs.472213	RRBP1	1.2	ribosome binding protein 1 homolog 180kda (dog)
	Hs.520182	TRAM2	1.4	translocation associated membrane protein 2
Functional Group 3: Programmed cell death				
GO terms	**UG ID**	**Symbol**	**FC**	**Genes**
regulation of apoptosis	Hs.494173	ANXA1	1.7	annexin a1
regulation of programmed cell death	Hs.436657	CLU	2.1	clusterin
negative regulation of programmed cell death	Hs.75189	DAP	1.2	death-associated protein
apoptosis	Hs.88556	HDAC1	1.1	histone deacetylase 1
	Hs.513463	P8	1.2	p8 protein (candidate of metastasis 1)
	Hs.35052	TEGT	0.7	testis enhanced gene transcript (bax inhibitor 1)

Three functional gene clusters could be identified which contained genes related to immune response, protein transport, and programmed cell death.
GO: Gene ontology. UG ID: Unigene cluster ID. FC: fold change.

Table 5: David functional annotation clustering results at the level of GO biological process level 5 for the AS3243 versus control comparison

Functional Group 1: Oxidative energy metabolism				
GO terms	**UG ID**	**Symbol**	**FC**	**Gene Title**
oxidative phosphorylation	Hs.295917	ATP6V1B2	1.3	atpase, h+ transporting, lysosomal 56/58kda, v1 subunit b2
ATP synthesis coupled electron transport	Hs.433419	COX4I1	1.2	cytochrome c oxidase subunit iv isoform 1
electron transport	Hs.69745	FDXR	1.4	ferredoxin reductase
	Hs.445350	FMO3	1.3	flavin containing monooxygenase 3
	Hs.523215	NDUFB8	1.4	nadh dehydrogenase (ubiquinone) 1 beta subcomplex, 8, 19kda
	Hs.84549	NDUFC1	1.2	nadh dehydrogenase (ubiquinone) 1 subcomplex unknown, 1, 6kda
	Hs.502528	NDUFS3	1.3	nadh dehydrogenase (ubiquinone) fe-s protein 3, 30kda (nadh-coenzyme q reductase)
	Hs.132370	NOX1	1.2	nadph oxidase 1

Functional Group 2: Programmed cell death				
GO terms	**UG ID**	**Symbol**	**FC**	**Genes**
positive regulation of programmed cell death	Hs.264482	ATG12	1.2	atg12 autophagy related 12 homolog (s. cerevisiae)
apoptosis	Hs.517517	EP300	1.1	e1a binding protein p300
regulation of apoptosis	Hs.487294	ERCC2	1.1	excision repair cross-complementing rodent repair deficiency, complementation group 2 (xeroderma pigmentosum d)
regulation of programmed cell death	Hs.397465	HIPK2	1.2	homeodomain interacting protein kinase 2
	Hs.87247	HRK	0.9	harakiri, bcl2 interacting protein (contains only bh3 domain)
	Hs.139896	MAEA	1.4	macrophage erythroblast attacher
	Hs.462590	MYO18A	1.5	myosin XVIIIA
	Hs.2200	PRF1	0.8	perforin 1 (pore forming protein)
	Hs.268887	STK17A	1.1	serine/threonine kinase 17a (apoptosis-inducing)
	Hs.408312	TP53	1.1	tumor protein p53 (li-fraumeni syndrome)
Functional Group 3: Protein synthesis				
GO terms	**UG ID**	**Symbol**	**FC**	**Genes**
regulation of protein biosynthesis	Hs.520205	EIF2AK1	1.2	eukaryotic translation initiation factor 2-alpha kinase 1
regulation of cellular biosynthesis	Hs.169474	EIF2B4	1.3	eukaryotic translation initiation factor 2b, subunit 4 delta, 67kda
regulation of protein metabolism	Hs.151777	EIF2S1	1.4	eukaryotic translation initiation factor 2, subunit 1 alpha, 35kda
protein biosynthesis	Hs.3254	MRPL23	1.3	mitochondrial ribosomal protein l23
	Hs.190968	RPS21	1.5	ribosomal protein s21
	Hs.404119,	TSTA3	1.2	tissue specific transplantation antigen p35b
	Hs.22616		1.3	kiaa0664
	Hs.3459		1.4	kiaa1970 protein
Functional Group 4: Intracellular protein trafficking				
GO terms	**UG ID**	**Symbol**	**FC**	**Genes**
intracellular transport	Hs.518460	AP2M1	1.3	adaptor-related protein complex 2, mu 1 subunit
establishment of cellular localization	Hs.12107	CHMP2A	1.4	chromatin modifying protein 2a
intracellular protein transport	Hs.546250	DYNC1I2	1.1	dynein, cytoplasmic 1, intermediate chain 2
protein transport	Hs.87726	GGA3	1.2	golgi associated, gamma adaptin ear containing, arf binding protein 3
	Hs.12457	NUP133	1.6	nucleoporin 133kda
	Hs.310645	RAB1A	1.2	rab1a, member ras oncogene family
	Hs.180711	STX3A	1.2	syntaxin 3a
	Hs.408312	TP53	1.1	tumor protein p53 (li-fraumeni syndrome)

Four functional gene clusters could be identified which contained genes related to oxidative energy metabolism, programmed cell death, protein synthesis, and protein transport.

GO: Gene ontology. UG ID: Unigene cluster ID. FC: fold change.

Table 6: Quantitative realtime PCR (QRT-PCR) results

			MicroArray (~ p<0.001)		*QRT-PCR (~ p<0.05)*	
Symbol	**Name**	**Process**	**Significant**	**FC**	**Significant**	**FC**
C1R	Complement component 1, r subcomponent	Complement	Mut3243	2.1	AS3243	2.7 ↑
					S3243	6.8 ↑
C1S	Complement component 1, s subcomponent	Complement	NS	-	Mut3243	4.6 ↑
C3	Complement component 3	Complement	NA	NA	Mut3243	4.1 ↑
CLU	Clusterin	Complement	Mut3243	2.1 ↑	Mut3243	4.3 ↑

The "significant" column lists whether and for which group comparison the gene expression was significantly different. NS: Not significant, NA: Not in microarray dataset, FC: fold change, ↑: up-regulated.

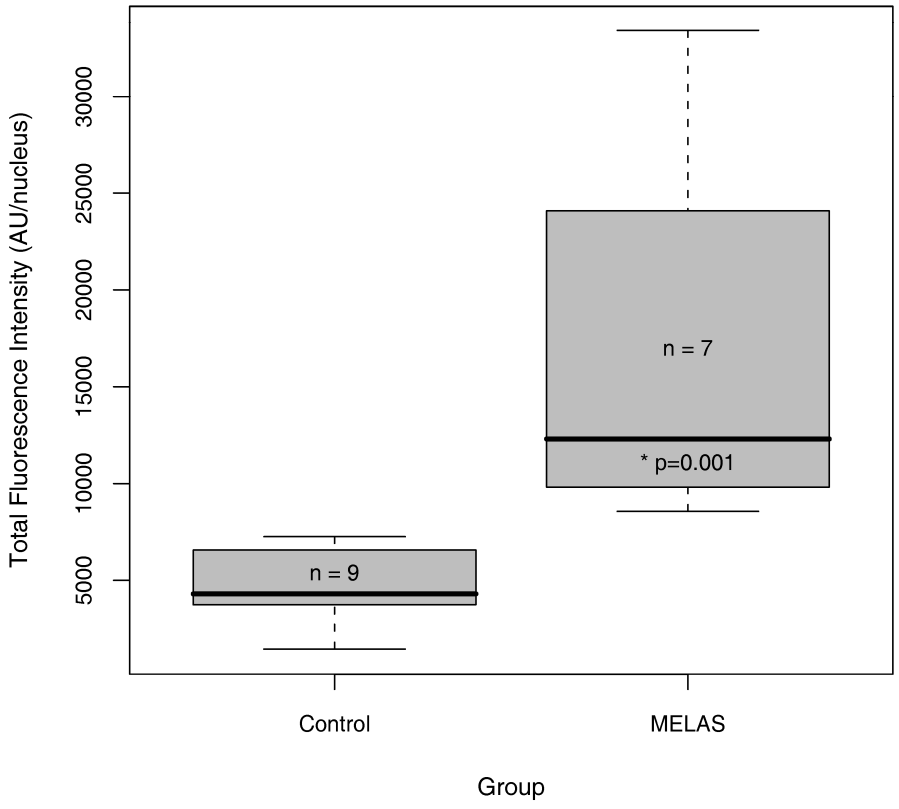

Figure 1: DHE staining

Cryosections of skeletal muscle samples of controls (n=9) and MELAS m.3243A>G mutation carriers (n=7) were stained with dihydroethidium (DHE) as described in the Materials and Methods section to assess the activity of enzymes able to produce superoxide radicals. A one-sided t-test showed that the expression of these enzymes in muscle of m.3243A>G mutation carriers was significantly 3.8-fold higher than in controls (p=0.001). The whiskers in the box plot indicate the extreme values. The boxes indicate the median (thick line) and the interquartile ranges (grey area).

AU: arbitrary units, reflecting the total fluorescence intensity of all events divided by the number of blue fluorescent nuclei (see Materials and Methods section).

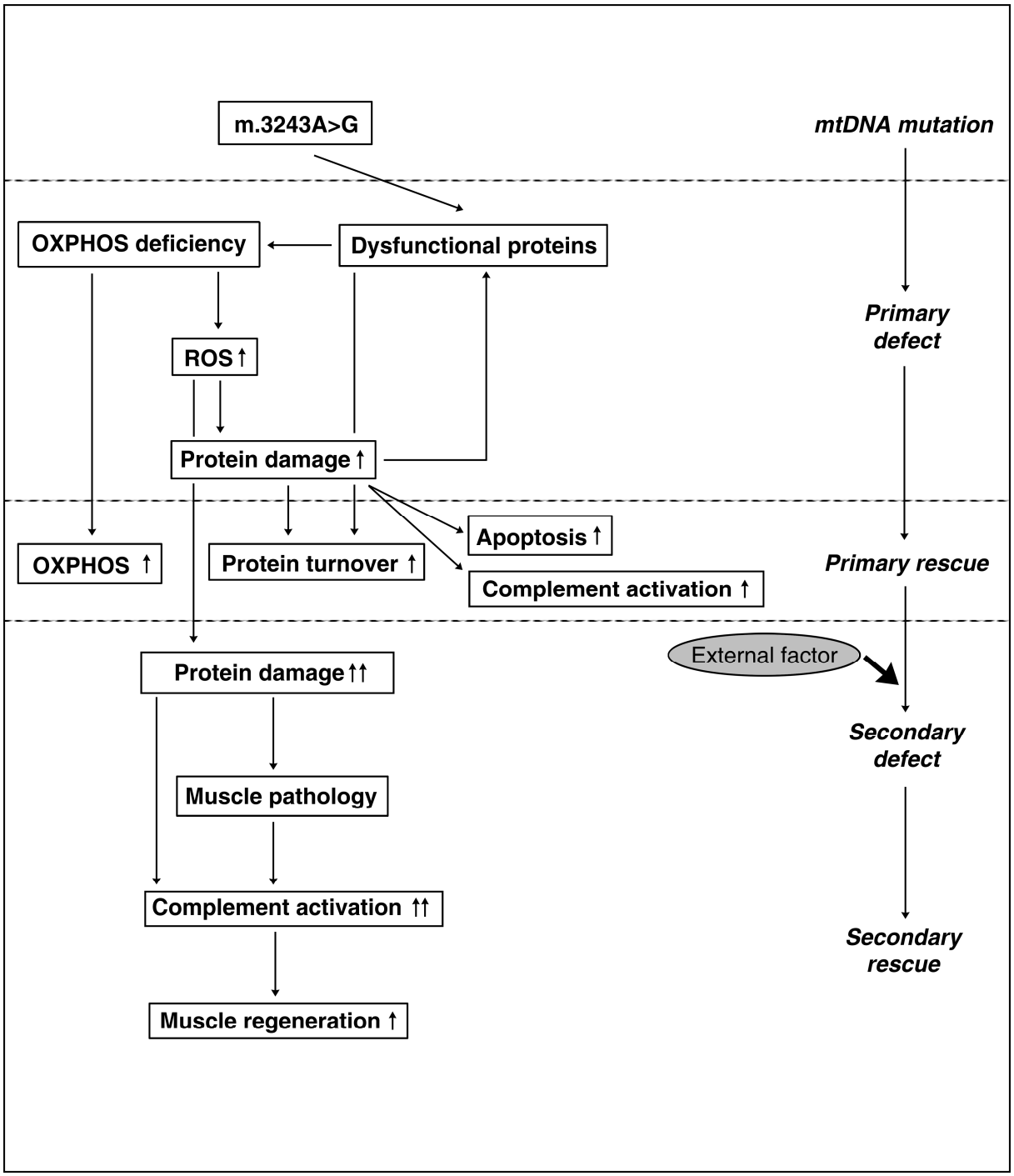

Figure 2: Pathobiological process flow of the m.3243A>G mutation

The m.3243A>G mutation gives rise to dysfunctional and damaged proteins. As a primary rescue attempt to this primary defect, OXPHOS is stimulated, protein turnover and apoptosis are increased, and the complement system is activated to initiate muscle regeneration. When the primary rescue mechanism fails, probably due to irreparable damage, it is terminated, protein damage increases further and muscle pathology arises as a secondary stage. The severe muscle pathology and increasing protein damage triggers a secondary rescue attempt through strengthening of complement activation, which may stimulate muscle regeneration further as a sole rescue process.

Discussion

Gene expression studies have been performed before on muscle of patients carrying the m.3243A>G mutation, in comparison to controls and other mtDNA mutations [118, 119]. In contrast to our study, no a-symptomatic mutation carriers were included. In the first study only specific processes were evaluated in muscle of three symptomatic MELAS patients carrying the m.3243A>G mutation (mutation loads of 50%, 72%, and 91%) compared to controls. Only in the patient with the highest mutation load, an induction of OXPHOS genes, genes involved in energy metabolism (glycolysis, glycogen metabolism, citric acid cycle), and ubiquitin mRNA levels indicating an increased protein turnover, was reported [118]. No gene expression changes in these processes were identified for the other two subjects. In contrast to our findings, these authors observe an increase in gene expression with mutation load. In the second study, which also investigated symptomatic MELAS patients carrying the m.3243A>G mutation compared to controls, genes related to arginine metabolism were up-regulated and genes involved in cell cycle regulation and apoptosis were up- and down-regulated indicating both a stimulation and an inhibition of these processes. No reference was made to an induction of OXPHOS genes in patients compared to controls [119]. In agreement with the results of the studies described above, our results indicate a minor stimulation of the OXPHOS system, but in a-symptomatic m.3243A>G mutation carriers only. Additionally, our results showed mixed changes in the apoptotic process and an increase in protein turnover. However, no significant gene expression changes were identified in glycogen metabolism, glycolysis, or the citric acid cycle. We were not able to identify gene expression changes concerning arginine metabolism. The arginine metabolism genes which were represented in our dataset were not differentially expressed between m.3243A>G mutation carriers and controls, but not all genes involved were covered in our dataset.

Our data has revealed a number of processes that occur in carriers of the m.3243A>G mutation. The most striking observations were the difference between the a-symptomatic and symptomatic carriers and which has not been reported before, the involvement of the complement system. The pathophysiological processes which can be derived from our data are depicted in figure 2 and the individual components of this process will be discussed below.

Compensation by increasing OXPHOS capacity in a-symptomatic m.3243A>G mutation carriers

A slight up-regulation of structural subunits of OXPHOS complexes I and IV, which are the most commonly deficient respiratory chain complexes in MELAS patients, is observed in a-symptomatic carriers of the m.3243A>G mutation, probably to compensate for the OXPHOS defect. This is in contrast to the S3243 subjects, where no gene expression changes for subunits of complex I and IV and even a down-regulation of the gene coding for the ATP5C1 subunit of the mitochondrial ATP synthase complex was detected. This is similar to patients having Leigh syndrome caused by

a mutation in the *SURF1* gene, except for the down-regulation of the *SURF1* gene itself (unpublished results). Additionally, compensation by stimulation of mitochondrial proliferation in the a-symptomatic m.3243A>G mutation carriers compared to controls could be identified, illustrated by the small but significant 1.1-fold up-regulation of the *PPRC1* gene (Peroxisome proliferative activated receptor, gamma, coactivator-related 1), as has been suggested before [120]. PPRC1 is similar to PPAR-gamma coactivator 1 (PPARGC1/PGC-1) which plays a role in the activation of mitochondrial biogenesis [121, 122], but in contrast to PGC-1 it is growth-regulated with the characteristic of an immediate early gene product. Given these results, it is likely that the up-regulation of OXPHOS structural subunits and mitochondrial biogenesis is a primary rescue attempt.

Stimulation of protein turnover in m.3243A>G mutation carriers

Stimulation of protein synthesis is a general process triggered by the m.3243A>G mutation, irrespective of the presence of clinical symptoms, possibly related to alterations in the translational process. A reduced leucine amino acid incorporation has been described in MELAS m.3243A>G subjects which results in dysfunctional protein production and protein synthesis rate reduction [103, 123]. The second DAVID cluster for the Mut3243 group (table 4) indicates up-regulation of protein synthesis, by up-regulation of ribosome and ER related genes (*RPL23, TRAM2,* and *RRBP1*). The up-regulation of the *TRAM2* gene might also be related to the disturbed calcium homeostasis in MELAS subjects, since the TRAM2 protein appears to interact with the Ca(2+) pump of the ER (SERCA2b) [107, 124]. Up-regulation of protein synthesis by a significant up-regulation of three translation initiation factors (*EIF2AK1, EIF2B4,* and *EIF2S1*), a subunit of the ribosomal 40S complex (*RPS21*), and a mitochondrial ribosomal protein (*MRPL23*) is a very prominent process in a-symptomatic carriers, probably in an effort to rebalance the dysfunctional protein content (see below). Investigation of the protein synthesis machinery in more detail shows that the majority of the other transcripts present in the dataset coding for members of the ribosomal subunits 40S and 60S had a tendency to be up-regulated as well. Eight out of fifteen transcripts for which data was available of the 60S ribosomal subunit (*RPL10A, RPL13, RPL14, RPL18, RPL23, RPL24, RPL27,* and *RPL32*) and four out of thirteen transcripts for which data was available of the 40S ribosomal subunit (*RPS6, RPS11, RPS23,* and *RPS24*) showed a trend to be more than 1.2-fold up-regulated. Although these changes were not significant on a single gene level, it suggests that the protein synthesis process as a whole is stimulated.

Bases on our data we hypothesise (figure 2) that dysfunctional proteins are degraded and replaced by new proteins, resulting in a stimulation of protein synthesis and intracellular protein trafficking. In line with this hypothesis, five out of nine transcripts of the 20S proteasome complex (*PSMA4, PSMA5, PSMB1, PSMB4,* and *PSMB5*), which is mainly associated with the breakdown of proteins with oxidative damage [83], showed a trend to be more than 1.2-fold up-regulated in a-symptomatic m.3243A>G mutation carriers compared to controls. Moreover, *PSME1*

and *PSME2*, both regulators of the 20S proteasome complex, showed a tendency to be more than 1.2-fold up-regulated. Stimulation of protein breakdown in the AS3243 group is further supported by the significant up-regulation of two transcripts from the fourth functional gene cluster from the DAVID analysis of which the function is related to lysosomal degradation of proteins. *CHMP2A*, which is involved in the formation of multivesicular bodies delivering transmembrane proteins into the lumen of the lysosome for degradation, was significantly up-regulated [125, 126]. *GGA3* was also significantly up-regulated and belongs to a protein family that regulates the trafficking of membrane proteins between the trans-Golgi network and the lysosome by binding to ubiquitin attached to membrane proteins [127]. Stimulation of protein synthesis and degradation was not detected in the S3243 group compared to controls, as no up-regulation of ribosomal subunits and no stimulation of the proteasomal protein degradation pathway was observed for this patient group. Even a subtle down-regulation (1.1-fold compared to controls) of two translation initiation factors (*EIF2B5* and *EIF4G1*) was observed in the S3243 group compared to controls.

A strong additional trigger for the stimulation of protein synthesis is increased oxidative protein damage, due to the impaired OXPHOS function. A significant higher amount of oxidatively damaged proteins and increased expression of ROS-producing enzymes was detected in muscle of m.3243A>G mutation carriers compared to controls (figure 1). The fact that the ability to produce ROS was increased at similar levels in symptomatic and a-symptomatic mutation carriers compared to controls, corresponds with the results of the oxprot assay, which indicated equal oxidative protein damage in symptomatic and a-symptomatic mutation carriers. Because the amount of carbonyl groups per mg protein for one a-symptomatic subject was much less than for the other two a-symptomatic subjects, one might suggest that some a-symptomatic mutation carriers might be able to more efficiently replace damaged proteins with functional ones compared to the symptomatic mutation carriers.

Apoptosis in m.3243A>G mutation carriers

Gene expression changes indicate both an inhibition and a stimulation of programmed cell death as a general effect of the m.3243A>G mutation (table 4), which might reflect heterogeneity among the carriers. For the a-symptomatic m.3243A>G mutation carriers compared to controls, there appears to be a pro-apoptotic effect of the gene expression changes (table 5). No changes in the apoptosis process have been identified for the S3243 group separately. Apoptosis has previously been reported in MELAS subjects with the m.3243A>G mutation and in OXPHOS disorders in general and was linked to cell proliferation and high mutation loads [120]. The trigger for apoptosis is not completely clear, but excessive ROS production leading to increased protein and cell damage beyond repair and malfunctioning due to a defective oxidative phosphorylation system resulting in energy deprivation might be involved. Possibly, during disease progression, the slight stimulation of apoptosis stops. An explanation might be that when the protein damage is less severe, damaged proteins can still be removed by increasing protein turnover followed by

the stimulation of apoptosis and muscle regeneration through complement activation (see below). When protein damage can not be repaired or removed, it persists probably to save energy for regeneration, and muscle pathology then manifests (figure 2).

Muscle regeneration by complement activation in m.3243A>G mutation carriers

In the m.3243A>G mutation carriers, a number of complement related genes were up-regulated. Microarray analysis showed that complement component 1 r (*C1R*), and clusterin (*CLU*) were significantly up-regulated. QRT-PCR confirmed these findings and also indicated a significant up-regulation of complement component 1 s (*C1S*) and complement component 3 (C3). These changes were specific for mutation carriers in general, irrespective of having symptoms or not. The up-regulation of complement components most likely reflects a process of muscle regeneration comparable to that observed in Leigh syndrome patients with a *SURF1* mutation (unpublished data). The 1.2 fold up-regulation of the *RPB1* gene, which is specifically expressed in neuromuscular junctions and showed a transient induction in concordance with previously known neuromuscular junction markers in a 27-time point muscle regeneration series experiment [128], is also related to regenerative processes [129]. The significantly stronger up-regulation of *C1R* for the symptomatic compared to the a-symptomatic mutation carriers (6.8-fold compared to 2.7-fold) may be due to the increasing damage to proteins, which is not removed anymore. This is bound to fail, as muscle damage prevails and the new muscle carries the same genetic defect. However, restoration of the wild type mtDNA has been reported in regenerating muscle fibres, some of which are mtDNA mutation free [130].

Conclusion

It appears that the detrimental effects of the m.3243A>G mutation can be compensated by up-regulation of genes coding for structural subunits of OXPHOS complexes and by stimulation of mitochondrial biogenesis, protein turnover, apoptosis, and muscle regeneration. When these compensating mechanisms fall short and are terminated, pathology becomes manifest and eventually regeneration of failing muscle by complement activation is triggered even further (figure 2). It is yet unclear which factors determine successful compensation. Mutation load may play a role, but as the mutation load of two of the investigated a-symptomatic m.3243A>G mutation carriers (subjects 25 and 30, table 1) fall in the higher mutation load range (60% and 65% respectively) of the symptomatic mutation carriers (32% - 73%) and one of the symptomatic subjects (subject 17, table 1) had a mutation load of 32%, falling in the lower range of the a-symptomatic subjects, this can not be the only factor involved. The involvement of (yet unknown) genetic and environmental factors has been proposed [99]. It is striking that a-symptomatic subject 25 (60% mutation load, table 1) is a fanatic sportsman who runs marathons. Physical exercise is known to stimulate mitochondrial proliferation in patients with mitochondrial myopathy [131], and therefore might have a favourable effect on this compensatory mechanism, as long as no symptoms are present. Moreover, it is well known that physical exercise delays the

reduction of muscle mass during aging and therefore might support the regenerative process which is stimulated in m.3243A>G mutation carriers by complement activation. Physical exercise has also been suggested as a tool to stimulate muscle regeneration in order to increase the proportion of wild-type mtDNA molecules in the muscle tissue. Exercise would lead to specific necrosis of exercise muscle fibres, which in turn would trigger muscle fibre regeneration populating the new muscle fibres with predominantly wild-type mtDNA molecules [132]. Therapeutic interventions aimed at stimulating mitochondrial proliferation, muscle regeneration and reducing ROS damage will be beneficial to delay the onset of symptoms in m.3243A>G carriers. These interventions should start at early age, before symptoms become manifest, as their effect may be detrimental for already affected patients. As protein turnover, apoptosis, and complement activation, with in specific the expression of the *C1R* gene, differ between the symptomatic and a-symptomatic m.3243A>G mutation carriers, the expression of these genes may be markers for the severity and progression of MELAS disease.

Acknowledgements

This research was supported by the Princess Beatrix Foundation, (Grant number: MAR99-0111) and the MitoCircle project (EU grant, Sixth Framework Program, contr. no. 005260). We would like to thank Mr. Pieter Derkx of the Pathology department at Erasmus MC, Rotterdam, The Netherlands, for the preparation of the muscle cryosections.

Supplementary table S1: Significantly differentially expressed genes

Unigene ID	Fold-change	Gene Description	Gene Symbol
S-3243			
Hs.498178	0.6	Actinin, alpha 2	ACTN2
Hs.82609	0.7	Hydroxymethylbilane synthase	HMBS
Hs.367992	0.7	Inositol(myo)-1(or 4)-monophosphatase 2	IMPA2
Hs.101337	0.7	Uncoupling protein 3 (mitochondrial, proton carrier)	UCP3
Hs.440960	0.7	RAD23 homolog A (S. cerevisiae)	RAD23A
Hs.12084	0.7	Tu translation elongation factor, mitochondrial	TUFM
Hs.406678	0.8	Acyl-CoA synthetase long-chain family member 1	ACSL1
Hs.13640	0.8	Roundabout, axon guidance receptor, homolog 1 (Drosophila)	ROBO1
Hs.515274	0.8	Splicing factor 4	SF4
Hs.6651	0.8	Vesicle-associated membrane protein 4	VAMP4
Hs.132902	0.8	CAP, adenylate cyclase-associated protein, 2 (yeast)	CAP2
Hs.514303	0.8	Prohibitin	PHB
Hs.642970	0.8	Transcribed locus	
Hs.43666	0.8	Protein tyrosine phosphatase type IVA, member 3	PTP4A3
Hs.465985	0.8	ArsA arsenite transporter, ATP-binding, homolog 1 (bacterial)	ASNA1
Hs.271135	0.8	ATP synthase, H+ transporting, mitochondrial F1 complex, gamma polypeptide 1	ATP5C1
Hs.36587	0.8	Protein phosphatase 1, regulatory subunit 7	PPP1R7
Hs.283551	0.8	Eukaryotic translation initiation factor 2B, subunit 5 epsilon, 82kDa	EIF2B5
Hs.433750	0.8	Eukaryotic translation initiation factor 4 gamma, 1	EIF4G1
Hs.52788	0.8	Fragile X mental retardation, autosomal homolog 2	FXR2
Hs.534338	0.8	Protein phosphatase 4 (formerly X), catalytic subunit	PPP4C
Hs.513522	0.8	Fusion (involved in t(12;16) in malignant liposarcoma)	FUS
Hs.515139	0.8	Transmembrane emp24 protein transport domain containing 1	TMED1
Hs.54460	0.9	Chemokine (C-C motif) ligand 11	CCL11
Hs.632340	0.9	Methylenetetrahydrofolate dehydrogenase (NADP+ dependent) 1, methenyltetrahydrofolate cyclohydrolase, formyltetrahydrofolate synthetase	MTHFD1
Hs.643147	0.9	Transcribed locus	
Hs.37092	0.9	Fibroblast growth factor 3 (murine mammary tumor virus integration site (v-int-2) oncogene homolog)	FGF3
Hs.419815	0.9	Epidermal growth factor (beta-urogastrone)	EGF
Hs.69089	0.9	Galactosidase, alpha	GLA
Hs.595187	0.9	Transcribed locus	
Hs.597347	0.9	Transcribed locus	
Hs.584887	0.9	Gamma tubulin ring complex protein (76p gene)	76P
Hs.593420	0.9	MRNA; cDNA DKFZp564G112 (from clone DKFZp564G112)	
Hs.631863	0.9	Neuropathy target esterase	PNPLA6
Hs.246381	0.9	Transcribed locus, strongly similar to NP_001242.1 CD68 antigen; Macrophage antigen CD68 (microsialin); macrosialin; scavenger receptor class D, member 1 [Homo sapiens]	
Hs.533022	0.9	Crystallin, beta B3	CRYBB3
Hs.332422	0.9	Aspartate beta-hydroxylase	ASPH
Hs.94367	0.9	Thyroid transcription factor 1	TITF1
Hs.532188	0.9	Integrator complex subunit 1	INTS1
Hs.94395	0.9	ATP-binding cassette, sub-family D (ALD), member 4	ABCD4
Hs.445489	0.9	Pleckstrin homology domain containing, family B (evectins) member 1	PLEKHB1
Hs.464469	0.9	Myomesin 1 (skelemin) 185kDa	MYOM1
Hs.37023	0.9	Growth hormone releasing hormone	GHRH
Hs.584806	0.9	Transcription elongation factor B (SIII), polypeptide 3 (110kDa, elongin A)	TCEB3
Hs.50727	0.9	Hydroxysteroid (17-beta) dehydrogenase 1	HSD17B1
Hs.408458	0.9	WW domain containing E3 ubiquitin protein ligase 2	WWP2
Hs.133444	0.9	PiggyBac transposable element derived 3	PGBD3
Hs.471405	0.9	Tubulin tyrosine ligase-like family, member 4	TTLL4
Hs.432818	0.9	UDP-N-acetyl-alpha-D-galactosamine:polypeptide N-acetylgalactosaminyltransferase 10 (GalNAc-T10)	GALNT10
Hs.591379	0.9	DOT1-like, histone H3 methyltransferase (S. cerevisiae)	DOT1L

Hs.122908	0.9	Chromatin licensing and DNA replication factor 1	CDT1
Hs.198249	0.9	Gap junction protein, beta 5 (connexin 31.1)	GJB5
Hs.74615	1.1	Platelet-derived growth factor receptor, alpha polypeptide	PDGFRA
Hs.24587	1.1	Embryonal Fyn-associated substrate	EFS
Hs.159223	1.1	NGFI-A binding protein 2 (EGR1 binding protein 2)	NAB2
Hs.618002	1.2	Transcribed locus	
Hs.128548	1.2	WD repeat domain 1	WDR1
Hs.390567	1.2	FYN oncogene related to SRC, FGR, YES	FYN
Hs.98594	1.2	Rho guanine nucleotide exchange factor (GEF) 10	ARHGEF10
Hs.202097	1.3	Procollagen C-endopeptidase enhancer	PCOLCE
Hs.174195	1.3	Interferon induced transmembrane protein 2 (1-8D)	IFITM2
Hs.508716	1.4	Collagen, type IV, alpha 2	COL4A2
Hs.296049	1.4	Microfibrillar-associated protein 4	MFAP4
Hs.513022	1.5	Immunoglobulin superfamily containing leucine-rich repeat	ISLR
Hs.458573	1.6	Platelet-derived growth factor receptor-like	PDGFRL
Hs.593775	1.8	NA	NA
Hs.103253	2.2	Perilipin	PLIN
AS-3243			
Hs.116244	0.7	WD repeat domain 62	WDR62
Hs.124940	0.8	Rho family GTPase 1	RND1
Hs.642952	0.8	SRY (sex determining region Y)-box 12	SOX12
Hs.2200	0.8	Perforin 1 (pore forming protein)	PRF1
Hs.442658	0.8	Aurora kinase B	AURKB
Hs.369759	0.8	Transient receptor potential cation channel, subfamily M, member 2	TRPM2
Hs.513484	0.9	Quinolinate phosphoribosyltransferase (nicotinate-nucleotide pyrophosphorylase (carboxylating))	QPRT
Hs.416848	0.9	Cathepsin W (lymphopain)	CTSW
Hs.159309	0.9	Uroplakin 1A	UPK1A
Hs.27183	0.9	Chromosome 14 open reading frame 79	C14orf79
Hs.87247	0.9	Harakiri, BCL2 interacting protein (contains only BH3 domain)	HRK
Hs.531563	0.9	Transmembrane protein 15	TMEM15
Hs.370267	1.1	Tankyrase, TRF1-interacting ankyrin-related ADP-ribose polymerase	TNKS
Hs.100299	1.1	Ligase III, DNA, ATP-dependent	LIG3
Hs.250712	1.1	Calcium channel, voltage-dependent, beta 3 subunit	CACNB3
Hs.513470	1.1	Nuclear factor of activated T-cells, cytoplasmic, calcineurin-dependent 2 interacting protein	NFATC2IP
Hs.461361	1.1	Craniofacial development protein 1	CFDP1
Hs.153022	1.1	TATA box binding protein (TBP)-associated factor, RNA polymerase I, C, 110kDa	TAF1C
Hs.1314	1.1	Tumor necrosis factor receptor superfamily, member 8	TNFRSF8
Hs.487294	1.1	Excision repair cross-complementing rodent repair deficiency, complementation group 2 (xeroderma pigmentosum D)	ERCC2
Hs.119689	1.1	Glycoprotein hormones, alpha polypeptide	CGA
Hs.631503	1.1	Ectonucleoside triphosphate diphosphohydrolase 6 (putative function)	ENTPD6
Hs.528299	1.1	HIV-1 Tat interacting protein, 60kDa	HTATIP
Hs.533551	1.1	Peroxisome proliferative activated receptor, gamma, coactivator-related 1	PPRC1
Hs.546250	1.1	Dynein, cytoplasmic 1, intermediate chain 2	DYNC1I2
Hs.268887	1.1	Serine/threonine kinase 17a (apoptosis-inducing)	STK17A
Hs.19012	1.1	Rab9 effector protein with kelch motifs	RABEPK
Hs.515598	1.1	PRP31 pre-mRNA processing factor 31 homolog (S. cerevisiae)	PRPF31
Hs.183800	1.1	Ran GTPase activating protein 1	RANGAP1
Hs.591054	1.1	BH3 interacting domain death agonist	BID
Hs.557646	1.1	Cyclin-dependent kinase 9 (CDC2-related kinase)	CDK9
Hs.602240	1.1	Transcribed locus	
Hs.463105	1.1	DEAH (Asp-Glu-Ala-His) box polypeptide 8	DHX8
Hs.408312	1.1	Tumor protein p53 (Li-Fraumeni syndrome)	TP53
Hs.642621	1.1	NA	NA
Hs.591189	1.1	KIAA0100	KIAA0100
Hs.2549	1.1	Adrenergic, beta-3-, receptor	ADRB3

Hs.441975	1.1	XIAP associated factor-1	BIRC4BP
Hs.513913	1.1	GABA(A) receptor-associated protein	GABARAP
Hs.493309	1.1	KIAA0020	KIAA0020
Hs.386470	1.1	Neuromedin B	NMB
Hs.606016	1.1	Twist homolog 1 (acrocephalosyndactyly 3; Saethre-Chotzen syndrome) (Drosophila)	TWIST1
Hs.592984	1.1	Scavenger receptor class B, member 2	SCARB2
Hs.159556	1.1	MTERF domain containing 2	MTERFD2
Hs.632368	1.1	Exosome component 10	EXOSC10
Hs.525629	1.1	Metastasis associated 1	MTA1
Hs.444356	1.1	Growth factor receptor-bound protein 2	GRB2
Hs.81134	1.1	Interleukin 1 receptor antagonist	IL1RN
Hs.466044	1.1	Protein kinase N1	PKN1
Hs.517517	1.1	E1A binding protein p300	EP300
Hs.518138	1.1	KIAA0040	KIAA0040
Hs.591946	1.1	Matrix metallopeptidase 20 (enamelysin)	MMP20
Hs.437599	1.1	Hermansky-Pudlak syndrome 5	HPS5
Hs.133539	1.1	Microtubule associated serine/threonine kinase family member 4	MAST4
Hs.35490	1.1	KIAA0350 protein	KIAA0350
Hs.567261	1.2	MAP/microtubule affinity-regulating kinase 2	MARK2
Hs.198853	1.2	Chromosome 12 open reading frame 32	C12orf32
Hs.126714	1.2	Class II, major histocompatibility complex, transactivator	CIITA
Hs.195667	1.2	KIAA0329	KIAA0329
Hs.473296	1.2	Tumor protein D52-like 2	TPD52L2
Hs.607883	1.2	Transcribed locus	
Hs.132370	1.2	Cleavage stimulation factor, 3' pre-RNA, subunit 2, 64kDa	CSTF2
Hs.493202	1.2	Cleavage and polyadenylation specific factor 1, 160kDa	CPSF1
Hs.352614	1.2	1-acylglycerol-3-phosphate O-acyltransferase 7 (lysophosphatidic acid acyltransferase, eta)	AGPAT7
Hs.172865	1.2	Cleavage stimulation factor, 3' pre-RNA, subunit 1, 50kDa	CSTF1
Hs.592088	1.2	Zinc finger protein 205	ZNF205
Hs.5920	1.2	Glucosamine (UDP-N-acetyl)-2-epimerase/N-acetylmannosamine kinase	GNE
Hs.632905	1.2	Transcribed locus	
Hs.472877	1.2	Eyes absent homolog 2 (Drosophila)	EYA2
Hs.272822	1.2	RuvB-like 1 (E. coli)	RUVBL1
Hs.10095	1.2	Myeloid/lymphoid or mixed-lineage leukemia (trithorax homolog, Drosophila); translocated to, 1	MLLT1
Hs.530940	1.2	Transcribed locus, strongly similar to XP_543397.2 PREDICTED: similar to BRCA1 associated protein [Canis familiaris]	
Hs.279913	1.2	Processing of precursor 5, ribonuclease P/MRP subunit (S. cerevisiae)	POP5
Hs.631863	1.2	Neuropathy target esterase	PNPLA6
Hs.592048	1.2	Ubiquinol-cytochrome c reductase core protein II	UQCRC2
Hs.297304	1.2	Glycosyltransferase 8 domain containing 1	GLT8D1
Hs.505033	1.2	V-Ki-ras2 Kirsten rat sarcoma viral oncogene homolog	KRAS
Hs.397918	1.2	KIN, antigenic determinant of recA protein homolog (mouse)	KIN
Hs.520205	1.2	Eukaryotic translation initiation factor 2-alpha kinase 1	EIF2AK1
Hs.84113	1.2	Cyclin-dependent kinase inhibitor 3 (CDK2-associated dual specificity phosphatase)	CDKN3
Hs.485471	1.2	CDC5 cell division cycle 5-like (S. pombe)	CDC5L
Hs.631240	1.2	Transcribed locus	
Hs.591936	1.2	Signal recognition particle receptor ('docking protein')	SRPR
Hs.9383	1.2	Cysteine-rich with EGF-like domains 1	CRELD1
Hs.300404	1.2	Esophageal cancer associated protein	MGC16824
Hs.554831	1.2	Polymerase (RNA) II (DNA directed) polypeptide D	POLR2D
Hs.500340	1.2	Thyroid hormone receptor interactor 4	TRIP4
Hs.159525	1.2	Cell growth regulator with EF-hand domain 1	CGREF1
Hs.558473	1.2	Chromosome 18 open reading frame 10	C18orf10
Hs.575381	1.2	Ankyrin repeat domain 6	ANKRD6
Hs.270043	1.2	KIAA0196	KIAA0196

Hs.631814	1.2	La ribonucleoprotein domain family, member 5	LARP5
Hs.84549	1.2	NADH dehydrogenase (ubiquinone) 1, subcomplex unknown, 1, 6kDa	NDUFC1
Hs.606668	1.2	Transcribed locus	
Hs.264482	1.2	ATG12 autophagy related 12 homolog (S. cerevisiae)	ATG12
Hs.368971	1.2	Nuclear receptor coactivator 6	NCOA6
Hs.1030	1.2	Ras and Rab interactor 1	RIN1
Hs.595201	1.2	Transcribed locus	
Hs.204041	1.2	AHA1, activator of heat shock 90kDa protein ATPase homolog 1 (yeast)	AHSA1
Hs.102308	1.2	Potassium inwardly-rectifying channel, subfamily J, member 8	KCNJ8
Hs.154073	1.2	Solute carrier family 35, member B1	SLC35B1
Hs.494192	1.2	Osteoclast stimulating factor 1	OSTF1
Hs.808	1.2	Heterogeneous nuclear ribonucleoprotein F	HNRPF
Hs.397465	1.2	Homeodomain interacting protein kinase 2	HIPK2
Hs.10848	1.2	BMS1-like, ribosome assembly protein (yeast)	BMS1L
Hs.580681	1.2	SAM domain and HD domain 1	SAMHD1
Hs.436646	1.2	Sodium channel, voltage-gated, type I, beta	SCN1B
Hs.532492	1.2	Acid phosphatase 2, lysosomal	ACP2
Hs.412870	1.2	Transcribed locus, strongly similar to NP_006618.1 POP4 (processing of precursor , S. cerevisiae) homolog; 1110023P21Rik [Homo sapiens]	
Hs.530251	1.2	TAF12 RNA polymerase II, TATA box binding protein (TBP)-associated factor, 20kDa	TAF12
Hs.180711	1.2	Syntaxin 3	STX3
Hs.485081	1.2	WD repeat domain 47	WDR47
Hs.591457	1.2	Polymerase (RNA) III (DNA directed) polypeptide C (62kD)	POLR3C
Hs.25527	1.2	Amyloid beta (A4) precursor protein-binding, family A, member 3 (X11-like 2)	APBA3
Hs.69328	1.2	Lymphocyte antigen 96	LY96
Hs.87726	1.2	Golgi associated, gamma adaptin ear containing, ARF binding protein 3	GGA3
Hs.595540	1.2	SEC24 related gene family, member A (S. cerevisiae)	SEC24A
Hs.151641	1.2	Leucine rich repeat containing 32	LRRC32
Hs.213389	1.2	Golgi autoantigen, golgin subfamily b, macrogolgin (with transmembrane signal), 1	GOLGB1
Hs.1481	1.2	Histidine decarboxylase	HDC
Hs.17883	1.2	Protein phosphatase 1G (formerly 2C), magnesium-dependent, gamma isoform	PPM1G
Hs.404119	1.2	Tissue specific transplantation antigen P35B	TSTA3
Hs.642714	1.2	Interleukin 24	IL24
Hs.591381	1.2	Insulin receptor	INSR
Hs.433419	1.2	Cytochrome c oxidase subunit IV isoform 1	COX4I1
Hs.153863	1.2	SMAD, mothers against DPP homolog 6 (Drosophila)	SMAD6
Hs.310645	1.2	RAB1A, member RAS oncogene family	RAB1A
Hs.492445	1.2	Transcribed locus, strongly similar to NP_056986.2 progestin-induced protein; ubiquitin-protein ligase; hyperplastic discs protein homolog; progestin induced protein [Homo sapiens]	
Hs.509718	1.2	Zinc finger protein 318	ZNF318
Hs.106511	1.2	Protocadherin 17	PCDH17
Hs.353035	1.2	TWIST neighbor	TWISTNB
Hs.519523	1.3	Serpin peptidase inhibitor, clade B (ovalbumin), member 6	SERPINB6
Hs.475334	1.3	KIAA0280	KIAA0280
Hs.592567	1.3	NA	NA
Hs.529846	1.3	Calcium modulating ligand	CAMLG
Hs.462732	1.3	Suppressor of zeste 12 homolog (Drosophila)	SUZ12
Hs.169474	1.3	Eukaryotic translation initiation factor 2B, subunit 4 delta, 67kDa	EIF2B4
Hs.278573	1.3	CD59 molecule, complement regulatory protein	CD59
Hs.510172	1.3	Human immunodeficiency virus type I enhancer binding protein 2	HIVEP2
Hs.518460	1.3	Adaptor-related protein complex 2, mu 1 subunit	AP2M1
Hs.269092	1.3	Chromodomain protein, Y-like	CDYL
Hs.513044	1.3	Chondroitin sulfate proteoglycan 4 (melanoma-associated)	CSPG4
Hs.584782	1.3	Nardilysin (N-arginine dibasic convertase)	NRD1
Hs.473087	1.3	CTP synthase	CTPS

Hs.258314	1.3	Brain and reproductive organ-expressed (TNFRSF1A modulator)	BRE
Hs.556018	1.3	Interleukin-1 receptor-associated kinase 1 binding protein 1	IRAK1BP1
Hs.31334	1.3	PRP6 pre-mRNA processing factor 6 homolog (S. cerevisiae)	PRPF6
Hs.12970	1.3	Proteasome (prosome, macropain) 26S subunit, non-ATPase, 3	PSMD3
Hs.475150	1.3	Death-inducing-protein	DIP
Hs.443465	1.3	Transcription elongation regulator 1	TCERG1
Hs.502528	1.3	NADH dehydrogenase (ubiquinone) Fe-S protein 3, 30kDa (NADH-coenzyme Q reductase)	NDUFS3
Hs.597390	1.3	Transcribed locus	
Hs.601814	1.3	Transcribed locus	
Hs.122346	1.3	MAD2L1 binding protein	MAD2L1BP
Hs.567380	1.3	Far upstream element (FUSE) binding protein 1	FUBP1
Hs.3439	1.3	Stomatin (EPB72)-like 2	STOML2
Hs.517948	1.3	DEAH (Asp-Glu-Ala-His) box polypeptide 30	DHX30
Hs.75782	1.3	General transcription factor IIIC, polypeptide 2, beta 110kDa	GTF3C2
Hs.22616	1.3	KIAA0664	KIAA0664
Hs.3873	1.3	Palmitoyl-protein thioesterase 1 (ceroid-lipofuscinosis, neuronal 1, infantile)	PPT1
Hs.465929	1.3	Calponin 1, basic, smooth muscle	CNN1
Hs.445350	1.3	Flavin containing monooxygenase 3	FMO3
Hs.182625	1.3	VAMP (vesicle-associated membrane protein)-associated protein B and C	VAPB
Hs.202470	1.3	UV radiation resistance associated gene	UVRAG
Hs.598003	1.3	Transcribed locus	
Hs.295917	1.3	ATPase, H+ transporting, lysosomal 56/58kDa, V1 subunit B2	ATP6V1B2
Hs.283111	1.3	KIAA0323	KIAA0323
Hs.79081	1.3	Protein phosphatase 1, catalytic subunit, gamma isoform	PPP1CC
Hs.528833	1.3	Fatso	FTO
Hs.201253	1.3	Cytoskeleton associated protein 5	CKAP5
Hs.601349	1.3	Transcribed locus	
Hs.591910	1.3	Tripartite motif-containing 32	TRIM32
Hs.467236	1.3	Zinc finger protein 160	ZNF160
Hs.3254	1.3	Mitochondrial ribosomal protein L23	MRPL23
Hs.500245	1.3	Discs, large homolog 5 (Drosophila)	DLG5
Hs.524484	1.4	Integrin, alpha 7	ITGA7
Hs.31387	1.4	Ariadne homolog 2 (Drosophila)	ARIH2
Hs.631618	1.4	Tropomyosin 4	TPM4
Hs.523238	1.4	Nucleolar and coiled-body phosphoprotein 1	NOLC1
Hs.524899	1.4	Sin3A-associated protein, 18kDa	SAP18
Hs.69745	1.4	Ferredoxin reductase	FDXR
Hs.26770	1.4	Fatty acid binding protein 7, brain	FABP7
Hs.2430	1.4	Vacuolar protein sorting 72 (S. cerevisiae)	VPS72
Hs.151777	1.4	Eukaryotic translation initiation factor 2, subunit 1 alpha, 35kDa	EIF2S1
Hs.157394	1.4	Hydroxyacylglutathione hydrolase	HAGH
Hs.269128	1.4	SNF1-like kinase 2	SNF1LK2
Hs.642820	1.4	Transcribed locus	
Hs.128548	1.4	WD repeat domain 1	WDR1
Hs.523215	1.4	NADH dehydrogenase (ubiquinone) 1 beta subcomplex, 8, 19kDa	NDUFB8
Hs.139896	1.4	Macrophage erythroblast attacher	MAEA
Hs.65234	1.4	DEAD (Asp-Glu-Ala-Asp) box polypeptide 27	DDX27
Hs.441926	1.4	Chromosome 13 open reading frame 24	C13orf24
Hs.291212	1.4	Tubulin-specific chaperone a	TBCA
Hs.523414	1.4	Insulin-like growth factor 2 (somatomedin A)	IGF2
Hs.12107	1.4	Chromatin modifying protein 2A	CHMP2A
Hs.569312	1.4	Dynein, cytoplasmic 1, heavy chain 1	DYNC1H1
Hs.564847	1.4	Small nuclear ribonucleoprotein polypeptide N	SNRPN
Hs.556600	1.4	Myosin, light polypeptide kinase	MYLK

Hs.3459	1.4	Ubiquitin-binding protein homolog	UBPH
Hs.463465	1.5	UTP18, small subunit (SSU) processome component, homolog (yeast)	UTP18
Hs.17441	1.5	Collagen, type IV, alpha 1	COL4A1
Hs.514435	1.5	Splicing factor 3b, subunit 3, 130kDa	SF3B3
Hs.190968	1.5	Ribosomal protein S21	RPS21
Hs.448589	1.5	Ankyrin repeat domain 1 (cardiac muscle)	ANKRD1
Hs.434937	1.5	Peptidylprolyl isomerase B (cyclophilin B)	PPIB
Hs.462590	1.5	Myosin XVIIIA	MYO18A
Hs.413801	1.6	Proteasome (prosome, macropain) activator subunit 4	PSME4
Hs.12457	1.6	Nucleoporin 133kDa	NUP133
Hs.189716	1.6	NADH dehydrogenase (ubiquinone) 1, alpha/beta subcomplex, 1, 8kDa	NDUFAB1
Hs.602622	1.7	Transcribed locus	
Hs.508716	2.1	Collagen, type IV, alpha 2	COL4A2
Hs.632144	4.9	Serum amyloid A1	SAA1
Mut-3243			
Hs.527919	0.7	Karyopherin alpha 3 (importin alpha 4)	KPNA3
Hs.35052	0.7	Testis enhanced gene transcript (BAX inhibitor 1)	TEGT
Hs.481551	0.7	5-methyltetrahydrofolate-homocysteine methyltransferase reductase	MTRR
Hs.432642	0.8	Mitogen-activated protein kinase 12	MAPK12
Hs.515003	0.8	Chromosome 19 open reading frame 6	C19orf6
Hs.247729	0.8	RAS (RAD and GEM)-like GTP-binding 1	REM1
Hs.99960	0.8	Membrane-spanning 4-domains, subfamily A, member 3 (hematopoietic cell-specific)	MS4A3
Hs.296949	0.9	Claudin 9	CLDN9
Hs.159509	0.9	Serpin peptidase inhibitor, clade F (alpha-2 antiplasmin, pigment epithelium derived factor), member 2	SERPINF2
Hs.32505	0.9	Potassium inwardly-rectifying channel, subfamily J, member 4	KCNJ4
Hs.631564	0.9	Protein kinase C, gamma	PRKCG
Hs.481466	0.9	Transcribed locus, strongly similar to NP_060610.1 hypothetical protein FLJ10565 [Homo sapiens]	
Hs.431792	0.9	Growth arrest-specific 8	GAS8
Hs.399800	0.9	A kinase (PRKA) anchor protein 8-like	AKAP8L
Hs.29282	0.9	Mitogen-activated protein kinase kinase kinase 3	MAP3K3
Hs.37860	0.9	Kruppel-like factor 1 (erythroid)	KLF1
Hs.631759	1.0	NA	NA
Hs.442182	1.1	ATP-binding cassette, sub-family C (CFTR/MRP), member 6	ABCC6
Hs.463045	1.1	GCN5 general control of amino-acid synthesis 5-like 2 (yeast)	GCN5L2
Hs.503546	1.1	Fatty acid desaturase 1	FADS1
Hs.100921	1.1	Zinc finger protein 193	ZNF193
Hs.279906	1.1	Cyclin T1	CCNT1
Hs.179565	1.1	MCM3 minichromosome maintenance deficient 3 (S. cerevisiae)	MCM3
Hs.584836	1.1	Transcribed locus, strongly similar to NP_004782.1 integrin, beta-like 1 (with EGF-like repeat domains) [Homo sapiens]	
Hs.503165	1.1	Centaurin, delta 2	CENTD2
Hs.523835	1.1	CDK2-associated protein 2	CDK2AP2
Hs.119014	1.1	Zinc finger protein 175	ZNF175
Hs.97616	1.1	SH3-domain GRB2-like 1	SH3GL1
Hs.533613	1.1	Troponin T type 2 (cardiac)	TNNT2
Hs.590970	1.1	AXL receptor tyrosine kinase	AXL
Hs.1570	1.1	Histamine receptor H1	HRH1
Hs.88556	1.1	Histone deacetylase 1	HDAC1
Hs.268107	1.1	Multimerin 1	MMRN1
Hs.166011	1.1	Catenin (cadherin-associated protein), delta 1	CTNND1
Hs.308340	1.1	Nucleoporin 188kDa	NUP188
Hs.517888	1.1	Cartilage associated protein	CRTAP
Hs.143288	1.1	Hypothetical protein MGC11271	MGC11271
Hs.155040	1.1	Zinc finger protein 217	ZNF217
Hs.274184	1.1	Transcription factor binding to IGHM enhancer 3	TFE3

Hs.502872	1.1	Mitogen-activated protein kinase kinase kinase 11	MAP3K11
Hs.611901	1.1	NA	NA
Hs.555936	1.1	APEX nuclease (apurinic/apyrimidinic endonuclease) 2	APEX2
Hs.524518	1.2	Signal transducer and activator of transcription 6, interleukin-4 induced	STAT6
Hs.632219	1.2	Small optic lobes homolog (Drosophila)	SOLH
Hs.467898	1.2	Adenylate cyclase 3	ADCY3
Hs.312098	1.2	ADAM metallopeptidase domain 15 (metargidin)	ADAM15
Hs.103834	1.2	Transmembrane protein 106C	TMEM106C
Hs.596164	1.2	Transcribed locus	
Hs.596205	1.2	Transcribed locus	
Hs.283844	1.2	Sideroflexin 3	SFXN3
Hs.433445	1.2	Jagged 2	JAG2
Hs.292843	1.2	Prostaglandin F receptor (FP)	PTGFR
Hs.507515	1.2	Olfactomedin-like 2B	OLFML2B
Hs.169998	1.2	Bone marrow stromal cell antigen 1	BST1
Hs.430551	1.2	IQ motif containing GTPase activating protein 1	IQGAP1
Hs.371617	1.2	Polycomb group ring finger 2	PCGF2
Hs.611934	1.2	Transcribed locus	
Hs.434888	1.2	Ring finger protein 44	RNF44
Hs.118631	1.2	Timeless homolog (Drosophila)	TIMELESS
Hs.516790	1.2	Transcribed locus, strongly similar to NP_004714.2 rho/rac guanine nucleotide exchange factor 2; proliferating cell nucleolar antigen p40 [Homo sapiens]	
Hs.271940	1.2	E74-like factor 4 (ets domain transcription factor)	ELF4
Hs.483635	1.2	Fibroblast growth factor 1 (acidic)	FGF1
Hs.85539	1.2	ATP synthase, H+ transporting, mitochondrial F0 complex, subunit E	ATP5I
Hs.472213	1.2	Ribosome binding protein 1 homolog 180kDa (dog)	RRBP1
Hs.89643	1.2	Transketolase (Wernicke-Korsakoff syndrome)	TKT
Hs.513463	1.2	P8 protein (candidate of metastasis 1)	NUPR1
Hs.3109	1.2	Rho GTPase activating protein 4	ARHGAP4
Hs.509067	1.2	Platelet-derived growth factor receptor, beta polypeptide	PDGFRB
Hs.16355	1.2	Myosin, heavy polypeptide 10, non-muscle	MYH10
Hs.153357	1.2	Procollagen-lysine, 2-oxoglutarate 5-dioxygenase 3	PLOD3
Hs.529044	1.2	RAB22A, member RAS oncogene family	RAB22A
Hs.642644	1.2	NA	NA
Hs.75189	1.2	Death-associated protein	DAP
Hs.213861	1.2	Laminin, alpha 4	LAMA4
Hs.436298	1.2	Epithelial membrane protein 1	EMP1
Hs.462214	1.2	Growth arrest-specific 7	GAS7
Hs.155919	1.3	Protein tyrosine phosphatase, receptor type, K	PTPRK
Hs.489284	1.3	Actin related protein 2/3 complex, subunit 1B, 41kDa	ARPC1B
Hs.490273	1.3	CAMP responsive element binding protein 3-like 2	CREB3L2
Hs.441783	1.3	Chromosome 14 open reading frame 78	C14orf78
Hs.438823	1.3	NA	NA
Hs.377090	1.3	Zinc fingers and homeoboxes 2	ZHX2
Hs.511952	1.3	NA	NA
Hs.592129	1.3	Cancer susceptibility candidate 3	CASC3
Hs.520102	1.3	KIAA0082	KIAA0082
Hs.501012	1.3	Adducin 3 (gamma)	ADD3
Hs.444767	1.3	Kinesin family member 13B	KIF13B
Hs.439312	1.3	Phospholipid transfer protein	PLTP
Hs.144492	1.3	Phospholipase C, epsilon 1	PLCE1
Hs.520740	1.3	Secernin 1	SCRN1
Hs.274313	1.3	Insulin-like growth factor binding protein 6	IGFBP6
Hs.631504	1.3	Ras association (RalGDS/AF-6) domain family 2	RASSF2
Hs.519909	1.3	Myristoylated alanine-rich protein kinase C substrate	MARCKS

Hs.439463	1.3	AE binding protein 1	AEBP1
Hs.12967	1.4	Spectrin repeat containing, nuclear envelope 1	SYNE1
Hs.198862	1.4	Fibulin 2	FBLN2
Hs.433222	1.4	Niemann-Pick disease, type C2	NPC2
Hs.502461	1.4	Diacylglycerol kinase, zeta 104kDa	DGKZ
Hs.642891	1.4	Transcribed locus	
Hs.117060	1.4	Extracellular matrix protein 2, female organ and adipocyte specific	ECM2
Hs.476092	1.4	C-type lectin domain family 3, member B	CLEC3B
Hs.507755	1.4	Doublecortin and CaM kinase-like 1	DCAMKL1
Hs.536663	1.4	Integrin, beta 5	ITGB5
Hs.520182	1.4	Translocation associated membrane protein 2	TRAM2
Hs.79299	1.4	Lipoma HMGIC fusion partner-like 2	LHFPL2
Hs.12956	1.4	Tax1 (human T-cell leukemia virus type I) binding protein 3	TAX1BP3
Hs.406300	1.5	Ribosomal protein L23	RPL23
Hs.9754	1.5	Activating transcription factor 5	ATF5
Hs.501280	1.5	HtrA serine peptidase 1	HTRA1
Hs.502756	1.5	AHNAK nucleoprotein (desmoyokin)	AHNAK
Hs.153381	1.5	Duffy blood group, chemokine receptor	DARC
Hs.143873	1.6	S100 calcium binding protein A10 (annexin II ligand, calpactin I, light polypeptide (p11))	S100A10
Hs.442378	1.6	Cysteine dioxygenase, type I	CDO1
Hs.201641	1.6	Brain abundant, membrane attached signal protein 1	BASP1
Hs.633826	1.6	Transcribed locus	
Hs.531081	1.6	Lectin, galactoside-binding, soluble, 3 (galectin 3)	LGALS3
Hs.391561	1.7	Fatty acid binding protein 4, adipocyte	FABP4
Hs.155597	1.7	Complement factor D (adipsin)	CFD
Hs.593123	1.7	Transcribed locus	
Hs.494173	1.7	Annexin A1	ANXA1
Hs.598135	1.8	Transcribed locus	
Hs.500572	1.8	Fer-1-like 3, myoferlin (C. elegans)	FER1L3
Hs.192233	1.9	Periplakin	PPL
Hs.384598	1.9	Serpin peptidase inhibitor, clade G (C1 inhibitor), member 1, (angioedema, hereditary)	SERPING1
Hs.213394	2.0	Erythrocyte membrane protein band 4.1-like 3	EPB41L3
Hs.436657	2.1	Clusterin	CLU
Hs.567497	2.1	Complement component 1, r subcomponent	C1R
Hs.533317	2.7	Vimentin	VIM

CHAPTER 5

Increasing levels of the m.9176T>C mutation in monoclonal human skin fibroblasts induces changes in apoptosis and cytoskeleton organisation

R.G.E. van Eijsden [1, 2, 3$], F.H.J. van Tienen [1, 4], L.M.T. Eijssen [1, 5$], H.J.M. Smeets [1, 2]

[1]Department Genetics and Cell Biology – Clinical Genetics, Maastricht University, Maastricht – The Netherlands.
[2]Research Institute Growth & Development, Maastricht University, Maastricht – The Netherlands.
[3]MicroArray Facility, VIB, Leuven – Belgium.
[4]Research Institute NUTRIM, Maastricht University, Maastricht – The Netherlands.
[5]BiGCaT Bioinformatics, Maastricht University, Maastricht – The Netherlands.

[$]Current affiliation.

In preparation

Abstract

Heteroplasmic mitochondrial DNA mutations have a threshold of expression above which clinical symptoms become manifest. This threshold is tissue-, mutation- and individual specific and usually the phenotypic expression or transcription profiles of different patients with different mutation loads are being compared to elucidate the underlying pathogenic mechanisms. To reduce sources of variation, which trouble the interpretation of these data, we performed - as a model experiment - gene expression profiling in isolated individual fibroblasts of a single patient with different levels of the m.9176T>C mutation. The m.9176T>C mutation in the adenosine triphosphate synthase 6 (*ATP6*) gene causes Leigh syndrome when exceeding a mutation load threshold of about 90%. Furthermore, the mutation load of this mutation is fairly constant among the different tissues analyzed. Fibroblasts were cultured from monoclonal cell populations with mutation loads above and under the level of clinical expression under forced aerobic culturing conditions in order to elicit a pathogenic effect, if present. Gene expression profiles were determined and the most prominent changes appeared to be related to apoptosis and cytoskeleton organisation as an apoptosis early event. Our data show that our model is accurate to study different mtDNA mutation levels in a homogeneous genetic background.

Introduction

A characteristic of mitochondrial DNA (mtDNA) mutations is the coexistence of mutated and wild-type mtDNA molecules within mitochondria, cells and tissues. This phenomenon of heteroplasmy partly explains the differences in severity and nature of clinical manifestations of oxidative phosphorylation (OXPHOS) disease, although it is no clear-cut and direct linear relation. The presentation of the m.3243A>G mutation, which is one of the most frequent mtDNA mutations and a major cause of the MELAS syndrome (Myopathy, Encephalopathy, Lactic Acidosis and Stroke-like episodes), is variable and only partially related to the mutation load, suggesting a role for modifying environmental or other genetic factors [99]. The m.8993T>C/G mutation in the adenosine triphosphate synthase 6 (*ATP6*) gene is an example of an mtDNA mutation with a more direct relation between heteroplasmy level and clinical symptoms. Clinical symptoms usually occur when the mutation load rises above 60% for the m.8993A>G or above 80% for the m.8993T>C mutation, resulting in Neuropathy, Ataxia, and Retinitis Pigmentosa (NARP) [11]. When mutation loads exceed 90% subjects present with the severe phenotype of maternally inherited Leigh syndrome [9-11]. A similar correlation between clinical features and mtDNA mutation load most likely exists for the m.9176T>C mutation in the ATP6 gene, although the number of patients and families studied is still small. When the mutation load is higher than the threshold of 90%, subjects present with Leigh syndrome. Mutation loads below the threshold value of 90% most often results in very mild or even no clinical symptoms at all [3-5, 133-137].

To study the molecular biological processes induced by different mtDNA mutation levels by gene expression profiling, in general, tissues or cell lines from different patients with different levels of the mtDNA mutation are being compared. A disadvantage of this approach is the difference in nuclear backgrounds, introducing experimental variability. To circumvent this, cell culture systems can be used where mitochondria from patient cells are transferred to a cell line lacking mtDNA (rho^0 cells) [138, 139], allowing the study of mutation loads ranging from 0% to 100%. A disadvantage is that rho^0 cells are in general tumour cells with an unstable nuclear background and that an experimental intervention is required to create cell lines with different mutation loads. This might cause unwanted experimental variability and affect gene expression levels. Therefore we established a new model system and analyzed gene expression profiles of cell cultures derived from individual primary skin fibroblasts from a single carrier of the m.9176T>C mutation. Each fibroblast has a different mutation load ranging from 0% to 100%, providing the opportunity to generate cell lines with different mutation levels of the m.9176T>C point mutation without introducing individual or experimental variability. Cells were cultured under forced aerobic conditions in order to elicit a pathogenic effect, if present.

Materials & methods

Cell cultures

A cell culture was setup using fibroblast cells from a female carrier of the m.9176T>C mutation in the ATP6 gene. The mutation load in this cell line was 77.7%. Cells were initially cultured in DMEM with a high glucose concentration (4500 mg/L) (Invitrogen, Carlsbad, CA, USA) supplemented with 10% foetal bovine serum (Invitrogen, Carlsbad, CA, USA) and 50 µg/mL (0.2 mM) uridine (Acros Organics, Geel, Belgium) in a T75 cell culture flask. After reaching ~90% confluence, cells were washed with 5 mL Hanks Balanced Salt Solution (HBSS) (Invitrogen, Carlsbad, CA), treated with trypLE (Invitrogen, Carlsbad, CA, USA) to detach them from the bottom of the cell culture flask, and resuspended in culture medium to a final concentration of 40 cells/mL of which 1 mL was transferred to each well of two 6-well culture plates. Conditional medium was prepared from a wild-type fibroblast control cell culture by sterilizing 2 day old medium from a 70% confluent culture through a 0.2 µm filter. Next, 1 mL conditional medium was added to each well. Each 4-5 days, 1 mL fresh culture medium was added to each well. After two weeks, when colonies of cells were formed in each well, medium was removed and cells were washed with 1 mL HBSS. Cells were treated with 100 µL of trypLE for 5 minutes at 37 °C to detach them from the bottom of the cell culture plate. From each well, one colony was manually transferred by pipette to a new well in a 6 well culture plate containing a mixture of 1 mL culture medium and 1 mL conditional medium. Every 4-5 days, 1 mL culture medium was added or the medium was refreshed with 2 mL culture medium. When a well reached 90% confluence, cells were treated with trypLE and one half was transferred to a new T75 culture flask containing 12 mL culture medium. The other half of the cell pellet was resuspended in 50 µL 1x phosphatebuffered Saline (PBS) + 1% polyvinylpyrolidone +

phenol red to use for later mutation load quantification (time point 1). When the cell culture reached 50% confluence, medium was removed and cells were washed with 5 mL PBS and 12 mL stringent medium was added. The stringent medium contained DMEM without glucose or sodium pyruvate (Invitrogen, Carlsbad, CA, USA), supplemented with 20% dialyzed foetal bovine serum (Invitrogen, Carlsbad, CA, USA), 5 mM galactose (Sigma-Aldrich, St. Louis, MO, USA), and 50 µg/mL (0.2 mM) uridine. Omitting glucose and sodium pyruvate from the medium forces the cells to use the OXPHOS system (aerobic energy metabolism). After 72 hours on the stringent medium, RNA and DNA (time point 2) were isolated from the cell cultures.

RNA and DNA isolation from fibroblasts

Total RNA was isolated from the fibroblast cell cultures according to the manufacturer's protocol using TRIzol reagent (Invitrogen, Carlsbad, CA, USA) and RNA was purified using the RNeasy clean-up kit (Qiagen, Hilden, Germany). RNA quantity and purity were determined spectrophotometrically with the Nanodrop ND-1000 (Nanodrop Technologies, Wilmington, DE, USA) and RNA integrity was assessed by determining the RNA 28S/18S ratio on a Bioanalyser 2100 (Agilent Technologies, Santa Clara, CA, USA).

DNA was isolated from the remaining interphase and organic phase from the TRIzol RNA isolation using a back extraction buffer. The back extraction buffer contained 4 M guanidine thiocyanate (Sigma-Aldrich, St. Louis, MO, USA), 50 mM sodiumcitrate (Merck & Co., Inc., Whitehouse Station, NJ, USA), and 1 M Tris (free base) (Roche, Basel, Switzerland). Back extraction buffer (500 µL per mL TRIzol) was added to the samples and the samples were vortexed for 15 seconds. Samples were incubated for 10 minutes at room temperature and centrifuged at maximum speed in an eppendorf centrifuge. Supernatant was removed and the DNA pellet was washed twice with 75% ethanol (750 µL per mL TRIzol). DNA pellets were air dried and dissolved in 30 µL nuclease free water. DNA purity and concentration were determined spectrophotometrically using the Nanodrop ND-1000.

m.9176T>C mutation load quantification

Forward (5'-TCATGCACCTAATTGGAAGCG-3') and reverse (5'-GTGTTGTCGTGCAGGTACCAGCTTACT-3') primers were used for amplification of the fragment carrying the m.9176T>C mutation by polymerase chain reaction (PCR). The reverse primer contained a three nucleotide mismatch at positions 18-20 of the primer sequence to create a restriction site in the PCR fragment for the *Bst*XI restriction enzyme, if the mutation is present. Cycling conditions were as follows: denaturation for 6' at 94°C, 35 cycles of 1' at 92°C, 1' at 52°C, and 45'' at 72°C, and a final elongation step for 7' at 72°C. A FAM-labelled forward primer was added to the final PCR cycle with a denaturation step for 2' at 94°C, annealing for 1' 52°C, and an elongation step for 7' at 72°C. PCR was carried out directly on 2 µL of the cell suspension stored previously (time point 1 - see above) after a cell lyses step, or on 2 µL DNA solution from the back extraction isolation (time point 2 -

see above). Cell lyses solution was prepared by dissolving 4.05 mg Dithiothreitol (DTT) in 210 µL NaOH (1 M) and 210 µL sterile water. Before use, the lyses solution was UV-irradiated for 1 hour to prevent DNA contamination. One µL lyses solution was added to 2 µL of the cell suspension. Lyses was performed at 65°C for 10 minutes.

Heteroplasmy levels were determined by digestion with the *Bst*XI enzyme (New England Biolabs, Ipswich - MA, USA) resulting in a wild-type fragment of 169 bp and mutant fragments of 148 and 21 bp. Digested products were analyzed on an ABI-PRISM 3100 genetic analyzer using the GeneScan Analysis 3.7 software package (Applied Biosystems, Foster City, CA, USA). The ratio of the area under the 148 bp mutant peak and the sum of the area's under the mutant (148 bp) and wild-type (169 bp) peaks was calculated to determine the heteroplasmy levels of the m.9176T>C mutation.

Gene expression profiling

One µg of total RNA from each sample was amplified using the Amino Allyl MessageAmp II aRNA kit (Ambion, Austin, TX, USA) to generate amino allyl aRNA (AA-aRNA), according to the manufacturer's protocol. A UTP: AA-UTP ratio of 7:3 was used instead of 1:1. The size distribution profile of the aRNA was assessed using a Bioanalyser 2100 (Agilent Technologies, Santa Clara, CA, USA). Each amino AA-aRNA sample was coupled to Cy3 or Cy5 dye (Amersham Biosciences, Uppsala, Sweden) and cleaned up with the RNeasy Minelute clean-up kit (Qiagen, Hilden, Germany). RNA quantity and dye incorporation efficiency were determined spectrophotometrically using the Nanodrop ND-1000. Hybridisation was performed on CodeLink slides (Amersham Biosciences, Uppsale - Sweden) containing the Operon Human oligo collection V2 with 21521 features (Operon Biotechnologies, Inc., Huntsville, AL, USA) printed by the UMC Microarray Facility (University Medical Centre Utrecht, Utrecht, The Netherlands). Slides were blocked in 5xSSC, 25% Formamide, 0.1% SDS, 1% BSA (Sigma-Aldrich, St. Louis, MO, USA) for 1 hour. Fragmentation was performed on 120 pmol of each dye-labelled aRNA sample (2% - 4.5% dye incorporation) using RNA fragmentation buffer (Ambion, Austin, TX, USA), mixed with 100 µg tRNA (Roche, Basel, Switzerland) and 50 µg Herring sperm DNA (Invitrogen, Carlsbad, CA, USA) in 120 µL hybridisation mix (5xSSC, 25% Formamide, 0.1% SDS), denaturated for 5 minutes at 95°C, hybridised for 16 hours at 42°C and washed 3 times with decreasing concentrations of SSC and SDS (1xSSC, 0.2%SDS, 0.1xSSC, 0.2%SDS, and 0.1xSSC respectively). Hybridisation, washing, and slide drying were performed on a HS 4800 hybridisation station (Tecan, Mannedorf/Zurich, Switzerland). Hybridisation was carried out according to the loop design illustrated in figure 1. Slides were scanned on a GenePix 4000B scanner (Molecular Devices, Sunnyvale, CA, USA) with laser power setting at 100% for both channels and photo multiplier settings at 625 and 746 for the green and the red channel respectively, which ensured a maximum of 0.05% of all spots to be saturated. Scanned images were analyzed and spots were quantified using Array-Pro analyzer software (Media Cybernetics, Bethesda, MD, USA). Bad spots were flagged manually.

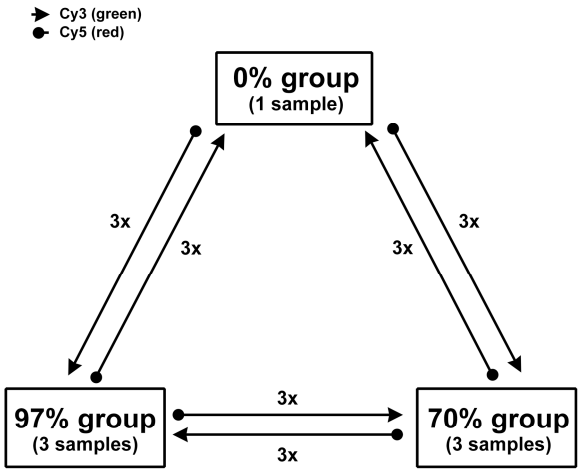

Figure 1: Microarray experimental design.
0% group: fibroblast cell line with 0% mutation load; 70% group: three fibroblast cell lines with mutation loads between 65% and 75%; 97% group: two fibroblast cell lines with mutation loads between 95% and 100%. Each sample was used four times for hybridisation because a dye-swap was carried out, except for the one sample in group 1 which was used 12 times.
Each arrow indicates a two colour hybridisation on a microarray slide, where the head of the arrow indicates a cy3-labeled samples and the tail of the arrow indicates a cy5-labeled sample.

Microarray data analysis and data mining

R, a free software environment for statistical computing and graphics, was used with the *LIMMA* library to perform the microarray data analysis [40, 140]. Background correction was carried out using the method "half", "print tip loes" was used as within array normalisation method, and the "scale" method was used for between array normalisation [141]. In the LIMMA procedure a correction was applied for the dye-effect and the dye-swaps were taken into account as technical replicates [142]. Before model fitting, data from all spots with foreground intensities smaller than twice the background intensities in all samples and in both colours were removed from the dataset. Since there was only one sample in group 1 (see figure 1) resulting in a small within group variance, it was likely that with standard stringency criteria (p-value<0.05) a lot of transcripts would be indicated as significantly differentially expressed of which the majority would be false positive. To overcome this and to correct for multiple testing, the restriction criteria were stringently adjusted and transcripts with an adjusted (Benjamini & Hochberg) p-value<0.001 and an absolute fold-change > 2-fold were selected as significantly differentially expressed [143]. To identify biological processes that were enriched for differentially expressed genes were involved, a process based analysis was carried out using the web-based Database for Annotation, Visualisation and Integrated Discovery (DAVID) [76].

Results and Discussion

Cell cultures and m.9176T>C mutation loads

Culturing single fibroblasts of a female carrier of the m.9176T>C mutation resulted in six cell cultures with different mutation loads and the same nuclear background. The remaining cell cultures grew very slowly or stopped growing for unknown reasons. The cultures could be sub-

divided into three groups based on their mutation loads. The first group comprising one sample with a mutation load of 0%, a second group containing three samples with mutation loads between 65% and 75%, and a third group of two samples with mutation loads between 95% and 100% (see table 1). Cells were cultured for three days under aerobic conditions, using galactose medium, to force them to use the OXPHOS system for their energy demand, after which RNA was isolated. Mutation loads remained more or less the same during these three days (table 1). The largest difference between time point one and two was 8% for cell culture B5. However, this did not have consequences for the mutation load group classification. There was no mutation load difference for cell culture A1 for which the mutation load remained 0%.

Table 1: Overview of cell cultures from the cell culture experiment as described in the materials and methods section

Cell culture	Mutation load at time point 1	Mutation load at time point 2	Group ID	Group description
A1	0,0%	0,0%	1	0%
A6	67,7%	65,6%	2	65-75%
B6	68,3%	69,7%	2	
B5	67,15	75,2%	2	
A4	96,6%	97,3%	3	95-100%
B2	96,5%	100%	3	

Cell culture A1 had an m.9176T>C mutation load of 0%. Cell cultures A6, B5, and B6 had mutation loads between 65% and 75%. Cell cultures A4 and B2 had mutation loads between 95% and 100%. Time point 1: just before applying the stringent galactose medium. Time point 2: After 72 hours on stringent galactose medium.

These cell lines are only theoretically monoclonal, because it is not completely certain that a single colony originates from a single cell, but the distribution of mutation levels will be much more confined to the mean than in the original fibroblast culture which shows a broad distribution with high and low mutation levels (carrier 3, chapter 4, figure 2 in [144]). Analysis of single cells from these cell lines could reveal the distribution pattern. Our approach is superior to the use of cybrid systems to study the effects of differences in mutation loads [138, 139] as cybrids are in general tumour cells with an unstable nuclear background, which introduces unwanted variability in gene expression experiments. This may be less of a disadvantage when studying specific processes, but makes them rather unsuitable for genome-wide gene expression profiling. The use of cell lines from different patients with different mutation loads of the m.9176T>C mutation has the disadvantage of differences in nuclear genetic background, which may mask the effect of the mutation load difference. From previous studies we know that the gene expression differences in fibroblasts with OXPHOS deficiency can be subtle. Our new approach of making 'monoclonal' cell lines allowed us to investigate gene expression differences in cultured skin fibroblast carrying different mutation loads of the m.9176T>C mutation with the same nuclear genetic background and minimal experimental and genetic variation. This approach might also be suitable to study heteroplasmy effects for other mtDNA mutations. However, this will depend on whether or not

the mutation is present in fibroblast cells at different levels and on the distribution and the stability of the mutation loads in individual cells.

Gene expression differences between fibroblasts with different m.9176T>C mutation loads

Microarray gene expression experiments were carried out using RNA from the three cell culture groups according to the experimental design depicted in figure 1. After removal of control spots and spots which did not reach a signal intensity higher than twice the background intensity, 10413 data points remained. For some transcripts more than one probe was spotted. This resulted in replicate entries within the list of significantly differentially expressed genes after LIMMA analysis. For the group 70% versus group 0% (70vs0) comparison, 882 unique transcripts were differentially expressed with 289 and 593 transcripts up- and down-regulated, respectively (supplementary table S1). For the group 97% versus group 0% (97vs0) comparison, 914 transcripts were differentially expressed, of which 365 and 549 were up- and down-regulated respectively (supplementary table S2). In the group 97% versus group 70% (97vs70) comparison 249 transcripts were differentially expressed with 135 up- and 114 down-regulated (supplementary table S3). Table 2 and the Venn diagram in figure 2 summarise the number of differentially expressed genes and illustrate that most gene expression changes occurred in the comparisons with group 0%. Moreover, there was a large overlap between the differentially expressed transcripts in the comparisons with group 0%. A number of 520 transcripts corresponding with a percentage of 59% (520/882) and 57% (520/914) of the differentially expressed genes for respectively the 70vs0 and 97vs0 comparisons overlapped.

Table 2: Significantly differentially expressed genes

Group 70% versus Group 0%					
all-total	**all-up**	**all-down**	**total-unique**	**up-unique**	**down-unique**
910	301	609	882	289	593
Group 97% versus Group 0%					
all-total	**all-up**	**all-down**	**total-unique**	**up-unique**	**down-unique**
937	372	665	914	365	549
Group 97% versus Group 70%					
all-total	**all-up**	**all-down**	**total-unique**	**up-unique**	**down-unique**
249	135	114	249	135	114

Significantly differentially expressed genes with an adjusted p-value<0.001 (Benjamini & Hochberg) and a minimum absolute fold-change>2. For a number of transcripts, more than one probe was spotted on the array, resulting in replicate entries in the differentially expressed gene lists. Here, the overall number of entries and the unique number of entries are listed.

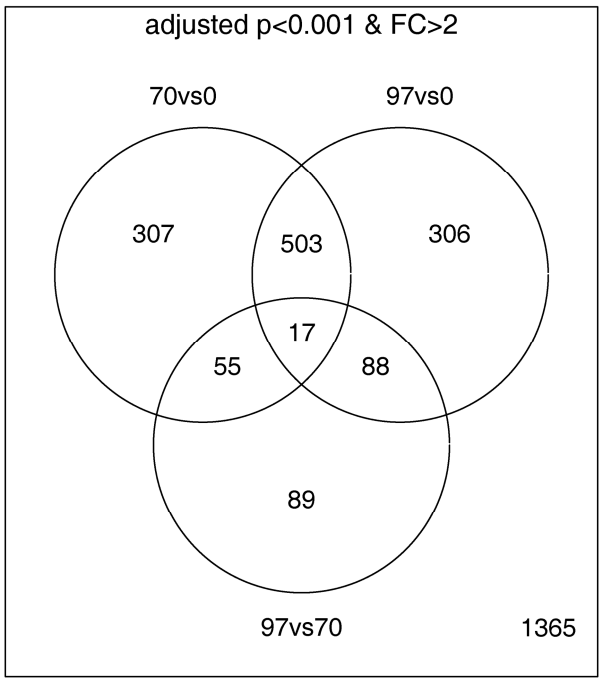

Figure 2: Venn diagram of the results from all three comparisons
Results in the Venn diagram are based on the unique genes in the differentially expressed gene lists only. The highest number of differentially expressed genes was found in the comparisons with group 0%. There is a large overlap between the differentially expressed genes in comparisons between group 70% and 0%, and group 97% and 0%.
p: p-value; FC: fold-change

The quality of the microarray experiment and data analysis is shown by the consistent appearance of genes which were present multiple times on the microarray and appear multiple times in the lists of differentially expressed genes. That most gene expression changes with substantial overlap occur in the comparisons with group 0% is expectable, since these comparisons correspond to the contrasting wild-type (no mutation) versus a fairly high mutation (>70% mutation load) situation. Another factor which might have contributed to the higher number of differentially expressed genes could be that there was only one sample in group 0%, causing the within group variance in this group to be smaller than in the other groups. This was taken into account by increasing the stringency criteria for a gene to be differentially expressed only when the adjusted p-value (corrected for multiple testing) was <0.001, in contrast to the often applied adjusted p-value cut-off of 0.05, and when the absolute fold-change was > 2-fold. The processes in the 70vs0 comparison could be the first processes elicited by the genetic defect, but could also reflect rescue processes as clinical manifestations do not occur at that level. Additionally, the 97vs0 and 97vs70 comparisons could identify processes directly related to the pathophysiology or failing of the rescue process and involved in the transition from non-symptomatic to symptomatic disease. However, it has to be kept in mind that symptoms do not occur in fibroblasts and that the processes in the affected tissues may differ.

Process based analysis comparison group 70% versus group 0%

DAVID functional annotation clustering of the differentially expressed genes from the 70vs0 comparison resulted in six gene clusters with at least one GO BP5 term having a p-value <0.05 (table 3). The first cluster contained genes with functions involved in programmed cell death. The cluster contained 48 unique transcripts (table 4) of which 40 were down-regulated and only 8 were up-regulated. Gene expression changes having a stimulatory effect on apoptosis were

significant down-regulations of apoptosis inhibitory genes. *TNFAIP3* was 5.4 fold down-regulated and is an inhibitor of tumour necrosis factor (TNF) induced apoptosis [145]. The 2.6 fold down-regulated gene *PPP1R13L* is capable of inhibiting apoptosis by inhibition of P53 [146]. *BCL2* is a well-known suppressor of the apoptotic process and was 2.3 fold down-regulated. *BIRC* was 2.0 fold down-regulated, and is an inhibitor of apoptosis (*IAP*) gene, suppressing apoptosis by the inhibition of caspases 3 and 7 [147]. In contrast, there were also down-regulations of apoptosis inducing genes, providing evidence for the inhibition of apoptosis. The *TP53BP2* gene has been shown to be able to induce apoptosis through the mitochondrial apoptotic pathway associated with a reduction of the mitochondrial trans-membrane potential and activation of caspase-9 [148] and was 3.0 fold down-regulated. The *TNFRSF10B* and *TNFRSF1B* genes, down-regulated 2.4 and 2.1 fold respectively, produce proteins which are members of the TNF-receptor superfamily, and on activation are capable of inducing apoptotic signals. *HRK* encodes a pro-apoptotic protein which is linked to the mitochondrial apoptotic pathway by possible interaction with the mitochondrial pore-forming protein p32, and was 2.1 fold down-regulated [149]. Another apoptosis inhibitory effect was the 2.4 fold up-regulation of *PRKCZ*, which has been shown to be able to phosphorylate caspase 9 and thereby inhibit the intrinsic apoptotic process [150].

All of the genes from the second cluster were also present in cluster 4 which contained mainly genes involved in transcription, translation and cytoskeleton organisation. The gene expression changes suggested a down-regulation of the transcriptional and translational processes and pointed to changes in cytoskeleton organisation activity. The *MAP2* gene was 4.0-fold down-regulated and is involved in the organisation and assembly of microtubules [151]. *SVIL,* which was 3.4-fold down-regulated, encodes a protein which forms a tight link between the actin-cytoskeleton and the membrane and therefore is thought to have a function in the recruitment of cytoskeleton proteins into the nucleus or the membrane [152]. *SPTAN1*, also known as alpha fodrin, was 2.1-fold up-regulated and has the ability to bind actin and has therefore been related to the binding of the cytoskeleton to the membrane [153]. Moreover, cleavage of fodrin by the plasmid-encoded toxin (Pet) of enteroaggregative Escherichia coli in epithelial cells results in cytoskeleton disruption [154]. Spectrin beta (*SPTBN1*) was 2.6-fold up-regulated. This cluster also contained the 2.4-fold down-regulated mitochondrial protein 18 Kda (*MTP18*) gene.

Table 3: DAVID functional annotation clustering of the differentially expressed genes from the 70vs0 comparison

Cluster 1	
GO BP Terms	*p-value*
apoptosis	0.00002
negative regulation of programmed cell death	0.00148
regulation of apoptosis	0.01199
regulation of programmed cell death	0.01287
positive regulation of programmed cell death	0.28872
Cluster 2	
GO BP Terms	*p-value*
negative regulation of protein metabolism	0.00403
negative regulation of cell organization and biogenesis	0.04284
regulation of actin polymerization and/or depolymerization	0.07368
actin polymerization and/or depolymerization	0.15979
Cluster 3	
GO BP Terms	*p-value*
protein kinase cascade	0.01167
positive regulation of signal transduction	0.06082
regulation of I-kappaB kinase/NF-kappaB cascade	0.07747
positive regulation of I-kappaB kinase/NF-kappaB cascade	0.13082
Cluster 4	
GO BP Terms	*p-value*
regulation of protein metabolism	0.00606
regulation of cellular biosynthesis	0.14654
regulation of protein biosynthesis	0.21603
Cluster 5	
GO BP Terms	*p-value*
carboxylic acid transport	0.02320
organic acid transport	0.02320
amino acid transport	0.14149
amine transport	0.22212
Cluster 6	
GO BP Terms	*p-value*
nitrogen compound biosynthesis	0.01304
amine biosynthesis	0.01304
amino acid derivative biosynthesis	0.32588
biogenic amine metabolism	0.63068
amino acid derivative metabolism	0.72054

Six clusters could be identified of which at least one of the gene ontology terms had a p-value<0.05.

Cluster 3 consisted of 23 unique transcripts of which 19 were down- and 4 were up-regulate. The genes in this cluster are mainly related to the processes cell proliferation and differentiation and apoptosis. The fifth cluster contained 9 down-regulated genes suggesting an inhibition of amino acid, lactate, and pyruvate transport. The sixth cluster contained 8 down-regulated transcripts and one up-regulated transcript, of which the gene expression changes pointed towards inhibition of amino acid metabolism.

Table 4: Gene members of the clusters identified by the DAVID functional annotation clustering of the differentially expressed genes from the group 70vs0 comparison

Cluster 1				
Genbank Accession No.	***Symbol***	***Title***	***2log fold-change***	***p-value***
NM_005345	HSPA1A	heat shock 70kda protein 1a	-4.3	3.41E-11
NM_005346	HSPA1B	heat shock 70kda protein 1b	-4.1	1.43E-10
NM_005347	HSPA5	heat shock 70kda protein 5 (glucose-regulated protein, 78kda)	-3.5	7.78E-07
NM_021158	TRIB3	tribbles homolog 3 (drosophila)	-3.5	1.30E-07
NM_001831	CLU	clusterin	-3.1	8.52E-09
NM_003299	HSP90B1	heat shock protein 90kda beta (grp94), member 1	-2.6	1.94E-05
AF022375	VEGFA	vascular endothelial growth factor	-2.4	6.47E-10
NM_006290	TNFAIP3	tumour necrosis factor, alpha-induced protein 3	-2.4	3.33E-05
NM_003655	CBX4	chromobox homolog 4 (pc class homolog, drosophila)	-2.2	1.06E-06
NM_006705	GADD45G	growth arrest and dna-damage-inducible, gamma	-2.2	4.64E-07
L24498	GADD45A	growth arrest and dna-damage-inducible, alpha	-2.1	1.12E-05
NM_015675	GADD45B	growth arrest and dna-damage-inducible, beta	-2.0	5.91E-08
NM_014330	PPP1R15A	protein phosphatase 1, regulatory (inhibitor) subunit 15a	-2.0	7.15E-08
BC013128	CEBPG	ccaat/enhancer binding protein (c/ebp), gamma	-1.8	3.57E-07
AK022859	UNC5B	unc-5 homolog b (c. elegans)	-1.7	1.49E-04
NM_013246	CLCF1	cardiotrophin-like cytokine factor 1	-1.6	2.30E-04
NM_005426	TP53BP2	tumour protein p53 binding protein, 2	-1.6	5.85E-08
AF220656	BCM:PHLDA1	pleckstrin homology-like domain, family a, member 1	-1.6	1.24E-04
NM_052815	IER3	immediate early response 3	-1.5	7.47E-06
NM_005923	MAP3K5	mitogen-activated protein kinase kinase kinase 5	-1.5	4.91E-08
NM_002583	PAWR	prkc, apoptosis, wt1, regulator	-1.5	6.51E-05
NM_033027	AXUD1	axin1 up-regulated 1	-1.4	5.04E-05
NM_006663	PPP1R13L	protein phosphatase 1, regulatory (inhibitor) subunit 13 like	-1.4	1.43E-05
NM_004862	LITAF	lipopolysaccharide-induced tnf factor	-1.4	6.62E-04
NM_004281	BAG3	bcl2-associated athanogene 3	-1.4	6.70E-05
AK026181	BCM:PHLDA1	pleckstrin homology-like domain, family a, member 1	-1.3	3.05E-04
NM_004343	CALR	calreticulin	-1.3	7.63E-05
AF016266	TNFRSF10B	tumour necrosis factor receptor superfamily, member 10b	-1.3	4.66E-05
AC004832	SEC14L3	sec14-like 2 (s. cerevisiae)	-1.3	5.48E-06
NM_004052	BNIP3	bcl2/adenovirus e1b 19kda interacting protein 3	-1.2	2.22E-04
NM_005627	SGK	serum/glucocorticoid regulated kinase	-1.2	9.99E-05
NM_000633	BCL2	b-cell cll/lymphoma 2	-1.2	2.15E-04
NM_002715	PPP2CA	protein phosphatase 2 (formerly 2a), catalytic subunit, alpha isoform	-1.1	4.37E-04
NM_001066	TNFRSF1B	tumour necrosis factor receptor superfamily, member 1b	-1.1	1.12E-04
NM_003806	HRK	harakiri, bcl2 interacting protein (contains only bh3 domain)	-1.1	6.90E-05
NM_003680	YARS	tyrosyl-trna synthetase	-1.1	5.43E-06
NM_002507	NGFR	nerve growth factor receptor (tnfr superfamily, member 16)	-1.1	2.95E-05
NM_006410	HTATIP2	hiv-1 tat interactive protein 2, 30kda	-1.1	5.29E-04
NM_005087	FXR1	fragile x mental retardation, autosomal homolog 1	-1.0	3.31E-04
AF070674	BIRC3	baculoviral iap repeat-containing 3	-1.0	1.15E-04
NM_001904	CTNNB1	catenin (cadherin-associated protein), beta 1, 88kda	1.0	3.94E-05
NM_000600	IL6	interleukin 6 (interferon, beta 2)	1.1	2.33E-04

NM_002744	PRKCZ	protein kinase c, zeta	1.3	1.61E-04
NM_000077	CDKN2A	cyclin-dependent kinase inhibitor 2a (melanoma, p16, inhibits cdk4)	1.4	4.36E-05
AK021874	TGFB2	transforming growth factor, beta 2	1.6	6.08E-07
NM_002527	NTF3	neurotrophin 3	2.1	4.72E-08
NM_002982	CCL2	chemokine (c-c motif) ligand 2	2.3	4.91E-08
NM_001562	IL18	interleukin 18 (interferon-gamma-inducing factor)	3.2	8.13E-08

Cluster 2

GB Accession No.	*Symbol*	*Title*	*2log fold-change*	*p-value*
NM_031846	MAP2	microtubule-associated protein 2	-2.0	1.47E-06
NM_004095	EIF4EBP1	eukaryotic translation initiation factor 4e binding protein 1	-1.9	8.94E-08
NM_000609	CXCL12	chemokine (c-x-c motif) ligand 12 (stromal cell-derived factor 1)	-1.8	8.75E-06
NM_021738	SVIL	supervillin	-1.8	2.35E-06
NM_022365	DNAJC1	dnaj (hsp40) homolog, subfamily c, member 1	-1.4	1.04E-06
NM_002715	PPP2CA	protein phosphatase 2 (formerly 2a), catalytic subunit, alpha isoform	-1.1	4.37E-04
NM_003127	SPTAN1	spectrin, alpha, non-erythrocytic 1 (alpha-fodrin)	1.0	7.43E-04
NM_000600	IL6	interleukin 6 (interferon, beta 2)	1.1	2.33E-04
AK025071	SPTBN1	spectrin, beta, non-erythrocytic 1	1.1	3.72E-06
NM_000177	GSN	gelsolin (amyloidosis, finnish type)	1.4	6.57E-06

Cluster 3

GB Accession No.	*Symbol*	*Title*	*2log fold-change*	*p-value*
NM_021158	TRIB3	tribbles homolog 3 (drosophila)	-3.5	1.30E-07
NM_002133	HMOX1	heme oxygenase (decycling) 1	-3.4	5.90E-08
NM_001946	DUSP6	dual specificity phosphatase 6	-2.7	3.04E-08
AF022375	VEGFA	vascular endothelial growth factor	-2.4	6.47E-10
NM_006290	TNFAIP3	tumour necrosis factor, alpha-induced protein 3	-2.4	3.33E-05
NM_006705	GADD45G	growth arrest and dna-damage-inducible, gamma	-2.2	4.64E-07
NM_015675	GADD45B	growth arrest and dna-damage-inducible, beta	-2.0	5.91E-08
NM_057159	EDG2	endothelial differentiation, lysophosphatidic acid g-protein-coupled receptor, 2	-2.0	1.65E-09
NM_006622	PLK2	polo-like kinase 2 (drosophila)	-1.9	1.06E-05
NM_000676	ADORA2B	adenosine a2b receptor	-1.6	2.22E-07
NM_013246	CLCF1	cardiotrophin-like cytokine factor 1	-1.6	2.30E-04
NM_005923	MAP3K5	mitogen-activated protein kinase kinase kinase 5	-1.5	4.91E-08
NM_017572	MKNK2	map kinase interacting serine/threonine kinase 2	-1.4	2.34E-04
NM_004862	LITAF	lipopolysaccharide-induced tnf factor	-1.4	6.62E-04
NM_007207	DUSP10	dual specificity phosphatase 10	-1.4	2.27E-04
AF016266	TNFRSF10B	tumour necrosis factor receptor superfamily, member 10b	-1.3	4.66E-05
NM_004418	DUSP2	dual specificity phosphatase 2	-1.3	1.38E-05
NM_002715	PPP2CA	protein phosphatase 2 (formerly 2a), catalytic subunit, alpha isoform	-1.1	4.37E-04
NM_000985	MIT:HsG2227	ribosomal protein l17	-1.1	1.24E-05
NM_032409	PINK1	pten induced putative kinase 1	1.1	3.42E-04
NM_002982	CCL2	chemokine (c-c motif) ligand 2	2.3	4.91E-08
NM_004335	BST2	bone marrow stromal cell antigen 2	2.8	1.46E-06
NM_000681	ADRA2A	adrenergic, alpha-2a-, receptor	3.2	2.88E-08

Cluster 4

GB Accession No.	*Symbol*	*Title*	*2log fold-change*	*p-value*
NM_013246	CLCF1	cardiotrophin-like cytokine factor 1	-1.6	2.30E-04
BC013128	CEBPG	ccaat/enhancer binding protein (c/ebp), gamma	-1.8	3.57E-07
NM_000609	CXCL12	chemokine (c-x-c motif) ligand 12 (stromal cell-derived factor 1)	-1.8	8.75E-06
NM_022365	DNAJC1	dnaj (hsp40) homolog, subfamily c, member 1	-1.4	1.04E-06
NM_006260	DNAJC3	dnaj (hsp40) homolog, subfamily c, member 3	-2.3	1.97E-07
NM_005228	EGFR	epidermal growth factor receptor (erythroblastic leukemia viral (v-erb-b) oncogene homolog, avian)	-1.4	2.44E-06
AL050005	EIF1	eukaryotic translation initiation factor 1	-1.2	4.37E-06
NM_005875	EIF1B	eukaryotic translation initiation factor 1b	-1.1	4.21E-04

NM_003753	EIF3S7	eukaryotic translation initiation factor 3, subunit 7 zeta, 66/67kda	-1.0	1.33E-04
NM_004095	EIF4EBP1	eukaryotic translation initiation factor 4e binding protein 1	-1.9	8.94E-08
NM_000177	GSN	gelsolin (amyloidosis, finnish type)	1.4	6.57E-06
AC004832	HSPC242	hypothetical protein hspc242	-1.3	5.48E-06
AK024941	DNAJC3	hypothetical protein loc144871	-1.9	1.17E-07
NM_000600	IL6	interleukin 6 (interferon, beta 2)	1.1	2.33E-04
NM_017572	MKNK2	map kinase interacting serine/threonine kinase 2	-1.4	2.34E-04
NM_031846	MAP2	microtubule-associated protein 2	-2.0	1.47E-06
AC004832	MTP18	mitochondrial protein 18 kda	-1.3	5.48E-06
NM_002659	PLAUR	plasminogen activator, urokinase receptor	-1.9	5.23E-07
NM_002715	PPP2CA	protein phosphatase 2 (formerly 2a), catalytic subunit, alpha isoform	-1.1	4.37E-04
AC004832	PTPNS1	protein tyrosine phosphatase, non-receptor type substrate 1	-1.3	5.48E-06
AC004832	PTPNS1L	protein tyrosine phosphatase, non-receptor type substrate 1-like	-1.3	5.48E-06
AC004832	SEC14L2	sec14-like 2 (s. cerevisiae)	-1.3	5.48E-06
AC004832	SEC14L3	sec14-like 3 (s. cerevisiae)	-1.3	5.48E-06
AC004832	SEC14L4	sec14-like 4 (s. cerevisiae)	-1.3	5.48E-06
NM_003127	SPTAN1	spectrin, alpha, non-erythrocytic 1 (alpha-fodrin)	1.0	7.43E-04
AK025071	SPTBN1	spectrin, beta, non-erythrocytic 1	1.1	3.72E-06
NM_021738	SVIL	supervillin	-1.8	2.35E-06

Cluster 5

GB Accession No.	*Symbol*	*Title*	*2log fold-change*	*p-value*
NM_001818	AKR1C4	aldo-keto reductase family 1, member c4 (chlordecone reductase; 3-alpha hydroxysteroid dehydrogenase, type i; dihydrodiol dehydrogenase 4)	-1.8	1.98E-06
NM_003038	SLC1A4	solute carrier family 1 (glutamate/neutral amino acid transporter), member 4	-2.0	5.39E-09
NM_005628	SLC1A5	solute carrier family 1 (neutral amino acid transporter), member 5	-1.7	8.54E-05
NM_003051	SLC16A1	solute carrier family 16 (monocarboxylic acid transporters), member 1	-1.3	5.54E-06
NM_004731	SLC16A7	solute carrier family 16 (monocarboxylic acid transporters), member 7	-1.1	5.46E-04
NM_002394	SLC3A2	solute carrier family 3 (activators of dibasic and neutral amino acid transport), member 2	-3.4	6.87E-11
NM_030674	SLC38A1	solute carrier family 38, member 1	-1.5	4.86E-05
AK024263	SLC38A1	solute carrier family 38, member 1	-1.4	4.63E-07
AF104032	SLC7A5	solute carrier family 7 (cationic amino acid transporter, y+ system), member 5	-2.9	4.00E-10
NM_014331	SLC7A11	solute carrier family 7, (cationic amino acid transporter, y+ system) member 11	-1.9	3.23E-07

Cluster 6

GB Accession No.	*Symbol*	*Title*	*2log fold-change*	*p-value*
NM_001673	ASNS	asparagine synthetase	-2.4	3.80E-10
NM_005504	BCAT1	branched chain aminotransferase 1, cytosolic	-1.8	9.88E-08
AL390172	BCAT1	branched chain aminotransferase 1, cytosolic	-1.4	2.70E-06
AK025615	BCAT1	branched chain aminotransferase 1, cytosolic	-1.3	1.71E-06
NM_001902	CTH	cystathionase (cystathionine gamma-lyase)	-3.1	1.93E-10
NM_000071	CBS	cystathionine-beta-synthase	-1.9	3.21E-05
AK027113	BCM:bcm714	ethanolamine kinase 1	-1.0	2.73E-04
NM_006907	PYCR1	pyrroline-5-carboxylate reductase 1	-1.2	3.58E-04
NM_012248	SEPHS2	selenophosphate synthetase 2	-1.6	1.64E-07
NM_002970	SAT1	spermidine/spermine n1-acetyltransferase	-2.1	9.91E-07
AK021874	TGFB2	transforming growth factor, beta 2	1.6	6.08E-07

Process based analysis comparison group 97% versus group 0%

Functional annotation clustering delivered four gene clusters for the 97vs0 comparison (tables 5 and 6). For the 97vs0 comparison, as in the 70vs0 comparison, the first cluster contained genes with functions related to programmed cell death. Twenty-eight out of the 35 down-regulated genes and four out of the 13 up-regulated genes overlapped with down- and up-regulated genes respectively in the 70vs0 comparison programmed cell death cluster. Three of the down-regulated apoptosis inhibitory genes from the 70vs0 comparison were also down-regulated in the 97vs0 comparison, pointing to stimulation of apoptosis. *PPP1R13L, TP53BP2,* and *HRK* were respectively 2.6, 2.3, and 2.3 fold down-regulated. Further apoptosis stimulation was elicited by the 2.6 fold down-regulation of another apoptosis inhibitory gene *DEDD2*, which is thought to play a role in death-receptor mediated apoptosis by targeting caspases 8 and 10 to the nucleus [155]. In addition, in this comparison also a number of apoptosis stimulatory genes were up-regulated. *PDCD4* was 2.3 fold up-regulated, and the PDCD4 protein is believed to be involved in TGF-beta1-induced apoptosis [156]. *SH3GLB1* has been shown to be able to promote apoptosis by Bax and Bak activation, and was 2.1 fold up-regulated [157]. *PYCARD* was 2.5 fold up-regulated and promotes apoptosis through activation of caspase 8 [158]. The *PDCD6* gene, which was 2.6 fold up-regulated, is involved in apoptosis via the caspase 3 dependent pathway [159, 160]. Inhibition of apoptosis occurred by the 2.4 fold down-regulation of the apoptosis inducing gene *LTBR*, which promotes apoptosis via *TRAF3* and *TRAF5* [161-163]. Also, the 2.2 fold up-regulation of the *PDCD6IP* gene, which is thought to be able to block apoptosis by interacting with *PDCD6* [164], points to an inhibition of the apoptotic process.

Table 5: DAVID functional annotation clustering of the differentially expressed genes from the group 97vs0 comparison

Cluster 1	
GO BP Terms	*p-value*
apoptosis	0.00001
negative regulation of programmed cell death	0.00817
regulation of apoptosis	0.00922
regulation of programmed cell death	0.00985
positive regulation of programmed cell death	0.16247
Cluster 2	
GO BP Terms	*p-value*
regulation of protein metabolism	0.00085
negative regulation of biosynthesis	0.00879
regulation of protein biosynthesis	0.05408
regulation of cellular biosynthesis	0.06866
Cluster 3	
GO BP Terms	*p-value*
Angiogenesis	0.02557
blood vessel morphogenesis	0.03139
cell migration	0.14846
Cluster 4	
GO BP Terms	*p-value*
negative regulation of immune response	0.04352
regulation of immune response	0.13106
immune cell activation	0.32526
lymphocyte activation	0.35406
lymphocyte differentiation	0.47940
regulation of lymphocyte activation	0.53295
positive regulation of immune response	0.67976

DAVID functional annotation clustering of the differentially expressed genes from the group 97vs0 comparison. Four clusters could be identified of which at least one of the gene ontology terms had a p-value<0.05.

The second cluster of the 97vs0 comparison included genes involved in transcriptional and translational processes and cytoskeleton and extracellular matrix (EM) organisation. The gene expression changes pointed to both stimulation and inhibition of these processes and illustrated an increased cytoskeleton and EM organisation activity. Inhibition of cytoskeleton formation is illustrated by the 4.2 fold down-regulation of the *MAP2* gene. As already mentioned above, MAP2 is involved in the organisation and assembly of microtubules [151]. The 3.0 fold down-regulation of the *TIMP* gene results in a protective effect against EM degradation. TIMP1 inhibits matrix metalloproteinases, thereby preventing EM degradation [165]. *SPTBN1* was on average 2.7 fold up-regulated and is involved in the binding of the cytoskeleton to the membrane (see above). Gelsolin (*GSN*) is 3.5 fold up-regulated and is able to bind actin filaments as well as to promote polymerisation of barbed ends. GSN is also capable of forming actin filaments by binding two monomeric actin molecules [166]. Furthermore, the up-regulation of *GSN* is indicative for an apoptosis inhibitory effect, as *GSN* has been shown to prevent Ras mediated apoptosis [167]. Moreover, *GSN* appears to provide resistance to apoptosis in senescent fibroblasts [168]. The

third cluster was labelled with GO terms related to angiogenesis and blood vessel morphogenesis and mainly included genes of which the expression changes pointed towards an inhibition of (endothelial) cell proliferation. The fourth cluster contains genes of which the gene expression changes result in an inhibitory effect on immune response.

Table 6: Gene members of the clusters identified by the DAVID functional annotation clustering of the differentially expressed genes from the 97vs0 comparison

Cluster 1				
Genbank Accession No.	***Symbol***	***Title***	***2log fold-change***	***p-value***
NM_005345	HSPA1A	heat shock 70kda protein 1a	-4.8	1.87E-11
NM_021158	TRIB3	tribbles homolog 3 (drosophila)	-4.6	1.57E-08
NM_005346	HSPA1B	heat shock 70kda protein 1a	-4.5	1.18E-10
NM_005347	HSPA5	heat shock 70kda protein 5 (glucose-regulated protein, 78kda)	-3.2	7.37E-06
NM_004862	LITAF	lipopolysaccharide-induced tnf factor	-3.0	4.83E-07
L24498	GADD45A	growth arrest and dna-damage-inducible, alpha	-2.4	5.68E-06
NM_015675	GADD45B	growth arrest and dna-damage-inducible, beta	-2.4	2.31E-08
NM_003655	CBX4	chromobox homolog 4 (pc class homolog, drosophila)	-2.4	1.62E-06
NM_006705	GADD45G	growth arrest and dna-damage-inducible, gamma	-2.3	6.91E-07
AF022375	VEGFA	vascular endothelial growth factor	-2.3	9.52E-09
NM_003900	SQSTM1	sequestosome 1	-2.1	1.85E-04
NM_002583	PAWR	prkc, apoptosis, wt1, regulator	-2.1	4.88E-06
NM_052815	IER3	immediate early response 3	-2.0	5.50E-07
NM_003299	HSP90B1	heat shock protein 90kda beta (grp94), member 1	-2.0	7.80E-04
NM_013246	CLCF1	cardiotrophin-like cytokine factor 1	-1.9	8.39E-05
NM_014330	PPP1R15A	protein phosphatase 1, regulatory (inhibitor) subunit 15a	-1.9	4.68E-07
NM_033027	AXUD1	axin1 up-regulated 1	-1.8	1.33E-05
NM_021972	SPHK1	sphingosine kinase 1	-1.7	4.22E-05
BC013128	CEBPG	ccaat/enhancer binding protein (c/ebp), gamma	-1.6	3.13E-06
NM_004343	CALR	calreticulin	-1.5	4.50E-05
NM_012385	NUPR1_HUMAN	p8 protein (candidate of metastasis 1)	-1.5	5.68E-06
NM_000600	IL6	interleukin 6 (interferon, beta 2)	-1.5	2.91E-05
NM_004281	BAG3	bcl2-associated athanogene 3	-1.5	8.02E-05
BC013372	DEDD2	death effector domain containing 2	-1.4	1.45E-05
NM_006663	PPP1R13L	protein phosphatase 1, regulatory (inhibitor) subunit 13 like	-1.4	4.69E-05
NM_002342	LTBR	lymphotoxin beta receptor (tnfr superfamily, member 3)	-1.3	1.39E-04
NM_003680	YARS	tyrosyl-trna synthetase	-1.3	3.13E-06
NM_005426	TP53BP2	tumour protein p53 binding protein, 2	-1.2	4.77E-06
NM_003806	HRK	harakiri, bcl2 interacting protein (contains only bh3 domain)	-1.2	7.70E-05
NM_004613	TGM2	transglutaminase 2 (c polypeptide, protein-glutamine gamma-glutamyltransferase)	-1.2	5.67E-04
NM_016639	TNFRSF12A	tumour necrosis factor receptor superfamily, member 12a	-1.1	2.30E-05
NM_006410	HTATIP2	hiv-1 tat interactive protein 2, 30kda	-1.1	8.71E-04
NM_005627	SGK	serum/glucocorticoid regulated kinase	-1.1	5.98E-04
NM_002507	NGFR	nerve growth factor receptor (tnfr superfamily, member 16)	-1.1	8.02E-05
NM_005923	MAP3K5	mitogen-activated protein kinase kinase kinase 5	-1.0	1.73E-05
D25304	ARHGEF6	rac/cdc42 guanine nucleotide exchange factor (gef) 6	1.0	7.88E-04
AB007960	SH3GLB1	sh3-domain grb2-like endophilin b1	1.1	6.82E-05
NM_022173	TIA1	tia1 cytotoxic granule-associated rna binding protein	1.1	4.14E-04
AB037796	PDCD6IP	programmed cell death 6 interacting protein	1.2	1.34E-05
NM_000077	CDKN2A	cyclin-dependent kinase inhibitor 2a (melanoma, p16, inhibits cdk4)	1.2	9.76E-04

NM_001904	CTNNB1	catenin (cadherin-associated protein), beta 1, 88kda	1.2	2.54E-05
NM_014456	PDCD4	programmed cell death 4 (neoplastic transformation inhibitor)	1.2	9.77E-05
NM_013258	PYCARD	pyd and card domain containing	1.3	1.64E-04
AB033060	PDCD6	programmed cell death 6	1.4	2.18E-06
AK057865	THY1	thy-1 cell surface antigen	1.7	1.32E-04
NM_000961	PTGIS	prostaglandin i2 (prostacyclin) synthase	1.9	9.22E-04
NM_002527	NTF3	neurotrophin 3	2.0	3.36E-07
NM_002982	CCL2	chemokine (c-c motif) ligand 2	3.2	1.68E-09

Cluster 2

Genbank Accession No.	*Symbol*	*Title*	*2log fold-change*	*p-value*
NM_004095	EIF4EBP1	eukaryotic translation initiation factor 4e binding protein 1	-2.4	1.31E-08
NM_006260	DNAJC3	dnaj (hsp40) homolog, subfamily c, member 3	-2.2	9.73E-07
NM_000169	GLA	galactosidase, alpha	-2.1	3.47E-08
NM_031846	MAP2	microtubule-associated protein 2	-2.1	3.13E-06
NM_013246	CLCF1	cardiotrophin-like cytokine factor 1	-1.9	8.39E-05
NM_022365	DNAJC1	dnaj (hsp40) homolog, subfamily c, member 1	-1.8	8.28E-08
NM_017572	MKNK2	map kinase interacting serine/threonine kinase 2	-1.7	8.00E-05
BC013128	CEBPG	ccaat/enhancer binding protein (c/ebp), gamma	-1.6	3.13E-06
NM_003254	TIMP1	timp metallopeptidase inhibitor 1	-1.6	1.80E-04
NM_005875	EIF1B	eukaryotic translation initiation factor 1b	-1.6	3.84E-05
NM_003732	EIF4EBP3	eukaryotic translation initiation factor 4e binding protein 3	-1.6	5.66E-06
NM_031232	APBA2BP	amyloid beta (a4) precursor protein-binding, family a, member 2 binding protein	-1.5	7.25E-07
NM_000600	IL6	interleukin 6 (interferon, beta 2)	-1.5	2.91E-05
NM_002659	PLAUR	plasminogen activator, urokinase receptor	-1.4	5.49E-05
AK024941	DNAJC3	dnaj (hsp40) homolog, subfamily c, member 3	-1.4	1.51E-05
AL050005	EIF1	eukaryotic translation initiation factor 1	-1.2	8.58E-06
NM_005228	EGFR	epidermal growth factor receptor (erythroblastic leukemia viral (v-erb-b) oncogene homolog, avian)	-1.1	8.99E-05
AB032972	ASB1	ankyrin repeat and socs box-containing 1	-1.1	2.77E-04
AJ420488	EEF1A1	eukaryotic translation elongation factor 1 alpha 1	1.1	8.56E-05
AL117621	ARF6	adp-ribosylation factor 6	1.1	5.06E-04
AK023762	SPTBN1	spectrin, beta, non-erythrocytic 1	1.4	4.21E-06
AK025071	SPTBN1	spectrin, beta, non-erythrocytic 1	1.5	5.98E-07
AK057865	THY1	thy-1 cell surface antigen	1.7	1.32E-04
NM_000177	GSN	gelsolin (amyloidosis, finnish type)	1.8	7.89E-07

Cluster 3

Genbank Accession No.	*Symbol*	*Title*	*2log fold-change*	*p-value*
NM_000584	IL8	interleukin 8	-2.4	6.61E-09
AL137311	DNER	delta-notch-like egf repeat-containing transmembrane	-2.3	6.64E-05
AF022375	VEGFA	vascular endothelial growth factor	-2.3	9.52E-09
NM_021972	SPHK1	sphingosine kinase 1	-1.7	4.22E-05
NM_002019	FLT1	fms-related tyrosine kinase 1 (vascular endothelial growth factor/ vascular permeability factor receptor)	-1.2	2.12E-05
NM_016639	TNFRSF12A	tumour necrosis factor receptor superfamily, member 12a	-1.1	2.30E-05
NM_006410	HTATIP2	hiv-1 tat interactive protein 2, 30kda	-1.1	8.71E-04
NM_005228	EGFR	epidermal growth factor receptor (erythroblastic leukemia viral (v-erb-b) oncogene homolog, avian)	-1.1	8.99E-05
NM_003711	PPAP2A	phosphatidic acid phosphatase type 2a	1.3	9.67E-04
NM_000859	HMGCR	3-hydroxy-3-methylglutaryl-coenzyme a reductase	1.4	3.28E-04
AK057865	THY1	thy-1 cell surface antigen	1.7	1.32E-04

NM_001150	ANPEP	alanyl (membrane) aminopeptidase (aminopeptidase n, aminopeptidase m, microsomal aminopeptidase, cd13, p150)	1.8	5.96E-05
Cluster 4				
Genbank Accession No.	***Symbol***	***Title***	***2log fold-change***	***p-value***
NM_000963	PTGS2	prostaglandin-endoperoxide synthase 2 (prostaglandin g/h synthase and cyclooxygenase)	-5.0	2.75E-09
NM_000584	IL8	interleukin 8	-2.4	6.61E-09
BC013128	CEBPG	ccaat/enhancer binding protein (c/ebp), gamma	-1.6	3.13E-06
NM_005088	CXYorf3	dna segment on chromosome x and y (unique) 155 expressed sequence, isoform 1	-1.5	8.91E-08
NM_000600	IL6	interleukin 6 (interferon, beta 2)	-1.5	2.91E-05
NM_018440	PAG1	phosphoprotein associated with glycosphingolipid microdomains 1	-1.2	2.58E-05
AB032972	ASB1	ankyrin repeat and socs box-containing 1	-1.1	2.77E-04
NM_014011	SOCS5	suppressor of cytokine signaling 5	1.5	2.27E-07
AK057865	THY1	thy-1 cell surface antigen	1.7	1.32E-04

Process based analysis comparison group 97% versus group 70%

For the 97vs70 comparison, only one functional gene cluster could be identified for which at least one of gene ontology groups had a p-value<0.05 (tables 7 and 8). The cluster was formed by 7 unique transcripts, 4 down- and 3 up-regulated, of which the gene expression changes resulted in an inhibition of the immune response. One of the gene members of this cluster was clusterin (*CLU*), which was 4.2 fold up-regulated in group 97% compared to group 70%. Although clusterin has an inhibitory function on the complement system of the innate immune response, it also has been reported to have pro-apoptotic but also pro-survival effects [115].

Table 7: DAVID functional annotation clustering of the differentially expressed genes from the 97vs70 comparison

Cluster 1	
GO BP Terms	*p-value*
humoral immune response	0.01049
humoral defense mechanism (sensu Vertebrata)	0.14615
antimicrobial humoral response	0.26808

One cluster could be identified of which at least one of the gene ontology terms had a p-value<0.05.

Table 8: Gene members of the cluster identified by the DAVID functional annotation clustering of the differentially expressed genes from the 97vs70 comparison

Cluster 1				
Genbank Accession No.	***Symbol***	***Title***	***2log fold-change***	***p-value***
NM_001562	IL18	interleukin 18 (interferon-gamma-inducing factor)	-3.0	8.12E-07
NM_000600	IL6	interleukin 6 (interferon, beta 2)	-2.6	5.53E-08
NM_004335	BST2	bone marrow stromal cell antigen 2	-1.7	5.44E-04
NM_002413	MGST2	microsomal glutathione s-transferase 2	-1.1	7.17E-05
NM_001311	CRIP1	cysteine-rich protein 1 (intestinal)	1.8	7.79E-05
NM_001831	CLU	clusterin	2.1	7.60E-06
NM_030781	COLEC12	collectin sub-family member 12	2.7	5.46E-04

Functional interpretation of the gene expression data

Energy pathways

The m.9176T>C mutation in the *ATP6* gene leads to an OXPHOS defect. Therefore, we checked for gene expression changes in the electron transport chain itself and in the glycolytic pathway, which is able to anaerobically supply energy. For the electron transport chain, only few genes coding for subunits of complexes I and IV, and the ATP synthase complex were significantly changed in expression. In the 70vs0 comparison, the genes coding for complex I subunit NDUFC2 and complex IV subunit COX7A1 were up-regulated 2.1 and 5.2 fold, respectively. In the 97vs0 comparison, complex IV subunit *COX7A1* gene was 3.5 fold up-regulated and ATP synthase subunit *ATP5G2* gene was 2.1 fold down-regulated. The 97vs70 comparison revealed a significant 2.1 fold down-regulation of the *ATP1* gene, coding for a subunit of the ATP synthase complex. In the 70vs0 comparison, the genes enolase 2 (*ENO2*) and glutamic-oxaloacetic transaminase 1 (*GOT1*) of the glycolytic pathway were down-regulated 3.4 and 3.7 fold respectively. For the lactate dehydrogenase A (*LDHA*) gene, multiple probes were spotted, all indicating a significant increase in expression with an average fold-change of 2.5 (σ = 0.3) for the 70vs0 comparison. In the 97vs0 comparison, *GOT1* was significantly 3.6 fold down-regulated and *LDHA* showed a significant increase in expression with an average fold-change of 2.5 (σ = 0.2). In the 97vs70 comparison, no significant gene expression changes were identified for the glycolytic pathway.

Almost no effort is made by the fibroblast carrying the m.9176T>C mutation to compensate for the OXPHOS defect at the transcriptional level by a direct induction of structural genes of the electron transport chain, as illustrated by the limited gene expression changes in this system. The few gene expression changes in the glycolytic pathway will most likely not have a strong effect on energy metabolism, since the changes do not concern the key regulatory genes of this pathway. Lactic acidosis is one of the biochemical features of Leigh syndrome patients carrying the m.9176T>C mutation [3, 4]. In these patients, pyruvate, which is the end-product of the glycolysis, is accumulated because it is not able to enter the citric acid cycle due to the impaired function of the ATP synthase complex of the electron transport chain. In order to remove the accumulating pyruvate, it can be converted to lactic acid by lactate dehydrogenase, explaining the up-regulation of *LDHA* in the 70vs0 and the 97vs0 comparisons, which leads to the lactic acidosis in these patients. This indicates that the cells are under energy stress.

Programmed cell death and cytoskeleton organisation

Programmed cell death, or apoptosis, was the main GO biological process which was identified by the DAVID functional clustering analysis in both the 70vs0 and the 97vs0 comparisons. For the 70vs0 comparison, nine apoptosis regulatory genes were identified from the genes from the first cluster of the DAVID functional annotation clustering. Additionally, the down-regulation of *MTP18,* listed in the fourth functional gene cluster from the DAVID analysis, might increase sensitivity of the cell to apoptotic stimuli. It has been reported that knockdown of the MTP18 protein results in

cytochrome-c release leading to apoptosis and that a reduced expression of the gene sensitises cells to apoptotic stimuli [169]. Although this might stimulate apoptosis, the majority of the apoptosis stimulatory effects were mostly the result of down-regulated apoptosis inhibitory genes, which in itself is not a direct stimulation of the apoptotic process, whereas the identified down-regulation of apoptosis stimulatory genes is indicative for direct inhibition of the apoptotic process. Therefore, based on these gene expression changes, there appears to be a tendency towards an inhibitory effect of apoptosis in the 70vs0 comparison.

For the 97vs0 comparison, the apoptosis related gene expression changes were also a mixture of inhibitory and stimulatory effects, making it difficult to indicate whether the apoptotic process is stimulated or inhibited or that the data reflects a mixture of cells, which are in different regulatory states with respect to the apoptotic process. The difference with the 70vs0 comparison is that in the 97vs0 comparison more apoptosis stimulatory genes were up-regulated (*PDCD4, SH3GLB1, PYCARD,* and *PDCD6*). Another difference between the 70vs0 and the 97vs0 comparison is that alpha spectrin and beta spectrin are down-regulated in the 70vs0 comparison, whereas alpha spectrin is 2.7-fold up-regulated in the 97vs0 comparison. Given the fact that degradation of alphaII- and betaII-spectrin appears to be an early event in apoptosis [170], there may be a possibility that the spectrins already are being degraded in group 97% fibroblasts, indicating apoptotic activity, causing the cells to respond with an up-regulation of spectrin alpha. Additionally, it has been suggested that the translocation of actin to mitochondria and the actin cytoskeleton reorganisation, as observed here according to the transcriptional changes of the genes in the second functional cluster of the 97vs0 comparison (table 6), are early processes in the initiation of apoptosis [171]. Because of these relationships between the cytoskeleton and apoptosis, the other gene expression changes related to cytoskeleton formation and organisation in both the 70vs0 and the 97vs0 comparison might be related to the changes in apoptotic gene expression. A trend can be observed from inhibition of apoptosis to stimulation of apoptosis, from the 70% to the 97% fibroblasts. This shift to a stimulation of apoptosis is probably also illustrated by the up-regulation of clusterin in the 97vs70 comparison. Clusterin has two isoforms, a nuclear form having pro-apoptotic effects and a secreted form having pro-survival effects [115]. Unfortunately, the microarray was unable to distinguish between these two isoforms. Measuring gene expression of the isoforms separately by quantitative realtime PCR will have to provide additional information.

Our results indicate that changes are occurring mainly in the regulation of apoptosis (no gene expression changes of apoptosis key effector genes) in the m.9176T>C fibroblasts and that some early apoptotic events are taking place when the mutation level reaches near homoplasmy. The mixed effects observed in our data may reflect cells in different stages of this process. In a previous paper no stimulation of apoptosis was reported in skeletal muscle of a NARP patient carrying the m.8993T>C mutation at a mutation load of 97%, and only rare apoptotic nuclei were present. This patient had a relatively mild phenotype, compared to the mutation load. Apoptotic

features, mainly localised in cytochrome *c* oxidase-negative fibres, were observed in muscle fibres of patients carrying a high percentage of single mtDNA deletions (>40%) and of tRNA point mutations (>70%) [172]. An inhibitory effect on apoptosis by the ATPase6 m.8993T>G and m.9176T>C mutations was proposed in a study where cybrids with and without one of these homoplasmic mutations were transplanted in nude mice. The early stage tumour growth in mice transplanted with these mtATP6 mutations showed larger tumours which grew faster, which could partly be explained by inhibition of apoptosis by the cybrid cells [173]. These findings seem to be inconsistent with a report that fibroblasts harbouring the 8993 *MTATP6* mutation were more sensitive to metabolic stress and apoptosis than wild-type fibroblasts [174]. However, this discrepancy is likely to be due to the difference between primary fibroblasts and cancer cells such as HeLa cybrids. For example, the glycolytic pathway in HeLa cells is more active than that in fibroblasts. In a recent study, mitochondrial and ER-stress mediated apoptosis was investigated in relation to a number of different mtDNA mutations, including mitochondrial cybrid cells carrying the homoplasmic NARP m.8993T>G mutation. The authors found that mitochondrial cybrid cells containing the m.8993T>G mutation were highly susceptible to both mitochondrial and ER-stress mediated apoptosis. It was proposed that the susceptibility of mtDNA mutated cells is related to the presence of OXPHOS complexes and the capability of generating an electron flux [175]. In contrast to the m.9176T>C cells in our study, in the m.8993T>G cells, apoptosis key effects were observed, as illustrated by significantly increased caspase 3 activation. This could be explained by the fact that in the study described, direct apoptosis stimulating agents (staurosporine, etoposide, thapsigargin, or tunicamycin) were used, which is likely to trigger a stronger effect than in a more natural situation as in our cell culturing experiment. Taken all data together, there appears to be no simple and single effect of mtDNA mutations on apoptosis. This depends on mutation type, mutation level and cell or tissue type. However, most data fits with our results where there appears to be a migration from inhibition to stimulation of apoptosis as m.9176T>C mutation loads rise to nearly homoplasmic levels. The controversial nature of the data clearly illustrates the need for a genetically homogeneous model to study the basic effect of these mtDNA mutations.

Conclusion

The cell culture model system that we have developed is particularly suited to study mtDNA mutation load differences in the same genetic background without the introduction of unwanted experimental and genetic biases. Gene expression profiling of monoclonal fibroblast cell cultures carrying different loads of the m.9176T>C mutation enabled the identification of a number of changes in biological processes between the different mutation load groups, with the most prominent changes in apoptosis with gene expression changes related to cytoskeleton organisation as an apoptotic early event. There appeared to be a shift from an inhibition to a stimulation of apoptosis when m.9176T>C mutation loads rise from ~70% to ~97%, i.e. from a-symptomatic to symptomatic. These biological processes need to be further characterised and

investigated in more detail, in more tissues and for more patients to provide further insight into the exact role of these processes in the context of this mutation related to Leigh syndrome.

Acknowledgements

This research was supported by the Princess Beatrix Foundation, (Grant number: MAR99-0111) and the MitoCircle project (EU grant, Sixth Framework Program, contr. no. 005260).

Supplementary table S1: Significantly differentially expressed genes for the 70 versus 0 comparison

Genbank accession No.	Gene symbol	Fold-change	Direction	p-value
NM_002421	MMP1	55.8	DOWN	2.54E-10
NM_002155	HSPA6	50.1	DOWN	1.38E-11
NM_000963	PTGS2	31.9	DOWN	6.39E-10
NM_001999	FBN2	29.6	DOWN	2.02E-05
NM_002923	RGS2	28.2	DOWN	2.16E-09
AK056355	Q7Z3M5_HUMAN	22.4	DOWN	6.33E-05
NM_004165	RRAD	22.2	DOWN	2.21E-11
NM_002220	ITPKA	20.5	DOWN	2.92E-11
NM_005345	HSPA1A	20.3	DOWN	3.41E-11
NM_005345	HSPA1A	20.3	DOWN	2.21E-11
NM_005345	HSPA1A	18.7	DOWN	2.66E-11
NM_005345	HSPA1A	18.4	DOWN	4.88E-11
NM_005345	HSPA1A	18.2	DOWN	1.38E-11
NM_005345	HSPA1A	18.1	DOWN	8.11E-11
NM_005345	HSPA1A	18.0	DOWN	2.86E-11
NM_005345	HSPA1A	17.8	DOWN	6.87E-11
NM_005532	IFI27	17.6	DOWN	1.51E-05
NM_005345	HSPA1A	17.4	DOWN	1.38E-11
NM_021127	PMAIP1	16.9	DOWN	2.85E-09
NM_005345	HSPA1A	16.9	DOWN	1.06E-10
NM_005346	HSPA1B	16.8	DOWN	1.43E-10
NM_005345	HSPA1A	16.8	DOWN	1.58E-11
NM_005345	HSPA1A	16.8	DOWN	1.38E-11
NM_005345	HSPA1A	16.7	DOWN	1.38E-11
BC012321	ARC	16.6	DOWN	3.49E-11
NM_005345	HSPA1A	16.5	DOWN	1.58E-11
NM_005345	HSPA1A	16.4	DOWN	1.29E-10
NM_007029	STMN2	16.4	DOWN	4.44E-07
NM_005345	HSPA1A	16.1	DOWN	3.12E-11
NM_005252	FOS	15.6	DOWN	2.55E-10
NM_004864	GDF15	15.1	DOWN	1.46E-07
NM_000799	EPO	15.0	DOWN	5.17E-09
NM_005345	HSPA1A	15.0	DOWN	3.41E-11
NM_000361	THBD	14.4	DOWN	9.43E-11
NM_032621	BEX2	13.9	DOWN	2.92E-11
NM_001451	FOXF1	13.6	DOWN	1.05E-09
NM_007036	ESM1	12.2	DOWN	3.03E-07
NM_006528	TFPI2	12.2	DOWN	1.74E-08
NM_001945	HBEGF	11.7	DOWN	3.04E-08
NM_005347	HSPA5	11.5	DOWN	7.78E-07
NM_021158	TRIB3	11.5	DOWN	1.30E-07
NM_006145	DNAJB1	11.3	DOWN	1.94E-11
NM_002133	HMOX1	10.7	DOWN	5.90E-08
NM_004398	DDX10	10.7	DOWN	3.40E-10
NM_002394	SLC3A2	10.5	DOWN	6.87E-11
NM_005261	GEM	10.1	DOWN	1.13E-09
NM_001353	AKR1C1	10.0	DOWN	3.56E-07
AK001031	TBX2	9.4	DOWN	3.94E-10
NM_007115	TNFAIP6	9.4	DOWN	1.51E-07
NM_001769	CD9	9.3	DOWN	4.81E-11
AB050476	LHX8	9.3	DOWN	2.55E-10
NM_006389	HYOU1	9.0	DOWN	2.43E-07
NM_004362	CLGN	8.9	DOWN	5.05E-10
NM_001533	HNRPL	8.9	DOWN	1.82E-10
NM_017947	MOCOS	8.7	DOWN	6.64E-06
NM_001902	CTH	8.6	DOWN	1.93E-10
NM_001831	CLU	8.4	DOWN	8.52E-09
NM_016084	RASD1	8.3	DOWN	3.20E-09
NM_012328	DNAJB9	8.2	DOWN	2.73E-10

BC017001	SCRT2	8.0	DOWN	3.30E-08
NM_022842	CDCP1	7.8	DOWN	6.57E-08
NM_002852	PTX3	7.6	DOWN	8.52E-09
AF104032	SLC7A5	7.5	DOWN	4.00E-10
NM_004350	RUNX3	7.3	DOWN	1.10E-05
NM_005985	SNAI1	7.0	DOWN	6.79E-07
NM_014751	MTSS1	6.9	DOWN	6.31E-08
X91348	C22:AC000095.2	6.9	DOWN	2.62E-04
NM_022743	SMYD3	6.8	DOWN	3.53E-08
AF212221	MYLIP	6.7	DOWN	1.62E-05
NM_006636	MTHFD2	6.7	DOWN	1.67E-10
NM_000627	LTBP1	6.6	DOWN	1.36E-05
NM_001946	DUSP6	6.5	DOWN	3.04E-08
BC013592	DDIT4L	6.4	DOWN	9.60E-08
NM_032691	NA	6.4	DOWN	1.43E-10
NM_002061	GCLM	6.3	DOWN	7.57E-10
NM_004419	DUSP5	6.3	DOWN	1.75E-06
NM_001793	CDH3	6.3	DOWN	4.91E-08
NM_018590	CGAT2_HUMAN	6.3	DOWN	3.03E-09
AF438313	TMEM158	6.2	DOWN	1.46E-07
NM_004024	ATF3	6.1	DOWN	5.62E-09
NM_003299	HSP90B1	6.0	DOWN	1.94E-05
NM_052966	NIBA_HUMAN	5.8	DOWN	2.45E-07
NM_004083	DDIT3	5.7	DOWN	2.54E-08
NM_016242	EMCN	5.6	DOWN	1.18E-06
NM_002479	MYOG	5.6	DOWN	3.79E-07
NM_003012	SFRP1	5.5	DOWN	8.83E-04
AF007152	ABHD3	5.5	DOWN	2.92E-11
AK056052	Q7Z3M5_HUMAN	5.5	DOWN	8.23E-05
NM_000167	GK	5.5	DOWN	3.63E-08
AF022375	VEGFA	5.4	DOWN	6.47E-10
NM_006732	FOSB	5.4	DOWN	1.17E-09
NM_006644	HSPH1	5.4	DOWN	4.42E-09
NM_006290	TNFAIP3	5.4	DOWN	3.33E-05
NM_001673	ASNS	5.4	DOWN	3.80E-10
NM_006010	ARMET	5.4	DOWN	5.81E-07
NM_012410	SEZ6L2	5.3	DOWN	6.74E-09
NM_000584	IL8	5.3	DOWN	1.65E-09
NM_005098	MSC	5.3	DOWN	2.20E-07
NM_005842	SPRY2	5.2	DOWN	1.43E-05
NM_023940	RASL11B	5.2	DOWN	3.97E-08
NM_019058	DDIT4	5.2	DOWN	1.17E-09
NM_020184	CNNM4	5.2	DOWN	7.57E-10
AF101051	CLDN1	5.2	DOWN	1.41E-04
AF124368	MIT:C8orf13	5.1	DOWN	1.77E-04
D31887	SLC39A14	5.1	DOWN	4.55E-10
BC016658	E2F7	5.1	DOWN	2.72E-07
NM_000231	SGCG	5.1	DOWN	1.99E-06
NM_025195	TRIB1	4.9	DOWN	4.16E-08
NM_057749	CCNE2	4.9	DOWN	6.08E-07
NM_006260	DNAJC3	4.9	DOWN	1.97E-07
NM_016262	TUBE1	4.9	DOWN	2.68E-09
NM_002047	GARS	4.8	DOWN	5.05E-10
NM_001498	GCLC	4.8	DOWN	7.57E-10
AB046853	CDK5RAP2	4.8	DOWN	7.58E-10
BC016285	PRKACB	4.7	DOWN	4.35E-09
NM_031456	FBXW10	4.7	DOWN	6.04E-07
NM_006931	SLC2A3	4.7	DOWN	2.76E-10
NM_003655	CBX4	4.7	DOWN	1.06E-06
BC007359	RTTN	4.7	DOWN	1.97E-08
NM_005402	RALA	4.7	DOWN	1.02E-07
NM_005279	GPR1	4.6	DOWN	1.93E-10

BC004538	LONRF1	4.6	DOWN	4.24E-05
AK001865	ERO1LB	4.6	DOWN	3.41E-08
NM_006705	GADD45G	4.5	DOWN	4.64E-07
NM_004933	CDH15	4.5	DOWN	1.92E-05
NM_007038	ADAMTS5	4.5	DOWN	4.70E-06
AL133096	DNAJA4	4.4	DOWN	1.72E-06
NM_013370	OSGIN1	4.4	DOWN	3.96E-07
NM_016614	TTRAP	4.4	DOWN	9.44E-08
M77140	GAL	4.4	DOWN	1.97E-05
NM_018259	TTC17	4.4	DOWN	1.16E-08
AB051479	VEPH1	4.4	DOWN	3.51E-09
AB051460	CPEB4	4.4	DOWN	9.46E-09
AL050090	MYRIP	4.4	DOWN	8.77E-07
NM_014191	SCN8A	4.3	DOWN	3.56E-08
NM_002970	SAT1	4.3	DOWN	9.91E-07
NM_006948	STCH	4.2	DOWN	1.47E-06
NM_004911	PDIA4	4.2	DOWN	3.50E-05
NM_000640	IL13RA2	4.2	DOWN	8.62E-06
NM_022044	SDF2L1	4.2	DOWN	1.17E-07
L24498	GADD45A	4.2	DOWN	1.12E-05
NM_012323	MAFF	4.1	DOWN	1.83E-06
NM_006470	TRIM16	4.1	DOWN	7.16E-06
NM_015675	GADD45B	4.1	DOWN	5.91E-08
NM_005080	XBP1	4.1	DOWN	2.97E-07
NM_002022	FMO4	4.1	DOWN	4.55E-10
NM_014330	PPP1R15A	4.0	DOWN	7.15E-08
BC015542	PVR	4.0	DOWN	6.47E-05
NM_057159	EDG2	4.0	DOWN	1.65E-09
NM_031846	MAP2	4.0	DOWN	1.47E-06
NM_018423	STYK1	4.0	DOWN	2.72E-07
NM_001675	ATF4	3.9	DOWN	6.57E-09
NM_006096	NDRG1	3.9	DOWN	1.10E-05
NM_005596	NFIB	3.9	DOWN	6.12E-06
AK024261	NA	3.9	DOWN	2.74E-07
NM_018015	CXorf57	3.9	DOWN	2.35E-07
NM_003038	SLC1A4	3.9	DOWN	5.39E-09
NM_016522	NTRI_HUMAN	3.8	DOWN	1.05E-09
NM_002659	PLAUR	3.8	DOWN	5.23E-07
NM_000876	IGF2R	3.8	DOWN	2.64E-05
AF212224	CLK1	3.8	DOWN	7.44E-07
NM_006622	PLK2	3.8	DOWN	1.06E-05
NM_024574	C4orf31	3.8	DOWN	4.92E-05
NM_032744	C6orf105	3.8	DOWN	1.93E-06
BC010563	ADAMTS6	3.8	DOWN	3.47E-06
NM_004095	EIF4EBP1	3.7	DOWN	8.94E-08
AF070606	ATP2B1	3.7	DOWN	1.72E-06
AK024941	DNAJC3	3.7	DOWN	1.17E-07
NM_004733	SLC33A1	3.7	DOWN	1.08E-09
NM_001912	CTSL	3.7	DOWN	3.35E-06
NM_000071	CBS	3.7	DOWN	3.21E-05
NM_002079	GOT1	3.7	DOWN	2.16E-09
NM_014331	SLC7A11	3.6	DOWN	3.23E-07
AK022459	CCPG1	3.6	DOWN	5.81E-07
NM_013417	IARS	3.6	DOWN	9.83E-07
AK025379	PLEKHM1	3.6	DOWN	4.00E-07
BC012337	HKDC1	3.6	DOWN	4.43E-07
NM_017515	SLC35F2	3.6	DOWN	3.71E-05
NM_004183	BEST1	3.6	DOWN	1.33E-06
AB024574	GTPBP2	3.5	DOWN	4.03E-07
AL353933	SLC22A15	3.5	DOWN	6.07E-06
NM_005746	PBEF1	3.5	DOWN	2.12E-06
NM_005504	BCAT1	3.5	DOWN	9.88E-08

NM_002943	RORA	3.5	DOWN	1.24E-05
AK055902	KIAA1324L	3.5	DOWN	4.36E-07
NM_000609	CXCL12	3.5	DOWN	8.75E-06
NM_021255	PELI2	3.5	DOWN	5.97E-05
NM_004403	DFNA5	3.4	DOWN	9.96E-08
AB051541	KIAA1754	3.4	DOWN	1.21E-05
NM_007289	MME	3.4	DOWN	3.69E-04
BC013128	CEBPG	3.4	DOWN	3.57E-07
NM_004524	LLGL2	3.4	DOWN	8.79E-07
NM_006546	IGF2BP1	3.4	DOWN	7.23E-06
NM_005502	ABCA1	3.4	DOWN	2.13E-05
NM_021738	SVIL	3.4	DOWN	2.35E-06
NM_001975	ENO2	3.4	DOWN	8.98E-05
NM_001818	AKR1C4	3.4	DOWN	1.98E-06
NM_005313	PDIA3	3.4	DOWN	4.12E-04
NM_004184	WARS	3.3	DOWN	4.13E-07
AK022859	UNC5B	3.3	DOWN	1.49E-04
AY044164	ALPK1	3.3	DOWN	4.48E-08
NM_023016	ANKRD57	3.3	DOWN	5.23E-07
AK055094	MARVELD2	3.3	DOWN	1.02E-06
NM_031471	URP2_HUMAN	3.3	DOWN	1.16E-06
NM_018057	SLC6A15	3.3	DOWN	1.04E-04
NM_000025	ADRB3	3.3	DOWN	5.90E-08
NM_024111	CHAC1	3.3	DOWN	6.46E-08
NM_003582	DYRK3	3.3	DOWN	1.07E-04
NM_001695	ATP6V1C1	3.3	DOWN	1.17E-07
NM_014059	C13orf15	3.3	DOWN	2.98E-04
AJ277587	SPIRE1	3.2	DOWN	7.64E-06
NM_032466	ASPH	3.2	DOWN	3.24E-06
AK056477	GZF1	3.2	DOWN	1.50E-07
NM_002014	FKBP4	3.2	DOWN	6.62E-07
BC016556	TMED5	3.2	DOWN	3.40E-07
NM_001550	IFRD1	3.2	DOWN	3.04E-08
NM_000270	NP	3.2	DOWN	6.34E-07
NM_000574	CD55	3.2	DOWN	3.05E-07
NM_004824	CDYL	3.2	DOWN	3.88E-07
BC001618	SLC1A4	3.2	DOWN	2.28E-09
NM_032315	SLC25A33	3.2	DOWN	1.50E-05
NM_000271	NPC1	3.2	DOWN	6.95E-08
NM_005628	SLC1A5	3.2	DOWN	8.54E-05
NM_032711	MAFG	3.2	DOWN	7.08E-06
NM_006988	ADAMTS1	3.2	DOWN	5.95E-06
D42055	NEDD4	3.2	DOWN	9.60E-08
NM_024324	CRELD2	3.2	DOWN	5.00E-05
AB033029	JGI:USP31	3.2	DOWN	3.07E-07
NM_002359	MAFG	3.2	DOWN	2.22E-05
NM_005239	ETS2	3.1	DOWN	9.29E-07
NM_001400	EDG1	3.1	DOWN	2.45E-06
NM_012421	RLF	3.1	DOWN	1.03E-06
NM_002641	PIGA	3.1	DOWN	1.73E-07
NM_016569	TBX3	3.1	DOWN	1.88E-05
AK025306	CLK1	3.1	DOWN	1.30E-06
NM_003364	UPP1	3.1	DOWN	9.83E-07
NM_003115	UAP1	3.1	DOWN	1.00E-05
AK057846	NIPA1	3.1	DOWN	1.84E-05
NM_012248	SEPHS2	3.1	DOWN	1.64E-07
NM_003505	FZD1	3.1	DOWN	1.37E-05
NM_002467	MYC	3.1	DOWN	5.83E-06
NM_001681	ATP2A2	3.1	DOWN	8.48E-06
AK025100	SNTB1	3.0	DOWN	4.48E-05
NM_015208	ANKRD12	3.0	DOWN	1.17E-07
AK056446	HSP90AA1	3.0	DOWN	1.08E-06

NM_052960	RBP7	3.0	DOWN	7.64E-06
NM_000804	FOLR3	3.0	DOWN	5.52E-06
NM_000676	ADORA2B	3.0	DOWN	2.22E-07
NM_005104	BRD2_HUMAN	3.0	DOWN	1.91E-04
AL136628	C4orf16	3.0	DOWN	3.68E-07
NM_053040	C1orf79	3.0	DOWN	1.12E-07
NM_015577	RAI14	3.0	DOWN	1.63E-05
NM_016535	ZNF581	3.0	DOWN	1.51E-06
NM_005681	TAF1A	3.0	DOWN	2.67E-06
NM_024642	GALNT12	3.0	DOWN	2.25E-06
NM_013246	CLCF1	3.0	DOWN	2.30E-04
NM_005426	TP53BP2	3.0	DOWN	5.85E-08
NM_016227	C1orf9	3.0	DOWN	6.26E-06
AL110126	NFIB	3.0	DOWN	7.68E-05
NM_025001	MTHFD2L	3.0	DOWN	3.31E-05
AF220656	BCM:PHLDA1	2.9	DOWN	1.24E-04
NM_007076	NP_009007.2	2.9	DOWN	1.22E-04
NM_018357	LARP6	2.9	DOWN	1.25E-06
NM_024610	HSPBAP1	2.9	DOWN	4.33E-06
BC016024	FOXA3	2.9	DOWN	2.44E-04
NM_002135	NR4A1	2.9	DOWN	4.30E-09
AK056926	SLC31A1	2.9	DOWN	3.88E-06
NM_002928	RGS16	2.9	DOWN	3.87E-06
AJ301564	C8orf13	2.9	DOWN	1.20E-06
NM_003407	ZFP36	2.9	DOWN	5.50E-04
NM_005800	USPL1	2.9	DOWN	8.14E-07
NM_025084	Q6P168_HUMAN	2.9	DOWN	7.86E-05
NM_004447	EPS8	2.9	DOWN	3.88E-06
BC012513	RND3	2.9	DOWN	3.44E-06
NM_018361	AGPAT5	2.9	DOWN	2.72E-07
NM_004464	FGF5	2.9	DOWN	8.38E-04
NM_001829	CLCN3	2.9	DOWN	3.74E-06
AL117608	FGFR1OP2	2.9	DOWN	6.30E-07
BC010112	HSPD1	2.9	DOWN	5.84E-07
NM_001539	DNAJA1	2.9	DOWN	1.17E-07
NM_030751	SNF1LK	2.9	DOWN	5.32E-05
NM_001122	ADFP	2.9	DOWN	6.74E-05
AK025800	NUPL1	2.9	DOWN	4.19E-07
BC001665	ABLIM3	2.9	DOWN	2.46E-05
NM_014778	NUPL1	2.9	DOWN	2.18E-05
D26067	TMEM41B	2.8	DOWN	1.50E-07
NM_003156	STIM1	2.8	DOWN	7.68E-04
AK056836	C22:IL17RA	2.8	DOWN	1.06E-06
BE884686	LTB4DH	2.8	DOWN	3.23E-07
NM_022751	FAM59A	2.8	DOWN	1.94E-07
U92285	GABRE	2.8	DOWN	3.98E-06
NM_033035	NP_149024.1	2.8	DOWN	4.88E-04
NM_003244	TGIF	2.8	DOWN	6.23E-06
NM_003764	STX11	2.8	DOWN	9.62E-07
NM_052815	IER3	2.8	DOWN	7.47E-06
NM_005527	HSPA1L	2.8	DOWN	2.12E-06
NM_001516	GTF2H3	2.8	DOWN	2.77E-07
NM_014246	CELSR1	2.8	DOWN	2.88E-04
BC011763	TRIM4	2.8	DOWN	1.25E-06
AK055774	PAQR3	2.8	DOWN	1.68E-05
NM_002631	PGD	2.8	DOWN	6.62E-07
NM_005923	MAP3K5	2.8	DOWN	4.91E-08
NM_005110	GFPT2	2.8	DOWN	2.74E-07
NM_024692	RSNL2	2.8	DOWN	2.27E-07
NM_030674	SLC38A1	2.8	DOWN	4.86E-05
NM_002448	MSX1	2.8	DOWN	1.88E-06
NM_002714	PPP1R10	2.8	DOWN	4.05E-04

NM_002583	PAWR	2.7	DOWN	6.51E-05
NM_016306	DNAJB11	2.7	DOWN	1.77E-05
AK025661	LIMS1	2.7	DOWN	4.35E-07
AL390172	NA	2.7	DOWN	2.70E-06
NM_024039	MIS12	2.7	DOWN	3.44E-09
NM_000637	GSR	2.7	DOWN	3.10E-05
NM_014161	MRPL18	2.7	DOWN	1.17E-07
NM_016947	G8_HUMAN	2.7	DOWN	3.56E-07
NM_000956	PTGER2	2.7	DOWN	8.29E-05
AB023142	CORO2B	2.7	DOWN	2.67E-05
NM_020645	NRIP3	2.7	DOWN	3.32E-06
NM_002090	CXCL3	2.7	DOWN	1.02E-05
AK055618	C18orf19	2.7	DOWN	5.19E-06
NM_033027	AXUD1	2.7	DOWN	5.04E-05
AL049265	IL6ST	2.7	DOWN	1.58E-05
AB046769	Q9H0M3_HUMAN	2.6	DOWN	2.75E-06
NM_002182	IL1RAP	2.6	DOWN	1.39E-05
AK056433	VAC14	2.6	DOWN	1.99E-05
NM_006043	HS3ST2	2.6	DOWN	2.62E-05
NM_003183	ADAM17	2.6	DOWN	3.68E-07
NM_017572	MKNK2	2.6	DOWN	2.34E-04
AK024263	NA	2.6	DOWN	4.63E-07
NM_006663	PPP1R13L	2.6	DOWN	1.43E-05
NM_032883	GCX1_HUMAN	2.6	DOWN	1.48E-04
NM_002835	PTPN12	2.6	DOWN	4.30E-07
NM_004862	LITAF	2.6	DOWN	6.62E-04
NM_005729	PPIF	2.6	DOWN	1.21E-06
NM_007207	DUSP10	2.6	DOWN	2.27E-04
AY032950	TRPM7	2.6	DOWN	1.31E-06
NM_005228	EGFR	2.6	DOWN	2.44E-06
BC017253	U31	2.6	DOWN	5.02E-05
BC010990	ZNF598	2.6	DOWN	8.74E-06
BC014523	Q7Z6M3_HUMAN	2.6	DOWN	5.00E-05
NM_003580	NSMAF	2.6	DOWN	1.39E-05
NM_004987	LIMS1	2.6	DOWN	6.47E-05
NM_014584	ERO1L	2.6	DOWN	1.33E-06
AB011164	NP_001005751.1	2.6	DOWN	1.45E-08
NM_001270	CHD1	2.6	DOWN	1.95E-06
NM_014167	CCDC59	2.6	DOWN	4.03E-06
NM_005088	CXYorf3	2.6	DOWN	9.96E-08
AB058745	KBTBD8	2.6	DOWN	6.71E-04
NM_000882	IL12A	2.6	DOWN	2.20E-05
NM_018112	TMEM38B	2.6	DOWN	8.77E-04
NM_000201	ICAM1	2.6	DOWN	6.17E-05
AB033112	BRPF3	2.6	DOWN	3.04E-07
NM_012124	CHORDC1	2.6	DOWN	8.94E-08
NM_002064	GLRX	2.6	DOWN	2.11E-04
NM_022365	DNAJC1	2.6	DOWN	1.04E-06
NM_004281	BAG3	2.6	DOWN	6.70E-05
NM_004787	SLIT2	2.5	DOWN	2.23E-04
AK024224	ERO1L	2.5	DOWN	4.21E-05
NM_017909	C6orf96	2.5	DOWN	7.06E-06
NM_004272	HOMER1	2.5	DOWN	5.45E-06
NM_005493	RANBP9	2.5	DOWN	3.06E-05
AK026095	SNTB1	2.5	DOWN	9.87E-05
AK026181	BCM:PHLDA1	2.5	DOWN	3.05E-04
NM_024506	GLB1L	2.5	DOWN	1.00E-04
NM_004414	DSCR1	2.5	DOWN	7.94E-06
NM_005544	IRS1	2.5	DOWN	1.04E-05
NM_001859	SLC31A1	2.5	DOWN	3.24E-06
NM_024525	TTC13	2.5	DOWN	1.43E-05
AK055903	KITLG	2.5	DOWN	4.45E-05

AK025615	NA	2.5	DOWN	1.71E-06
NM_001457	FLNB	2.5	DOWN	3.47E-05
NM_005524	HES1	2.5	DOWN	1.46E-06
NM_006516	SLC2A1	2.5	DOWN	4.12E-06
NM_006072	CCL26	2.5	DOWN	3.17E-05
NM_003051	SLC16A1	2.5	DOWN	5.54E-06
AF444779	SYNE1	2.5	DOWN	8.93E-06
NM_004990	MARS	2.5	DOWN	2.89E-05
AF055007	MARCH3	2.5	DOWN	7.98E-05
NM_022840	METTL4	2.5	DOWN	1.21E-05
NM_006769	LMO4	2.5	DOWN	1.70E-06
NM_005354	JUND	2.5	DOWN	5.49E-04
NM_032839	DIRC2	2.5	DOWN	3.96E-05
NM_004343	CALR	2.5	DOWN	7.63E-05
NM_001134	AFP	2.5	DOWN	8.50E-06
NM_001568	EIF3S6	2.5	DOWN	4.27E-04
NM_022447	PAPD5	2.5	DOWN	1.02E-04
AB018274	LARP1	2.5	DOWN	4.21E-04
NM_001881	CREM	2.5	DOWN	2.08E-06
NM_006681	NMU	2.5	DOWN	3.71E-05
NM_002106	H2AFZ	2.5	DOWN	6.23E-05
NM_012463	ATP6V0A2	2.5	DOWN	3.42E-05
NM_002526	NT5E	2.4	DOWN	3.40E-05
NM_001895	CSNK2A1	2.4	DOWN	6.65E-05
NM_012296	GAB2	2.4	DOWN	1.87E-04
NM_003340	UBE2D3	2.4	DOWN	3.90E-05
NM_014674	EDEM1	2.4	DOWN	5.85E-07
NM_005655	KLF10	2.4	DOWN	7.03E-04
AL021327	RP1-124O9.1	2.4	DOWN	2.63E-07
BC008580	GDNF	2.4	DOWN	3.04E-06
NM_004673	ANGPTL1	2.4	DOWN	1.63E-05
NM_020038	ABCC3	2.4	DOWN	7.65E-04
AF016266	TNFRSF10B	2.4	DOWN	4.66E-05
AC004832	SEC14L3	2.4	DOWN	5.48E-06
D50926	MORC3	2.4	DOWN	1.38E-07
NM_001751	CARS	2.4	DOWN	1.19E-05
NM_004418	DUSP2	2.4	DOWN	1.38E-05
BC013764	KCTD12	2.4	DOWN	1.13E-05
NM_032270	LRRC8C	2.4	DOWN	1.39E-05
NM_002041	GABPAP	2.4	DOWN	1.34E-06
NM_006670	TPBG	2.4	DOWN	2.26E-04
NM_003171	SUPV3L1	2.4	DOWN	7.64E-06
NM_003368	USP1	2.4	DOWN	3.42E-06
AB018285	JMJD1A	2.4	DOWN	9.50E-07
NM_003155	STC1	2.4	DOWN	1.10E-05
NM_032873	STS1_HUMAN	2.4	DOWN	7.36E-05
NM_003033	ST3GAL1	2.4	DOWN	1.04E-04
NM_001746	CANX	2.4	DOWN	8.05E-07
NM_017793	RPP25	2.4	DOWN	7.34E-05
NM_006819	STIP1	2.4	DOWN	3.69E-04
D83702	CRY1	2.4	DOWN	2.67E-06
NM_003489	NRIP1	2.4	DOWN	6.39E-07
NM_014423	AFF4	2.4	DOWN	6.11E-06
AB011542	MEGF9	2.4	DOWN	4.96E-04
NM_024755	SLTM	2.4	DOWN	1.01E-05
NM_020424	LYRM1	2.4	DOWN	5.95E-06
AF278605	SEC31A	2.4	DOWN	5.88E-07
NM_005896	IDH1	2.4	DOWN	2.81E-04
BC009033	ASPHD1	2.3	DOWN	5.25E-05
NM_003851	CREG1	2.3	DOWN	2.06E-04
NM_003670	BHLHB2	2.3	DOWN	4.70E-06
NM_000558	HBA_HUMAN	2.3	DOWN	2.34E-05

NM_006362	NXF1	2.3	DOWN	4.48E-06
NM_014710	GPRASP1	2.3	DOWN	7.22E-05
NM_031412	GABARAPL1	2.3	DOWN	6.36E-04
NM_002423	MMP7	2.3	DOWN	6.47E-05
NM_024686	TTLL7	2.3	DOWN	1.46E-06
NM_023076	C16orf28	2.3	DOWN	1.81E-05
AB037801	JMJD1C	2.3	DOWN	1.97E-05
AB058713	SYVN1	2.3	DOWN	5.65E-04
AK026142	GATAD1	2.3	DOWN	8.83E-04
BC009367	ZNF317	2.3	DOWN	1.19E-04
NM_004052	BNIP3	2.3	DOWN	2.22E-04
NM_014278	HSPA4L	2.3	DOWN	1.11E-04
NM_000942	PPIB	2.3	DOWN	4.98E-04
NM_022750	PARP12	2.3	DOWN	2.72E-04
AK027647	DNAJC10	2.3	DOWN	6.20E-06
AK026747	Q9UMH3_HUMAN	2.3	DOWN	6.00E-04
NM_000169	GLA	2.3	DOWN	1.00E-05
NM_006492	ALX3	2.3	DOWN	4.13E-04
AK021570	NA	2.3	DOWN	3.95E-05
NM_005727	TSPAN1	2.3	DOWN	4.37E-06
NM_002019	FLT1	2.3	DOWN	7.51E-06
NM_006537	USP3	2.3	DOWN	2.12E-06
AB051505	SK:KIAA1718	2.3	DOWN	5.59E-05
NM_005627	SGK	2.3	DOWN	9.99E-05
NM_004087	DLG1	2.3	DOWN	1.99E-04
NM_000158	GBE1	2.3	DOWN	1.30E-06
NM_003243	TGFBR3	2.3	DOWN	1.21E-06
NM_000633	BCL2	2.3	DOWN	2.15E-04
NM_024303	ZSCAN5	2.3	DOWN	3.23E-04
AK021789	Q8NHV5_HUMAN	2.3	DOWN	4.04E-05
NM_031431	COG3	2.3	DOWN	4.51E-06
AK055243	CCBE1	2.3	DOWN	1.87E-04
AK055975	ZNF746	2.3	DOWN	3.10E-04
AB040916	ZBTB2	2.3	DOWN	5.34E-05
BC010612	Q96FP1_HUMAN	2.3	DOWN	3.59E-05
NM_014914	CENTG2	2.3	DOWN	5.83E-06
NM_012290	TLK1	2.3	DOWN	1.32E-05
AF395440	Q96RF1_HUMAN	2.3	DOWN	3.92E-05
NM_016325	ZNF274	2.3	DOWN	6.26E-07
NM_022780	RMND5A	2.3	DOWN	2.75E-06
BC012044	SGTB	2.3	DOWN	1.07E-04
NM_000179	MSH6	2.3	DOWN	1.71E-04
AK023505	RSNL2	2.3	DOWN	8.89E-04
NM_006392	NOL5A	2.3	DOWN	7.64E-06
NM_003662	PIR	2.2	DOWN	9.02E-04
NM_003576	STK24	2.2	DOWN	1.47E-05
NM_006907	PYCR1	2.2	DOWN	3.58E-04
NM_006693	CPSF4	2.2	DOWN	1.76E-05
NM_003344	UBE2H	2.2	DOWN	7.82E-05
NM_015513	CRELD1	2.2	DOWN	1.25E-04
NM_030759	NRBF2	2.2	DOWN	1.98E-06
NM_006756	TCEA1_HUMAN	2.2	DOWN	7.62E-06
AB051498	ZCCHC6	2.2	DOWN	5.54E-06
AK057782	ANKRD29	2.2	DOWN	9.10E-04
NM_016545	IER5	2.2	DOWN	1.86E-05
NM_020122	KCMF1	2.2	DOWN	1.02E-06
AB051513	ZC3H12C	2.2	DOWN	9.84E-06
NM_002243	KCNJ15	2.2	DOWN	8.41E-04
NM_003567	BCAR3	2.2	DOWN	4.23E-04
NM_021958	HLX1	2.2	DOWN	5.11E-04
NM_000735	CGA	2.2	DOWN	7.86E-05
AL050005	EIF1	2.2	DOWN	4.37E-06

NM_000079	CHRNA1	2.2	DOWN	1.08E-05
NM_002252	KCNS3	2.2	DOWN	3.05E-04
NM_002056	GFPT1	2.2	DOWN	7.18E-05
NM_002078	GOLGA4	2.2	DOWN	3.17E-04
AK055649	ERICH1	2.2	DOWN	4.51E-06
NM_020233	C17orf48	2.2	DOWN	7.82E-05
AB051516	NP_444270.2	2.2	DOWN	3.41E-06
AK000933	CHML	2.2	DOWN	9.62E-07
NM_031459	SESN2	2.2	DOWN	2.88E-04
AK027789	STT3B	2.2	DOWN	3.02E-05
NM_000311	PRNP	2.2	DOWN	7.82E-05
AB059277	AHCTF1	2.2	DOWN	2.96E-05
AL110139	NP_997329.1	2.2	DOWN	3.95E-04
BC017117	CREM	2.2	DOWN	1.27E-06
NM_006746	SCML1	2.2	DOWN	7.17E-05
NM_007314	ABL2	2.2	DOWN	5.61E-06
NM_000710	BDKRB1	2.2	DOWN	3.27E-05
NM_005875	EIF1B	2.2	DOWN	4.21E-04
NM_052868	IGSF8	2.2	DOWN	1.28E-04
NM_002219	STT3A	2.2	DOWN	1.01E-04
AB058747	WAC	2.2	DOWN	4.13E-04
NM_004731	SLC16A7	2.2	DOWN	5.46E-04
NM_000081	LYST	2.2	DOWN	3.17E-05
NM_032895	NP_001001870.1	2.2	DOWN	4.82E-05
NM_002715	PPP2CA	2.2	DOWN	4.37E-04
NM_006207	PDGFRL	2.2	DOWN	1.75E-04
AF148949	NA	2.2	DOWN	6.51E-04
NM_000935	PLOD2	2.2	DOWN	7.71E-05
NM_024633	CN139_HUMAN	2.2	DOWN	4.35E-07
AL136807	NP_055260.1	2.2	DOWN	2.38E-04
BC011715	Q8WTY6_HUMAN	2.2	DOWN	2.32E-04
NM_021194	SLC30A1	2.2	DOWN	4.19E-04
AK024896	SLC5A3	2.2	DOWN	2.86E-06
AK026902	GNA13	2.2	DOWN	8.64E-06
AK022547	PARP6	2.2	DOWN	1.77E-05
NM_005587	MEF2A	2.2	DOWN	1.97E-05
NM_002717	DOCK5	2.1	DOWN	1.22E-05
NM_001066	TNFRSF1B	2.1	DOWN	1.12E-04
AK057820	PTGES3	2.1	DOWN	6.44E-06
AJ420423	UGCG	2.1	DOWN	6.70E-05
NM_002846	PTPRN	2.1	DOWN	4.24E-04
AB007931	ZUBR1	2.1	DOWN	1.77E-05
NM_003806	HRK	2.1	DOWN	6.90E-05
AK023623	GLDN	2.1	DOWN	9.66E-05
NM_003680	YARS	2.1	DOWN	5.43E-06
NM_000985	MIT:HsG2227	2.1	DOWN	1.24E-05
NM_017983	WIPI1	2.1	DOWN	2.41E-05
NM_007107	SSR3	2.1	DOWN	7.05E-05
AB029551	RYBP	2.1	DOWN	2.62E-05
NM_021928	SPCS3	2.1	DOWN	1.24E-04
NM_018096	NLE1	2.1	DOWN	6.74E-05
NM_002930	RIT2	2.1	DOWN	6.57E-04
AF121255	EIF2C2	2.1	DOWN	2.87E-04
AK026217	TTC17	2.1	DOWN	6.96E-06
NM_031437	RASSF5	2.1	DOWN	4.13E-04
BC014527	FBXO27	2.1	DOWN	4.82E-05
NM_024580	EFTUD1	2.1	DOWN	3.12E-04
NM_006835	CCNI	2.1	DOWN	6.63E-05
NM_002507	NGFR	2.1	DOWN	2.95E-05
AK056817	NA	2.1	DOWN	1.38E-04
NM_006410	HTATIP2	2.1	DOWN	5.29E-04
AJ420461	QSCN6L1	2.1	DOWN	1.68E-06

BC017650	C1orf201	2.1	DOWN	2.58E-04
U82319	C6orf68	2.1	DOWN	1.16E-04
NM_006513	SARS	2.1	DOWN	1.09E-05
NM_003875	GMPS	2.1	DOWN	4.64E-04
NM_016470	CT111_HUMAN	2.1	DOWN	4.55E-04
AB011100	KIAA0528	2.1	DOWN	4.59E-06
NM_018630	DERL1	2.1	DOWN	5.96E-05
AK024597	TRIM25	2.1	DOWN	1.41E-04
NM_032717	NP_116106.2	2.1	DOWN	6.39E-06
NM_017993	NP_060463.1	2.1	DOWN	7.64E-06
NM_004337	OSGIN2	2.1	DOWN	7.14E-06
NM_004405	DLX2	2.1	DOWN	6.69E-05
NM_006164	NFE2L2	2.1	DOWN	9.77E-06
NM_014812	CEP170	2.1	DOWN	4.04E-05
M12679	HLA-C	2.1	DOWN	6.10E-05
NM_000638	VTN	2.1	DOWN	1.69E-04
NM_052888	LRRC37B	2.1	DOWN	8.31E-07
AB051551	LRRCC1	2.1	DOWN	6.31E-04
AF263613	PNPLA10P	2.1	DOWN	1.44E-05
NM_007214	SEC63	2.1	DOWN	4.24E-05
NM_024640	YRDC	2.1	DOWN	3.12E-05
AK024276	Q8ND77_HUMAN	2.1	DOWN	2.42E-05
NM_002116	HLA-H	2.1	DOWN	2.92E-04
NM_013376	SERTAD1	2.1	DOWN	2.18E-05
NM_016582	SLC15A3	2.0	DOWN	4.26E-04
NM_003904	ZNF259	2.0	DOWN	2.59E-05
AK027113	BCM:bcm714	2.0	DOWN	2.73E-04
AB067493	BCM:Q96PY1	2.0	DOWN	2.54E-04
NM_024052	C17orf39	2.0	DOWN	1.30E-05
AB037797	ARRDC3	2.0	DOWN	7.86E-04
AL137480	FNBP4	2.0	DOWN	1.04E-04
NM_004063	CDH17	2.0	DOWN	6.59E-05
NM_025000	C2orf37	2.0	DOWN	7.88E-05
AB046794	FAM29A	2.0	DOWN	1.19E-04
L21934	SOAT1	2.0	DOWN	1.41E-04
NM_015497	TMEM87A	2.0	DOWN	2.75E-04
BC003353	MED10	2.0	DOWN	9.15E-04
NM_006170	NOL1	2.0	DOWN	2.88E-04
NM_014811	KIAA0649	2.0	DOWN	5.30E-06
NM_003414	ZNF267	2.0	DOWN	4.98E-04
AK024858	LEMD2	2.0	DOWN	6.41E-06
NM_004865	TBPL1	2.0	DOWN	5.61E-06
BC011000	CDCA5	2.0	DOWN	1.76E-04
NM_003866	INPP4B	2.0	DOWN	1.05E-04
NM_005087	FXR1	2.0	DOWN	3.31E-04
NM_015946	PELO	2.0	DOWN	7.64E-06
NM_032842	NP_116231.2	2.0	DOWN	4.06E-05
NM_004623	TTC4	2.0	DOWN	2.03E-05
NM_017945	SLC35A5	2.0	DOWN	2.61E-06
NM_016078	FAM18B	2.0	DOWN	5.42E-04
NM_003753	EIF3S7	2.0	DOWN	1.33E-04
NM_020156	C1GALT1	2.0	DOWN	3.19E-05
NM_003659	AGPS	2.0	DOWN	1.19E-04
AF070674	BIRC3	2.0	DOWN	1.15E-04
NM_002874	RAD23B	2.0	UP	3.01E-04
AB007857	RUTBC1	2.0	UP	1.69E-04
AK001536	C22:AP000525.4	2.0	UP	1.70E-04
NM_007286	SYNPO	2.0	UP	5.41E-04
BC010145	DNAJC4	2.0	UP	5.65E-05
NM_006319	CDIPT	2.0	UP	1.54E-04
NM_015544	TMEM98	2.0	UP	5.82E-06
AJ420812	SLC44A1	2.0	UP	3.32E-04

NM_024509	LRFN3	2.0	UP	3.97E-05
AL080219	RTCD1	2.0	UP	7.22E-05
NM_014604	P2RX5	2.0	UP	5.87E-04
NM_001972	ELA2	2.0	UP	1.22E-05
NM_001904	CTNNB1	2.0	UP	3.94E-05
NM_005982	SIX1	2.0	UP	7.66E-04
NM_001703	BAI2	2.0	UP	4.35E-04
BC000039	FAM26B	2.0	UP	2.86E-05
NM_014217	KCNK2	2.0	UP	2.76E-04
NM_014051	TMEM14A	2.0	UP	2.35E-05
AK027274	MARCKS	2.0	UP	2.18E-05
NM_000900	MGP	2.1	UP	3.64E-04
NM_000380	XPA	2.1	UP	8.20E-04
NM_000858	GUK1	2.1	UP	1.37E-04
AF070641	ETV1	2.1	UP	2.42E-04
NM_002695	POLR2E	2.1	UP	4.91E-05
NM_018347	CT029_HUMAN	2.1	UP	1.12E-04
NM_018719	CDCA7L	2.1	UP	1.08E-05
NM_003127	SPTAN1	2.1	UP	7.43E-04
AK054707	ROGDI	2.1	UP	4.49E-06
AK022939	CEP27	2.1	UP	3.46E-06
NM_015976	SNX7	2.1	UP	2.34E-05
NM_004663	RAB11A	2.1	UP	7.03E-05
NM_005766	FARP1	2.1	UP	3.13E-04
BC007323	NDUFC2	2.1	UP	1.19E-04
NM_024863	TCEAL4	2.1	UP	1.39E-05
NM_018355	ZNF415	2.1	UP	3.84E-04
NM_000093	COL5A1	2.1	UP	3.44E-06
AL137535	C9orf3	2.1	UP	3.20E-04
NM_002861	PCYT2	2.1	UP	5.13E-04
NM_004809	STOML1	2.1	UP	7.13E-05
NM_032409	PINK1	2.1	UP	3.42E-04
NM_016199	LSM7	2.1	UP	4.62E-04
AB046781	UACA	2.1	UP	1.99E-06
BC008744	PLEKHQ1	2.1	UP	4.10E-05
AK057652	NA	2.1	UP	7.81E-04
NM_014248	RBX1	2.1	UP	2.77E-05
NM_021210	TRAPPC1	2.1	UP	7.92E-05
BC000977	ALAD	2.1	UP	1.35E-04
AK023815	GALNT10	2.1	UP	2.00E-06
NM_012135	FAM50B	2.1	UP	3.47E-06
NM_024042	METRN	2.1	UP	5.72E-05
AK026666	NP_001026897.1	2.1	UP	7.34E-05
NM_024833	ZNF671	2.1	UP	1.90E-04
NM_000600	IL6	2.1	UP	2.33E-04
NM_015392	NPDC1	2.1	UP	4.16E-05
NM_022823	FNDC4	2.1	UP	4.02E-04
NM_005432	XRCC3	2.1	UP	4.77E-05
AK055683	ZMAT2	2.1	UP	2.69E-05
NM_001060	TBXA2R	2.1	UP	3.57E-05
NM_003893	LDB1	2.1	UP	3.49E-06
AL049980	HSD17B12	2.1	UP	4.38E-05
NM_006848	CCDC85B	2.2	UP	1.12E-04
NM_016113	TRPV2	2.2	UP	2.75E-04
AK054986	RP5-998N21.2	2.2	UP	9.44E-06
NM_032601	MCEE	2.2	UP	9.75E-07
NM_021570	BARX1	2.2	UP	3.88E-05
NM_000859	HMGCR	2.2	UP	7.75E-04
AF156100	HMCN1	2.2	UP	2.57E-04
NM_006810	PDIA5	2.2	UP	3.40E-05
NM_004638	BAT2	2.2	UP	2.14E-06
NM_006412	AGPAT2	2.2	UP	1.86E-05

NM_024825	PODNL1	2.2	UP	1.32E-05
BC018118	ARHGAP1	2.2	UP	1.94E-05
AB037823	CHGUT_HUMAN	2.2	UP	2.48E-04
AK056039	NA	2.2	UP	5.90E-05
AK025071	SPTBN1	2.2	UP	3.72E-06
NM_016206	BCM:NM_016206	2.2	UP	3.23E-04
NM_012317	LDOC1	2.2	UP	4.84E-05
NM_006074	TRIM22	2.2	UP	9.73E-05
BC009566	TAF9B	2.2	UP	1.04E-04
AK056499	PRICKLE1	2.2	UP	1.19E-04
NM_005566	LDHA	2.2	UP	1.77E-04
NM_005009	NME4	2.2	UP	1.27E-06
NM_014324	AMACR	2.3	UP	1.51E-05
AJ272212	PSKH1	2.3	UP	1.25E-06
NM_003491	ARD1A	2.3	UP	3.16E-06
AK021925	SLC41A3	2.3	UP	1.94E-05
U60873	NA	2.3	UP	5.62E-04
NM_000138	FBN1	2.3	UP	8.46E-04
AK025371	ASAHL	2.3	UP	7.97E-05
AK055506	VGCNL1	2.3	UP	3.65E-05
NM_000107	DDB2	2.3	UP	2.44E-06
NM_003528	HIST2H2BE	2.3	UP	2.06E-04
AK056513	NP_653327.1	2.3	UP	7.02E-06
NM_005566	LDHA	2.3	UP	7.22E-05
AK000672	FAM82B	2.3	UP	4.62E-04
NM_021643	TRIB2	2.3	UP	1.80E-05
NM_005111	CRYZL1	2.3	UP	3.80E-04
NM_024062	VANGL1	2.3	UP	4.66E-05
NM_003492	CXorf12	2.3	UP	1.10E-05
NM_003634	NIPSNAP1	2.3	UP	2.74E-05
AB011540	LRP4	2.3	UP	4.61E-04
NM_015373	PGEA1	2.3	UP	1.41E-05
AK055699	LYPD6	2.3	UP	5.69E-05
AK023619	CRIM1	2.3	UP	1.10E-05
NM_004538	NAP1L3	2.3	UP	4.45E-05
NM_032262	NP_115638.1	2.3	UP	1.78E-04
AK021851	NA	2.3	UP	3.45E-05
NM_001611	ACP5	2.3	UP	2.63E-04
NM_001215	CA6	2.3	UP	4.77E-04
NM_003118	SPARC	2.4	UP	8.94E-04
NM_000476	AK1	2.4	UP	3.37E-06
AK027351	RHOJ	2.4	UP	7.50E-04
NM_004528	MGST3	2.4	UP	1.28E-04
NM_001336	CTSZ	2.4	UP	9.43E-05
AL359052	ITGBL1	2.4	UP	4.39E-04
NM_006822	RAB40B	2.4	UP	1.86E-05
NM_004642	CDK2AP1	2.4	UP	1.38E-06
AK055294	SHROOM3	2.4	UP	3.31E-05
AK021486	BMP5	2.4	UP	2.78E-04
AK057566	ANKRD13D	2.4	UP	2.45E-07
NM_003516	HIST2H2AA3	2.4	UP	4.98E-04
NM_002452	NUDT1	2.4	UP	1.00E-04
AK056203	LRSAM1	2.4	UP	1.20E-04
NM_016429	COPZ2	2.4	UP	9.87E-05
NM_017702	NP_997397.1	2.4	UP	8.50E-06
NM_025149	NP_079425.2	2.4	UP	1.08E-04
NM_003528	HIST2H2BE	2.4	UP	1.07E-04
NM_002744	PRKCZ	2.4	UP	1.61E-04
AK057356	GGN	2.4	UP	4.36E-05
NM_005767	P2RY5	2.5	UP	4.16E-04
BC013049	MRRF	2.5	UP	3.87E-06
NM_003528	HIST2H2BE	2.5	UP	3.76E-04

AB011539	MEGF6	2.5	UP	4.33E-05
NM_022783	DEPDC6	2.5	UP	4.34E-04
NM_002863	PYGL	2.5	UP	2.79E-05
NM_003528	HIST2H2BE	2.5	UP	2.38E-04
NM_005418	ST5	2.5	UP	5.99E-06
AK025953	MYLK	2.5	UP	5.23E-04
M62896	NA	2.5	UP	1.24E-04
NM_031302	GLT8D2	2.5	UP	8.59E-08
AK025627	MIT:HsG2201	2.5	UP	4.96E-06
AK056473	FAM33A	2.5	UP	3.84E-05
NM_003528	HIST2H2BE	2.5	UP	2.10E-04
BC012170	C3orf54	2.5	UP	7.64E-06
NM_005566	LDHA	2.5	UP	3.57E-05
NM_021923	FGFRL1	2.5	UP	1.51E-04
NM_002725	PRELP	2.5	UP	2.83E-04
NM_003250	THRA	2.6	UP	9.81E-07
NM_005101	ISG15	2.6	UP	5.42E-04
NM_003528	HIST2H2BE	2.6	UP	7.71E-05
AL133084	PGBD3	2.6	UP	6.87E-05
AY008268	SAR1A	2.6	UP	1.73E-05
AK027191	NA	2.6	UP	7.15E-05
NM_001822	CHN1	2.6	UP	2.43E-06
NM_000177	GSN	2.6	UP	6.57E-06
AK055808	NP_001070148.1	2.6	UP	1.99E-05
NM_033138	CALD1	2.6	UP	7.03E-05
NM_003528	HIST2H2BE	2.6	UP	3.35E-05
NM_057161	KLHDC3	2.6	UP	4.30E-07
NM_005566	LDHA	2.6	UP	6.45E-05
NM_005469	ACOT8	2.6	UP	7.98E-05
AF380356	XG	2.6	UP	2.45E-04
NM_005572	LMNA	2.6	UP	9.96E-06
NM_003246	THBS1	2.6	UP	6.37E-07
NM_003956	CH25H	2.6	UP	2.75E-04
NM_004701	CCNB2	2.6	UP	3.76E-04
NM_016332	SEPX1	2.6	UP	4.35E-07
BC012625	PPP1R3C	2.6	UP	2.85E-07
AB011110	RASA4	2.6	UP	4.39E-07
NM_032800	C1orf198	2.7	UP	1.77E-04
NM_003528	HIST2H2BE	2.7	UP	7.01E-05
U97105	DPYSL2	2.7	UP	7.48E-07
NM_002966	S100A10	2.7	UP	3.33E-04
NM_032291	SGIP1	2.7	UP	2.56E-05
NM_001548	IFIT1	2.7	UP	4.86E-05
NM_052969	RPL39L	2.7	UP	3.86E-06
NM_021874	CDC25B	2.7	UP	3.71E-05
AL080111	NEK7	2.7	UP	7.44E-04
NM_000820	GAS6	2.7	UP	3.31E-05
NM_022343	GAPR1_HUMAN	2.7	UP	1.03E-06
NM_000077	CDKN2A	2.7	UP	4.36E-05
AK026164	MYL6	2.7	UP	4.76E-08
AK057333	C11orf66	2.7	UP	7.04E-05
BC013438	Q96D13_HUMAN	2.8	UP	5.41E-06
NM_005491	CXorf6	2.8	UP	4.91E-08
NM_002313	ABLIM1	2.8	UP	1.99E-04
NM_018953	HOXC5	2.8	UP	6.37E-06
AB051459	DJBP_HUMAN	2.8	UP	1.15E-06
NM_006579	EBP	2.8	UP	2.01E-05
AL049957	CD59	2.8	UP	2.25E-06
NM_016471	ORMDL3	2.8	UP	1.06E-06
NM_002413	MGST2	2.8	UP	4.33E-07
NM_005423	TFF2	2.9	UP	2.84E-05
NM_003070	SMARCA2	2.9	UP	5.66E-06

AK023464	BCM:bcm899	2.9	UP	8.56E-07
AL050137	OLFML2B	2.9	UP	2.42E-08
AK026717	SEPW1	2.9	UP	4.33E-06
NM_002609	PDGFRB	2.9	UP	5.24E-07
NM_020166	MCCC1	2.9	UP	1.97E-06
NM_005566	LDHA	2.9	UP	1.69E-06
X68742	PELO	2.9	UP	6.63E-04
NM_014583	LMCD1	2.9	UP	2.78E-04
NM_053025	MYLK	2.9	UP	1.05E-04
NM_003528	HIST2H2BE	2.9	UP	7.71E-05
NM_004765	BCL7C	2.9	UP	8.87E-07
NM_006986	MAGED1	2.9	UP	1.99E-08
AF043897	hsa-mir-23b	2.9	UP	5.59E-07
AB046764	NBEA	3.0	UP	1.69E-05
AB037750	SORCS2	3.0	UP	8.10E-06
L10374	Q5W0J2_HUMAN	3.0	UP	3.46E-06
NM_000022	ADA	3.0	UP	2.36E-04
AK024192	RBPMS	3.0	UP	3.11E-04
NM_000163	GHR	3.0	UP	6.63E-05
AK021874	TGFB2	3.0	UP	6.08E-07
NM_030786	SYNC1	3.0	UP	4.72E-08
AF090693	CUGBP2	3.1	UP	6.71E-04
AK022222	CALD1	3.1	UP	2.13E-04
NM_001845	COL4A1	3.1	UP	3.95E-05
NM_003512	HIST1H2AC	3.1	UP	3.42E-06
NM_003247	THBS2	3.1	UP	5.41E-04
NM_003289	TPM2	3.1	UP	3.36E-05
AL359558	MCC	3.1	UP	2.97E-07
NM_000943	PPIC	3.1	UP	1.12E-08
BC015134	THBS1	3.1	UP	1.02E-07
NM_022129	MAWBP_HUMAN	3.2	UP	4.51E-06
NM_054033	FKBP1B	3.2	UP	1.47E-06
NM_003280	TNNC1	3.2	UP	1.97E-05
NM_032348	MXRA8	3.2	UP	1.27E-07
NM_014867	KBTBD11	3.2	UP	5.31E-07
NM_016557	NA	3.3	UP	2.19E-04
NM_001512	GSTA4	3.3	UP	7.09E-08
AB046796	K1576_HUMAN	3.3	UP	1.83E-04
NM_004512	GALT	3.3	UP	1.82E-06
NM_021730	Q96AM0_HUMAN	3.4	UP	8.15E-09
AY039760	ATP6V1G3	3.4	UP	2.70E-06
NM_004409	DMPK	3.4	UP	1.02E-08
AF245505	MXRA5	3.4	UP	3.56E-05
NM_002775	HTRA1	3.4	UP	1.56E-06
NM_012134	LMOD1	3.4	UP	2.69E-05
NM_002048	GAS1	3.4	UP	1.79E-05
NM_000253	MTTP	3.5	UP	1.31E-07
NM_001792	CDH2	3.5	UP	2.01E-05
NM_000393	COL5A2	3.5	UP	5.24E-07
AK021982	DYM	3.5	UP	7.59E-08
BC013971	HOXA10	3.5	UP	1.32E-07
AB032947	CADPS	3.5	UP	1.71E-07
NM_018936	PCDHB2	3.5	UP	4.07E-04
AK057501	CMTM2	3.5	UP	4.21E-07
NM_030915	LBH	3.6	UP	2.54E-04
NM_032603	LOXL3	3.7	UP	9.96E-08
NM_000090	COL3A1	3.7	UP	1.00E-06
AK001007	GRAMD3	3.7	UP	5.21E-05
NM_005195	Q504X4_HUMAN	3.7	UP	1.39E-04
NM_004265	FADS2	3.8	UP	7.45E-04
NM_020404	CD248	3.8	UP	2.00E-09
NM_004772	C5orf13	4.1	UP	8.15E-08

AK025346	NA	4.3	UP	7.64E-06
NM_052880	NP_443112.2	4.3	UP	5.66E-06
NM_014298	QPRT	4.3	UP	5.29E-04
NM_002527	NTF3	4.4	UP	4.72E-08
NM_004415	DSP	4.4	UP	9.85E-06
AK057328	NA	4.5	UP	1.12E-07
AF444143	SPG3A	4.5	UP	1.06E-05
AK058001	DENND3	4.5	UP	4.46E-07
NM_032623	NP_116012.2	4.6	UP	5.69E-05
NM_014762	DHCR24	4.6	UP	2.42E-05
NM_023927	GRAMD3	4.6	UP	1.59E-07
AL137734	NA	4.6	UP	3.82E-06
NM_031289	GSG1	4.8	UP	5.19E-06
NM_002961	S100A4	4.8	UP	1.35E-05
NM_023067	FOXL2	4.8	UP	9.10E-05
NM_004881	TP53I3	4.8	UP	3.12E-11
NM_002982	CCL2	4.9	UP	4.91E-08
AF213459	EPHA3	5.0	UP	1.31E-06
NM_000147	FUCA1	5.1	UP	2.24E-08
NM_001864	COX7A1	5.2	UP	9.50E-08
NM_005584	MAB21L1	5.2	UP	8.15E-08
BC012486	KRA24_HUMAN	5.2	UP	5.97E-05
AJ245539	GALNT5	5.4	UP	2.79E-10
AK055249	UCHL1	5.6	UP	5.82E-10
NM_001175	ARHGDIB	5.6	UP	1.56E-06
NM_000346	SOX9	5.7	UP	1.47E-05
AL137678	C20orf50	6.0	UP	3.10E-08
NM_004181	UCHL1	6.1	UP	7.45E-10
NM_003783	B3GALT2	6.1	UP	3.86E-05
AK002039	MRVI1	6.2	UP	5.69E-05
NM_004335	BST2	6.7	UP	1.46E-06
NM_030967	KRTAP1-3	7.2	UP	1.31E-06
NM_000095	COMP	7.5	UP	7.59E-06
NM_000088	COL1A1	7.7	UP	1.02E-07
NM_004669	CLIC3	8.5	UP	4.36E-07
NM_000681	ADRA2A	8.9	UP	2.88E-08
NM_001562	IL18	9.1	UP	8.13E-08
NM_020169	LXN	9.1	UP	2.16E-09
NM_006308	HSPB3	10.3	UP	5.95E-08
NM_002276	KRT19	10.6	UP	7.14E-08
AK022198	GALNT5	12.6	UP	1.13E-09
AB032953	ODZ2	13.3	UP	1.38E-11
NM_000089	COL1A2	13.9	UP	3.12E-11
AB067499	Q96PX6_HUMAN	14.4	UP	8.31E-07
AK021484	SYNPO2	22.0	UP	4.44E-08

Supplementary table S2: Significantly differentially expressed genes for the 97 versus 0 comparison

Genbank accession No.	Gene symbol	Fold-change	Direction	p-value
NM_000799	EPO	67.7	DOWN	5.94E-11
NM_002155	HSPA6	52.1	DOWN	2.14E-11
NM_002421	MMP1	38.8	DOWN	3.82E-09
NM_004864	GDF15	37.3	DOWN	1.29E-08
NM_000963	PTGS2	32.4	DOWN	2.75E-09
NM_005345	HSPA1A	28.8	DOWN	1.87E-11
NM_005345	HSPA1A	28.3	DOWN	5.88E-12
NM_005345	HSPA1A	27.9	DOWN	5.88E-12
NM_005345	HSPA1A	27.7	DOWN	1.87E-11
NM_005345	HSPA1A	27.7	DOWN	5.88E-12
NM_005345	HSPA1A	27.6	DOWN	4.84E-11
NM_005345	HSPA1A	27.5	DOWN	2.14E-11
NM_005345	HSPA1A	27.1	DOWN	4.84E-11
NM_005345	HSPA1A	26.2	DOWN	5.88E-12
NM_005345	HSPA1A	26.1	DOWN	4.55E-11
NM_005345	HSPA1A	26.1	DOWN	5.88E-12
NM_005345	HSPA1A	25.9	DOWN	5.94E-11
NM_005345	HSPA1A	25.4	DOWN	5.88E-12
NM_005345	HSPA1A	25.3	DOWN	4.84E-11
NM_021158	TRIB3	23.9	DOWN	1.57E-08
NM_005345	HSPA1A	23.6	DOWN	2.14E-11
NM_005345	HSPA1A	23.1	DOWN	7.36E-11
NM_005346	HSPA1B	23.0	DOWN	1.18E-10
NM_005345	HSPA1A	22.8	DOWN	2.14E-11
NM_002220	ITPKA	20.1	DOWN	9.52E-11
NM_022842	CDCP1	19.9	DOWN	1.47E-09
NM_004165	RRAD	19.3	DOWN	9.90E-11
NM_002727	PRG1	18.4	DOWN	6.91E-10
NM_002923	RGS2	18.0	DOWN	6.20E-08
NM_005252	FOS	18.0	DOWN	5.09E-10
NM_032621	BEX2	17.3	DOWN	3.46E-11
NM_002394	SLC3A2	15.8	DOWN	3.46E-11
BC012321	ARC	13.8	DOWN	3.49E-10
NM_001353	AKR1C1	11.6	DOWN	5.45E-07
NM_017947	MOCOS	11.5	DOWN	4.91E-06
NM_012328	DNAJB9	11.2	DOWN	1.46E-10
NM_006145	DNAJB1	11.2	DOWN	4.84E-11
NM_001533	HNRPL	10.5	DOWN	2.44E-10
NM_007115	TNFAIP6	10.3	DOWN	3.09E-07
NM_001945	HBEGF	10.3	DOWN	2.12E-07
NM_000640	IL13RA2	10.2	DOWN	8.84E-08
NM_002133	HMOX1	9.8	DOWN	3.27E-07
NM_021127	PMAIP1	9.7	DOWN	2.16E-07
NM_001902	CTH	9.6	DOWN	3.69E-10
AB050476	LHX8	9.5	DOWN	8.59E-10
BC017001	SCRT2	9.4	DOWN	4.16E-08
NM_005347	HSPA5	9.3	DOWN	7.37E-06
NM_001451	FOXF1	9.2	DOWN	4.19E-08
NM_007289	MME	9.1	DOWN	2.13E-06
NM_005532	IFI27	8.9	DOWN	6.41E-04
NM_002837	PTPRB	8.8	DOWN	5.82E-08
NM_005098	MSC	8.8	DOWN	2.50E-08
NM_000361	THBD	8.6	DOWN	7.69E-09
NM_000804	FOLR3	8.6	DOWN	4.54E-09
AF438313	TMEM158	8.2	DOWN	8.53E-08
NM_004862	LITAF	8.0	DOWN	4.83E-07
NM_013370	OSGIN1	7.7	DOWN	2.33E-08
NM_004083	DDIT3	7.7	DOWN	1.24E-08
NM_004398	DDX10	7.6	DOWN	1.29E-08

NM_002479	MYOG	7.5	DOWN	1.78E-07
NM_006010	ARMET	7.4	DOWN	2.26E-07
NM_007036	ESM1	7.4	DOWN	1.40E-05
NM_016084	RASD1	7.3	DOWN	2.90E-08
AK001031	TBX2	7.2	DOWN	1.02E-08
NM_003364	UPP1	7.1	DOWN	3.05E-09
NM_017723	NP_060193.2	7.0	DOWN	1.71E-04
NM_006636	MTHFD2	7.0	DOWN	4.50E-10
BC016658	E2F7	6.8	DOWN	1.25E-07
NM_003038	SLC1A4	6.6	DOWN	2.21E-10
AL390153	MBD3	6.5	DOWN	6.44E-04
NM_020038	ABCC3	6.5	DOWN	7.63E-07
NM_030674	SLC38A1	6.3	DOWN	1.56E-07
NM_006389	HYOU1	6.3	DOWN	6.72E-06
AL133096	DNAJA4	6.1	DOWN	5.24E-07
NM_006470	TRIM16	6.1	DOWN	1.26E-06
NM_014751	MTSS1	6.0	DOWN	5.50E-07
NM_004362	CLGN	6.0	DOWN	3.58E-08
NM_001673	ASNS	5.9	DOWN	6.91E-10
NM_022044	SDF2L1	5.9	DOWN	2.66E-08
NM_006732	FOSB	5.8	DOWN	3.10E-09
NM_006528	TFPI2	5.8	DOWN	4.69E-06
NM_032691	NA	5.8	DOWN	1.25E-09
NM_003330	Q6YNQ1_HUMAN	5.7	DOWN	1.69E-05
NM_014331	SLC7A11	5.6	DOWN	2.60E-08
NM_005402	RALA	5.5	DOWN	9.32E-08
NM_006644	HSPH1	5.5	DOWN	1.70E-08
BC007359	RTTN	5.5	DOWN	1.94E-08
NM_019058	DDIT4	5.4	DOWN	3.58E-09
NM_004419	DUSP5	5.4	DOWN	1.47E-05
NM_000584	IL8	5.4	DOWN	6.61E-09
M77140	GAL	5.4	DOWN	1.36E-05
NM_001498	GCLC	5.4	DOWN	1.23E-09
NM_004024	ATF3	5.4	DOWN	5.72E-08
NM_005985	SNAI1	5.4	DOWN	1.19E-05
AF101051	CLDN1	5.4	DOWN	3.02E-04
NM_020299	AKR1B10	5.4	DOWN	1.59E-05
L24498	GADD45A	5.3	DOWN	5.68E-06
NM_004095	EIF4EBP1	5.3	DOWN	1.31E-08
BC016285	PRKACB	5.3	DOWN	6.63E-09
NM_015675	GADD45B	5.3	DOWN	2.31E-08
NM_002061	GCLM	5.3	DOWN	1.43E-08
NM_022743	SMYD3	5.2	DOWN	7.30E-07
AB018289	NP_056002.1	5.2	DOWN	1.78E-04
NM_000231	SGCG	5.2	DOWN	5.60E-06
NM_000071	CBS	5.2	DOWN	6.90E-06
NM_003655	CBX4	5.2	DOWN	1.62E-06
NM_000271	NPC1	5.1	DOWN	2.54E-09
AF007152	ABHD3	5.1	DOWN	1.46E-10
NM_003582	DYRK3	5.1	DOWN	1.10E-05
NM_003662	PIR	5.1	DOWN	1.82E-06
NM_052966	NIBA_HUMAN	5.0	DOWN	2.07E-06
NM_001793	CDH3	5.0	DOWN	8.20E-07
NM_002135	NR4A1	5.0	DOWN	6.03E-11
NM_006705	GADD45G	5.0	DOWN	6.91E-07
NM_000167	GK	5.0	DOWN	2.58E-07
NM_006516	SLC2A1	4.9	DOWN	1.29E-08
NM_002047	GARS	4.9	DOWN	1.80E-09
BC001618	SLC1A4	4.9	DOWN	1.13E-10
NM_018259	TTC17	4.9	DOWN	1.78E-08
AL137311	DNER	4.8	DOWN	6.64E-05
NM_016242	EMCN	4.8	DOWN	1.07E-05

NM_025001	MTHFD2L	4.8	DOWN	1.41E-06
NM_023940	RASL11B	4.8	DOWN	2.49E-07
AF022375	VEGFA	4.8	DOWN	9.52E-09
NM_005261	GEM	4.7	DOWN	8.77E-07
AF104032	SLC7A5	4.7	DOWN	6.15E-08
AL353933	SLC22A15	4.7	DOWN	1.74E-06
X63759	TNP2	4.6	DOWN	2.34E-05
NM_006260	DNAJC3	4.6	DOWN	9.73E-07
NM_031456	FBXW10	4.6	DOWN	2.21E-06
AK056433	VAC14	4.6	DOWN	3.09E-07
NM_004933	CDH15	4.6	DOWN	5.06E-05
NM_001818	AKR1C4	4.6	DOWN	4.55E-07
NM_004524	LLGL2	4.5	DOWN	2.49E-07
NM_020184	CNNM4	4.5	DOWN	1.24E-08
D31887	SLC39A14	4.4	DOWN	8.08E-09
BC012337	HKDC1	4.4	DOWN	2.49E-07
NM_022359	PDE4DIP	4.4	DOWN	6.50E-05
NM_003900	SQSTM1	4.4	DOWN	1.85E-04
NM_016306	DNAJB11	4.3	DOWN	6.65E-07
NM_018590	CGAT2_HUMAN	4.3	DOWN	2.46E-07
NM_000169	GLA	4.3	DOWN	3.47E-08
NM_018112	TMEM38B	4.3	DOWN	3.30E-05
NM_002943	RORA	4.3	DOWN	6.47E-06
NM_024111	CHAC1	4.3	DOWN	1.58E-08
NM_012410	SEZ6L2	4.3	DOWN	1.81E-07
NM_031846	MAP2	4.2	DOWN	3.13E-06
AK025379	PLEKHM1	4.2	DOWN	3.13E-07
NM_054012	ASS1	4.2	DOWN	1.31E-04
NM_004183	BEST1	4.2	DOWN	1.01E-06
NM_004911	PDIA4	4.2	DOWN	1.04E-04
NM_025195	TRIB1	4.2	DOWN	5.75E-07
NM_002640	SERPINB8	4.2	DOWN	1.12E-08
NM_002583	PAWR	4.1	DOWN	4.88E-06
NM_000270	NP	4.1	DOWN	2.05E-07
NM_052815	IER3	4.1	DOWN	5.50E-07
NM_004418	DUSP2	4.1	DOWN	1.64E-07
NM_007076	NP_009007.2	4.1	DOWN	2.05E-05
NM_032744	C6orf105	4.1	DOWN	2.97E-06
NM_016614	TTRAP	4.1	DOWN	5.95E-07
AF070606	ATP2B1	4.1	DOWN	2.39E-06
NM_005504	BCAT1	4.1	DOWN	8.11E-08
NM_006769	LMO4	4.0	DOWN	2.83E-08
NM_017793	RPP25	4.0	DOWN	1.19E-06
NM_032883	GCX1_HUMAN	4.0	DOWN	9.26E-06
NM_032413	C15orf48	4.0	DOWN	3.38E-05
AC004010	AMIGO2	4.0	DOWN	2.90E-05
NM_004010	DMD	4.0	DOWN	4.45E-05
BC015687	FLCN	4.0	DOWN	1.69E-05
NM_006670	TPBG	4.0	DOWN	5.60E-06
NM_002359	MAFG	3.9	DOWN	9.42E-06
AK022459	CCPG1	3.9	DOWN	9.27E-07
NM_003299	HSP90B1	3.9	DOWN	7.80E-04
NM_002970	SAT1	3.9	DOWN	6.65E-06
NM_001859	SLC31A1	3.9	DOWN	8.99E-08
NM_004403	DFNA5	3.9	DOWN	1.14E-07
NM_004184	WARS	3.9	DOWN	3.27E-07
NM_012082	ZFPM2	3.8	DOWN	4.09E-04
NM_005842	SPRY2	3.8	DOWN	3.35E-04
NM_014191	SCN8A	3.8	DOWN	3.18E-07
NM_001946	DUSP6	3.8	DOWN	5.86E-06
AB046853	CDK5RAP2	3.8	DOWN	2.83E-08
NM_006948	STCH	3.8	DOWN	1.02E-05

NM_013246	CLCF1	3.8	DOWN	8.39E-05
NM_003953	MPZL1	3.8	DOWN	4.26E-06
NM_000574	CD55	3.8	DOWN	2.12E-07
NM_004047	ATP6V0B	3.8	DOWN	6.01E-07
AK001865	ERO1LB	3.8	DOWN	6.29E-07
NM_014330	PPP1R15A	3.8	DOWN	4.68E-07
NM_000120	EPHX1	3.7	DOWN	4.06E-10
NM_021928	SPCS3	3.7	DOWN	6.93E-07
NM_001912	CTSL	3.7	DOWN	8.91E-06
NM_000025	ADRB3	3.7	DOWN	5.74E-08
AK055094	MARVELD2	3.7	DOWN	1.13E-06
NM_002064	GLRX	3.7	DOWN	2.00E-05
NM_018423	STYK1	3.6	DOWN	1.93E-06
NM_002079	GOT1	3.6	DOWN	1.07E-08
NM_053040	C1orf79	3.6	DOWN	5.56E-08
NM_000311	PRNP	3.6	DOWN	9.95E-07
NM_024692	RSNL2	3.6	DOWN	4.20E-08
AK056477	GZF1	3.6	DOWN	1.85E-07
NM_022365	DNAJC1	3.6	DOWN	8.28E-08
NM_005596	NFIB	3.6	DOWN	3.84E-05
AL050090	MYRIP	3.5	DOWN	1.60E-05
AB051460	CPEB4	3.5	DOWN	2.76E-07
NM_001888	CRYM	3.5	DOWN	1.29E-04
AK024263	NA	3.5	DOWN	6.20E-08
NM_014900	COBLL1	3.5	DOWN	4.09E-05
NM_031471	URP2_HUMAN	3.5	DOWN	2.13E-06
NM_030751	SNF1LK	3.5	DOWN	2.61E-05
BC012513	RND3	3.4	DOWN	1.85E-06
NM_023016	ANKRD57	3.4	DOWN	1.22E-06
AK024261	NA	3.4	DOWN	3.13E-06
NM_024324	CRELD2	3.4	DOWN	7.36E-05
BC017667	NAV3	3.4	DOWN	5.78E-04
NM_024531	GPR172A	3.4	DOWN	4.83E-07
AF212224	CLK1	3.4	DOWN	7.42E-06
NM_033027	AXUD1	3.4	DOWN	1.33E-05
NM_057749	CCNE2	3.4	DOWN	4.25E-05
NM_017572	MKNK2	3.3	DOWN	8.00E-05
NM_001122	ADFP	3.3	DOWN	5.08E-05
BC015542	PVR	3.3	DOWN	7.59E-04
NM_005080	XBP1	3.3	DOWN	7.44E-06
NM_052960	RBP7	3.3	DOWN	1.11E-05
NM_031412	GABARAPL1	3.3	DOWN	6.80E-05
NM_031459	SESN2	3.3	DOWN	1.30E-05
NM_006546	IGF2BP1	3.2	DOWN	3.27E-05
NM_016535	ZNF581	3.2	DOWN	2.12E-06
NM_021972	SPHK1	3.2	DOWN	4.22E-05
NM_014584	ERO1L	3.2	DOWN	3.56E-07
AB040959	DFNB31	3.2	DOWN	3.37E-06
NM_002014	FKBP4	3.2	DOWN	2.29E-06
NM_012081	ELL2	3.2	DOWN	3.24E-04
NM_005746	PBEF1	3.2	DOWN	1.61E-05
NM_001134	AFP	3.2	DOWN	1.44E-06
NM_004733	SLC33A1	3.2	DOWN	2.36E-08
AB007931	ZUBR1	3.2	DOWN	4.23E-07
NM_001881	CREM	3.2	DOWN	3.51E-07
AK001619	PDE4DIP	3.1	DOWN	1.11E-05
BC009033	ASPHD1	3.1	DOWN	6.47E-06
NM_000876	IGF2R	3.1	DOWN	3.85E-04
AF131821	MGLL	3.1	DOWN	9.03E-07
NM_022447	PAPD5	3.1	DOWN	2.56E-05
BC013128	CEBPG	3.1	DOWN	3.13E-06
NM_004673	ANGPTL1	3.1	DOWN	3.13E-06

NM_002910	RENBP	3.1	DOWN	1.37E-05
AK021789	Q8NHV5_HUMAN	3.1	DOWN	3.65E-06
NM_012323	MAFF	3.1	DOWN	7.18E-05
NM_005524	HES1	3.1	DOWN	3.81E-07
NM_005279	GPR1	3.1	DOWN	5.18E-08
NM_032711	MAFG	3.1	DOWN	2.79E-05
NM_014674	EDEM1	3.1	DOWN	1.14E-07
NM_022751	FAM59A	3.1	DOWN	2.56E-07
BC011715	Q8WTY6_HUMAN	3.1	DOWN	1.33E-05
NM_005527	HSPA1L	3.1	DOWN	2.61E-06
NM_001675	ATF4	3.1	DOWN	3.71E-07
AB051541	KIAA1754	3.0	DOWN	1.03E-04
NM_018015	CXorf57	3.0	DOWN	8.09E-06
NM_002041	GABPAP	3.0	DOWN	2.58E-07
NM_021938	BRUNOL5	3.0	DOWN	1.07E-04
NM_003851	CREG1	3.0	DOWN	3.83E-05
BC016024	FOXA3	3.0	DOWN	4.69E-04
AK056926	SLC31A1	3.0	DOWN	7.98E-06
NM_033280	SEC11C	3.0	DOWN	5.35E-07
NM_003254	TIMP1	3.0	DOWN	1.80E-04
NM_005875	EIF1B	3.0	DOWN	3.84E-05
BC017650	C1orf201	3.0	DOWN	1.30E-05
NM_002849	PTPRR	3.0	DOWN	4.53E-07
NM_002182	IL1RAP	3.0	DOWN	1.11E-05
AL136628	C4orf16	3.0	DOWN	1.41E-06
NM_003732	EIF4EBP3	3.0	DOWN	5.66E-06
NM_000079	CHRNA1	3.0	DOWN	9.38E-07
NM_016069	TIM16_HUMAN	3.0	DOWN	9.18E-09
AJ301564	C8orf13	2.9	DOWN	3.34E-06
NM_018421	TBC1D2	2.9	DOWN	4.74E-04
NM_013376	SERTAD1	2.9	DOWN	5.89E-07
NM_005729	PPIF	2.9	DOWN	1.04E-06
NM_024610	HSPBAP1	2.9	DOWN	1.38E-05
NM_025084	Q6P168_HUMAN	2.9	DOWN	2.13E-04
AK023769	C17orf27	2.9	DOWN	1.20E-05
NM_031232	APBA2BP	2.9	DOWN	7.25E-07
NM_014710	GPRASP1	2.9	DOWN	2.03E-05
NM_005088	CXYorf3	2.9	DOWN	8.91E-08
NM_004343	CALR	2.9	DOWN	4.50E-05
NM_016262	TUBE1	2.9	DOWN	2.02E-06
NM_002631	PGD	2.9	DOWN	1.67E-06
NM_000882	IL12A	2.9	DOWN	1.99E-05
AJ277587	SPIRE1	2.8	DOWN	8.10E-05
NM_022468	MMP25	2.8	DOWN	7.53E-06
NM_016522	NTRI_HUMAN	2.8	DOWN	1.36E-07
NM_021102	SPINT2	2.8	DOWN	8.89E-04
AK024858	LEMD2	2.8	DOWN	1.91E-07
NM_012385	NUPR1_HUMAN	2.8	DOWN	5.68E-06
NM_024506	GLB1L	2.8	DOWN	8.90E-05
NM_000637	GSR	2.8	DOWN	5.97E-05
AK024597	TRIM25	2.8	DOWN	1.10E-05
AK055618	C18orf19	2.8	DOWN	8.36E-06
NM_018357	LARP6	2.8	DOWN	6.64E-06
NM_002641	PIGA	2.8	DOWN	2.02E-06
AL080118	CN109_HUMAN	2.8	DOWN	2.02E-06
NM_005628	SLC1A5	2.8	DOWN	6.89E-04
NM_000600	IL6	2.8	DOWN	2.91E-05
AK025983	MGLL	2.8	DOWN	1.78E-04
NM_002928	RGS16	2.8	DOWN	1.83E-05
NM_032315	653698	2.8	DOWN	1.62E-04
NM_004281	BAG3	2.8	DOWN	8.02E-05
NM_001628	AKR1B1	2.8	DOWN	6.83E-05

NM_015364	LY96	2.8	DOWN	1.31E-04
NM_005727	TSPAN1	2.8	DOWN	1.30E-06
NM_003670	BHLHB2	2.8	DOWN	1.85E-06
AL122070	Q6ZUG4_HUMAN	2.8	DOWN	7.12E-06
NM_001553	IGFBP7	2.7	DOWN	2.47E-04
NM_001746	CANX	2.7	DOWN	4.55E-07
NM_002090	CXCL3	2.7	DOWN	2.25E-05
BC015711	SPSB1	2.7	DOWN	3.38E-07
AL389943	OSBPL10	2.7	DOWN	4.88E-05
NM_021732	AVPI1	2.7	DOWN	3.45E-05
BC014523	Q7Z6M3_HUMAN	2.7	DOWN	8.25E-05
AB024574	GTPBP2	2.7	DOWN	1.80E-05
NM_001695	ATP6V1C1	2.7	DOWN	3.09E-06
AF121255	EIF2C2	2.7	DOWN	4.50E-05
NM_016947	G8_HUMAN	2.7	DOWN	1.15E-06
NM_000942	PPIB	2.7	DOWN	2.73E-04
NM_032873	STS1_HUMAN	2.7	DOWN	5.66E-05
NM_002022	FMO4	2.7	DOWN	2.04E-07
NM_002659	PLAUR	2.7	DOWN	5.49E-05
AK056836	C22:IL17RA	2.7	DOWN	6.28E-06
NM_020645	NRIP3	2.7	DOWN	1.02E-05
NM_025000	C2orf37	2.7	DOWN	7.16E-06
NM_006509	RELB	2.7	DOWN	6.33E-04
NM_024123	LY6G6E	2.6	DOWN	9.09E-07
NM_032258	TBCD3_HUMAN	2.6	DOWN	1.03E-04
NM_018234	STEAP3	2.6	DOWN	5.17E-05
NM_012296	GAB2	2.6	DOWN	2.26E-04
NM_032325	NP_115701.2	2.6	DOWN	1.62E-06
BC011763	TRIM4	2.6	DOWN	7.98E-06
BC017253	U31	2.6	DOWN	1.27E-04
NM_021106	RGS3	2.6	DOWN	2.05E-07
AB033112	BRPF3	2.6	DOWN	7.35E-07
AK026142	GATAD1	2.6	DOWN	6.79E-04
NM_001550	IFRD1	2.6	DOWN	1.10E-06
NM_006043	HS3ST2	2.6	DOWN	8.05E-05
BC013372	DEDD2	2.6	DOWN	1.45E-05
AK024941	DNAJC3	2.6	DOWN	1.51E-05
NM_006663	PPP1R13L	2.6	DOWN	4.69E-05
NM_001728	BSG	2.6	DOWN	3.01E-05
NM_017784	OSBPL10	2.6	DOWN	3.92E-06
AB033029	JGI:USP31	2.6	DOWN	8.95E-06
BC010616	WBP2	2.6	DOWN	4.81E-06
AL110126	NFIB	2.6	DOWN	6.94E-04
BC010990	ZNF598	2.6	DOWN	2.68E-05
AB051479	VEPH1	2.6	DOWN	3.68E-06
NM_052868	IGSF8	2.6	DOWN	4.61E-05
NM_014167	CCDC59	2.6	DOWN	1.14E-05
NM_013417	IARS	2.6	DOWN	8.63E-05
AK025100	SNTB1	2.6	DOWN	5.93E-04
NM_003904	ZNF259	2.6	DOWN	3.63E-06
NM_001751	CARS	2.6	DOWN	1.66E-05
AK024653	BCM:bcm2075	2.6	DOWN	5.56E-04
NM_004272	HOMER1	2.6	DOWN	1.46E-05
NM_000849	GSTM3	2.5	DOWN	8.99E-06
NM_015513	CRELD1	2.5	DOWN	8.00E-05
NM_006756	TCEA1_HUMAN	2.5	DOWN	4.61E-06
NM_016594	FKBP11	2.5	DOWN	5.32E-05
AB046769	Q9H0M3_HUMAN	2.5	DOWN	1.54E-05
NM_000201	ICAM1	2.5	DOWN	2.17E-04
NM_001516	GTF2H3	2.5	DOWN	3.63E-06
NM_000904	NQO2	2.5	DOWN	1.85E-07
BC014527	FBXO27	2.5	DOWN	1.52E-05

NM_004337	OSGIN2	2.5	DOWN	1.62E-06
NM_003414	ZNF267	2.5	DOWN	1.11E-04
NM_004990	MARS	2.5	DOWN	7.96E-05
NM_018556	SIRPG	2.5	DOWN	9.35E-07
AB058702	POU2F1	2.5	DOWN	2.22E-05
BC009558	TMEM58	2.5	DOWN	2.58E-07
NM_006287	TFPI	2.5	DOWN	3.64E-04
AK055484	STXBP5	2.5	DOWN	2.99E-05
NM_002314	LIMK1	2.5	DOWN	1.06E-06
BC013592	DDIT4L	2.5	DOWN	8.63E-04
NM_000676	ADORA2B	2.5	DOWN	8.49E-06
NM_003367	USF2	2.5	DOWN	8.17E-05
BC016556	TMED5	2.5	DOWN	2.32E-05
AF000560	ZNF787	2.4	DOWN	3.76E-06
NM_006513	SARS	2.4	DOWN	4.03E-06
NM_002342	LTBR	2.4	DOWN	1.39E-04
NM_022780	RMND5A	2.4	DOWN	3.17E-06
NM_012124	CHORDC1	2.4	DOWN	6.35E-07
BC010112	HSPD1	2.4	DOWN	1.45E-05
AF161383	C6orf129	2.4	DOWN	8.63E-05
NM_019044	CCDC93	2.4	DOWN	7.98E-06
NM_003580	NSMAF	2.4	DOWN	8.99E-05
NM_002561	P2RX5	2.4	DOWN	1.63E-04
AL117608	FGFR1OP2	2.4	DOWN	1.61E-05
NM_023076	C16orf28	2.4	DOWN	3.41E-05
NM_003764	STX11	2.4	DOWN	1.93E-05
NM_019037	EXOSC4	2.4	DOWN	1.67E-05
NM_003576	STK24	2.4	DOWN	1.73E-05
AY044164	ALPK1	2.4	DOWN	6.56E-06
NM_004987	LIMS1	2.4	DOWN	3.97E-04
NM_003680	YARS	2.4	DOWN	3.13E-06
NM_032717	NP_116106.2	2.4	DOWN	2.64E-06
NM_000558	HBA_HUMAN	2.4	DOWN	5.06E-05
NM_024525	TTC13	2.4	DOWN	7.60E-05
NM_014278	HSPA4L	2.4	DOWN	2.13E-04
NM_003875	GMPS	2.4	DOWN	2.69E-04
NM_012463	ATP6V0A2	2.4	DOWN	1.32E-04
NM_002268	KPNA4	2.4	DOWN	2.64E-06
NM_032384	Q9H5Q3_HUMAN	2.4	DOWN	1.61E-05
NM_022448	Q96E37_HUMAN	2.4	DOWN	2.22E-06
AK055774	PAQR3	2.4	DOWN	2.67E-04
NM_006558	KHDRBS3	2.4	DOWN	6.45E-05
AF121858	SNX8	2.4	DOWN	6.44E-06
NM_000433	NCF2	2.4	DOWN	2.76E-04
NM_002056	GFPT1	2.4	DOWN	9.07E-05
NM_006755	TALDO1	2.4	DOWN	4.82E-04
NM_005283	XCR1	2.4	DOWN	1.07E-04
BC007429	STX3	2.4	DOWN	2.15E-05
U82319	C6orf68	2.3	DOWN	8.00E-05
NM_002105	H2AFX	2.3	DOWN	2.12E-04
NM_022117	TSPYL2	2.3	DOWN	9.52E-05
AK025651	C1orf121	2.3	DOWN	5.92E-04
NM_004623	TTC4	2.3	DOWN	6.40E-06
NM_021194	SLC30A1	2.3	DOWN	4.44E-04
NM_004447	EPS8	2.3	DOWN	1.31E-04
BE884686	LTB4DH	2.3	DOWN	1.17E-05
BC000320	SH3BP1	2.3	DOWN	5.79E-05
NM_018440	PAG1	2.3	DOWN	2.58E-05
AF308297	PPP1R14C	2.3	DOWN	1.75E-04
NM_005426	TP53BP2	2.3	DOWN	4.77E-06
NM_002019	FLT1	2.3	DOWN	2.12E-05
AK025306	CLK1	2.3	DOWN	1.24E-04

AL137438	EXOC6	2.3	DOWN	5.97E-05
NM_018361	AGPAT5	2.3	DOWN	1.46E-05
NM_000713	BLVRB	2.3	DOWN	7.11E-04
AL050005	EIF1	2.3	DOWN	8.58E-06
NM_003806	HRK	2.3	DOWN	7.70E-05
NM_006931	SLC2A3	2.3	DOWN	3.40E-06
NM_014778	NUPL1	2.3	DOWN	6.25E-04
NM_032340	C6orf125	2.3	DOWN	1.88E-06
NM_007245	ATXN2L	2.3	DOWN	5.93E-04
NM_004613	TGM2	2.3	DOWN	5.67E-04
AK025661	LIMS1	2.3	DOWN	1.37E-05
BC009493	DOLPP1	2.3	DOWN	4.03E-06
NM_006693	CPSF4	2.3	DOWN	3.98E-05
NM_032712	C19orf48	2.3	DOWN	6.04E-04
NM_024303	ZSCAN5	2.3	DOWN	8.54E-04
AF395440	Q96RF1_HUMAN	2.3	DOWN	1.01E-04
NM_005887	DLEU1	2.3	DOWN	1.27E-05
NM_002486	NCBP1	2.3	DOWN	3.70E-04
NM_017983	WIPI1	2.3	DOWN	2.79E-05
NM_000935	PLOD2	2.3	DOWN	1.13E-04
NM_001539	DNAJA1	2.3	DOWN	7.98E-06
BC017085	SERINC2	2.3	DOWN	8.32E-05
AK023635	BCM:bcm2077	2.3	DOWN	3.35E-04
NM_016274	PLEKHO1	2.3	DOWN	2.20E-04
NM_004824	CDYL	2.3	DOWN	6.20E-05
NM_024640	YRDC	2.3	DOWN	2.24E-05
NM_003033	ST3GAL1	2.3	DOWN	5.77E-04
NM_014068	PSORS1C1	2.3	DOWN	5.96E-05
NM_017909	C6orf96	2.3	DOWN	8.82E-05
NM_024052	C17orf39	2.2	DOWN	9.01E-06
NM_006186	NR4A2	2.2	DOWN	1.77E-05
NM_005689	ABCB6	2.2	DOWN	1.47E-04
NM_003183	ADAM17	2.2	DOWN	1.07E-05
NM_002448	MSX1	2.2	DOWN	7.96E-05
NM_020122	KCMF1	2.2	DOWN	3.18E-06
NM_014851	KLHL21	2.2	DOWN	3.10E-05
NM_003244	TGIF	2.2	DOWN	2.73E-04
AK055902	KIAA1324L	2.2	DOWN	2.00E-04
AK026295	SERINC5	2.2	DOWN	2.54E-05
NM_000916	OXTR	2.2	DOWN	5.16E-04
NM_002467	MYC	2.2	DOWN	6.03E-04
D26067	TMEM41B	2.2	DOWN	1.33E-05
NM_023935	CT116_HUMAN	2.2	DOWN	2.03E-04
NM_016545	IER5	2.2	DOWN	6.26E-05
NM_032270	LRRC8C	2.2	DOWN	1.21E-04
NM_004414	DSCR1	2.2	DOWN	1.25E-04
AL050151	NA	2.2	DOWN	4.73E-05
NM_021013	KRT34	2.2	DOWN	7.92E-05
AB023142	CORO2B	2.2	DOWN	6.60E-04
NM_018162	NAV2	2.2	DOWN	6.62E-04
NM_000638	VTN	2.2	DOWN	2.14E-04
NM_004584	RAD9A	2.2	DOWN	4.67E-04
NM_004087	DLG1	2.2	DOWN	8.62E-04
NM_018214	LRRC1	2.2	DOWN	8.92E-06
NM_018840	CT024_HUMAN	2.2	DOWN	2.91E-05
NM_016639	TNFRSF12A	2.2	DOWN	2.30E-05
NM_002157	HSPE1	2.2	DOWN	1.52E-05
NM_006410	HTATIP2	2.2	DOWN	8.71E-04
NM_005415	SLC20A1	2.2	DOWN	4.07E-05
NM_002846	PTPRN	2.2	DOWN	8.88E-04
AK022745	NA	2.2	DOWN	3.47E-05
NM_014951	ZNF365	2.2	DOWN	8.00E-05

NM_016034	MRPS2	2.2	DOWN	6.87E-05
BC007644	YIF1B	2.2	DOWN	7.59E-04
AB007923	PDE4DIP	2.2	DOWN	3.80E-05
U92285	GABRE	2.2	DOWN	2.67E-04
NM_001064	TKT	2.2	DOWN	7.57E-05
NM_004405	DLX2	2.2	DOWN	1.07E-04
NM_006278	ST3GAL4	2.2	DOWN	1.42E-06
NM_001909	CTSD	2.2	DOWN	8.85E-06
NM_007314	ABL2	2.2	DOWN	2.03E-05
AK026436	ARRDC4	2.2	DOWN	5.14E-04
NM_005228	EGFR	2.2	DOWN	8.99E-05
AB032972	NA	2.2	DOWN	2.77E-04
NM_005627	SGK	2.2	DOWN	5.98E-04
AL137488	C12orf29	2.1	DOWN	3.56E-04
NM_005176	ATP5G2	2.1	DOWN	9.21E-04
BC008580	GDNF	2.1	DOWN	5.05E-05
Z46376	HK2	2.1	DOWN	2.42E-04
NM_005194	CEBPB	2.1	DOWN	1.61E-05
NM_022102	NP_001026883.1	2.1	DOWN	3.60E-04
NM_024945	RMI1	2.1	DOWN	1.61E-05
AK026217	TTC17	2.1	DOWN	1.83E-05
NM_016227	C1orf9	2.1	DOWN	7.05E-04
NM_030759	NRBF2	2.1	DOWN	1.32E-05
AK057591	DGKE	2.1	DOWN	7.21E-05
AL136770	CLDN12	2.1	DOWN	2.28E-04
NM_014423	AFF4	2.1	DOWN	8.29E-05
NM_032331	ECE2	2.1	DOWN	5.97E-04
NM_003155	STC1	2.1	DOWN	1.64E-04
AB011164	NP_001005751.1	2.1	DOWN	1.04E-06
NM_006042	HS3ST3A1	2.1	DOWN	2.39E-04
NM_002507	NGFR	2.1	DOWN	8.02E-05
NM_000735	CGA	2.1	DOWN	4.14E-04
NM_004388	CTBS	2.1	DOWN	1.31E-04
NM_004563	PCK2	2.1	DOWN	9.58E-04
BC017117	CREM	2.1	DOWN	7.98E-06
NM_024039	MIS12	2.1	DOWN	6.19E-07
AK022547	PARP6	2.1	DOWN	7.36E-05
NM_021226	ARHGAP22	2.1	DOWN	7.82E-04
NM_013326	C18orf8	2.1	DOWN	3.33E-04
NM_024937	LRP12	2.1	DOWN	3.04E-04
NM_018231	NP_060701.1	2.1	DOWN	2.30E-05
NM_001294	CLPTM1	2.1	DOWN	2.94E-04
NM_002423	MMP7	2.1	DOWN	6.74E-04
NM_000903	NQO1	2.1	DOWN	8.93E-05
NM_025128	MUS81	2.1	DOWN	8.53E-05
NM_014725	STARD8	2.1	DOWN	1.75E-04
NM_005706	TSSC4	2.1	DOWN	1.75E-04
BC012469	YIPF6	2.1	DOWN	3.59E-05
NM_004717	DGKI	2.1	DOWN	7.25E-04
NM_012099	CD3EAP	2.1	DOWN	4.90E-06
AL021327	RP1-124O9.1	2.1	DOWN	9.02E-06
AF161415	SELK_HUMAN	2.1	DOWN	7.26E-06
NM_003301	TRHR	2.1	DOWN	6.08E-04
AF151867	TICAM2	2.1	DOWN	1.01E-05
AK023623	GLDN	2.1	DOWN	4.44E-04
NM_013379	DPP7	2.1	DOWN	2.77E-04
NM_005681	TAF1A	2.0	DOWN	6.39E-04
NM_005336	HDLBP	2.0	DOWN	9.52E-04
NM_006207	PDGFRL	2.0	DOWN	8.88E-04
AK055649	ERICH1	2.0	DOWN	4.53E-05
NM_019025	SMOX	2.0	DOWN	4.16E-05
AF062733	IGSF4B	2.0	DOWN	1.33E-04

M12679	HLA-C	2.0	DOWN	2.21E-04
NM_022758	C6orf106	2.0	DOWN	8.29E-04
NM_024686	TTLL7	2.0	DOWN	3.65E-05
NM_015449	C1orf43	2.0	DOWN	4.95E-04
NM_005738	ARL4A	2.0	DOWN	1.85E-04
BC010612	Q96FP1_HUMAN	2.0	DOWN	4.73E-04
NM_002249	KCNN3	2.0	DOWN	1.03E-04
NM_007355	HSP90AB1	2.0	DOWN	1.56E-04
NM_005923	MAP3K5	2.0	DOWN	1.73E-05
NM_012111	AHSA1	2.0	DOWN	1.48E-04
M75883	SCP2	2.0	UP	2.27E-04
NM_057161	KLHDC3	2.0	UP	5.54E-05
AK001731	C12orf23	2.0	UP	1.51E-05
NM_018007	FBXO4	2.0	UP	1.22E-04
AL049949	C10orf56	2.0	UP	4.53E-04
AB020689	TBC1D9	2.0	UP	2.56E-04
NM_024833	ZNF671	2.0	UP	9.53E-04
NM_015559	SETBP1	2.0	UP	2.61E-05
AK021851	NA	2.0	UP	5.77E-04
NM_000235	LIPA	2.0	UP	4.31E-04
AB007855	ZHX3	2.0	UP	8.63E-05
NM_017458	MVP	2.0	UP	8.86E-05
NM_000947	PRIM2A	2.0	UP	5.98E-05
AK021807	LRP11	2.0	UP	4.34E-04
NM_005327	HADH	2.0	UP	4.62E-05
AK056552	ZNF528	2.0	UP	3.21E-04
NM_023037	FRY	2.0	UP	7.01E-05
D25304	ARHGEF6	2.0	UP	7.88E-04
NM_000110	DPYD	2.0	UP	1.39E-06
AB033056	PPFIBP1	2.0	UP	7.36E-04
NM_002129	HMGB2	2.0	UP	5.41E-04
AK057365	TLOC1	2.1	UP	7.63E-05
BC013153	LOXL4	2.1	UP	6.22E-04
AK001553	AK3	2.1	UP	3.60E-04
NM_018719	CDCA7L	2.1	UP	3.01E-05
NM_014928	OTUD4	2.1	UP	1.27E-04
AK055981	NA	2.1	UP	2.77E-04
AK058159	DHRS1	2.1	UP	3.97E-04
NM_012446	SSBP2	2.1	UP	3.96E-05
AB007916	SLC35E2	2.1	UP	1.75E-04
NM_014055	IFT81	2.1	UP	1.11E-04
NM_018222	PARVA	2.1	UP	7.67E-04
AL080186	C6orf111	2.1	UP	9.00E-05
AK056245	ZMAT3	2.1	UP	7.37E-04
AJ420416	GCNT1	2.1	UP	3.04E-04
NM_022918	TMEM135	2.1	UP	3.09E-04
NM_001635	AMPH	2.1	UP	3.13E-04
BC014890	SNAI2	2.1	UP	5.93E-04
AJ420488	EEF1A1	2.1	UP	8.56E-05
D50683	TGFBR2	2.1	UP	8.75E-04
NM_006275	SFRS6	2.1	UP	1.09E-04
NM_014799	HEPH	2.1	UP	3.79E-04
AF010236	SGCD	2.1	UP	5.51E-04
AL049471	ARID5B	2.1	UP	9.91E-06
AK001478	RHOU	2.1	UP	4.50E-05
NM_022470	ZMAT3	2.1	UP	2.67E-04
D42043	RFTN1	2.1	UP	6.48E-05
NM_018486	HDAC8	2.1	UP	2.67E-04
AB007960	SH3GLB1	2.1	UP	6.82E-05
NM_000093	COL5A1	2.1	UP	8.44E-06
AB020671	MRIP_HUMAN	2.1	UP	7.02E-04
NM_021210	TRAPPC1	2.1	UP	1.97E-04

NM_024582	FAT4	2.1	UP	4.90E-05
NM_024062	VANGL1	2.1	UP	3.60E-04
NM_004765	BCL7C	2.1	UP	1.37E-04
NM_000107	DDB2	2.1	UP	1.90E-05
NM_018355	ZNF415	2.1	UP	7.57E-04
NM_002655	PLAG1	2.1	UP	2.42E-04
AL136680	GBP3	2.1	UP	8.99E-05
NM_006645	STARD10	2.1	UP	1.43E-04
AK026717	SEPW1	2.1	UP	4.12E-04
NM_005512	LRRC32	2.1	UP	7.81E-04
NM_018649	H2AFY2	2.1	UP	1.25E-04
NM_000430	PAFAH1B1	2.1	UP	9.67E-04
NM_016201	AMOTL2	2.1	UP	1.81E-05
AB040929	CNTN3	2.1	UP	3.85E-04
X62048	WEE1	2.2	UP	6.91E-05
NM_020215	C14orf132	2.2	UP	1.52E-05
AB037775	KLHL9	2.2	UP	6.56E-05
NM_006074	TRIM22	2.2	UP	3.62E-04
NM_004776	B4GALT5	2.2	UP	4.09E-04
AB020710	EHBP1	2.2	UP	8.86E-05
NM_025149	NP_079425.2	2.2	UP	9.59E-04
NM_019035	PCDH18	2.2	UP	2.67E-04
AL117621	ARF6	2.2	UP	5.06E-04
NM_001114	ADCY7	2.2	UP	4.50E-04
AF131851	FAM19A5	2.2	UP	4.67E-06
AY039760	ATP6V1G3	2.2	UP	7.30E-04
NM_005766	FARP1	2.2	UP	4.46E-04
NM_006111	ACAA2	2.2	UP	1.67E-06
NM_014621	NA	2.2	UP	5.98E-04
NM_001330	CTF1	2.2	UP	2.15E-04
AK056473	FAM33A	2.2	UP	4.89E-04
NM_005637	SS18	2.2	UP	9.90E-04
AK057180	C16orf45	2.2	UP	1.13E-04
NM_005584	MAB21L1	2.2	UP	8.40E-04
NM_022173	TIA1	2.2	UP	4.14E-04
AK026666	NP_001026897.1	2.2	UP	1.26E-04
BC008377	EPB41L3	2.2	UP	1.58E-04
NM_032305	POLR3GL	2.2	UP	7.35E-05
AK026977	MYH10	2.2	UP	2.34E-05
NM_024830	AYTL2	2.2	UP	5.33E-06
NM_014362	HIBCH	2.2	UP	6.38E-06
NM_005578	BCM:LPP	2.2	UP	7.91E-04
AB051491	KIAA1704	2.2	UP	4.91E-04
AB037796	PDCD6IP	2.2	UP	1.34E-05
NM_000077	CDKN2A	2.2	UP	9.76E-04
NM_014970	KIFAP3	2.2	UP	4.74E-06
NM_006226	PLCL1	2.2	UP	7.44E-04
AB051515	TANC1	2.2	UP	2.21E-05
AL157488	NA	2.2	UP	6.28E-04
BC013920	NP_997259.1	2.2	UP	4.02E-05
NM_005566	LDHA	2.2	UP	2.81E-04
NM_005573	LMNB1	2.2	UP	1.38E-05
AL110152	CD109	2.2	UP	7.66E-04
NM_001182	ALDH7A1	2.2	UP	3.14E-04
AB014540	SWP70_HUMAN	2.2	UP	1.82E-04
NM_005891	ACAT2	2.3	UP	6.70E-04
NM_014965	TRAK1	2.3	UP	4.28E-04
NM_001904	CTNNB1	2.3	UP	2.54E-05
NM_005630	SLCO2A1	2.3	UP	2.43E-04
BC006428	CXXC5	2.3	UP	2.66E-06
AL049331	NME7	2.3	UP	3.04E-04
AF161403	CLEC14A	2.3	UP	6.13E-04

NM_005566	LDHA	2.3	UP	1.17E-04
NM_005423	TFF2	2.3	UP	8.58E-04
NM_005566	LDHA	2.3	UP	7.67E-05
AB032261	SCD	2.3	UP	5.98E-04
AB046781	UACA	2.3	UP	1.82E-06
NM_007083	NUDT6	2.3	UP	1.87E-04
AB014589	CSTF2T	2.3	UP	7.50E-05
NM_057174	PEX16	2.3	UP	2.42E-04
D42047	GPD1L	2.3	UP	1.00E-04
AK025703	NP_001001701.1	2.3	UP	1.23E-04
NM_000846	GSTA1	2.3	UP	3.06E-05
AB029018	PDZRN3	2.3	UP	3.02E-05
NM_003634	NIPSNAP1	2.3	UP	7.04E-05
BC013049	MRRF	2.3	UP	2.32E-05
NM_014867	KBTBD11	2.3	UP	7.23E-05
NM_000527	LDLR	2.3	UP	7.84E-05
NM_014456	PDCD4	2.3	UP	9.77E-05
AK027274	MARCKS	2.3	UP	1.03E-05
NM_003278	CLEC3B	2.3	UP	4.45E-04
AK055553	C22:RP3-477H23.1	2.3	UP	3.09E-04
AJ312319	40057	2.3	UP	1.65E-06
NM_006579	EBP	2.3	UP	3.75E-04
NM_003069	SMARCA1	2.3	UP	7.89E-06
NM_000671	ADH5	2.3	UP	4.64E-06
NM_018159	NUDT11	2.4	UP	4.95E-04
NM_017885	HCFC1R1	2.4	UP	8.01E-05
AK057328	NA	2.4	UP	2.21E-04
NM_018422	Q7L3Y3_HUMAN	2.4	UP	3.13E-05
NM_012484	HMMR	2.4	UP	5.56E-04
AL049957	CD59	2.4	UP	5.08E-05
AK025759	NA	2.4	UP	2.74E-04
AK057652	NA	2.4	UP	5.06E-04
NM_012304	FBXL7	2.4	UP	2.42E-06
NM_001548	IFIT1	2.4	UP	4.70E-04
NM_014937	INPP5F	2.4	UP	5.68E-06
NM_006412	AGPAT2	2.4	UP	1.54E-05
AF070617	C5orf21	2.4	UP	1.61E-05
AK058001	DENND3	2.4	UP	4.91E-04
AL137535	C9orf3	2.4	UP	1.45E-04
NM_002775	HTRA1	2.4	UP	1.75E-04
NM_014244	ADAMTS2	2.4	UP	8.27E-06
AL117234	MCF2	2.4	UP	2.24E-04
AB028976	GC:SAMD4A	2.4	UP	2.54E-05
NM_032943	SYTL2	2.4	UP	1.44E-04
NM_005864	EFS	2.5	UP	4.14E-04
AB038653	NA	2.5	UP	1.13E-06
AK056513	NP_653327.1	2.5	UP	7.89E-06
AK055087	C1orf59	2.5	UP	1.62E-06
NM_013258	PYCARD	2.5	UP	1.64E-04
NM_018171	DP13B_HUMAN	2.5	UP	2.72E-04
NM_005418	ST5	2.5	UP	1.82E-05
NM_032601	MCEE	2.5	UP	4.40E-07
BC000268	PSMB2	2.5	UP	8.46E-04
NM_016121	KCTD3	2.5	UP	5.69E-05
NM_006810	PDIA5	2.5	UP	1.85E-05
AL137938	PXK	2.5	UP	2.11E-05
NM_052954	CYYR1	2.5	UP	3.11E-04
AK055466	C7orf41	2.5	UP	5.58E-05
AB011153	PLCB1	2.5	UP	1.58E-04
AB033025	KIAA1199	2.5	UP	9.60E-04
NM_012157	FBXL2	2.5	UP	3.60E-04
AK056791	MUC16	2.5	UP	3.65E-05

NM_005566	LDHA	2.5	UP	1.15E-04
BC000977	ALAD	2.5	UP	3.83E-05
NM_017671	C20orf42	2.5	UP	8.03E-04
NM_003711	PPAP2A	2.5	UP	9.67E-04
AK023762	SPTBN1	2.6	UP	4.21E-06
NM_005566	LDHA	2.6	UP	2.24E-04
AK026140	FAM20C	2.6	UP	1.69E-04
AK024677	ASAHL	2.6	UP	9.76E-04
AK055808	NP_001070148.1	2.6	UP	6.14E-05
BC015050	OIP5	2.6	UP	9.90E-04
AF380356	XG	2.6	UP	7.28E-04
NM_000859	HMGCR	2.6	UP	3.28E-04
NM_005463	HNRPDL	2.6	UP	1.45E-06
NM_005566	LDHA	2.6	UP	4.50E-05
NM_003250	THRA	2.6	UP	2.29E-06
NM_019555	ARHGEF3	2.6	UP	8.91E-04
NM_033115	NP_149106.2	2.6	UP	8.08E-06
AB033060	PDCD6	2.6	UP	2.18E-06
NM_001336	CTSZ	2.6	UP	8.18E-05
NM_004772	C5orf13	2.6	UP	2.44E-05
AB051459	DJBP_HUMAN	2.6	UP	7.52E-06
NM_000393	COL5A2	2.6	UP	3.01E-05
NM_000791	DHFRL1	2.6	UP	1.62E-05
AF019226	NA	2.6	UP	2.85E-05
AK026035	NA	2.6	UP	6.14E-05
AK021980	TCF4	2.6	UP	8.56E-04
AK057477	HYLS1	2.6	UP	2.85E-05
AK055341	DAB1	2.7	UP	3.62E-05
NM_002874	RAD23B	2.7	UP	2.27E-05
AK023464	BCM:bcm899	2.7	UP	5.72E-06
NM_002609	PDGFRB	2.7	UP	4.10E-06
AL162068	NAP1L1	2.7	UP	1.08E-06
BC000039	FAM26B	2.7	UP	1.82E-06
NM_021953	FOXM1	2.7	UP	1.09E-04
NM_001431	EPB41L2	2.7	UP	4.50E-05
NM_000557	GDF5	2.7	UP	8.98E-05
NM_002863	PYGL	2.7	UP	2.51E-05
NM_001387	DPYSL3	2.7	UP	4.53E-05
NM_004881	TP53I3	2.7	UP	5.23E-08
NM_005566	LDHA	2.7	UP	4.21E-05
BC009566	TAF9B	2.7	UP	2.61E-05
AK023607	SASH1	2.7	UP	1.75E-06
NM_000163	GHR	2.7	UP	4.05E-04
NM_005308	GRK5	2.8	UP	1.74E-08
AK025071	SPTBN1	2.8	UP	5.98E-07
NM_014051	TMEM14A	2.8	UP	1.23E-06
NM_022129	MAWBP_HUMAN	2.8	UP	4.97E-05
NM_000900	MGP	2.8	UP	2.87E-05
AK057333	C11orf66	2.8	UP	1.66E-04
NM_007066	PKIG	2.8	UP	6.22E-04
M62895	ANXA2P3	2.8	UP	1.26E-04
AJ245539	GALNT5	2.8	UP	7.86E-07
NM_000147	FUCA1	2.8	UP	1.75E-05
NM_022343	GAPR1_HUMAN	2.8	UP	2.31E-06
NM_005566	LDHA	2.8	UP	8.02E-06
NM_024049	RP11-445H22.3	2.8	UP	9.33E-04
NM_005572	LMNA	2.8	UP	1.33E-05
NM_001788	39326	2.8	UP	5.71E-06
NM_014011	SOCS5	2.8	UP	2.27E-07
NM_005032	PLS3	2.9	UP	7.42E-06
NM_003022	SH3BGRL	2.9	UP	6.86E-07
NM_007222	ZHX1	2.9	UP	1.79E-05

NM_014217	KCNK2	2.9	UP	1.36E-05
BC013939	NA	2.9	UP	4.30E-05
NM_003243	TGFBR3	2.9	UP	2.01E-07
NM_014750	DLG7	2.9	UP	5.17E-05
U61166	ITSN1	2.9	UP	4.23E-07
NM_001889	CRYZ	2.9	UP	6.10E-07
NM_054033	FKBP1B	2.9	UP	1.02E-05
NM_002725	PRELP	2.9	UP	1.94E-04
NM_032800	C1orf198	2.9	UP	1.82E-04
NM_004512	GALT	2.9	UP	1.81E-05
NM_020166	MCCC1	2.9	UP	5.93E-06
AK027351	RHOJ	2.9	UP	2.36E-04
NM_005576	LOXL1	2.9	UP	8.88E-04
NM_004701	CCNB2	3.0	UP	3.60E-04
AK025371	ASAHL	3.0	UP	1.06E-05
NM_002430	NM_002430.2	3.0	UP	2.03E-05
NM_003246	THBS1	3.0	UP	5.19E-07
NM_006307	SRPX	3.0	UP	1.17E-06
AK023999	NA	3.0	UP	5.18E-05
NM_032674	LRRFIP1	3.0	UP	8.04E-06
NM_004663	RAB11A	3.0	UP	2.22E-06
NM_030926	ITM2C	3.0	UP	3.04E-07
AK057721	NA	3.0	UP	1.86E-05
NM_005786	TSHZ1	3.0	UP	1.87E-04
NM_004538	NAP1L3	3.0	UP	6.33E-06
NM_032348	MXRA8	3.0	UP	7.87E-07
NM_004404	37500	3.1	UP	5.66E-06
NM_000253	MTTP	3.1	UP	1.65E-06
NM_052947	ALPK2	3.1	UP	4.83E-06
AB011110	RASA4	3.1	UP	2.54E-07
NM_052932	TMEM123	3.1	UP	8.35E-07
NM_006822	RAB40B	3.1	UP	2.73E-06
AK025953	MYLK	3.1	UP	1.80E-04
NM_015976	SNX7	3.1	UP	4.23E-07
AB037750	SORCS2	3.1	UP	1.52E-05
AB067801	QKI	3.1	UP	4.20E-06
NM_052969	RPL39L	3.1	UP	2.21E-06
NM_004349	RUNX1T1	3.2	UP	3.22E-05
NM_020190	OLFML3	3.2	UP	5.80E-04
NM_005733	KIF20A	3.2	UP	6.34E-04
AK057865	THY1	3.2	UP	1.32E-04
NM_024745	SHCBP1	3.2	UP	2.83E-05
NM_004642	CDK2AP1	3.2	UP	1.21E-07
NM_001998	FBLN2	3.3	UP	4.57E-04
NM_002736	PRKAR2B	3.3	UP	1.65E-07
NM_012413	QPCT	3.3	UP	8.02E-06
NM_001512	GSTA4	3.3	UP	2.23E-07
NM_016240	SCARA3	3.3	UP	4.58E-06
NM_004480	FUT8	3.4	UP	4.02E-06
AK024475	PLEKHG4	3.4	UP	1.60E-07
AF043897	hsa-mir-23b	3.4	UP	4.49E-07
NM_003070	SMARCA2	3.4	UP	3.18E-06
AK026784	ITGBL1	3.4	UP	8.35E-05
AL136842	CDC42EP3	3.4	UP	3.59E-05
NM_005195	Q504X4_HUMAN	3.4	UP	6.59E-04
NM_001150	ANPEP	3.4	UP	5.96E-05
BC012625	PPP1R3C	3.5	UP	4.58E-08
NM_001864	COX7A1	3.5	UP	8.28E-06
AK057501	CMTM2	3.5	UP	1.60E-06
BC015134	THBS1	3.5	UP	1.14E-07
NM_000177	GSN	3.5	UP	7.89E-07
M62896	NA	3.5	UP	1.17E-05

NM_006986	MAGED1	3.5	UP	1.01E-08
NM_001067	P11388-3	3.5	UP	8.01E-05
AK021982	DYM	3.5	UP	2.38E-07
NM_002380	MATN2	3.5	UP	1.21E-05
AL137734	NA	3.5	UP	9.09E-05
AK025909	EFNA5	3.6	UP	5.99E-04
NM_001822	CHN1	3.6	UP	2.95E-07
AK027276	ATXN7L4	3.6	UP	3.74E-04
NM_019105	P22105-2	3.6	UP	2.82E-05
NM_030786	SYNC1	3.6	UP	2.02E-08
NM_031302	GLT8D2	3.7	UP	3.05E-09
BC013971	HOXA10	3.7	UP	2.51E-07
NM_000961	PTGIS	3.7	UP	9.22E-04
NM_020404	CD248	3.7	UP	9.70E-09
NM_001312	CRIP2	3.8	UP	9.99E-06
NM_021730	Q96AM0_HUMAN	3.8	UP	8.55E-09
NM_024812	BAALC	3.9	UP	7.52E-07
NM_001449	FHL1	3.9	UP	2.24E-04
AB046796	K1576_HUMAN	3.9	UP	1.27E-04
NM_002527	NTF3	4.0	UP	3.36E-07
NM_032048	EMILIN2	4.0	UP	1.06E-06
NM_001311	CRIP1	4.0	UP	2.59E-05
NM_032623	NP_116012.2	4.0	UP	3.51E-04
AF444143	SPG3A	4.0	UP	7.23E-05
NM_000165	GJA1	4.1	UP	8.20E-04
AK022997	BCM:bcm4083	4.1	UP	2.34E-07
AL359558	MCC	4.2	UP	5.23E-08
AK000776	ROR1	4.2	UP	7.60E-05
NM_007286	SYNPO	4.3	UP	5.81E-07
AL050137	OLFML2B	4.3	UP	1.22E-09
NM_001920	DCN	4.3	UP	9.24E-06
NM_016824	ADD3	4.4	UP	9.32E-08
NM_005491	CXorf6	4.4	UP	1.06E-09
NM_005704	PTPRU	4.5	UP	2.53E-04
NM_004098	EMX2	4.6	UP	5.04E-08
NM_014762	DHCR24	4.6	UP	6.59E-05
AB002365	KIAA0367	4.7	UP	4.55E-07
NM_001129	AEBP1	4.7	UP	5.32E-04
NM_003783	B3GALT2	4.8	UP	4.56E-04
AF156100	HMCN1	4.8	UP	3.36E-07
AK055710	EBF3	4.8	UP	2.85E-05
NM_003247	THBS2	4.8	UP	5.36E-05
NM_006206	PDGFRA	4.9	UP	2.38E-08
NM_002160	TNC	4.9	UP	4.91E-06
U97105	DPYSL2	5.0	UP	5.09E-09
NM_002048	GAS1	5.0	UP	2.40E-06
NM_000090	COL3A1	5.1	UP	2.43E-07
NM_030965	ST6GALNAC5	5.2	UP	2.70E-06
NM_052880	NP_443112.2	5.2	UP	4.06E-06
NM_021637	TMEM35	5.2	UP	8.63E-04
NM_006308	HSPB3	5.5	UP	8.84E-06
NM_002966	S100A10	5.6	UP	2.68E-06
NM_002961	S100A4	5.7	UP	1.19E-05
AK025346	NA	5.8	UP	2.59E-06
AK026424	GNG2	6.3	UP	3.01E-05
NM_002276	KRT19	6.4	UP	4.69E-06
NM_016206	BCM:NM_016206	6.5	UP	5.82E-08
NM_021111	RECK	6.6	UP	5.60E-08
NM_001753	CAV1	6.9	UP	4.01E-07
AK022198	GALNT5	6.9	UP	1.84E-07
NM_000095	COMP	7.4	UP	2.30E-05
AL137578	CTA-109P11.3	8.3	UP	4.23E-07

AF216077	TNFRSF19	8.4	UP	5.75E-07
AF245505	MXRA5	8.9	UP	1.14E-07
NM_002982	CCL2	9.4	UP	1.68E-09
NM_016557	NA	10.5	UP	2.89E-07
NM_000088	COL1A1	10.8	UP	5.23E-08
AK021484	SYNPO2	11.5	UP	2.70E-06
NM_000681	ADRA2A	12.7	UP	1.43E-08
NM_000089	COL1A2	13.6	UP	1.03E-10
AB067499	Q96PX6_HUMAN	13.9	UP	3.13E-06
AB032953	ODZ2	14.0	UP	2.14E-11

Supplementary table S3: Significantly differentially expressed genes for the 97 versus 70 comparison

Genbank accession No.	Gene symbol	Fold-change	Direction	p-value
NM_002727	PRG1	23.4	DOWN	5.23E-10
NM_020169	LXN	8.9	DOWN	1.76E-08
NM_001562	IL18	8.0	DOWN	8.12E-07
BC012486	KRA24_HUMAN	7.2	DOWN	3.16E-05
NM_000600	IL6	6.0	DOWN	5.53E-08
NM_017723	NP_060193.2	5.3	DOWN	5.90E-04
NM_001175	ARHGDIB	5.2	DOWN	1.21E-05
AL137678	C20orf50	4.9	DOWN	7.24E-07
AF213459	EPHA3	4.7	DOWN	9.99E-06
NM_000799	EPO	4.5	DOWN	2.65E-05
AC004010	AMIGO2	4.5	DOWN	1.49E-05
NM_002837	PTPRB	4.5	DOWN	8.45E-06
AK055249	UCHL1	4.5	DOWN	2.62E-08
NM_018421	TBC1D2	4.5	DOWN	2.14E-05
NM_001321	CSRP2	4.4	DOWN	6.68E-04
AK021874	TGFB2	4.4	DOWN	7.33E-08
AB029000	SULF1	4.3	DOWN	4.45E-05
NM_004181	UCHL1	4.3	DOWN	7.87E-08
NM_004669	CLIC3	4.1	DOWN	1.32E-04
AB032947	CADPS	4.0	DOWN	2.13E-07
NM_001845	COL4A1	3.6	DOWN	3.45E-05
NM_012082	ZFPM2	3.6	DOWN	5.98E-04
NM_004335	BST2	3.3	DOWN	5.44E-04
NM_005070	SLC4A3	3.3	DOWN	4.35E-05
AK021486	BMP5	3.2	DOWN	4.35E-05
AF111170	NUDT14	3.2	DOWN	5.65E-06
NM_003280	TNNC1	3.1	DOWN	6.95E-05
L10374	Q5W0J2_HUMAN	3.1	DOWN	1.04E-05
NM_004010	DMD	3.1	DOWN	3.13E-04
NM_004862	LITAF	3.0	DOWN	4.07E-04
NM_031438	NUDT12	3.0	DOWN	2.91E-04
NM_033642	FGF13	3.0	DOWN	8.19E-04
NM_001553	IGFBP7	3.0	DOWN	1.06E-04
NM_000120	EPHX1	2.9	DOWN	1.54E-08
NM_031289	GSG1	2.9	DOWN	7.42E-04
NM_002561	P2RX5	2.8	DOWN	3.56E-05
NM_000804	FOLR3	2.8	DOWN	3.85E-05
NM_023927	GRAMD3	2.8	DOWN	4.89E-05
NM_014578	RHOD	2.7	DOWN	3.01E-05
AK055506	VGCNL1	2.7	DOWN	1.74E-05
NM_020038	ABCC3	2.7	DOWN	6.63E-04
U60873	NA	2.7	DOWN	2.40E-04
NM_032603	LOXL3	2.7	DOWN	1.47E-05
NM_012099	CD3EAP	2.6	DOWN	2.22E-07
NM_018214	LRRC1	2.6	DOWN	1.28E-06
NM_014068	PSORS1C1	2.6	DOWN	1.39E-05
AF161383	C6orf129	2.6	DOWN	4.39E-05
NM_014900	COBLL1	2.6	DOWN	5.51E-04
NM_022842	CDCP1	2.6	DOWN	8.63E-04
NM_023935	CT116_HUMAN	2.5	DOWN	4.24E-05
NM_021938	BRUNOL5	2.5	DOWN	5.22E-04
NM_004047	ATP6V0B	2.5	DOWN	4.51E-05
AK056831	ANR52_HUMAN	2.5	DOWN	8.12E-07
NM_014951	ZNF365	2.5	DOWN	1.88E-05
BC017996	Q8WVI0_HUMAN	2.5	DOWN	5.02E-06
AK026761	NA	2.4	DOWN	8.96E-05
AB037823	CHGUT_HUMAN	2.4	DOWN	2.01E-04
NM_004992	MECP2	2.4	DOWN	1.72E-04
NM_002640	SERPINB8	2.4	DOWN	8.13E-06

NM_032514	MAP1LC3A	2.4	DOWN	1.50E-04
NM_005584	MAB21L1	2.4	DOWN	3.40E-04
NM_033448	KRT71	2.4	DOWN	1.72E-04
NM_004409	DMPK	2.3	DOWN	5.29E-06
NM_003214	TEAD3	2.3	DOWN	7.60E-06
AB040883	Q9H994_HUMAN	2.3	DOWN	4.90E-04
AF109681	ITGA11	2.3	DOWN	2.14E-05
NM_016069	TIM16_HUMAN	2.3	DOWN	3.84E-07
NM_003364	UPP1	2.3	DOWN	1.06E-04
NM_030674	SLC38A1	2.3	DOWN	8.14E-04
NM_018281	ECHDC2	2.3	DOWN	1.74E-04
NM_015645	MFRP	2.2	DOWN	1.53E-04
NM_007263	COPE	2.2	DOWN	9.18E-04
BC009849	SDSL	2.2	DOWN	1.84E-05
AF131821	MGLL	2.2	DOWN	5.18E-05
NM_000389	CDKN1A	2.2	DOWN	4.47E-05
NM_032340	C6orf125	2.2	DOWN	5.29E-06
NM_018973	DPM3	2.2	DOWN	4.78E-05
AB040959	DFNB31	2.2	DOWN	2.33E-04
NM_005094	SLC27A4	2.2	DOWN	3.07E-04
BC000737	RGS4	2.2	DOWN	6.86E-04
NM_018556	SIRPG	2.2	DOWN	9.53E-06
AK025627	MIT:HsG2201	2.2	DOWN	9.26E-05
AK056388	UBE2Q1	2.2	DOWN	3.54E-04
NM_017874	CT027_HUMAN	2.1	DOWN	1.50E-04
NM_016732	RALY	2.1	DOWN	9.18E-04
NM_003491	ARD1A	2.1	DOWN	2.64E-05
AL080219	RTCD1	2.1	DOWN	9.74E-05
NM_002314	LIMK1	2.1	DOWN	1.28E-05
BC009493	DOLPP1	2.1	DOWN	1.71E-05
NM_024038	C19orf43	2.1	DOWN	2.48E-04
NM_007100	ATP5I	2.1	DOWN	4.39E-05
NM_002413	MGST2	2.1	DOWN	7.17E-05
NM_021170	HES4	2.1	DOWN	3.03E-04
AL136826	RGMA	2.1	DOWN	5.44E-04
NM_003893	LDB1	2.1	DOWN	2.14E-05
NM_001029	RPS26P10	2.1	DOWN	1.06E-04
NM_021570	BARX1	2.1	DOWN	2.08E-04
NM_006368	CREB3	2.1	DOWN	3.55E-05
NM_002069	GNAI1	2.1	DOWN	3.84E-04
NM_017767	SLC39A4	2.1	DOWN	7.58E-04
NM_003494	DYSF	2.1	DOWN	5.29E-05
NM_003815	ADAM15	2.0	DOWN	1.20E-04
AK026750	GPR20	2.0	DOWN	3.68E-04
NM_003732	EIF4EBP3	2.0	DOWN	4.04E-04
AJ272212	PSKH1	2.0	DOWN	2.30E-05
NM_032350	NP_115726.1	2.0	DOWN	4.14E-04
NM_018438	FBXO6	2.0	DOWN	5.18E-05
NM_031232	APBA2BP	2.0	DOWN	7.20E-05
NM_000964	RARA	2.0	DOWN	3.95E-04
NM_003313	TSTA3	2.0	DOWN	2.83E-04
NM_006284	TAF10	2.0	DOWN	4.24E-05
AB020649	PLEKHM2	2.0	DOWN	8.18E-04
NM_031484	MARVELD1	2.0	DOWN	6.35E-04
NM_001725	BPI	2.0	DOWN	1.06E-04
NM_005032	PLS3	2.0	UP	4.49E-04
NM_033116	NEK9	2.0	UP	9.65E-05
NM_006915	RP2	2.0	UP	2.02E-04
NM_001358	DHX15	2.0	UP	2.21E-04
AK056809	NA	2.0	UP	9.19E-05
AK024475	PLEKHG4	2.0	UP	8.51E-05
D42055	NEDD4	2.0	UP	8.66E-05

NM_006931	SLC2A3	2.0	UP	2.54E-05
NM_003205	TCF12	2.0	UP	4.00E-05
AB018353	UNC84A	2.1	UP	3.92E-04
NM_003692	C9orf30	2.1	UP	4.07E-04
AK023607	SASH1	2.1	UP	7.79E-05
BC017972	SRGAP2P1	2.1	UP	4.50E-05
NM_014799	HEPH	2.1	UP	4.07E-04
AF061733	NP_689482.1	2.1	UP	1.29E-04
AK002085	CCNT1	2.1	UP	5.05E-05
AK022008	NOTCH2	2.1	UP	4.72E-04
NM_032832	LRP11	2.1	UP	7.85E-06
AB058733	TXNDC10	2.1	UP	4.94E-05
NM_005610	RBBP4	2.1	UP	1.20E-04
NM_002822	TWF1	2.1	UP	4.78E-05
NM_007286	SYNPO	2.1	UP	6.10E-04
NM_002736	PRKAR2B	2.1	UP	3.90E-05
AB051551	LRRCC1	2.1	UP	8.92E-04
AK001478	RHOU	2.1	UP	4.33E-05
NM_016121	KCTD3	2.1	UP	3.16E-04
NM_003278	CLEC3B	2.1	UP	9.24E-04
AK024356	SOCS6	2.1	UP	1.10E-05
NM_002430	NM_002430.2	2.2	UP	5.44E-04
AB037748	FAM44A	2.2	UP	7.17E-05
AB046794	FAM29A	2.2	UP	1.29E-04
AL132665	BNIP3L	2.2	UP	7.79E-05
NM_005637	SS18	2.2	UP	9.18E-04
AF156100	HMCN1	2.2	UP	5.71E-04
NM_000179	MSH6	2.2	UP	4.82E-04
NM_004354	CCNG2	2.2	UP	3.82E-05
AB051516	NP_444270.2	2.2	UP	1.29E-05
AL080186	C6orf111	2.2	UP	4.20E-05
AK057180	C16orf45	2.2	UP	9.26E-05
NM_001788	39326	2.2	UP	9.58E-05
NM_000861	HRH1	2.2	UP	2.89E-05
AK056791	MUC16	2.3	UP	1.32E-04
AJ420481	AOF1	2.3	UP	5.19E-04
AK054863	ABI2	2.3	UP	4.39E-05
NM_006346	C13orf24	2.3	UP	8.92E-06
NM_022826	MARCH7	2.3	UP	7.09E-05
NM_006417	IFI44	2.3	UP	1.09E-05
BC000195	METTL9	2.3	UP	2.66E-04
AL136680	GBP3	2.3	UP	3.85E-05
D50926	MORC3	2.3	UP	1.50E-06
NM_022831	NA	2.3	UP	4.90E-04
NM_006264	PTPN13	2.3	UP	6.90E-04
AB040929	CNTN3	2.4	UP	1.19E-04
NM_000956	PTGER2	2.4	UP	7.58E-04
NM_000846	GSTA1	2.4	UP	3.08E-05
NM_005493	RANBP9	2.4	UP	1.32E-04
NM_004098	EMX2	2.4	UP	3.90E-05
AL161952	GLUL	2.4	UP	2.88E-04
NM_001937	DPT	2.4	UP	8.63E-04
AF208850	PTP4A2	2.4	UP	1.19E-04
NM_018422	Q7L3Y3_HUMAN	2.4	UP	2.80E-05
AL137938	PXK	2.4	UP	3.45E-05
AK057721	NA	2.5	UP	1.50E-04
NM_000930	PLAT	2.5	UP	2.79E-04
U83115	AIM1	2.5	UP	3.91E-05
NM_033664	CDH11	2.5	UP	1.34E-05
NM_007150	ZNF185	2.5	UP	9.18E-04
NM_019105	P22105-2	2.5	UP	6.10E-04
AF177377	EML4	2.5	UP	1.85E-05

NM_016824	ADD3	2.6	UP	2.72E-05
BC008377	EPB41L3	2.6	UP	3.19E-05
NM_012413	QPCT	2.6	UP	9.58E-05
NM_024609	NES	2.6	UP	8.37E-04
AK023999	NA	2.6	UP	1.90E-04
BC013592	DDIT4L	2.6	UP	4.07E-04
AF245505	MXRA5	2.6	UP	7.42E-04
NM_003368	USP1	2.6	UP	5.29E-06
NM_004369	COL6A3	2.6	UP	4.14E-04
NM_052954	CYYR1	2.7	UP	1.48E-04
AB033056	PPFIBP1	2.7	UP	3.74E-05
AK021807	LRP11	2.7	UP	1.84E-05
AL049321	NP_060404.3	2.7	UP	6.26E-06
AB020689	TBC1D9	2.7	UP	8.78E-06
NM_032813	TMTC4	2.7	UP	6.78E-05
NM_024642	GALNT12	2.8	UP	2.16E-05
NM_030926	ITM2C	2.8	UP	1.28E-06
NM_007038	ADAMTS5	2.8	UP	4.56E-04
NM_024745	SHCBP1	2.8	UP	9.26E-05
NM_005630	SLCO2A1	2.8	UP	2.33E-05
NM_017515	SLC35F2	2.8	UP	6.05E-04
NM_024633	CN139_HUMAN	2.9	UP	3.90E-08
NM_001067	P11388-3	2.9	UP	3.71E-04
NM_016206	BCM:NM_016206	2.9	UP	4.45E-05
NM_014246	CELSR1	3.0	UP	3.85E-04
NM_006307	SRPX	3.0	UP	1.61E-06
NM_032048	EMILIN2	3.1	UP	1.69E-05
NM_015310	PSD3	3.1	UP	3.85E-05
NM_005864	EFS	3.2	UP	3.67E-05
NM_016557	NA	3.2	UP	5.30E-04
NM_002160	TNC	3.3	UP	1.21E-04
NM_007063	TBC1D8	3.4	UP	1.19E-04
AK000776	ROR1	3.4	UP	3.46E-04
NM_004480	FUT8	3.4	UP	5.29E-06
NM_001920	DCN	3.4	UP	5.97E-05
NM_021738	SVIL	3.5	UP	8.99E-06
NM_006622	PLK2	3.5	UP	5.92E-05
NM_001311	CRIP1	3.5	UP	7.79E-05
NM_024812	BAALC	3.6	UP	2.47E-06
AK000933	CHML	3.6	UP	1.46E-08
AL137578	CTA-109P11.3	3.6	UP	1.18E-04
NM_030965	ST6GALNAC5	3.7	UP	4.39E-05
AK022997	BCM:bcm4083	3.7	UP	8.62E-07
AK025909	EFNA5	3.7	UP	3.87E-04
BC013939	NA	3.8	UP	5.29E-06
NM_016240	SCARA3	3.8	UP	1.97E-06
AB020710	EHBP1	3.9	UP	1.94E-07
NM_001998	FBLN2	3.9	UP	1.14E-04
NM_021111	RECK	3.9	UP	5.06E-06
AK055243	CCBE1	4.0	UP	3.19E-06
NM_006206	PDGFRA	4.1	UP	1.69E-07
NM_020190	OLFML3	4.1	UP	7.65E-05
NM_001831	CLU	4.2	UP	7.60E-06
NM_000609	CXCL12	4.3	UP	6.26E-06
NM_057159	EDG2	4.6	UP	3.90E-09
AK055710	EBF3	5.0	UP	2.95E-05
AF216077	TNFRSF19	5.0	UP	1.88E-05
NM_001753	CAV1	5.3	UP	3.69E-06
AB002365	KIAA0367	6.1	UP	7.87E-08
NM_000627	LTBP1	6.4	UP	4.81E-05
NM_002380	MATN2	6.6	UP	1.27E-07
NM_003243	TGFBR3	6.7	UP	2.61E-10

NM_030781	COLEC12	6.7	UP	5.46E-04
NM_007029	STMN2	7.0	UP	8.99E-05
NM_001769	CD9	7.2	UP	1.96E-09
NM_002852	PTX3	8.4	UP	2.64E-08

CHAPTER 6

General Discussion

Diagnosis of OXPHOS disorders

A genetic diagnosis of oxidative phosphorylation (OXPHOS) disorders is with some exceptions difficult to make because of the clinical and genetic heterogeneity. A single mutation can lead to a variety of clinical symptoms and syndromes, and the same phenotype can also be caused by a number of different mutations. The current genetic diagnostic procedures are often symptom based protocols, in which the clinical, pathological and biochemical manifestations are used to select the genes which are most likely to contain the pathogenic mutation. Leigh syndrome with a cytochrome *c* oxidase (COX) deficiency is an example where these phenotypic characteristics provide an indication of the genotypic defect. Tiranti *et al.* demonstrated that in Leigh syndrome with COX deficiency 75% of the patients had a mutation in the *SURF1* gene, resulting in loss of function of the SURF1 protein [7, 63]. Although another study reported a lower frequency of 26% [64], more Leigh syndrome patients with COX deficiency have been genetically diagnosed with mutations in the *SURF1* gene [6, 176-179], illustrating that Leigh syndrome associated with COX deficiency is a good indication of a genetic defect in the *SURF1* gene. Leber Hereditary Optic Atrophy (LHON) is another example of an OXPHOS disorder with a direct relation between clinical symptoms and genetic defect, since three primary mtDNA mutations have been shown to be present in over 90% of the affected families [180]. When such a direct link between phenotype and genotype does not exist, a number of relatively common mitochondrial DNA (mtDNA) mutations and, dependent on the phenotype, mutations in nuclear genes are usually screened. Unfortunately, this approach is often inconclusive and can be costly and time consuming if multiple genes have to be tested.

Specific approaches have been developed and tested to make the identification of the genetic defects easier. The first distinction is between mutations in the mtDNA or in the nDNA. A clear maternal transmission of the disease will point to an mtDNA mutation and consanguinity or paternal transmission to a nuclear gene defect, but the available information or number of patients is not always sufficient to draw an unambiguous conclusion. Measurement of enzyme activities does not resolve the mutation origin directly, although the knowledge whether or not complex II, which is completely of nuclear origin, is involved, may provide a clue. Complementation studies by fusing patient fibroblast cells with mtDNA-less (ρ^o) cells can provide a definite answer whether the genetic defect lies in the mtDNA or the nDNA. For example, fibroblasts of a patient with a severe mtDNA depletion were enucleated and complemented with a human-derived ρ^o cell line. The hybdrid cells were able to grow on culture medium lacking uridine and pyruvate, indicating that the origin of the mtDNA depletion had to be under the control of the nuclear genome [181]. Tiranti *et al.* identified the chromosome on which the genetic defect resided in Leigh syndrome patients with cytochrome *c* deficiency by chromosome transfer technology [7]. This, in combination with linkage analysis, lead to the identification of mutations in the *SURF1* gene. However, this approach is technically demanding, costly and time consuming

and will only work for patients who have fibroblast cells expressing the OXPHOS deficiency. In case sub chromosomal mapping is not possible by linkage analysis, then this has to be done by complementation analysis using chromosomal fragments. In another preselection method, OXPHOS complex assembly by SDS-PAGE or Blue Native-PAGE immunoblotting is studied. This can provide information about genetic defects in structural genes or genes involved in the assembly of the OXPHOS complexes. OXPHOS disorders characterised by complex I deficiency are one of the fields in which this technique appears to be promising [182, 183]. These studies showed that a specific decrease of intact mitochondrial complex III is indicative for mutations in *NDUFS2* and *NDUFS4*. Mutations in *NDUFS4* appeared to be further related to decreased levels of fully assembled complex I combined with high levels of a defective sub complex not present in controls.

Classification of patients by their gene expression profile is evaluated as an alternative approach. However, this appears to be difficult due to the small number of patients available for classification experiments to find a classification signature. In one study, differences in expression were shown in cell lines with complex I defects as a result of genetic defects in different complex I genes [184], but a specific gene expression signature for complex I defects related to specific mutations was not reported. Despite the numerous methods described above to facilitate the genetic diagnosis of OXPHOS disorders, other approaches to improve and speed up genetic diagnosis must be considered. The development of better mutation screening techniques is a necessary alternative. Furthermore, more knowledge about the molecular pathological processes involved in OXPHOS disorders will be of great value in the genetic diagnosis of OXPHOS disorders.

Because 25% of all paediatric OXPHOS patients is expected to have a mutation in the mtDNA [23] and because the ability to discriminate between mtDNA and nDNA is important for genetic counselling, mutation screening of the entire mtDNA will be an essential step, complementing the methods mentioned above. In Chapter 2, a chip-based resequencing method was tested to resequence the entire mtDNA of patients with OXPHOS disorders. The method appeared to be very robust, delivering an average call rate of 94%, which was comparable to reports from Affymetrix and others [33]. Heteroplasmy levels could be detected in a range from 5 to 50%. Although the call rate was relatively high, it needs to be further improved for a diagnostic setting [185]. Furthermore, the sensitivity of heteroplasmy detection was lower than heteroduplex based methods like denaturing high-performance liquid chromatography (dHPLC). Optimisation of the data analysis procedure and software tools will most likely make it possible to reach detection levels in the same range. For example, we have observed a better performance in signal calling for the reverse strand compared to the forward strand on the MitoChip. It is not clear if this is a characteristic for specific regions in the mtDNA, but the generation of more data will gradually provide more insight into the region specific performance of the MitoChip, which must be considered when optimizing the data analysis. The signals from the forward and reverse strand on the MitoChip should be evaluated separately and should be incorporated in the analysis having

a different weight specific for particular mtDNA regions. Several approaches are currently considered and several companies are working on this [185].

High-throughput sequencing of the complete mtDNA cannot be dealt with without interpretation issues. Many nucleotide variations are being detected, which in most cases are neutral polymorphisms. However, a substantial proportion could be pathogenic nucleotide variations. To evaluate the pathogenic properties of unknown nucleotide variations, calculation of a pathogenicity score as described by Mitchell *et al.* for complex I mutations may help to decide whether a nucleotide variation is likely to be pathogenic [50]. A slightly adapted version of this scoring scheme has been applied to primary pathogenic mutations in the mRNA coding region [186]. A similar scoring scheme exists for mitochondrial tRNA mutations [60]. However, calculation of such scores appears not to be straightforward, because not always all data is available and it remains for a large part circumstantial evidence. Moreover, it should be repeated regularly to cover the new genomic information which is being produced at an extremely rapid pace. This indicates that there is a need for a standardised diagnostic flowchart in which, if possible, all aspects of the scoring mechanism are integrated, including automated database searches as well as easy functional assays. An initiative for the former has already been taken by the MitoCircle project (EU grant, Sixth Framework Program, contr. no. 005260), which started with the development of standardised diagnostic guidelines for OXPHOS disorders and the development of a standardised database, in which phenotypic information together with mtDNA genetic variations, both pathogenic and unclassified variants, is being listed [22]. Further expansion of the database by including complete mtDNA sequences will eventually facilitate genetic diagnosis and improve prognostic predictions. Initial MitoChip screening of 28 patients with OXPHOS disease resulted in the identification of three known pathogenic mutations and four new unclassified variants which were likely to be pathogenic (Chapter 2). Meanwhile, one of the four latter variants has been reported to be the pathogenic mtDNA mutation in a family with a prevalent ocular phenotype [187]. This illustrates that results which might initially seem to be inconclusive have to be followed up and reviewed periodically. Furthermore, this shows that 25% of all paediatric OXPHOS patients can be genetically diagnosed with this technique. At the same time, this technique can be used to exclude mtDNA involvement to a certain level, although the number of unclassified variants (a mean value of three to four per patients) should be taken into account. Additionally, chip-based resequencing could also be valuable for the candidate gene mutation screening approach, for example to screen all known structural genes or assembly factors for (one of the complexes of) the respiratory genes. This is for example being done in a diagnostic setting for Inherited syndromes of intrahepatic cholestasis [188]. Such an approach might be much more favourable for resolving the genetic basis of OXPHOS disorders than any of the genotype-phenotype based approaches.

The development of next-generation sequencers, with faster and cheaper sequencing techniques, like the 454-sequencing system (Roche), the Solexa sequencing system (Illumina) or the SOLID

system (Applied Biosystems), brings this approach even closer. These systems are able to sequence millions of bases per hour and are based on massive parallel single template sequencing. A sequence by synthesis strategy is used in the 454 and Solexa where round by round nucleotides are added which results in a fluorescent signal (Solexa) or a luciferase light emission signal (454) which can be detected and recorded. The 454 sequencing system is able to yield relatively large DNA sequences (250-350 bp) compared to the shorter fragments (<40 bp) with the Solexa system. In both systems, a reference sequence is used to align and compare the sequenced sample fragments to in order to determine nucleotide variations, although the 454 can also be used for *de novo* sequencing. The complexity of the human genome hampers these techniques from being used for high throughput mutation screening. Long-range PCR and an enrichment step of the preferred sequences from the genomic DNA prior to sequencing provide a solution for this problem, e.g. by selecting the exons of interest for resequencing. Recently, the use of microarray based techniques has been reported to enrich genomic target sequences of interest [189-191]. In short, these techniques use probes on a microarray directed against specific genomic targets (e.g. exons). Genomic DNA is fragmented and hybridised to the array, after which the array is washed to remove a-specifically bound targets. Subsequently, the hybridised targets are eluted from the microarray and amplified after which the sample is ready for sequencing. Another publication described the use of a microarray to synthesise target specific oligonucleotide probes. After synthesis, the probes are released from the array to capture the genomic sequences of interest. After capturing, amplification was carried out of the captured targets resulting in a circular product, after which all linear and thus non-target sequences were removed by restriction digestion [192]. Using these techniques, between 6,000 and 200,000 exons could be enriched for subsequent sequencing, bringing the application of these technologies for molecular genetic diagnostics nearby.

A drawback of these techniques is the huge amount of data generated, i.e. images have to be saved and quantified after each sequencing round, which has to be analyzed. Specialised software will be necessary for analysis and a huge storage capacity is needed for data storage. Furthermore, screening thousands of enriched genomic targets will deliver an enormous amount of unknown nucleotide variations, which will make the interpretation about pathogenicity of a variation difficult and which will lead to considerable uncertainty. This will be the trade-off for the increasing number of cases for which an accurate diagnosis can be made. This emphasises again the need to store all nucleotide variations in a central database and a strong need for easy, fast, and cheap functional assays to confirm pathogenicity. Up until now, there are no reports of these techniques being capable of the detection of heteroplasmic nucleotide variations in the mtDNA, although they are being used for ultra-deep sequencing of pathology specimens [193, 194] and detection of heteroplasmic mutations with a low mutation load should be possible. Although the cost per nucleotide has become about 100-fold cheaper compared to traditional sequencing methods [195], the required coverage for reaching a reliable 1% detection level may make this approach too expensive compared to alternatives. Comparing chip-based resequencing with

these massive parallel sequencers, it appears that the chip is more appropriate to rapidly screen many genes for individual cases, whereas massive parallel sequencing is more effective for large number of patients and genes.

As an alternative to large-scale sequencing, simple, cheap and sensitive pre-screening methods may still be considered. A high-throughput method which currently is able to detect heteroplasmic mtDNA mutations at a sensitivity level comparable to dHPLC is the high-resolution melting analysis (Lightscanner Idaho), which is able to analyze 96 samples in about 10 minutes [196-198]. Although this technique is based on heteroduplex analysis, detection of homoplasmic variations is directly possible, probably with lesser sensitivity, or as heteroduplex after annealing to a wild-type reference sample. It has even been reported that homozygous variations with a nearest neighbour thermodynamic symmetry, i.e. the bases adjacent to the SNP are identical on both DNA strands and the SNP consists of an interchange between complementary bases, can be detected by high resolution melting analysis [199]. A second fast method for the detection of mtDNA variations is the mutation surveyor technique. This method is based on restriction enzyme digestion by a specific endonuclease which cleaves double stranded DNA at any mismatch site. Subsequently, products are separated and analyzed by agarose gel electrophoresis. Because mutation detection is based on the identification of differences in size of the digestion products, homoplasmic mutations can not be detected, but heteroplasmic mutations can be detected at mutation loads as low as 3% [200, 201]. In conclusion, the number of samples which will provide the opportunity for automated analysis, the possibilities of improving the data analysis, the costs of the chip itself, and the speed with which other new high throughput sequencing and mutation detection techniques are developed, will determine whether MitoChip resequencing of the mtDNA will prevail to be the preferred method for mtDNA resequencing for the next couple of years. Whether candidate gene screening by chip resequencing will become the preferred method for candidate gene screening will depend on the same factors. However, it is very likely that the solution for the genetic diagnosis of OXPHOS disorders will come from one of these technologies.

Pathophysiology of OXPHOS disorders: patient derived and non-patient derived experimental models for gene expression profiling

Microarray gene expression studies have proven their value in unravelling pathological processes underlying diseases and also in classifying patients groups using gene expression signatures. The microarray gene expression technique would be very wanted as an aid in the study of OXPHOS disorders. However, classification of patients with OXPHOS disease remains a challenge because of the limited availability of homogeneous patient groups due to the genetic and clinical heterogeneity. Furthermore, since OXPHOS defects usually affect tissues with a high energy demand like brain, heart, skeletal muscle, renal, and the endocrine system [32], it is necessary to

obtain one of these tissues to perform diagnostic and experimental tests on. Most often skeletal muscle (needle) biopsies are used for diagnostic purposes. They are also the preferred tissue type to use for research purposes. Since the quantity of muscle biopsies is often limited, only a small fraction will be available for research. These limitations urged us to explore different approaches in order to use microarray gene expression profiling for the study of OXPHOS disorders, and experimental models have been used by us and others as an alternative, some of which will be discussed below.

Non-patient derived experimental models for OXPHOS disorders and gene expression profiling

Very often, animal models are used to simulate human disease conditions and to extrapolate results and conclusions to the human situation. Yeast, mouse, fly, and worm models have been used to study OXPHOS disorders. The advantage of the mouse as a model organism is its phylogenetically short distance to the human. Advantages of yeast, fly, and worm as model organisms are mainly the short life cycles of these organisms. They are relatively easy to work with, the genomes are fully sequenced, and the genetic manipulation is straightforward. It has been reported that mutations in a gene in yeast that is homologous gene to the human *SURF1*, the *SHY1* (Surf Homolog of Yeast) gene, also results in cytochrome *c* oxidase deficiency, just as in Leigh syndrome patients with mutations in the *SURF1* gene [202]. The yeast SHY1 protein has a similar function to the human SURF1 protein [203] and the yeast SHY1-model has been used to investigate the role of SHY1 in the cytochrome *c* oxidase complex assembly [203-206]. A mouse-model for Leigh syndrome caused by mutations in the *SURF1* gene has also been created [207] and the knock-out mouse had a phenotype very similar to that observed in the patients with a substantially decreased muscle strength and motor performance, isolated cytochrome *c* oxidase deficiency in muscle, liver, heart and brain, and morphological abnormalities in skeletal muscle mainly reflected by COX negative muscle fibres and decrease mitochondrial proliferation. Despite the fact that numerous aspects resemble the human situation, a prominent characteristic of Leigh syndrome is unfortunately not present in this mouse knockout model, which is the characteristic neurological pathology of Leigh syndrome identified as focal, bilateral symmetrical necrotic lesions in the basal ganglia, thalamus, brainstem, and spinal cord.

Various other mouse models have been created, some of which have been reviewed by Wallace [208, 209]. One of the models is the Tfam deficient mouse model which might be a good model to study mtDNA depletion syndrome in humans. These mice presented with systemic, cardiac, and pancreatic β-cell defects, probably as a result of mtDNA depletion. *TFAM* encodes a mitochondrial transcription factor and reduced levels of this protein has been shown to results in mtDNA depletion in human [210]. ANT1 deficient mice most importantly present with mitochondrial myopathy and hypertrophic cardiomyopathy [211]. The characteristics of the *ANT1* knockout mice illustrate that these mice share pathology with patients with autosomal dominant progressive external ophthalmoplegia (adPEO, OMIM#157640) and therefore might be a good model to study

this mtDNA multiple deletion syndrome. Mouse models have also been created for a frequently affected nuclear gene in humans, which is the polymerase gamma gene. Mice were created containing a proof-reading deficient polymerase gamma (*POLG*) gene in the heart, which caused an accumulation of mtDNA mutations. The mitochondrial apoptotic process was activated and the mice developed dilated cardiomyopathy [212, 213]. In another study, transgenic mice were generated with a mutant polymerase gamma gene expressed in a neuron-specific manner in order to create a genetic model for bipolar disorder, and more specifically for the mitochondrial disease chronic progressive external ophthalmoplegia (CPEO). CPEO is often caused by a mutation in *POLG*, which results in the accumulation of mtDNA deletions. Just as in CPEO patients, transgenic mice produced mtDNA deletions and mutations in the brain [214].

The creation of mouse models with a defect in the mtDNA has shown to be extremely difficult and only few models exist. Chimeric mice have been created carrying the m.2433T>C mutation in the 16S rRNA gene leading to resistance to the mitochondrial ribosome inhibitor chloramphenicol (CAP). These CAP resistant chimeric mice presented with clinical features similar to OXPHOS disorders, i.e. congenital cataracts, mitochondrial myopathy and cardiomyopathy [215]. In a second model, mice were generated harbouring an mtDNA deletion. The deletion size was 4,696 bp and included 6 tRNA genes and 7 structural genes which also resulted in OXPHOS disorder phenotypes. Histochemical and morphological investigation of skeletal and heart muscle showed mosaic distribution of COX-negative and –positive cells with ragged-red fibre-like characteristics and blood lactate levels were elevated [216].

A variety of models are available for *Drosophila*, of which some are reviewed by Sánchez-Martínez *et al.* [217]. One of the models discussed in this review is a functional knock-down of the *Surf1* gene in *Drosophila* [218]. Ubiquitous silencing of the *Surf1* gene in *Drosophila* resulted in high mortality before entering pupariation, which resembles the high embryonic lethality of the *SURF1* knock-out mice [207]. When silencing *Surf1* in the central nervous system alone, larval muscle contained altered mitochondria. Furthermore, a decreased COX activity in cephalic sections could be shown. These abnormalities are characteristics of patients with Leigh syndrome caused by a *SURF1* mutation. The first model in *C. elegans* was the target-selected mutagenesis of the *nuo-1* gene, which encodes the 51-kDa active site subunit of complex I [219]. Mutants are characterised by behavioural defects indicative of muscular and/or neuronal defects, which is very similar to the human situation were mutations in the human homolog *NDUFV1* result in myoclonic epilepsy, hypotonia, ataxia, Leigh syndrome, leukodystrophy, and other neurological conditions [220, 221]. The *C. elegans* mutant having a mutation in the *mev1* gene, encoding a subunit of complex II, has been helpful in understanding the involvement of a defective electron transport chain in increased ROS production. *Mev1* mutants have an increased ROS production and an abnormal energy metabolism [222].

Experimental animal models for OXPHOS disorders are very useful in gene expression studies, especially since they overcome the problem of the sample scarcity. Furthermore, working with animal models is much more flexible, e.g. animals can be exposed to conditions in favour of the experimental setup, and genetic manipulation is often relatively easy.

Patient derived experimental models for gene expression profiling

Animal models, having a homogeneous genetic background, not always represent the wild-type or pathological situation in human to the best extent, making extrapolation of the results difficult. Therefore, patient-derived model systems can be a better alternative from that perspective. It would be preferable to use the patient's primary tissue and the tissue in which the OXPHOS defect is most pronounced, like skeletal muscle, directly. Because of the limited availability of such material, cell cultures of patient cells can be used as an alternative. This has the advantage that taking blood for lymphocytes or a skin biopsy for fibroblast cells is less disturbing for patients compared to undergoing a muscle biopsy. Moreover, cells can be grown in large quantities and can be stored and reused for long periods of time. However, *in vitro* cultured cells are not the same as *in vivo* tissues and these cells are often not affected by the condition. In order to use cell culture systems to explore the molecular biological processes involved in the pathology of OXPHOS disorders, cultured cells have to suffer from the OXPHOS defect as well. One of the measurable manifestations can be a biochemical deficiency of one or more of the five complexes of the electron transport chain. Lymphocytes, primary skin fibroblasts, and myoblasts are the most prominent cell types which have been used as cell culture models to study OXPHOS disorders. Besides the use of primary patient cell cultures, primary cells can also be genetically manipulated to simulate OXPHOS defects. Osteosarcoma cell lines depleted of their mtDNA (ρ^o cells) transfected with mtDNA from patient cells are often used to create cells with identical nuclear genetic background, but different types of mtDNA mutations or heteroplasmy levels (cybrid cells).

There have been a number of microarray gene expression studies reporting the use of patient-derived cell cultures to study OXPHOS disorders. Van der Westhuizen *et al.* studied complex I deficiencies using primary fibroblasts from patients with mutations in five different genes encoding complex I subunits. Because fibroblasts mainly rely on anaerobic energy metabolism (glycolysis) for their energy supply, they chose to compare gene expression of these cells under anaerobic culture conditions to aerobic (OXPHOS) culture conditions. One of the observations from this study was a significant induction of methallothioneins, which was believed to be related to their antioxidant function as a protection from an increase in ROS production [184]. In another study using microarray and realtime-PCR, matrix metalloproteinase 1 (*MMP1*) expression was shown to be significantly increased in cultured skin fibroblasts from patients with the myoclonic epilepsy and ragged-red fibres (MERRF) syndrome. Supported by the measurement of a significant increase in intracellular H_2O_2 concentration in these patient cells and previous reports

in literature, the induction of MMP1 was related to an increase in ROS production [223]. In a study of Leber's hereditary optic neuropathy (LHON), microarray gene expression analysis was carried out on cybrid cells constructed from five patient cell lines containing LHON mtDNA mutations compared to controls cell lines. An important observation was that the majority of the gene expression changes was due to the ρ^0 and the cybridisation process, instead of resulting from LHON mtDNA mutations. Nevertheless, several significant gene expression changes could be identified, which were related to the presence of the LHON mtDNA mutations [224]. Jahangir Tafrechi *et al.* compared gene expression profiles of cybrid cells with 100% wild-type mtDNA, cybrid cells with 100% m.3243A>G mutant mtDNA, and ρ^0 cells. Their conclusion was that different mtDNA mutations result in distinct nuclear gene expression changes, suggesting the involvement of different molecular pathways, partly explaining the clinical heterogeneity observed in OXPHOS disorders [225]. Cortopassi *et al.* performed an extensive gene expression study in which they compared gene expression profiles from five mitochondrial diseases (LHON, Friedreich's ataxia, MELAS, Kearns-Sayre Syndrome, and NARP) using lymphoblasts, osteosarcomas, fibroblasts, myoblasts, differentiated muscle, undifferentiated and differentiated NT2 neural cells, and undifferentiated and differentiated SH-SY5Y neuroblastoma cells. Transcripts of the unfolded protein response and of the cell cycle pathway were commonly induced. Transcripts involved in vesicular secretion and protein synthesis were commonly reduced [226]. These studies show that a prominent process taking place in various OXPHOS disorders is an increased ROS production. The resulting ROS damage may lead to secondary responses like ROS defence, and changes in protein turnover and cell cycle related processes. A very important aspect when using cell culture models is that one must be very careful not to draw conclusions on the basis of artefacts.

As mentioned above, the effects of different mutation loads of mtDNA mutations can be studied in cybrid cells. A disadvantage is that these cell lines are predominantly tumour cells with a genetically modified and unstable nuclear background, introducing extra experimental variability, as illustrated by the study of Danielson *et al.* [224]. Another option is to use cell lines from different patients with varying mutation loads of the mtDNA mutation. The advantage is that these cells are not genetically manipulated, but the disadvantage of this method is the different nuclear backgrounds of each cell culture. The introduction of the extra variation by these two methods complicates the identification of the effect of the mtDNA mutation and the effect of the differences in mutation load. In chapter five, a cell culture model system is presented which circumvents these problems by exploiting the mutation load differences between single cultured fibroblast cells. Fibroblast cells from one single patient carrying the m.9176T>C mutation in the *ATP6* gene were cloned by seeding the cells in a very low concentration, allowing cell colonies to arise from only one single cell. This gave rise to various cell lines with the same genetic background, but with different m.9176T>C mutation loads. This system is the preferred method to study mutation load effects of the m.9176T>C mutation. The applicability of this cell culture model system for other mtDNA mutations depends on a number of factors. Firstly, as already mentioned previously, the OXPHOS defect has to be expressed in the cultured cells, e.g. it has to result in a

biochemical phenotype. Secondly, the distribution of the mutation loads of individual fibroblast cells has to be broad, providing the possibility of cloning cells with varying mutation loads and preferably also with only wild-type mtDNA molecules. Finally, the mutation load has to be stable during the culturing procedure. For example, the common heterogeneous MELAS m.3243A>G mutation has a biochemical phenotype in cultured skin fibroblasts, and the mutation load is stable during culturing as long as an exogenous uridine supply is provided [227]. Single muscle fibres and single lymphocyte cells have been analyzed for this mutation and the widest mutation load ranges were from 12% to 100% for single muscle fibres and from 19% to 92% for single lymphocyte cells [104, 105, 228]. Single fibroblast cells unfortunately have not been analyzed, but it can be expected that fibroblast mutation loads are in the range of the muscle fibre and lymphocyte mutation loads. The MELAS m.3243A>G mutation most likely fulfils all criteria, and therefore is a good candidate for this cell culture model system, although a 0% mutation load monoclonal cell culture may be difficult to achieve. The cell culture model system might also be useful for the m.8993T>G/C mutation in the ATP6 gene resulting in Neuropathy, Ataxia, and Retinitis Pigmentosa (NARP) or Leigh syndrome [9-11, 149]. This mutation has been shown to be stable with respect to its mutation load over cell culture passages and the mutation also results in a biochemical phenotype in cultured skin fibroblasts. However, the distribution of the mutation load in single fibroblast cells has not yet been determined, but since the characteristics of this mutation are very much like those of the m.9176T>C mutation in the same gene, it is plausible that this criterion will also be fulfilled.

The use of animal or cell culture model systems for gene expression studies of OXPHOS disorders are alternatives for the use of primary patient tissue, but have considerable pitfalls. Gene expression profiling of primary patient tissue remains to be the preferred approach, and validation of results from experimental models to the human *in vivo* situation always needs to be strived for.

Molecular biological processes involved in OXPHOS disorders

Besides improvement of genetic diagnosis for OXPHOS disorders (chapter 2) and the development of good experimental models in order to study OXPHOS disorders (chapter 5), this thesis shows that microarray gene expression technology has proven to be a valuable tool to study the molecular pathology of OXPHOS disorders and to identify (new) entries for therapeutic interventions. We were able to identify a number of known, but also novel molecular biological pathways related to the specific disorders under study, which may imply to other OXPHOS disorders as well. Moreover, microarray gene expression analysis led to the identification of gene expression markers for OXPHOS disease stages. Lastly, through the newly identified molecular biological pathways in the investigated OXPHOS disorders, new therapeutic possibilities were identified which are worthwhile for follow-up investigations.

In chapters three and four, two microarray gene expression studies are described comparing skeletal muscle from Leigh syndrome patients with a mutation in the *SURF1* gene and skeletal muscle from carriers of the MELAS m.3243A>G mutation respectively with skeletal muscle from control subjects. To perform a more specific analysis for the m.3243A>G mutation, the m.3243A>G mutation carriers were divided into three groups, and each group was compared to the controls. One group comprised a-symptomatic mutation carriers (AS3243) and another consisted of symptomatic mutation carriers (S3243). A third group combined all mutation carriers (Mut3243), irrespective of having symptoms or not. In chapter five, a study is described in which monoclonal primary skin fibroblast originating from one patient are used for the investigation of gene expression differences between different mutation loads of the m.9176T>C mutation. The goal of these studies was to gain insight into the molecular biological processes involved in the pathology of these diseases, and, more specifically for the m.3243A>G and m.9176T>C mutations, to investigate the effect of the mutation load on gene expression. Table 1 gives an overview of the most important processes which were identified as changed in the comparisons made in these studies.

Energy pathways, OXPHOS, and mitochondrial biogenesis

Because there is a defect in OXPHOS, which is one of the most important parts of the aerobic energy metabolism, one might expect that compensatory changes would occur in the expression of genes involved in other energy metabolism systems such as the glycolysis or the citric acid cycle. Furthermore, changes in the expression of OXPHOS related genes and genes involved in mitochondrial biogenesis would be expected to occur as well. However, only in muscle of a-symptomatic m.3243A>G mutation carriers, we observed stimulation of OXPHOS and mitochondrial biogenesis, but no other changes in energy metabolism occurred. None of these expected compensatory mechanisms were identified in muscle of the symptomatic m.3243A>G mutation carriers, *SURF1* Leigh patients, or in fibroblasts carrying the m.9176T>C mutation. However, these results are in line with previous microarray gene expression studies on OXPHOS disorders. Van der Westhuizen *et al.* carried out a microarray gene expression study on cell lines from patients with complex I deficiency due to mutations in genes coding for different complex I subunits. The majority of these cell lines showed no change in gene expression of mtDNA encoded structural OXPHOS components when cultured under aerobic compared to anaerobic conditions [184]. In another study, gene expression of cybrid cells with 100% wild-type mtDNA, 100% mutant m.3243A>G mtDNA, and ρ^0 cells were compared using microarray gene expression. Similar to our results in muscle of symptomatic m.3243A>G mutation carriers, mostly having high mutation loads, the gene set 'oxidative phosphorylation' showed no change when the m.3243 mutant cells were compared to wild-type cells [225]. Furthermore, two other microarray gene expression studies have been reported on muscle biopsies from OXPHOS patients. One study investigated three MELAS patients carrying the m.3243A<G mutation, and only in the patient with

the highest mutation load (91%) an induction of OPXHOS genes was identified [118]. The other study, in which also symptomatic MELAS subjects with the m.3243A<G mutation were studied, did not report any gene expression changes of OXPHOS genes [119].

On the basis of the reports in literature and from our results, we can conclude that stimulation of OXPHOS and mitochondrial biogenesis does not occur when pathology is present, but may contribute to prevention of a-symptomatic m.3243A>G mutation carriers becoming symptomatic. Mutations in the *SURF1* gene and the m.9176T>C mutation in the *ATP6* gene both result in deficiencies of electron transport chain complexes, i.e. the cytochrome *c* oxidase complex and the ATP synthase subunit respectively. It is likely that these defects are more severe than the defect of the $tRNA^{Leu}$ molecule caused by the m.3243A>G mutation, because they directly affect the energy production system, whereas the defective $tRNA^{Leu}$ molecule indirectly affects the oxidative energy metabolism. In contrast to muscle, the fibroblast cells carrying the m.9176T>C mutation only show a biochemical phenotype. Therefore, these cells might have a different response than muscle cells. In conclusion, the stimulation of OXPHOS and mitochondrial biogenesis appears to be able to initially protect the cells carrying the m.3243A>G mutation, in contrast to cells with a *SURF1* or the m.9176T>C mutation.

Protein turnover, ROS production, apoptosis, and complement activation

An increased protein turnover, characterised by increased protein synthesis and degradation, appears to be present in muscle cells from Leigh syndrome patients with a *SURF1* mutation and in muscle cells from m.3243A>G mutation carriers. An increase in protein turnover was previously reported when increased ubiquitin mRNA levels were found in MELAS m.3243A>G muscle cells [118]. However, this was not observed in affected m.3243A>G MELAS patients, which is in agreement with the findings in cybrid cells carrying 100% of the m.3243A>G mutation. In these cybrids, ribosomal protein gene expression was down-regulated and transcripts coding for proteins involved in ubiquitin-mediated proteolysis were also significantly down-regulated. The measurement of a decreased cytosolic protein synthesis rate in these cybrid cells confirmed the microarray results [225]. The explanation which was suggested for the decrease in protein synthesis was, that energy demanding processes like protein synthesis are down-regulated to compensate for the OXPHOS defect. A suppression of protein synthesis was also identified in a microarray study of fibroblasts carrying the m.8344A>G mutation in the $tRNA^{Lys}$ gene resulting in myoclonic epilepsy and ragged red fibres (MERRF) syndrome [223]. In a study where 9 different cell types from five different OXPHOS disorders were analyzed by microarray gene expression, protein biosynthesis was identified as a changed process, however, in this study it was not explained whether the process was stimulated or inhibited [226].

In addition to the increases protein turnover, increased ROS production and complement activation are found in skeletal muscle from Leigh syndrome patients with a *SURF1* mutation and

in muscle from m.3243A>G mutation carriers and patients. Our hypothesis is that increased ROS production resulting from a defective OXPHOS system and a defect in the translation machinery in case of the m.3243A>G mutation, results in oxidatively damaged and dysfunctional proteins. In an effort to replace the damaged and dysfunctional proteins, protein turnover is increased, but this apparently is insufficient, or in case of the m.3243A>G mutation still gives rise to dysfunctional proteins. When damage persists, increases, and compensation fails, muscle pathology arises, and in turn triggers the activation of apoptosis and complement components (see below). Not all of these changes were identified in fibroblasts with the m.9176T>C mutation. ROS production and oxidative protein damage was not experimentally determined in these fibroblasts, but there were no gene expression changes related to ROS defence which could be indicative for an increased ROS production. Surprisingly, this is in contrast with previous reports on fibroblast cell cultures with OXPHOS defects [174, 223, 229]. In complex I deficient fibroblasts, an up-regulation of metallothioneins was identified, which is also an indication for increased ROS production since metallothioneins are have an antioxidant function [184]. Further study on our m.9176T>C fibroblast cell cultures is needed in order to find an explanation for this discrepancy.

Table 1: Biological processes altered in muscle from Surf Leigh patients and m.3243A>G mutation carriers and in fibroblasts with the m.9176T>C mutation compared to controls

	Skeletal Muscle				*Fibroblasts*
Process	**SURF1 Leigh**	**MELAS AS3243**	**MELAS S3243**	**MELAS Mut3243**	**m.9176T>C**
Apoptosis	ND	↑	NC	↑↓	↑↓
Protein synthesis	↑	↑↑	NC	↑	NC
Protein degradation	↑	↑	NC	ND	NC
ROS production*	↑	↑	↑	-	ND / NC**
Oxidative protein damage*	NC	↑	↑	-	ND
OXPHOS	NC	↑	NC	ND	NC
Mitochondrial biogenesis	ND	↑	NC	ND	NC
Energy pathways	NC	NC	NC	NC	NC
Complement system	↑	↑	↑↑	ND	NC

ND: Not determined by the process based analysis, but some individual genes might be changed. NC: No change. ↑: Stimulation of the process. ↓: Inhibition of the process. For the determination of ROS production and oxidative protein damage, no general mutation effects were estimated, as is indicated by a dash (-).

* ROS production and oxidative protein damage were determined through a DHE-staining and an oxprot assay (see chapters three and four for assay details).

** Not determined by DHE-staining and no change according to the gene expression information.

Apoptosis has been identified as an altered process in skeletal muscle of m.3243A>G mutation carriers. Also the monoclonal fibroblasts carrying the m.9176T>C mutation showed apoptotic changes in comparison with fibroblasts containing only wild-type mtDNA. For the m.3243A>G mutation carriers, a stimulation of apoptosis was mainly identified in a-symptomatic mutation carriers, whereas both stimulation and inhibition of the process occurred in mutation carriers irrespective of the presence of symptoms or not. No apoptotic changes were identified for the

m.3243A>G symptomatic mutation carriers. This illustrates that there appears to be a transition during disease progression from a-symptomatic to symptomatic from stimulation to inhibition of the apoptotic process. An explanation for these changes might be related to the progression of the disease, where in the a-symptomatic mutation carriers, stimulation of apoptosis appears to be a rescue mechanism in order to remove the damaged cells containing the dysfunctional and damaged proteins due to the increased ROS production. In combination with protein turnover and the complement activation (see below), stimulating muscle regeneration, this forms the coping mechanism for cells carrying the m.3243A>G mutation. However, when damage increases, this mechanism apparently does not hold up or requires too much energy, and apoptosis is inhibited in combination with a stronger stimulation of the complement system as the sole final rescue attempt. The situation is probably similar in the monoclonal fibroblast carrying the m.9176T>C mutation. In these cells, apoptosis appeared to be both stimulated as inhibited, which might reflect different cell populations in a different phase of the process. The gene expression changes were all on the level of regulation. No actual apoptosis effector genes were changed in expression, which indicates that actual apoptosis was not occurring. Further studies will be necessary to explain the role of these apoptotic changes with respect to the m.9176T>C mutation and its pathological consequences.

In chapters three and four it was demonstrated that activation of complement in the skeletal muscle from the investigated patients does not lead to cell lyses by the membrane attack complex (MAC), which is the final step in the classical complement pathway. Furthermore it was shown that according to the gene expression information it is not the result of infiltration of inflammatory cells like B-lymphocytes or macrophages. Complement activation in the muscle of patients having these two OXPHOS disorders most likely is an effort to stimulate muscle regenerative processes, as complement has been shown to be able to stimulate tissue and organ regeneration [78-80, 106]. One might argue that this complement activation is purely a reaction to the muscle pathology, and that it is not specific to these disorders. However, comparison of data from Duchene muscular dystrophy (DMD) patients, who suffer from severe muscle pathology, with data from *SURF1* Leigh patients illustrated that activation of complement components most likely has different objectives in these two disorders. In DMD, the activation of complement is probably triggered by the infiltration of inflammatory cells and results in necrosis of the muscle fibres. In contrast, we have illustrated that complement activation in muscle from *SURF1* Leigh patients is not the results of infiltrating inflammatory cells and that muscle fibre necrosis is not occurring (chapter 3). Changes in gene expression and immunohistochemical data have provided support for the hypothesis that complement activation most likely is an effort to stimulate muscle fibre regeneration and development in *SURF1* Leigh patients (chapter 3), and probably also in subjects carrying the MELAS m.3243A>G mutation. Further study on skeletal muscle of other OXPHOS disorders will have to show whether the complement activation is specific to the muscle pathology in general, or to these two OXPHOS disorders or maybe OXPHOS disorders in general. The expression of complement components in muscle, and possibly complement component C3

in particular, in combination with the protein turnover rate, may be a marker for the severity and progression of the OXPHOS disorders.

Conclusions

This thesis describes the successful application of a chip-based resequencing method to facilitate genetic diagnosis of OXPHOS disorders (chapter 2). The advantages of this approach demonstrate the feasibility to tackle mutation detection in genetically and clinically heterogeneous disorders by this or alternative high throughput sequencing technologies. It can be concluded that much can be gained from these new techniques, but that experimental methods and data analysis and interpretation have to be optimised. To study pathophysiological processes involved in OXPHOS disorders, a cell culture model system was proposed which allowed different mtDNA mutation loads to be compared without introducing experimental or genetic bias (chapter 5). This technique is the preferred method to study mtDNA mutation load differences in a genetically controlled environment. Chapters 3 and 4 describe two gene expression studies on skeletal muscle from Leigh syndrome patients with a *SURF1* mutation and carriers of the m.3243A>G mutation compared to controls. This led to the identification of pathological processes which are directly or indirectly related to these OXPHOS disorders, some of which might provide new clues for the development of therapies for OXPHOS disorders. A number of rescue or coping mechanisms as a reaction to mutations in the nuclear encoded *SURF1* gene and the mtDNA encoded $tRNA^{Leu1}$ gene (m.3243A>G) and *ATP6* gene (m.9176T>C) leading to Leigh syndrome or MELAS were identified (chapters 3, 4, and 5 respectively). As OXPHOS components appear to be stimulated prior to disease manifestation, increasing energy capacity could provide similar effects. Preventing ROS damage to proteins, DNA and tissue by preventing excessive ROS production, but also improving ROS protection, seems to be important. When protein and/or tissue damage occurs after all, stimulating protein turnover and supplying the required energy capacity might be helpful in order to compensate for the defects and postpone disease manifestation. Our studies have provided solid evidence to explore further routes of intervention along these lines.

References

1. Anderson, S., et al., *Sequence and organization of the human mitochondrial genome.* Nature, 1981. **290**(5806): p. 457-65.
2. Jukes, T.H. and S. Osawa, *The genetic code in mitochondria and chloroplasts.* Experientia, 1990. **46**(11-12): p. 1117-26.
3. Campos, Y., et al., *Leigh syndrome associated with the T9176C mutation in the ATPase 6 gene of mitochondrial DNA.* Neurology, 1997. **49**(2): p. 595-7.
4. Dionisi-Vici, C., et al., *Fulminant Leigh syndrome and sudden unexpected death in a family with the T9176C mutation of the mitochondrial ATPase 6 gene.* J Inherit Metab Dis, 1998. **21**(1): p. 2-8.
5. Makino, M., et al., *Confirmation that a T-to-C mutation at 9176 in mitochondrial DNA is an additional candidate mutation for Leigh's syndrome.* Neuromuscul Disord, 1998. **8**(3-4): p. 149-51.
6. Pequignot, M.O., et al., *Mutations in the SURF1 gene associated with Leigh syndrome and cytochrome C oxidase deficiency.* Hum Mutat, 2001. **17**(5): p. 374-81.
7. Tiranti, V., et al., *Mutations of SURF-1 in Leigh disease associated with cytochrome c oxidase deficiency.* Am J Hum Genet, 1998. **63**(6): p. 1609-21.
8. Zhu, Z., et al., *SURF1, encoding a factor involved in the biogenesis of cytochrome c oxidase, is mutated in Leigh syndrome.* Nat Genet, 1998. **20**(4): p. 337-43.
9. Makela-Bengs, P., et al., *Correlation between the clinical symptoms and the proportion of mitochondrial DNA carrying the 8993 point mutation in the NARP syndrome.* Pediatr Res, 1995. **37**(5): p. 634-9.
10. Tatuch, Y., et al., *The 8993 mtDNA mutation: heteroplasmy and clinical presentation in three families.* Eur J Hum Genet, 1994. **2**(1): p. 35-43.
11. White, S.L., et al., *Genetic counseling and prenatal diagnosis for the mitochondrial DNA mutations at nucleotide 8993.* Am J Hum Genet, 1999. **65**(2): p. 474-82.
12. Matthews, P.M., et al., *Comparison of the relative levels of the 3243 (A-->G) mtDNA mutation in heteroplasmic adult and fetal tissues.* J Med Genet, 1994. **31**(1): p. 41-4.
13. Vilarinho, L., et al., *The mitochondrial A3243G mutation presenting as severe cardiomyopathy.* J Med Genet, 1997. **34**(7): p. 607-9.
14. van den Ouweland, J.M., et al., *Mutation in mitochondrial tRNA(Leu)(UUR) gene in a large pedigree with maternally transmitted type II diabetes mellitus and deafness.* Nat Genet, 1992. **1**(5): p. 368-71.
15. Reardon, W., et al., *Diabetes mellitus associated with a pathogenic point mutation in mitochondrial DNA.* Lancet, 1992. **340**(8832): p. 1376-9.
16. Schulz, J.B., et al., *Mitochondrial gene mutations and diabetes mellitus.* Lancet, 1993. **341**(8842): p. 438-9.
17. Manouvrier, S., et al., *Point mutation of the mitochondrial tRNA(Leu) gene (A 3243 G) in maternally inherited hypertrophic cardiomyopathy, diabetes mellitus, renal failure, and sensorineural deafness.* J Med Genet, 1995. **32**(8): p. 654-6.
18. Goto, Y., I. Nonaka, and S. Horai, *A mutation in the tRNA(Leu)(UUR) gene associated with the MELAS subgroup of mitochondrial encephalomyopathies.* Nature, 1990. **348**(6302): p. 651-3.
19. Kobayashi, Y., et al., *A point mutation in the mitochondrial tRNA(Leu)(UUR) gene in MELAS (mitochondrial myopathy, encephalopathy, lactic acidosis and stroke-like episodes).* Biochem Biophys Res Commun, 1990. **173**(3): p. 816-22.
20. Enter, C., et al., *A specific point mutation in the mitochondrial genome of Caucasians with MELAS.* Hum Genet, 1991. **88**(2): p. 233-6.

21. Ciafaloni, E., et al., *MELAS: clinical features, biochemistry, and molecular genetics.* Ann Neurol, 1992. **31**(4): p. 391-8.
22. Brandon, M.C., et al., *MITOMAP: a human mitochondrial genome database--2004 update.* Nucleic Acids Res, 2005. **33**(Database issue): p. D611-3.
23. Thorburn, D.R., *Mitochondrial disorders: prevalence, myths and advances.* J Inherit Metab Dis, 2004. **27**(3): p. 349-62.
24. Valnot, I., et al., *A mutation in the human heme A:farnesyltransferase gene (COX10) causes cytochrome c oxidase deficiency.* Hum Mol Genet, 2000. **9**(8): p. 1245-9.
25. Venter, J.C., et al., *The sequence of the human genome.* Science, 2001. **291**(5507): p. 1304-51.
26. McPherson, J.D., et al., *A physical map of the human genome.* Nature, 2001. **409**(6822): p. 934-41.
27. Golub, T.R., et al., *Molecular classification of cancer: class discovery and class prediction by gene expression monitoring.* Science, 1999. **286**(5439): p. 531-7.
28. van 't Veer, L.J., et al., *Gene expression profiling predicts clinical outcome of breast cancer.* Nature, 2002. **415**(6871): p. 530-6.
29. Mootha, V.K., et al., *PGC-1alpha-responsive genes involved in oxidative phosphorylation are coordinately downregulated in human diabetes.* Nat Genet, 2003. **34**(3): p. 267-73.
30. Eijssen, L.M.T., *Analysis of microarray gene expression data sets.* Department of Genetics and Cell Biology, Cardiovascular Research Institute Maastricht (CARIM). Maastricht University. Maastricht, 2006.
31. Chinnery, P.F., *New approaches to the treatment of mitochondrial disorders.* Reprod Biomed Online, 2004. **8**(1): p. 16-23.
32. Wallace, D.C., *Mitochondrial diseases in man and mouse.* Science, 1999. **283**(5407): p. 1482-8.
33. Maitra, A., et al., *The Human MitoChip: a high-throughput sequencing microarray for mitochondrial mutation detection.* Genome Res, 2004. **14**(5): p. 812-9.
34. Jakupciak, J.P., et al., *Mitochondrial DNA as a cancer biomarker.* J Mol Diagn, 2005. **7**(2): p. 258-67.
35. Mullenbach, R., P.J. Lagoda, and C. Welter, *An efficient salt-chloroform extraction of DNA from blood and tissues.* Trends Genet, 1989. **5**(12): p. 391.
36. Comi, G.P., et al., *Cytochrome c oxidase subunit I microdeletion in a patient with motor neuron disease.* Ann Neurol, 1998. **43**(1): p. 110-6.
37. Pease, A.C., et al., *Light-generated oligonucleotide arrays for rapid DNA sequence analysis.* Proc Natl Acad Sci U S A, 1994. **91**(11): p. 5022-6.
38. Lipshutz, R.J., et al., *High density synthetic oligonucleotide arrays.* Nat Genet, 1999. **21**(1 Suppl): p. 20-4.
39. Andrews, R.M., et al., *Reanalysis and revision of the Cambridge reference sequence for human mitochondrial DNA.* Nat Genet, 1999. **23**(2): p. 147.
40. R Development Core Team. *R: A language and environment for statistical computing*. 2004. Vienna, Austria: R Foundation for Statistical Computing.
41. Shaag, A., et al., *Mitochondrial encephalomyopathy associated with a novel mutation in the mitochondrial tRNA(leu)(UUR) gene (A3243T).* Biochem Biophys Res Commun, 1997. **233**(3): p. 637-9.
42. Kirby, D.M., et al., *Mutations of the mitochondrial ND1 gene as a cause of MELAS.* J Med Genet, 2004. **41**(10): p. 784-9.
43. Santorelli, F.M., et al., *Identification of a novel mutation in the mtDNA ND5 gene associated with MELAS.* Biochem Biophys Res Commun, 1997. **238**(2): p. 326-8.
44. Pulkes, T., et al., *The mitochondrial DNA G13513A transition in ND5 is associated with a LHON/MELAS overlap syndrome and may be a frequent cause of MELAS.* Ann Neurol, 1999. **46**(6): p. 916-9.
45. Penisson-Besnier, I., et al., *Recurrent brain hematomas in MELAS associated with an ND5 gene mitochondrial mutation.* Neurology, 2000. **55**(2): p. 317-8.

46. Chol, M., et al., *The mitochondrial DNA G13513A MELAS mutation in the NADH dehydrogenase 5 gene is a frequent cause of Leigh-like syndrome with isolated complex I deficiency.* J Med Genet, 2003. **40**(3): p. 188-91.
47. Kirby, D.M., et al., *Low mutant load of mitochondrial DNA G13513A mutation can cause Leigh's disease.* Ann Neurol, 2003. **54**(4): p. 473-8.
48. Sudo, A., et al., *Leigh syndrome caused by mitochondrial DNA G13513A mutation: frequency and clinical features in Japan.* J Hum Genet, 2004. **49**(2): p. 92-6.
49. Helm, M., et al., *Search for characteristic structural features of mammalian mitochondrial tRNAs.* Rna, 2000. **6**(10): p. 1356-79.
50. Mitchell, A.L., et al., *Sequence Variation In Mitochondrial Complex I Genes: Mutation Or Polymorphism?* J Med Genet, 2006. **43**(3): p. 175-9.
51. Suomalainen, A., et al., *Use of single strand conformation polymorphism analysis to detect point mutations in human mitochondrial DNA.* J Neurol Sci, 1992. **111**(2): p. 222-6.
52. van Orsouw, N.J., et al., *Mutational scanning of mitochondrial DNA by two-dimensional electrophoresis.* Genomics, 1998. **52**(1): p. 27-36.
53. van den Bosch, B.J., et al., *Mutation analysis of the entire mitochondrial genome using denaturing high performance liquid chromatography.* Nucleic Acids Res, 2000. **28**(20): p. E89.
54. Bjorheim, J. and P.O. Ekstrom, *Review of denaturant capillary electrophoresis in DNA variation analysis.* Electrophoresis, 2005. **26**(13): p. 2520-30.
55. Wartell, R.M., S.H. Hosseini, and C.P. Moran, Jr., *Detecting base pair substitutions in DNA fragments by temperature-gradient gel electrophoresis.* Nucleic Acids Res, 1990. **18**(9): p. 2699-705.
56. Wong, L.J. and R.G. Boles, *Mitochondrial DNA analysis in clinical laboratory diagnostics.* Clin Chim Acta, 2005. **354**(1-2): p. 1-20.
57. Sohm, B., et al., *Towards understanding human mitochondrial leucine aminoacylation identity.* J Mol Biol, 2003. **328**(5): p. 995-1010.
58. Corona, P., et al., *A novel mtDNA mutation in the ND5 subunit of complex I in two MELAS patients.* Ann Neurol, 2001. **49**(1): p. 106-10.
59. DiMauro, S. and E.A. Schon, *Mitochondrial DNA mutations in human disease.* Am J Med Genet, 2001. **106**(1): p. 18-26.
60. McFarland, R., et al., *Assigning pathogenicity to mitochondrial tRNA mutations: when "definitely maybe" is not good enough.* Trends Genet, 2004. **20**(12): p. 591-6.
61. Ingman, M. and U. Gyllensten, *mtDB: Human Mitochondrial Genome Database, a resource for population genetics and medical sciences.* Nucleic Acids Res, 2006. **34**(Database issue): p. D749-51.
62. Dahl, H.H., *Getting to the nucleus of mitochondrial disorders: identification of respiratory chain-enzyme genes causing Leigh syndrome.* Am J Hum Genet, 1998. **63**(6): p. 1594-7.
63. Tiranti, V., et al., *Loss-of-function mutations of SURF-1 are specifically associated with Leigh syndrome with cytochrome c oxidase deficiency.* Ann Neurol, 1999. **46**(2): p. 161-6.
64. Sue, C.M., et al., *Differential features of patients with mutations in two COX assembly genes, SURF-1 and SCO2.* Ann Neurol, 2000. **47**(5): p. 589-95.
65. Tiranti, V., et al., *Characterization of SURF-1 expression and Surf-1p function in normal and disease conditions.* Hum Mol Genet, 1999. **8**(13): p. 2533-40.
66. Bruno, C., et al., *A novel mutation in the SURF1 gene in a child with Leigh disease, peripheral neuropathy, and cytochrome-c oxidase deficiency.* J Child Neurol, 2002. **17**(3): p. 233-6.
67. den Dunnen, J.T. and S.E. Antonarakis, *Mutation nomenclature extensions and suggestions to describe complex mutations: a discussion.* Hum Mutat, 2000. **15**(1): p. 7-12.
68. Gautier, L., et al., *affy--analysis of Affymetrix GeneChip data at the probe level.* Bioinformatics, 2004. **20**(3): p. 307-15.
69. Lindsey, J.K., *Models for Repeated Measurements*. 1999, Oxford: Oxford University Press.

70. Lindsey, J.K. *R modeling libraries.* [cited; Available from: http://popgen.unimaas.nl/~jlindsey/rcode.html.
71. Dai, M., et al., *Evolving gene/transcript definitions significantly alter the interpretation of GeneChip data.* Nucleic Acids Res, 2005. **33**(20): p. e175.
72. Akaike, H. *Information theory and an extension of the maximum likelihood principle.* in *Second International Symposium on Inference Theory*. 1973. Budapest: Akadémiai Kiadó.
73. Atkinson, A.C., *A note on the generalized information criterion for choice of a model.* Biometrika, 1980. **67**: p. 413-418.
74. Dahlquist, K.D., et al., *GenMAPP, a new tool for viewing and analyzing microarray data on biological pathways.* Nat Genet, 2002. **31**(1): p. 19-20.
75. Doniger, S.W., et al., *MAPPFinder: using Gene Ontology and GenMAPP to create a global gene-expression profile from microarray data.* Genome Biol, 2003. **4**(1): p. R7.
76. Dennis, G., Jr., et al., *DAVID: Database for Annotation, Visualization, and Integrated Discovery.* Genome Biol, 2003. **4**(5): p. P3.
77. Hsiao, L.L., et al., *A compendium of gene expression in normal human tissues.* Physiol Genomics, 2001. **7**(2): p. 97-104.
78. Alamdari, D.H., et al., *High sensitivity enzyme-linked immunosorbent assay (ELISA) method for measuring protein carbonyl in samples with low amounts of protein.* Free Radic Biol Med, 2005. **39**(10): p. 1362-7.
79. Zhao, H., et al., *Superoxide reacts with hydroethidine but forms a fluorescent product that is distinctly different from ethidium: potential implications in intracellular fluorescence detection of superoxide.* Free Radic Biol Med, 2003. **34**(11): p. 1359-68.
80. Wilson, M.C., et al., *Lactic acid efflux from white skeletal muscle is catalyzed by the monocarboxylate transporter isoform MCT3.* J Biol Chem, 1998. **273**(26): p. 15920-6.
81. Baker, S.K., M.A. Tarnopolsky, and A. Bonen, *Expression of MCT1 and MCT4 in a patient with mitochondrial myopathy.* Muscle Nerve, 2001. **24**(3): p. 394-8.
82. Pilegaard, H., et al., *Effect of high-intensity exercise training on lactate/H+ transport capacity in human skeletal muscle.* Am J Physiol, 1999. **276**(2 Pt 1): p. E255-61.
83. Grune, T., T. Reinheckel, and K.J. Davies, *Degradation of oxidized proteins in K562 human hematopoietic cells by proteasome.* J Biol Chem, 1996. **271**(26): p. 15504-9.
84. Esposito, L.A., et al., *Mitochondrial disease in mouse results in increased oxidative stress.* Proc Natl Acad Sci U S A, 1999. **96**(9): p. 4820-5.
85. Walport, M.J., *Complement. First of two parts.* N Engl J Med, 2001. **344**(14): p. 1058-66.
86. Song, W.C., M.R. Sarrias, and J.D. Lambris, *Complement and innate immunity.* Immunopharmacology, 2000. **49**(1-2): p. 187-98.
87. Porter, J.D., et al., *A chronic inflammatory response dominates the skeletal muscle molecular signature in dystrophin-deficient mdx mice.* Hum Mol Genet, 2002. **11**(3): p. 263-72.
88. Turk, R., et al., *Common pathological mechanisms in mouse models for muscular dystrophies.* Faseb J, 2006. **20**(1): p. 127-9.
89. Cornelio, F. and I. Dones, *Muscle fiber degeneration and necrosis in muscular dystrophy and other muscle diseases: cytochemical and immunocytochemical data.* Ann Neurol, 1984. **16**(6): p. 694-701.
90. Engel, A.G. and G. Biesecker, *Complement activation in muscle fiber necrosis: demonstration of the membrane attack complex of complement in necrotic fibers.* Ann Neurol, 1982. **12**(3): p. 289-96.
91. Gasque, P., et al., *Human skeletal myoblasts spontaneously activate allogeneic complement but are resistant to killing.* J Immunol, 1996. **156**(9): p. 3402-11.
92. Legoedec, J., et al., *Complement classical pathway expression by human skeletal myoblasts in vitro.* Mol Immunol, 1997. **34**(10): p. 735-41.
93. Mastellos, D. and J.D. Lambris, *Complement: more than a 'guard' against invading pathogens?* Trends Immunol, 2002. **23**(10): p. 485-91.

94. Del Rio-Tsonis, K., et al., *Expression of the third component of complement, C3, in regenerating limb blastema cells of urodeles.* J Immunol, 1998. **161**(12): p. 6819-24.
95. Markiewski, M.M., et al., *C3a and C3b activation products of the third component of complement (C3) are critical for normal liver recovery after toxic injury.* J Immunol, 2004. **173**(2): p. 747-54.
96. Strey, C.W., et al., *The proinflammatory mediators C3a and C5a are essential for liver regeneration.* J Exp Med, 2003. **198**(6): p. 913-23.
97. van Dartel, M. and T.J. Hulsebos, *Characterization of PMP22 expression in osteosarcoma.* Cancer Genet Cytogenet, 2004. **152**(2): p. 113-8.
98. Gutierrez, J., et al., *Free radicals, mitochondria, and oxidized lipids: the emerging role in signal transduction in vascular cells.* Circ Res, 2006. **99**(9): p. 924-32.
99. Hammans, S.R., et al., *The mitochondrial DNA transfer RNALeu(UUR) A-->G(3243) mutation. A clinical and genetic study.* Brain, 1995. **118 (Pt 3)**: p. 721-34.
100. Chinnery, P.F., et al., *Molecular pathology of MELAS and MERRF. The relationship between mutation load and clinical phenotypes.* Brain, 1997. **120 (Pt 10)**: p. 1713-21.
101. Torroni, A., et al., *Mitochondrial DNA haplogroups do not play a role in the variable phenotypic presentation of the A3243G mutation.* Am J Hum Genet, 2003. **72**(4): p. 1005-12.
102. van Essen, E.H., et al., *HLA-DQ polymorphism and degree of heteroplasmy of the A3243G mitochondrial DNA mutation in maternally inherited diabetes and deafness.* Diabet Med, 2000. **17**(12): p. 841-7.
103. Flierl, A., H. Reichmann, and P. Seibel, *Pathophysiology of the MELAS 3243 transition mutation.* J Biol Chem, 1997. **272**(43): p. 27189-96.
104. Silvestri, G., et al., *Single-fiber PCR in MELAS(3243) patients: correlations between intratissue distribution and phenotypic expression of the mtDNA(A3243G) genotype.* Am J Med Genet, 2000. **94**(3): p. 201-6.
105. Ozawa, M., I. Nonaka, and Y. Goto, *Single muscle fiber analysis in patients with 3243 mutation in mitochondrial DNA: comparison with the phenotype and the proportion of mutant genome.* J Neurol Sci, 1998. **159**(2): p. 170-5.
106. van Empel, V.P., et al., *Downregulation of apoptosis-inducing factor in harlequin mutant mice sensitizes the myocardium to oxidative stress-related cell death and pressure overload-induced decompensation.* Circ Res, 2005. **96**(12): p. e92-e101.
107. Stefanovic, B., et al., *TRAM2 protein interacts with endoplasmic reticulum Ca2+ pump Serca2b and is necessary for collagen type I synthesis.* Mol Cell Biol, 2004. **24**(4): p. 1758-68.
108. Wanker, E.E., et al., *Functional characterization of the 180-kD ribosome receptor in vivo.* J Cell Biol, 1995. **130**(1): p. 29-39.
109. Liou, M.L. and H.C. Liou, *The ubiquitin-homology protein, DAP-1, associates with tumor necrosis factor receptor (p60) death domain and induces apoptosis.* J Biol Chem, 1999. **274**(15): p. 10145-53.
110. Chen, R.H., W.J. Wang, and J.C. Kuo, *The tumor suppressor DAP-kinase links cell adhesion and cytoskeleton reorganization to cell death regulation.* J Biomed Sci, 2006. **13**(2): p. 193-9.
111. Ishida, M., et al., *The SYT-SSX fusion protein down-regulates the cell proliferation regulator COM1 in t(x;18) synovial sarcoma.* Mol Cell Biol, 2007. **27**(4): p. 1348-55.
112. Xue, D. and H.R. Horvitz, *Inhibition of the Caenorhabditis elegans cell-death protease CED-3 by a CED-3 cleavage site in baculovirus p35 protein.* Nature, 1995. **377**(6546): p. 248-51.
113. Bump, N.J., et al., *Inhibition of ICE family proteases by baculovirus antiapoptotic protein p35.* Science, 1995. **269**(5232): p. 1885-8.
114. Mork, C.N., D.V. Faller, and R.A. Spanjaard, *A mechanistic approach to anticancer therapy: targeting the cell cycle with histone deacetylase inhibitors.* Curr Pharm Des, 2005. **11**(9): p. 1091-104.
115. Shannan, B., et al., *Clusterin and DNA repair: a new function in cancer for a key player in apoptosis and cell cycle control.* J Mol Histol, 2006. **37**(5-7): p. 183-8.

116. D'Orazi, G., et al., *Homeodomain-interacting protein kinase-2 phosphorylates p53 at Ser 46 and mediates apoptosis.* Nat Cell Biol, 2002. **4**(1): p. 11-9.
117. Sanjo, H., T. Kawai, and S. Akira, *DRAKs, novel serine/threonine kinases related to death-associated protein kinase that trigger apoptosis.* J Biol Chem, 1998. **273**(44): p. 29066-71.
118. Heddi, A., et al., *Coordinate induction of energy gene expression in tissues of mitochondrial disease patients.* J Biol Chem, 1999. **274**(33): p. 22968-76.
119. Crimi, M., et al., *Skeletal muscle gene expression profiling in mitochondrial disorders.* Faseb J, 2005. **19**(7): p. 866-8.
120. Aure, K., et al., *Apoptosis in mitochondrial myopathies is linked to mitochondrial proliferation.* Brain, 2006. **129**(Pt 5): p. 1249-59.
121. Andersson, U. and R.C. Scarpulla, *Pgc-1-related coactivator, a novel, serum-inducible coactivator of nuclear respiratory factor 1-dependent transcription in mammalian cells.* Mol Cell Biol, 2001. **21**(11): p. 3738-49.
122. Gleyzer, N., K. Vercauteren, and R.C. Scarpulla, *Control of mitochondrial transcription specificity factors (TFB1M and TFB2M) by nuclear respiratory factors (NRF-1 and NRF-2) and PGC-1 family coactivators.* Mol Cell Biol, 2005. **25**(4): p. 1354-66.
123. Park, H., E. Davidson, and M.P. King, *The pathogenic A3243G mutation in human mitochondrial tRNALeu(UUR) decreases the efficiency of aminoacylation.* Biochemistry, 2003. **42**(4): p. 958-64.
124. Moudy, A.M., et al., *Abnormal calcium homeostasis and mitochondrial polarization in a human encephalomyopathy.* Proc Natl Acad Sci U S A, 1995. **92**(3): p. 729-33.
125. Howard, T.L., et al., *CHMP1 functions as a member of a newly defined family of vesicle trafficking proteins.* J Cell Sci, 2001. **114**(Pt 13): p. 2395-404.
126. Tsang, H.T., et al., *A systematic analysis of human CHMP protein interactions: additional MIT domain-containing proteins bind to multiple components of the human ESCRT III complex.* Genomics, 2006. **88**(3): p. 333-46.
127. Bilodeau, P.S., et al., *The GAT domains of clathrin-associated GGA proteins have two ubiquitin binding motifs.* J Biol Chem, 2004. **279**(52): p. 54808-16.
128. Nazarian, J., K. Bouri, and E.P. Hoffman, *Intracellular expression profiling by laser capture microdissection: three novel components of the neuromuscular junction.* Physiol Genomics, 2005. **21**(1): p. 70-80.
129. Zhao, P. and E.P. Hoffman, *Embryonic myogenesis pathways in muscle regeneration.* Dev Dyn, 2004. **229**(2): p. 380-92.
130. Shoubridge, E.A., T. Johns, and G. Karpati, *Complete restoration of a wild-type mtDNA genotype in regenerating muscle fibres in a patient with a tRNA point mutation and mitochondrial encephalomyopathy.* Hum Mol Genet, 1997. **6**(13): p. 2239-42.
131. Taivassalo, T., et al., *Aerobic conditioning in patients with mitochondrial myopathies: physiological, biochemical, and genetic effects.* Ann Neurol, 2001. **50**(2): p. 133-41.
132. Taivassalo, T., et al., *Gene shifting: a novel therapy for mitochondrial myopathy.* Hum Mol Genet, 1999. **8**(6): p. 1047-52.
133. Akagi, M., et al., *A point mutation of mitochondrial ATPase 6 gene in Leigh syndrome.* Neuromuscul Disord, 2002. **12**(1): p. 53-5.
134. Wilson, C.J., et al., *Mitochondrial DNA point mutation T9176C in Leigh syndrome.* J Child Neurol, 2000. **15**(12): p. 830-3.
135. Makino, M., et al., *Mitochondrial DNA mutations in Leigh syndrome and their phylogenetic implications.* J Hum Genet, 2000. **45**(2): p. 69-75.
136. Thyagarajan, D., et al., *A novel mitochondrial ATPase 6 point mutation in familial bilateral striatal necrosis.* Ann Neurol, 1995. **38**(3): p. 468-72.
137. Jacobs, L.J., et al., *Transmission and prenatal diagnosis of the T9176C mitochondrial DNA mutation.* Mol Hum Reprod, 2005. **11**(3): p. 223-8.
138. King, M.P. and G. Attardi, *Injection of mitochondria into human cells leads to a rapid replacement of the endogenous mitochondrial DNA.* Cell, 1988. **52**(6): p. 811-9.

139. King, M.P. and G. Attardi, *Human cells lacking mtDNA: repopulation with exogenous mitochondria by complementation.* Science, 1989. **246**(4929): p. 500-3.
140. Smyth, G.K., *Linear models and empirical bayes methods for assessing differential expression in microarray experiments.* Stat Appl Genet Mol Biol, 2004. **3**: p. Article3.
141. Smyth, G.K. and T. Speed, *Normalization of cDNA microarray data.* Methods, 2003. **31**(4): p. 265-73.
142. Smyth, G.K., J. Michaud, and H.S. Scott, *Use of within-array replicate spots for assessing differential expression in microarray experiments.* Bioinformatics, 2005. **21**(9): p. 2067-75.
143. Benjamini, Y. and Y. Hochberg, *Controlling the false discovery rate: a practical andpowerful approach to multiple testing.* J. R. Statist. Soc. B, 1995. **57**: p. 289-300.
144. Jacobs, J.A.M., *The transmission and seggregation of mitochondrial DNA mutations.* Department of Genetics and Cell Biology, Research institute GROW (Growth and development). Maastricht University. Maastricht, 2007.
145. Lademann, U., T. Kallunki, and M. Jaattela, *A20 zinc finger protein inhibits TNF-induced apoptosis and stress response early in the signaling cascades and independently of binding to TRAF2 or 14-3-3 proteins.* Cell Death Differ, 2001. **8**(3): p. 265-72.
146. Liu, Z.J., X. Lu, and S. Zhong, *ASPP--Apoptotic specific regulator of p53.* Biochim Biophys Acta, 2005. **1756**(1): p. 77-80.
147. Deveraux, Q.L., et al., *IAPs block apoptotic events induced by caspase-8 and cytochrome c by direct inhibition of distinct caspases.* Embo J, 1998. **17**(8): p. 2215-23.
148. Kobayashi, S., et al., *53BP2 induces apoptosis through the mitochondrial death pathway.* Genes Cells, 2005. **10**(3): p. 253-60.
149. Sunayama, J., et al., *Physical and functional interaction between BH3-only protein Hrk and mitochondrial pore-forming protein p32.* Cell Death Differ, 2004. **11**(7): p. 771-81.
150. Brady, S.C., L.A. Allan, and P.R. Clarke, *Regulation of caspase 9 through phosphorylation by protein kinase C zeta in response to hyperosmotic stress.* Mol Cell Biol, 2005. **25**(23): p. 10543-55.
151. Paschal, B.M., R.A. Obar, and R.B. Vallee, *Interaction of brain cytoplasmic dynein and MAP2 with a common sequence at the C terminus of tubulin.* Nature, 1989. **342**(6249): p. 569-72.
152. Oh, S.W., et al., *Archvillin, a muscle-specific isoform of supervillin, is an early expressed component of the costameric membrane skeleton.* J Cell Sci, 2003. **116**(Pt 11): p. 2261-75.
153. Harris, A.S. and J.S. Morrow, *Calmodulin and calcium-dependent protease I coordinately regulate the interaction of fodrin with actin.* Proc Natl Acad Sci U S A, 1990. **87**(8): p. 3009-13.
154. Canizalez-Roman, A. and F. Navarro-Garcia, *Fodrin CaM-binding domain cleavage by Pet from enteroaggregative Escherichia coli leads to actin cytoskeletal disruption.* Mol Microbiol, 2003. **48**(4): p. 947-58.
155. Alcivar, A., et al., *DEDD and DEDD2 associate with caspase-8/10 and signal cell death.* Oncogene, 2003. **22**(2): p. 291-7.
156. Zhang, H., et al., *Involvement of programmed cell death 4 in transforming growth factor-beta1-induced apoptosis in human hepatocellular carcinoma.* Oncogene, 2006. **25**(45): p. 6101-12.
157. Takahashi, Y., et al., *Loss of Bif-1 suppresses Bax/Bak conformational change and mitochondrial apoptosis.* Mol Cell Biol, 2005. **25**(21): p. 9369-82.
158. Hasegawa, M., et al., *Mechanism of ASC-mediated apoptosis: bid-dependent apoptosis in type II cells.* Oncogene, 2007. **26**(12): p. 1748-56.
159. Lee, J.H., S.B. Rho, and T. Chun, *Programmed cell death 6 (PDCD6) protein interacts with death-associated protein kinase 1 (DAPk1): additive effect on apoptosis via caspase-3 dependent pathway.* Biotechnol Lett, 2005. **27**(14): p. 1011-5.
160. Vito, P., E. Lacana, and L. D'Adamio, *Interfering with apoptosis: Ca(2+)-binding protein ALG-2 and Alzheimer's disease gene ALG-3.* Science, 1996. **271**(5248): p. 521-5.

161. Chen, M.C., et al., *The role of apoptosis signal-regulating kinase 1 in lymphotoxin-beta receptor-mediated cell death.* J Biol Chem, 2003. **278**(18): p. 16073-81.
162. Nakano, H., et al., *TRAF5, an activator of NF-kappaB and putative signal transducer for the lymphotoxin-beta receptor.* J Biol Chem, 1996. **271**(25): p. 14661-4.
163. Kuai, J., et al., *Endogenous association of TRAF2, TRAF3, cIAP1, and Smac with lymphotoxin beta receptor reveals a novel mechanism of apoptosis.* J Biol Chem, 2003. **278**(16): p. 14363-9.
164. Chatellard-Causse, C., et al., *Alix (ALG-2-interacting protein X), a protein involved in apoptosis, binds to endophilins and induces cytoplasmic vacuolization.* J Biol Chem, 2002. **277**(32): p. 29108-15.
165. Gomez, D.E., et al., *Tissue inhibitors of metalloproteinases: structure, regulation and biological functions.* Eur J Cell Biol, 1997. **74**(2): p. 111-22.
166. Silacci, P., et al., *Gelsolin superfamily proteins: key regulators of cellular functions.* Cell Mol Life Sci, 2004. **61**(19-20): p. 2614-23.
167. Klampfer, L., et al., *Oncogenic Ras promotes butyrate-induced apoptosis through inhibition of gelsolin expression.* J Biol Chem, 2004. **279**(35): p. 36680-8.
168. Ahn, J.S., et al., *Gelsolin for senescence-associated resistance to apoptosis.* Ann N Y Acad Sci, 2003. **1010**: p. 493-5.
169. Tondera, D., et al., *Knockdown of MTP18, a novel phosphatidylinositol 3-kinase-dependent protein, affects mitochondrial morphology and induces apoptosis.* J Biol Chem, 2004. **279**(30): p. 31544-55.
170. Wang, K.K., et al., *Simultaneous degradation of alphaII- and betaII-spectrin by caspase 3 (CPP32) in apoptotic cells.* J Biol Chem, 1998. **273**(35): p. 22490-7.
171. Tang, H.L., A.H. Le, and H.L. Lung, *The increase in mitochondrial association with actin precedes Bax translocation in apoptosis.* Biochem J, 2006. **396**(1): p. 1-5.
172. Mirabella, M., et al., *Apoptosis in mitochondrial encephalomyopathies with mitochondrial DNA mutations: a potential pathogenic mechanism.* Brain, 2000. **123 (Pt 1)**: p. 93-104.
173. Shidara, Y., et al., *Positive contribution of pathogenic mutations in the mitochondrial genome to the promotion of cancer by prevention from apoptosis.* Cancer Res, 2005. **65**(5): p. 1655-63.
174. Geromel, V., et al., *Superoxide-induced massive apoptosis in cultured skin fibroblasts harboring the neurogenic ataxia retinitis pigmentosa (NARP) mutation in the ATPase-6 gene of the mitochondrial DNA.* Hum Mol Genet, 2001. **10**(11): p. 1221-8.
175. Kwong, J.Q., et al., *The mitochondrial respiratory chain is a modulator of apoptosis.* J Cell Biol, 2007. **179**(6): p. 1163-77.
176. Ostergaard, E., et al., *Hypertrichosis in patients with SURF1 mutations.* Am J Med Genet A, 2005. **138**(4): p. 384-8.
177. Rahman, S., et al., *A SURF1 gene mutation presenting as isolated leukodystrophy.* Ann Neurol, 2001. **49**(6): p. 797-800.
178. Salviati, L., et al., *Novel SURF1 mutation in a child with subacute encephalopathy and without the radiological features of Leigh Syndrome.* Am J Med Genet A, 2004. **128**(2): p. 195-8.
179. Tiranti, V., et al., *Leigh syndrome transmitted by uniparental disomy of chromosome 9.* J Med Genet, 1999. **36**(12): p. 927-8.
180. Riordan-Eva, P. and A.E. Harding, *Leber's hereditary optic neuropathy: the clinical relevance of different mitochondrial DNA mutations.* J Med Genet, 1995. **32**(2): p. 81-7.
181. Bodnar, A.G., et al., *Nuclear complementation restores mtDNA levels in cultured cells from a patient with mtDNA depletion.* Am J Hum Genet, 1993. **53**(3): p. 663-9.
182. Ugalde, C., et al., *Differences in assembly or stability of complex I and other mitochondrial OXPHOS complexes in inherited complex I deficiency.* Hum Mol Genet, 2004. **13**(6): p. 659-67.

183. Scacco, S., et al., *Pathological mutations of the human NDUFS4 gene of the 18-kDa (AQDQ) subunit of complex I affect the expression of the protein and the assembly and function of the complex.* J Biol Chem, 2003. **278**(45): p. 44161-7.
184. van der Westhuizen, F.H., et al., *Human mitochondrial complex I deficiency: investigating transcriptional responses by microarray.* Neuropediatrics, 2003. **34**(1): p. 14-22.
185. Pandya, G.A., et al., *A bioinformatic filter for improved base-call accuracy and polymorphism detection using the Affymetrix GeneChip whole-genome resequencing platform.* Nucleic Acids Res, 2007. **35**(21): p. e148.
186. Wong, L.J., *Pathogenic mitochondrial DNA mutations in protein-coding genes.* Muscle Nerve, 2007. **36**(3): p. 279-93.
187. Valentino, M.L., et al., *The 13042G --> A/ND5 mutation in mtDNA is pathogenic and can be associated also with a prevalent ocular phenotype.* J Med Genet, 2006. **43**(7): p. e38.
188. Liu, C., et al., *Novel resequencing chip customized to diagnose mutations in patients with inherited syndromes of intrahepatic cholestasis.* Gastroenterology, 2007. **132**(1): p. 119-26.
189. Albert, T.J., et al., *Direct selection of human genomic loci by microarray hybridization.* Nat Methods, 2007. **4**(11): p. 903-5.
190. Hodges, E., et al., *Genome-wide in situ exon capture for selective resequencing.* Nat Genet, 2007.
191. Okou, D.T., et al., *Microarray-based genomic selection for high-throughput resequencing.* Nat Methods, 2007. **4**(11): p. 907-9.
192. Porreca, G.J., et al., *Multiplex amplification of large sets of human exons.* Nat Methods, 2007. **4**(11): p. 931-6.
193. Wang, C., et al., *Characterization of mutation spectra with ultra-deep pyrosequencing: application to HIV-1 drug resistance.* Genome Res, 2007. **17**(8): p. 1195-201.
194. Hoffmann, C., et al., *DNA bar coding and pyrosequencing to identify rare HIV drug resistance mutations.* Nucleic Acids Res, 2007. **35**(13): p. e91.
195. Olson, M., *Enrichment of super-sized resequencing targets from the human genome.* Nat Methods, 2007. **4**(11): p. 891-2.
196. Wittwer, C.T., et al., *High-resolution genotyping by amplicon melting analysis using LCGreen.* Clin Chem, 2003. **49**(6 Pt 1): p. 853-60.
197. Liew, M., et al., *Genotyping of single-nucleotide polymorphisms by high-resolution melting of small amplicons.* Clin Chem, 2004. **50**(7): p. 1156-64.
198. Reed, G.H. and C.T. Wittwer, *Sensitivity and specificity of single-nucleotide polymorphism scanning by high-resolution melting analysis.* Clin Chem, 2004. **50**(10): p. 1748-54.
199. Palais, R.A., M.A. Liew, and C.T. Wittwer, *Quantitative heteroduplex analysis for single nucleotide polymorphism genotyping.* Anal Biochem, 2005. **346**(1): p. 167-75.
200. Bannwarth, S., V. Procaccio, and V. Paquis-Flucklinger, *Surveyor Nuclease: a new strategy for a rapid identification of heteroplasmic mitochondrial DNA mutations in patients with respiratory chain defects.* Hum Mutat, 2005. **25**(6): p. 575-82.
201. Bannwarth, S., V. Procaccio, and V. Paquis-Flucklinger, *Rapid identification of unknown heteroplasmic mutations across the entire human mitochondrial genome with mismatch-specific Surveyor Nuclease.* Nat Protoc, 2006. **1**(4): p. 2037-47.
202. Mashkevich, G., et al., *SHY1, the yeast homolog of the mammalian SURF-1 gene, encodes a mitochondrial protein required for respiration.* J Biol Chem, 1997. **272**(22): p. 14356-64.
203. Nijtmans, L.G., et al., *Shy1p occurs in a high molecular weight complex and is required for efficient assembly of cytochrome c oxidase in yeast.* FEBS Lett, 2001. **498**(1): p. 46-51.
204. Barrientos, A., D. Korr, and A. Tzagoloff, *Shy1p is necessary for full expression of mitochondrial COX1 in the yeast model of Leigh's syndrome.* Embo J, 2002. **21**(1-2): p. 43-52.
205. Barrientos, A., A. Zambrano, and A. Tzagoloff, *Mss51p and Cox14p jointly regulate mitochondrial Cox1p expression in Saccharomyces cerevisiae.* Embo J, 2004. **23**(17): p. 3472-82.

206. Mick, D.U., et al., *Shy1 couples Cox1 translational regulation to cytochrome c oxidase assembly.* Embo J, 2007. **26**(20): p. 4347-58.
207. Agostino, A., et al., *Constitutive knockout of Surf1 is associated with high embryonic lethality, mitochondrial disease and cytochrome c oxidase deficiency in mice.* Hum Mol Genet, 2003. **12**(4): p. 399-413.
208. Wallace, D.C., *Mouse models for mitochondrial disease.* Am J Med Genet, 2001. **106**(1): p. 71-93.
209. Wallace, D.C., *Animal models for mitochondrial disease.* Methods Mol Biol, 2002. **197**: p. 3-54.
210. Poulton, J., et al., *Deficiency of the human mitochondrial transcription factor h-mtTFA in infantile mitochondrial myopathy is associated with mtDNA depletion.* Hum Mol Genet, 1994. **3**(10): p. 1763-9.
211. Graham, B.H., et al., *A mouse model for mitochondrial myopathy and cardiomyopathy resulting from a deficiency in the heart/muscle isoform of the adenine nucleotide translocator.* Nat Genet, 1997. **16**(3): p. 226-34.
212. Zhang, D., et al., *Mitochondrial DNA mutations activate the mitochondrial apoptotic pathway and cause dilated cardiomyopathy.* Cardiovasc Res, 2003. **57**(1): p. 147-57.
213. Zhang, D., et al., *Construction of transgenic mice with tissue-specific acceleration of mitochondrial DNA mutagenesis.* Genomics, 2000. **69**(2): p. 151-61.
214. Kasahara, T., et al., *Mice with neuron-specific accumulation of mitochondrial DNA mutations show mood disorder-like phenotypes.* Mol Psychiatry, 2006. **11**(6): p. 577-93, 523.
215. Sligh, J.E., et al., *Maternal germ-line transmission of mutant mtDNAs from embryonic stem cell-derived chimeric mice.* Proc Natl Acad Sci U S A, 2000. **97**(26): p. 14461-6.
216. Inoue, K., et al., *Generation of mice with mitochondrial dysfunction by introducing mouse mtDNA carrying a deletion into zygotes.* Nat Genet, 2000. **26**(2): p. 176-81.
217. Sanchez-Martinez, A., et al., *Modeling human mitochondrial diseases in flies.* Biochim Biophys Acta, 2006. **1757**(9-10): p. 1190-8.
218. Zordan, M.A., et al., *Post-transcriptional silencing and functional characterization of the Drosophila melanogaster homolog of human Surf1.* Genetics, 2006. **172**(1): p. 229-41.
219. Tsang, W.Y., et al., *Mitochondrial respiratory chain deficiency in Caenorhabditis elegans results in developmental arrest and increased life span.* J Biol Chem, 2001. **276**(34): p. 32240-6.
220. Benit, P., et al., *Large-scale deletion and point mutations of the nuclear NDUFV1 and NDUFS1 genes in mitochondrial complex I deficiency.* Am J Hum Genet, 2001. **68**(6): p. 1344-52.
221. Schuelke, M., et al., *Mutant NDUFV1 subunit of mitochondrial complex I causes leukodystrophy and myoclonic epilepsy.* Nat Genet, 1999. **21**(3): p. 260-1.
222. Senoo-Matsuda, N., et al., *A defect in the cytochrome b large subunit in complex II causes both superoxide anion overproduction and abnormal energy metabolism in Caenorhabditis elegans.* J Biol Chem, 2001. **276**(45): p. 41553-8.
223. Ma, Y.S., et al., *Upregulation of matrix metalloproteinase 1 and disruption of mitochondrial network in skin fibroblasts of patients with MERRF syndrome.* Ann N Y Acad Sci, 2005. **1042**: p. 55-63.
224. Danielson, S.R., et al., *Isolation of transcriptomal changes attributable to LHON mutations and the cybridization process.* Brain, 2005. **128**(Pt 5): p. 1026-37.
225. Jahangir Tafrechi, R.S., et al., *Distinct nuclear gene expression profiles in cells with mtDNA depletion and homoplasmic A3243G mutation.* Mutat Res, 2005. **578**(1-2): p. 43-52.
226. Cortopassi, G., et al., *Mitochondrial disease activates transcripts of the unfolded protein response and cell cycle and inhibits vesicular secretion and oligodendrocyte-specific transcripts.* Mitochondrion, 2006. **6**(4): p. 161-75.
227. Gerard, B., et al., *Uridine preserves the expression of respiratory enzyme deficiencies in cultured fibroblasts.* Eur J Pediatr, 1993. **152**(3): p. 270.

228. Saitoh, S., et al., *Single-cell analysis of mitochondrial DNA in patients and a carrier of the tRNA(Leu)(UUR) gene mutation.* J Inherit Metab Dis, 1999. **22**(5): p. 608-14.
229. Geromel, V., et al., *Coenzyme Q10 depletion is comparatively less detrimental to human cultured skin fibroblasts than respiratory chain complex deficiencies.* Free Radic Res, 2002. **36**(4): p. 375-9.

Summary

One of the most important functions of mitochondria is the production of energy through the process of oxidative phosphorylation (OXPHOS). The first part of OXPHOS is carried out by the electron transport chain, consisting of OXPHOS enzyme complexes I to IV. In the final step, which is catalysed by the fifth OXPHOS enzyme complex, ATP synthase or complex V, energy is generated in the form of ATP. OXPHOS is under dual genetic control of the nuclear DNA (nDNA) and the mitochondrial DNA (mtDNA). The mtDNA encodes 13 subunits of the OXPHOS enzyme complexes, 22 tRNA and two rRNA molecules. The vast majority of the subunits and all other mitochondrial proteins, involved in mtDNA transcription, translation, replication, or in mitochondrial transport, assembly and biogenesis, are encoded by nuclear genes. Mutations in the mtDNA are either *de novo*, segregate in the maternal lineage or are somatically acquired. MtDNA mutations can be either heteroplasmic (mutant and wild-type mtDNA molecules co-segregate within cells and tissues) or homoplasmic (all mtDNA molecules are mutated). Mutations in mtDNA genes and in nuclear OXPHOS genes can lead to OXPHOS deficiency and energy deficit. Disorders in which OXPHOS deficiency is a central characteristic, are referred to as oxidative phosphorylation or OXPHOS disorders.

OXPHOS disorders are clinically and genetically heterogeneous. This means that the same mutation can lead to different symptoms and that different mutations can lead to the same symptoms respectively. This makes it difficult to determine the genetic defect and to explain the disease pathology. Clinical heterogeneity is particularly an issue for mtDNA mutations, which can only partly be explained by different levels of heteroplasmy. Other factors must play a role as well. Symptom-based protocols have been explored to link clinical symptoms directly to a specific mtDNA mutation, but the suitability is limited to certain specific syndromes, as for example with Leber hereditary optic atrophy (LHON). Alternatively the entire mtDNA could be screened to identify a genetic defect or to exclude the mtDNA as a causative factor, which is important for genetic counseling. For example, mtDNA mutations are causative in 25% of the pediatric OXPHOS disorder cases, making it is reasonable to screen the complete mtDNA. In **chapter 2** a microarray based method is applied to resequence the complete mtDNA in OXPHOS patients. Call rates were high (94% on average) and heteroplasmic mutations were detectable at levels above 5%, although the lower limits were not systematically evaluated. In a quarter of the OXPHOS patients a genetic diagnosis could be made, but one has to be aware that unclassified variants are frequently detected, which cause interpretation problems and, if not properly counseled, anxiety in the families involved. Optimisation of data analysis and software tools will improve call rates and heteroplasmy level detection limits comparable to the currently used heteroduplex based methods. Databases and functional assays will need to solve the interpretation problems, which is common to all large-scale sequencing approaches. A first step will be central storage of all detected nucleotide variants and the development of standardised diagnostic flow charts in

which as many aspects as possible of a pathogenicity scoring mechanisms are taken into account. The improvements in data analysis and the costs of the chip compared with new high throughput sequencing and mutation detection techniques will determine whether MitoChip resequencing remains the preferred method for mtDNA resequencing for the next couple of years.

Microarray gene expression profiling has been shown to be extremely powerful to study pathological molecular processes of diseases. This approach was applied to OXPHOS disorders on skeletal muscle from Leigh syndrome patients with a mutation in the nuclear *SURF1* gene, which is fatal at infancy (**chapter 3**) and from symptomatic and a-symptomatic carriers of the m.3243A>G mutation in the mtDNA, which can cause a variety of symptoms, including mitochondrial myopathy, encephalopathy, lactic acidosis, and stroke-like episodes (MELAS, **chapter 4**). Our data show that stimulation of OXPHOS and mitochondrial biogenesis does not occur to compensate the energy deficiency in symptomatic *SURF1* Leigh and MELAS patients. The number of altered processes was fairly limited, but included an unexpected elevation of the complement system. In a-symptomatic carriers of the m.3243A>G mutation many more processes were altered, including protein turn-over, apoptosis and also, at a lower level, the complement system. Protein studies showed that ROS-damage was elevated in *SURF1*- and MELAS-muscle biopsies. Based on our data, we hypothesise that increased ROS production, resulting from a defective OXPHOS system and a defect in the translation machinery in case of the m.3243A>G mutation, results in oxidative damaged and dysfunctional proteins. In an effort to replace the damaged and dysfunctional proteins, protein turnover and apoptosis is increased. However, as dysfunctional proteins are constantly produced, this can not prevent, but only delay pathology from occurring, probably depending on the energy capacity of the tissue. When damage is insufficiently removed, irreparable pathology arises. Compensation and rescue mechanisms are shut-down and, as a final rescue process, complement components are strongly activated as stimulators of muscle regeneration. As the genetic defect is present in all cells this final effort is doomed to fail.

Gene expression studies on OXPHOS disorders are limited by the rareness of specific syndromes and the scarcity of available tissue. Alternative animal models not always represent the wild-type or pathological situation in human to the best extent, making extrapolation of the results difficult. Therefore, patient-derived model systems should be better alternatives. In **chapter 5**, a cell culture model system is presented which exploits the mutation load differences between monoclonal fibroblast cultures. This circumvents the main problems of other cell culture model systems, i.e. differences in genetic backgrounds between individuals or genetically modified and unstable genetic backgrounds in transformed cell lines. Fibroblast cells from one single patient carrying the m.9176T>C mutation in the *ATP6* gene were cloned by seeding the cells in a very low concentration, allowing cell colonies to arise from only one single cell. This gave rise to various cell lines with the same genetic background, but with different m.9176T>C mutation loads. This system is the preferred method to study mutation load effects of the m.9176T>C mutation. Moreover, this cell culture model system may be applicable to other mtDNA mutations as well,

like the MELAS m.3243A>G and the Neuropathy, Ataxia, and Retinitis Pigmentosa (NARP) or Leigh syndrome m.8993T>G/C mutation.

In conclusion, chip-based approaches have been shown to be valuable tools for studying OXPHOS diseases. Classification based on gene expression profiling or other clinical or biochemical criteria remains difficult and only applicable to a small subgroup of patients, due to the extreme genetic and clinical heterogeneity of these disorders. Therefore, high-throughput screening methods, like the mtDNA resequencing chips, have been developed as an alternative to rapidly screen large amounts of genes, if no educated choice can be made in advance. Gene expression profiling is particularly suited to identify the pathological molecular genetic pathways, involved in OXPHOS disease. Apparently, the OXPHOS system itself reacts only limitedly at the transcriptional level and for the m.3243A>G mutation only before symptoms occur. Other processes involved are ROS damage, protein turnover and tissue regeneration, which may provide new clues for the development of therapies for OXPHOS disorders. Increasing energy capacity may delay pathology. Preventing ROS damage to proteins, DNA and tissue, by preventing excessive ROS production, but also by improving ROS protection, seems to be beneficial. Finally, stimulating protein turnover and supplying the required energy capacity might be helpful in order to compensate for the defects and postpone disease manifestation. Further studies will have to be performed to demonstrate the efficacy of these approaches.

Samenvatting

Een van de meest belangrijkste functies van mitochondria is de productie van energie via het proces van oxidatieve fosforylering (OXPHOS). Het eerste deel van OXPHOS wordt gevormd door de electronentransportketen die bestaat uit de OXPHOS enzymcomplexen I tot en met IV. In de laatste stap, die gekatalyseerd wordt door het vijfde OXPHOS enzymcomplex, ATP synthase of complex V, wordt energie gegenereerd in de vorm van ATP. OXPHOS is zowel onder controle van het nucleaire DNA (nDNA) als het mitochondriële DNA (mtDNA). Het mtDNA codeert voor 13 subunits van het OXPHOS enzymcomplex, 22 tRNA en twee rRNA moleculen. De meerderheid van de subunits en alle andere mitochondriële eiwitten, betrokken bij mtDNA transcriptie, translatie, replicatie, of bij mitochondrieel transport, opbouw en biogenese, worden gecodeerd door nucleaire genen. Mutaties in het mtDNA kunnen *de novo* zijn, worden overgedragen via de maternale lijn of worden somatisch verworven. MtDNA mutaties kunnen heteroplasmisch (mutante en wild-type mtDNA moleculen zijn samen aanwezig in cellen en weefsels) of homoplasmisch (alle mtDNA moleculen zijn gemuteerd) zijn. Mutaties in mtDNA genen en in nucleaire OXPHOS genen kunnen leiden tot OXPHOS deficiëntie en een energietekort. Ziektes waarbij OXPHOS deficiëntie een centrale rol speelt worden oxidatieve fosforyleringsstoornissen of OXPHOS stoornissen genoemd.

OXPHOS stoornissen zijn klinisch en genetisch heterogeen. Dit betekent respectievelijk dat dezelfde mutatie kan leiden tot verschillende symptomen, en dat verschillende mutaties kunnen leiden tot dezelfde symptomen. Dit bemoeilijkt het bepalen van het genetisch defect en het verklaren van de pathologie achter de ziekte. Klinische heterogeniteit is vooral een knelpunt in het geval van mtDNA mutaties, wat alleen gedeeltelijk verklaard kan worden door verschillen in heteroplasmieniveaus. Andere factoren zullen ook een rol spelen. Er zijn symptoomgebaseerde protocollen ontwikkeld die trachten een directe link tussen de klinische symptomen en een mtDNA mutatie te leggen, maar de bruikbaarheid hiervan blijft beperkt tot bepaalde specifieke syndromen, zoals Leber hereditary optic atrophy (LHON). Als alternatief zou het volledige mtDNA gescreend kunnen worden om het genetisch defect te identificeren of om het mtDNA als oorzakelijke factor uit te sluiten, wat belangrijk is voor de genetische counseling. MtDNA mutaties zijn bijvoorbeeld de ziekteoorzaak in 25% van de pediatrische OXPHOS stoornis gevallen, dat het nut van het screenen van het gehele mtDNA benadrukt. In **hoofdstuk 2** wordt een op microarray gebaseerde techniek gebruikt om het gehele mtDNA van patiënten met een OXPHOS stoornis te resequencen. Callrates waren hoog (gemiddeld 94%) en heteroplasmische mutaties waren detecteerbaar tot niveaus boven de 5%, hoewel de lagere limiet niet systematisch geëvalueerd is. In een kwart van de OXPHOS patiënten kon een genetische diagnose worden gesteld, maar er moet niet vergeten worden dat er vaak ongeclassificeerde varianten worden gedetecteerd, die de interpretatie kunnen bemoeilijken en die, wanneer niet goed gecounseld, angst in de betrokken families kan veroorzaken. Optimalisatie van de data analyse en software tools zal de callrates en

de heterplasmiedetectielimiet doen verbeteren tot een vergelijkbaar niveau als de huidige op heteroduplex gebaseerde methodes. Databases en functionele tests zullen het interpretatieprobleem dat voorkomt bij alle grootformaat sequencing aanpakken moeten verhelpen. De centrale opslag van alle gedetecteerd nucleotidevarianten, en de ontwikkeling van gestandaardiseerde diagnostische werkschema's waarin zo veel mogelijk aspecten van een pathogeniciteitsscroringsmechanisme worden aangehaald, zal een eerste stap vormen. De verbeteringen in de data analyse en de kosten van de chip in vergelijking met nieuwe high throughput sequencing- en mutatiedetectietechnieken zullen bepalend zijn voor de vraag of MitoChip resequencing de voorkeursmethode zal blijven voor het resequencen van het mtDNA in de komende jaren.

Het is gebleken dat microarray genexpressie profilering zeer waardevol is voor het bestuderen van pathologisch moleculaire processen van ziektes. Deze aanpak werd toegepast op skeletspier van patiënten met een OXPHOS stoornis zoals Leigh syndroom patiënten met een mutatie in het nucleaire *SURF1* gen die fataal is tijdens de kinderjaren (**hoofdstuk 3**) en symptomatische en a-symptomatische dragers van de m.3243A>G mutatie in het mtDNA die kan resulteren in verschillende symptomen, waaronder mitochondrial myopathy, encephalopathy, lactic acidosis, and stroke-like episodes (MELAS, **hoofdstuk 4**). Onze data illustreert dat stimulatie van OXPHOS en mitochondriële biogenese niet optreedt ter compensatie van het energietekort in symptomatische *SURF1* Leigh en MELAS patiënten. Het aantal veranderde processen was aan de lage kant, maar bevatte een onverwachte stimulatie van het complement systeem. In a-symptomatische dragers van de m.3243A>G mutatie waren veel meer processen veranderd, waaronder eiwitturnover, apoptose en ook, weliswaar minder sterk, het complement systeem. Eiwitstudies hebben aangetoond dat de mate van ROS-schade verhoogd was in *SURF1* en MELAS spierbiopten. Op basis van onze data stellen wij de hypothese dat de toename in ROS-productie, veroorzaakt door het defecte OXPHOS systeem en een defect in het translatieapparaat bij de m.3243A>G mutatie, leidt tot oxidatief beschadigde en disfunctionele eiwitten. Omdat disfunctionele eiwitten constant geproduceerd worden, kan dit mechanisme het ontstaan van de pathologie niet voorkomen, maar alleen vertragen, wat afhankelijk is van de energiecapaciteit van het weefsel. Wanneer de schade inefficiënt verwijderd wordt, ontstaat er een onomkeerbare pathologie. Compensatie- en reddingsmechanismen worden gestopt en complement componenten worden sterk geactiveerd voor de stimulatie van spierregeneratie als een laatste redmiddel. Omdat het genetisch defect in alle cellen aanwezig is, is deze laatste poging gedoemd om te mislukken.

De aanwezigheid van genexpressiestudies op OXPHOS stoornissen is beperkt door de zeldzaamheid van specifieke syndromen en de schaarsheid aan beschikbaar weefsel. Alternatieve diermodellen representeren de wild-type of de pathologische situatie in de mens niet altijd even goed, wat extrapolatie van de resultaten bemoeilijkt. Daarom zouden van de patiënt afgeleide modelsystemen betere alternatieven zijn. In **hoofdstuk 5** wordt een celkweekmodelsysteem

beschreven dat gebruik maakt van de verschillen in mutatiepercentage tussen monoklonale fibroblastenkweken. Dit omzeilt de belangrijkste problemen van andere celkweekmodelsystemen, namelijk de verschillen in genetische achtergronden tussen individuen of genetische gemodificeerde en onstabiele genetische achtergronden in getransformeerde cellijnen. Fibroblastcellen van één patiënt die drager was van de m.9176T>C mutatie in het *ATP6* gen werden gekloneerd door de cellen uit te zaaien in een zeer lage concentratie waardoor celkolonies konden ontstaan vanuit één enkele cel. Hierdoor ontstonden verschillende cellijnen met dezelfde genetische achtergrond, maar met verschillende m.9176T>C mutatiepercentages. Dit systeem is de voorkeursmethode voor het bestuderen van mutatiepercentage effecten van de m.9176T>C mutatie. Daarnaast zou dit celkweekmodelsysteem ook toepasbaar zijn op andere mtDNA mutaties, zoals de MELAS m.3243A>G en de Neuropathy, Ataxia, and Retinitis Pigmentosa (NARP) of Leigh syndrome m.8993T>G/C mutatie.

Concluderend kunnen we stellen dat de op chip-gebaseerde aanpakken waardevol zijn gebleken voor de bestudering van OXPHOS stoornissen. Classificatie op basis van genexpressieprofilering of andere klinische of biochemische criteria blijft lastig vanwege de extreme genetische en klinische heterogeniteit van deze stoornissen, en alleen toepasbaar op een kleine subgroep patiënten. Daarom zijn alternatieve high-throughput screeningsmethodes ontwikkeld, zoals de mtDNA resequencing chip, als een alternatief om snel een grote hoeveelheid genen te screenen wanneer geen weloverwogen gerichte keuze op voorhand gemaakt kan worden. Genexpressieprofilering is vooral geschikt voor het identificeren van de pathologische moleculaire genetische pathways die betrokken zijn bij OXPHOS stoornissen. Blijkbaar is er maar een beperkte reactie van het OXPHOS systeem zelf op het transcriptionele niveau, en bij de m.3243A>G mutatie alleen vóórdat symptomen optreden. Andere processen die een rol spelen zijn ROS schade, eiwit turnover en weefselregeneratie, welke nieuwe ingangen kunnen vormen voor de ontwikkeling van therapieën voor OXPHOS stoornissen. Het doen toenemen van de energiecapaciteit zou het optreden van pathologische verschijnselen kunnen vertragen. Het voorkomen van ROS-schade aan eiwitten, DNA en weefsel, door het voorkomen van buitensporige ROS-productie, maar ook door het verbeteren van de ROS-bescherming, zal een positieve invloed hebben. Als laatste zou het stimuleren van de eiwitturnover en het aanreiken van de benodigde energie hiervoor helpen bij de compensatie van het defect, waardoor het optreden van ziektesymptomen uitgesteld wordt. Er zal aanvullend onderzoek uitgevoerd moeten worden om de doeltreffendheid van deze aanpakken vast te stellen.

Dankwoord

Ik kan bijna niet geloven dat het eindelijk zover is. Het eindproduct van een aantal jaren hard werken is er eindelijk. Deze periode had zowel ups als downs, maar beide hebben ervoor gezorgd dat ik gegroeid ben als mens en als wetenschappelijk onderzoeker en hebben daarmee bijgedragen aan de totstandkoming van dit proefschrift. Dit alles heb ik natuurlijk niet alleen aan mezelf te danken. Ook de hulp en steun van anderen is in dit traject van groot belang geweest.

Als eerste wil ik mijn promotor en copromotor bedanken. Joep, jij was een promotor in de vorm van een "stille vennoot", vooral in de eerste jaren. Een stille vennoot houdt de gang van zaken van een afstandje in de gaten. Je was er dan ook wanneer je er moest zijn, met name in de eindfase. Beste Joep, bedankt voor je bijdrage. Bert, jou wil ik vooral bedanken voor je steun en begrip in moeilijke tijden, vooral ook tijdens moeilijke tijden buiten het werkvlak. Mede dankzij deze steun en hulp, heb ik dit traject met succes kunnen afronden. Wat het onderzoek betreft lagen we niet altijd op één lijn, wat soms voor stevige discussies zorgde. Ook dat heeft eraan bijgedragen dat ik in wetenschappelijk opzicht gegroeid ben.

Natuurlijk verdienen mijn directe collega's een dankjewel. Ik wil beginnen met de harde AIO-kern, die in het begin gevormd werd door Lorraine, Bianca en Lars, en later werd uitgebreid met Nicole, Florence, Ruben en An. Lorraine, ons raakvlak op onderzoeksgebied was de m.9176T>C mutatie, waarvoor jij een PGD ging opzetten. Van jouw vooronderzoek heb ik dankbaar gebruik gemaakt bij het opzetten van mijn PCR's en mutatiepercentage analyses. Bedankt voor het delen van je expertise op dit gebied. Jij was ook altijd van de partij als er gestapt moest worden. Herinner je je nog die grote neger in het Haagse café? Hoewel hij Frans sprak, wist hij je duidelijk te maken dat hij je wel zag zitten. Jammer genoeg (voor hem) was dat niet wederzijds. Bianca, wij kennen elkaar al veel langer. We zijn in hetzelfde jaar (in 1995 - zijn we al zo oud?!) aan de studie Gezondheidswetenschappen begonnen, maar na een jaar of 2-3 werd ons contact wat minder. Het was voor jou dan ook een verassing dat ik in 2002 bij PopGen/KlinGen begon als AIO. Op mijn eerste werkdag was Bert er niet, en jij moest mij maar even opvangen. Dat was een beetje onwennig, maar het was fijn om een bekend gezicht te zien. Dat onwennige ging er gelukkig weer snel af. Hoewel jouw onderzoeksonderwerp met de muizen wat verder van mijn onderwerp af stond, heb ik toch veel aan jou gehad. Je hebt me een beetje wegwijs gemaakt in het AIO zijn en de gang van zaken geïntroduceerd op de afdeling Popgen. Verder heb je mijn woordenschat uit weten te breiden. Dankzij jou weet ik nu wat "poepig" is. Ik betrap mezelf erop dat ik het woord ook soms gebruik. Lars en Nicole, naast mijn AIO collega's ook mijn paranimfen, ik wil jullie natuurlijk bedanken voor jullie hulp en steun tijdens het hele traject. Zowel op het werkvlak en privé heb ik veel steun aan jullie gehad. Ook al had ons onderzoek soms weinig raakvlakken, doordat we op dezelfde afdeling werkten hadden we toch dingen gemeen waardoor we toch veel steun aan elkaar hebben gehad. Lars, het afgelopen (bijna) anderhalf jaar heb ik door mijn

"dubbele baan" (mijn werk in Leuven en daarnaast het schrijven van mijn proefschrift) een beetje jouw slaappatroon overgenomen. Maar ik ben blij dat ik ervan af kan stappen; 4-5 uurtjes slaap per dag is toch wat weinig, ik heb er toch wel 6 nodig. Van jou heb ik ook veel geleerd over het analyseren van microarray data. Het programmeren in R was voor jou als spreken in een tweede moedertaal, en mede dankzij jou spreek ik deze taal nu ook redelijk vloeiend. Nicole, wat werk betreft hadden wij weinig gemeen, maar verder konden we het goed vinden. Er was altijd tijd voor een praatje, of een discussie waarbij jij net als ik altijd je gelijk wilde halen; een goede eigenschap vind ik zelf ;-) Laat me weten wanneer de kinderboerderij klaar is, want ik heb Olivia beloofd dat we een keer naar Nicole en Dennis met hun eigen kinderboerderij gaan. De <100 heb ik misschien niet gehaald, maar we drinken toch een goede pint op het resultaat dat ik al geboekt heb, zowel voor wat betreft aantal pagina's als aantal verloren kilo's! Florence, jij begon als stagiair bij Caroline en mij. In het begin was je heel stil, maar later toen je eenmaal een tijdje als AIO bij ons werkte kwam je los. Je was nog steeds redelijk rustig, zeker in vergelijking met de rest, maar áls je wat zei dan was het ook meteen raak. Ruben, jij gekke Hollander! Je bent een vreemde vogel, maar je kunt heerlijk Chinees koken……lekkerrrrr! An, zotteke, een gekke Belg! Tja, wat kan ik zeggen, een beetje onnozel natuurlijk, maar wel een *toffe* en *plezante* collega (ja, ik spreek inmiddels ook al een aardig woordje Vlaams).

Naast de AIO's zijn er nog andere mensen op de afdelingen Populatiegenetica en Klinische genetica die ik moet bedanken. Caroline, bedankt voor al het praktisch werk dat je voor mijn project verricht hebt. De resultaten van de arrays die voornamelijk door jou gerund zijn heb je nu in je handen! Erika, gek schaap jij met je schaap, samen met jou heb ik mijn eerste RNA isolaties gedaan. Ik kan me herinneren dat ik vond dat jij zo soepeltjes met die pipet omging. Bedankt voor de leuke en ontspannen praatjes, zomaar even op de gang of in de koffiekamer. Wanneer ga je nog eens met je moeder bellen zodat ik het Betuws dialect eens kan horen? Alexandra, mijn vraagbaak op 3X. Toen Rosy mij een rondleiding gaf, zei ze: "Dit is Alexandra, en als je hier iets nodig hebt dan moet je bij haar zijn". Laat ik het zo zeggen, Rosy heeft niet gelogen! Bedankt voor je hulp! Torik, jou wil ik bedanken voor het feit dat je deur altijd open stond voor het stellen van een vraagje. Dat vraagje ontketende dan wel vaak een lange discussie, maar daar heb ik wel veel aan gehad. Bij deze wil ik me ook vast aanmelden voor de *cruiseference* op Curaçao of ergens anders waar het lekker warm is. Als ik als spreker kom, betaal jij vast mijn ticket en hotel, toch? Ton, bedankt voor je instant IT-hulp. Ook als je het erg druk had maakte je wel even tijd om mijn probleem op te lossen, zelfs op je wekelijkse vrije dag vanuit thuis. Succes met je nieuwe baan! Patrick, na een aantal jaren in Nederland gewerkt te hebben, neem ik aan dat je inmiddels je Nederlands cursus met succes hebt afgerond. Ik bedank jou dan ook in het Nederlands dat je R aan mij geïntroduceerd hebt en een aantal analyses voor mij hebt gedaan. Je scripts waren niet altijd even eenvoudig, maar op den duur kon ik er toch goed wijs uit komen en zelfs wat zaken aanpassen. Rob, Ellen, Marion (of moet ik zeggen "Márion"), Jos D, Mike, Bieke, Marij en Fons, jullie natuurlijk ook bedankt voor mijn leuke tijd bij Popgen/Klingen. Rosy, jou moet ik natuurlijk niet vergeten te bedanken. Jij wist me altijd wegwijs te maken als er iets geregeld moest worden.

Jij wist altijd waar en bij wie ik moest zijn. Ook waren de koffiekamersessies met jou altijd zeer vermakend.

Naast alle mensen van mijn oude werkplek, ben ik ook een "dikke merci" verschuldigd aan mijn nieuwe collega's in het verre Leuven (v.w.b. treintijd dan…). Ruth ("de ouw van de MAF"), Kizi (is het nu "Kiezzie", "Kizzie" of "Kèzzie"?), Lieze (zeikwijf ;-)), Joke ("dikke kak"), Kris ("is dah?") en Paul, jullie wil ik bedanken voor het feit dat jullie het aangedurfd hebben om een Hollander in jullie groep op te nemen. Ik heb het erg naar mijn zin bij jullie, en hoop dat ik nog een tijd mag blijven. Joke, bedankt voor je luisterend oor in de tijden dat ik het even nodig had. Paul, het "binnen afzienbare tijd" afronden van mijn doctoraat (zie mijn sollicitatiebrief) heeft langer geduurd dan verwacht, maar nu ben ik eindelijk ook officieel een volwaardige postdoc. Ik wil jou daarom in het bijzonder bedanken voor je geduld, je steun, en je vertrouwen in mij.

Mijn familie moet ik zeker bedanken! Guido, grote broer ;-), wij hadden het wel eens over de verschillen tussen jouw en mijn werk. Jij als consultant in de hoek van bank- en verzekeringszaken, en ik als wetenschappelijk onderzoeker in de genetica. We snapten weinig van elkaars werk, maar één ding was duidelijk: veel zaken zijn anders geregeld in deze sectoren. Bedankt voor onze spaarzame, maar toch ontspannen gesprekken hierover, die mij geholpen hebben bij het relativeren van sommige zaken. En dan nu het moeilijkste stuk…… Pap en Mam, jullie mag ik natuurlijk niet vergeten. Ik wil jullie met de woorden bedanken, precies zoals ze op dit moment in me opkomen. Pap en Mam, geer höb miech altied begeleid en gesteund in mien ganse studietrajec. Allewel geer neet altied begreep boe iech mèt bezig waor, vroog geer altied wie ut op 't wèrrek waor en of 't al get opsjoot. Zonder eure steun en raod, waor 't mesjiens gans aanders oetgepak. Iech weit nog tot iech op 't punt stond um te stoppe mèt mien studie um mien favoriete biijbäönsje tot mien wèrrek te make. Allewel geer dat eigelik gein good idee vónt, stónt geer toch achter mien beslissing, moch iech de beslissing numme um te stoppe. Mer gelökkig höb geer miech toch weite te euvertuige um nog evekes door te zètte. 'T resultaat is d'r noe en iech bin kóntent, en iech hoop tot geer daor zjus zoe euver dink. Pap, ik sjrief dit stök vaan mien daankwoord mèt traone in mien ouge. Iech weit totsdiech hiij hiel gere biij hads wèlle zien, en veer hadde aoch allemaol hiel gere gehad totste d'rbiij waors, mèr het heet neet zoe mage zien. Iech mis diech daan oach hiel erg hiijbiij. Iech hoop totsdiech 't toch allemaol u bitteke mètkrijgs en totsdiech tróts op miech bis. Pa en Ma, bedaank!

Ik moet natuurlijk niet vergeten mijn eigen gezinnetje, dat weer uitgebreid wordt met een tweede dochtertje, te bedanken. Olivia, je kunt dit nu nog niet lezen, maar misschien kijk je later nog eens in het dan stoffige boekje van Papa. Hoewel het zeker het afgelopen jaar heel zwaar is geweest, was jij altijd in staat om mij op te vrolijken na weer een lange dag werken. Stiekem hebben we je altijd wat langer op laten blijven, zodat ik je nog een uurtje kon zien als ik 's avonds thuiskwam van mijn werk in Leuven. Jouw lach, je lieve stemmetje en je knuffeltjes hebben mij erdoorheen gesleept! Ik hoop dat je zusje net zo lief en braaf wordt als jij, dan hebben mama en ik het héél erg

goed. Claudia, jij hebt waarschijnlijk de meeste nadelen ondervonden van mijn promoveren. Vooral in de eindfase was er heel vaak geen tijd voor jou, zeker toen je de spaarzame vrije tijd ook nog moest delen met Olivia en andere zaken die noodgedwongen om mijn aandacht vroegen. Thuis van mijn werk, na het eten en nadat we Olivia in bed hadden gelegd, moest ik vaak nog "even snel" iets afmaken waar ik in de trein al aan begonnen was. Dat "even" werd vaak tot in de kleine uurtjes 's nachts. Toch heb jij zelden hierover geklaagd en ben je altijd mijn steunpilaar geweest en gebleven als er weer eens iets tegenzat. Ik kon altijd mijn verhaal bij jou kwijt, ook al begreep je soms niet waar het over ging en ook al klonk het soms allemaal wat onwerkelijk. Nu dit eindelijk is afgerond, kunnen we weer wat meer ontspannen van elkaar en van Olivia en haar zusje genieten. Claudia, jij bent de beste!

Ik heb ongetwijfeld mensen niet genoemd of ben mensen vergeten te noemen. Dat wil niet zeggen dat ik jullie niet dankbaar ben, maar het is gewoon onmogelijk om op dit moment aan iedereen te denken en dat op papier te zetten. Mensen, bedankt!

Rudy!

Curriculum Vitae

Rudy Gerardus Elisabeth van Eijsden werd geboren op 3 augustus 1977 in Maastricht. Van 1989 tot 1995 doorliep hij het Voorbereidend Wetenschappelijk Onderwijs (VWO) aan het St. Maartenscollege te Maastricht waarna hij koos voor de opleiding Biologische Gezondheidkunde aan de Universiteit Maastricht. Na zijn afstudeerstage bij de afdeling Pathologie van het Academisch Ziekenhuis Maastricht met "een klonaliteitsanalyse van Non-Hodgkin lymfomen" als onderwerp, behaalde hij zijn universitair diploma in 2001. In 2001 werkte hij een korte tijd als wetenschappelijk onderzoeker bij de Universiteit Maastricht op de afdeling Gezondheidsrisico Analyse en Toxicologie en hielp daar bij het schrijven van een wetenschappelijk rapport over de toepassing van high-throughput genexpressieprofileringstechnieken in de exotoxicologie. Dit bleek later een goede voorbereiding geweest te zijn voor zijn promotieonderzoek waaraan hij in maart 2002 begon als assistent in opleiding (AIO) aan de Universiteit Maastricht bij de afdeling Klinische Genetica binnen de capaciteitsgroep Genetica en Celbiologie, verbonden aan het onderzoeksinstituut Groei en Ontwikkeling (GROW). Het onderzoek was gericht op oxidatieve fosforyleringsstoornissen en had als doel meer inzicht te verkrijgen in de moleculair biologische processen die bij deze stoornissen betrokken zijn. Het voornaamste middel waarvan binnen dit onderzoekstraject gebruik werd gemaakt was de microarray techniek, voor zowel genexpressiebepalingen als voor resequencing doeleinden. Vanaf 1 december 2007 is hij werkzaam als wetenschappelijk onderzoeker bij de MicroArray Faciliteit van het VIB te Leuven in België waar hij als postdoc meewerkt aan het YING (Yeast In No Gravity) project, waarbij de invloed van microgravitéit bestudeerd wordt op cellulaire adhesie, biofilmvorming en invasieve groei bij het modelorganisme *Saccharomyces cerevisiae*. Daarnaast is hij bij de VIB MicroArray Facility betrokken bij de planning van experimenten, het uitvoeren van data- en functionele analyses, en bij bioinformaticaprojecten in de meest brede zin van het woord.

Abbreviations

adPEO	autosomal dominant progressive external ophthalmoplegia
AIC	Akaike information criterion
BN-PAGE	blue native polyacrylamide gel electrophoresis
CDF	probe set definition
cDNA	complementary DNA
COX	cytochrom *c* oxidase
CPEO	chronic progressive external ophthalmoplegia
DAVID	Database for Annotation, Visualisation and Integrated Discovery
DCE	denaturant capillary electrophoresis
DFP	diisopropyl fluorophosphate
DGGE	denaturing gradient gel electrophoresis
DHE	dihydroethidium
dHPLC	denaturing high-performance liquid chromatography
DMD	Duchene muscular dystrophy
DTT	dithiothreitol
EM	extracellular matrix
ER	endoplasmatic reticulum
GDAS	GeneChip DNA Analysis Software
GENMAPP	Gene Map Annotator and Pathway Profiler
HBSS	Hanks balanced salt solution
KSS	Kearns-Sayre syndrome
LHON	Leber hereditary optic atrophy
MAC	membrane attack complex
MELAS	mitochondrial myopathy, encephalopathy, lactic Acidosis, and stroke-like episodes
MERRF	myoclonus epilepsy and ragged red Fibres
MRI	magnetic resonance imaging
mtDNA	mitochondrial DNA
NARP	neuropathy, ataxia, and retinitis pigmentosa
nDNA	nuclear DNA
OXPHOS	oxidative phosphorylation
PBS	phosphate-buffered saline
PCR	polymerase chain reaction
PDHC	pyruvate dehydrogenase complex
PIM	protease inhibitor mixture
QRT-PCR	quantitative real-time polymerase chain reaction
RCRS	revised cambridge reference sequence
ROS	reactive oxygen species
RRF	ragged red fibres
SD	standard deviation
SSCP	single strand conformation polymorphism
TGGE	temperature gradient gel electrophoresis
UV	unclassified variant
ww	wet weight

Stellingen behorende bij het proefschrift

Microarray analysis of oxidative phosphorylation disorders

Rudy Gerardus Elisabeth van Eijsden

Maastricht, 22 mei 2008

1. Nieuwe krachtige sequencingtechnieken zullen eerder de oplossing vormen voor de genetische diagnostiek van complexe stoornissen dan slimme klinische classificaties. (dit proefschrift)
2. Stimulering van het OXPHOS systeem en de aanmaak van mitochondria stelt het optreden van klinische symptomen bij dragers van de m.3243A>G mutatie uit. (dit proefschrift)
3. De expressie van complement component C3 in spier is een indicatie voor de pathologie, ernst en progressie van OXPHOS aandoeningen. (dit proefschrift)
4. Inductie van weefselregeneratie middels complement component C3 is een centraal, maar ontoereikend herstelproces bij OXPHOS aandoeningen. (dit proefschrift)
5. Kleine genexpressieveranderingen krijgen pas betekenis wanneer ze gezamenlijk op groeps- of procesniveau bestudeerd worden.
6. Het sequencen van het complete genoom is een steeds nader komend feit in de genetische diagnostiek waarbij interpretatieproblemen als nevenverschijnsel geaccepteerd zullen moeten worden.
7. Hoe complexer de ziekte, hoe meer patiënten er nodig zijn voor een genexpressiestudie.
8. Dataopslag en –transport zal met de nieuwe generatie sequencingtechnologieën een groot probleem worden.
9. Het begrip *resequencing* suggereert een herhaling die er niet is.
10. Het gebruik van nieuwe krachtige sequencingapparaten zal aanzienlijk toenemen als bij elk apparaat een bioinformaticus geleverd wordt.
11. Het mtDNA is *the circle of life*.